



THE UNIVERSITY OF QUEENSLAND
AUSTRALIA

Targeted skin delivery of topically applied drugs by optimised formulation design

Eman Abd

*A thesis submitted for the degree of Doctor of Philosophy at
The University of Queensland in 2015
School of Medicine (Southern Clinical Division)*

Abstract

Early research concentrated on the relationship between a solute's physicochemical properties and its skin permeation, mostly from simple solutions. Relatively less is known about how vehicles, particularly complex ones, might also affect skin permeation by altering the properties of the skin, although this is an area that has attracted much interest. Key requirements for topical delivery is understanding the relationships between drug-vehicle, drug-skin or drug –vehicle –skin interaction. In this project, understanding this relationship was crucial to designing novel formulations able to deliver drugs with different lipophilicity topically or systemically. The first aim was to explore the impact of various solution compositions on skin permeation of some model drugs. I compared *in vitro* maximum penetration fluxes (J_{max}) and solubilities of the vehicles (S_v) and of the stratum corneum (S_{SC}) and derived diffusivities (D^*) for four drugs (caffeine, minoxidil, lidocaine and naproxen) having a range of lipophilicities. I used a range of solvent vehicles that were hypothesised to affect the skin to differing degrees to evaluate vehicle effects on permeability parameters.

If neither the vehicle nor the solute alters the properties of the skin, maximum (or saturated) solute flux is independent of both the vehicle composition and the solute's saturated solubility in that vehicle. These findings were confirmed in this study for all four drugs used. The permeation of caffeine, minoxidil, lidocaine and naproxen were found to be selectively enhanced by vehicles containing specific excipients that were hypothesised to alter the properties of the skin. The greatest effects were seen on flux and diffusivity by the eucalyptol (EU) and oleic acid (OA) vehicles on the more hydrophilic compounds, caffeine and minoxidil. We concluded that enhanced solute fluxes were mainly driven by increased diffusivity in the stratum corneum.

I also examined the extent of skin permeation enhancement of the hydrophilic drug caffeine and lipophilic drug naproxen applied in nanoemulsions incorporating skin penetration enhancers. Infinite doses of fully characterised oil-in-water nanoemulsions containing the skin penetration enhancers oleic acid or eucalyptol as oil phases and caffeine (3%) or naproxen (2%) were applied to full-thickness skin and human epidermal membranes in Franz diffusion cells, along with aqueous control solutions. Caffeine and naproxen fluxes were determined over 8 h. Solute solubility in the formulations and in the stratum corneum, as well as the uptake of product components into the stratum corneum were measured.

The nanoemulsions significantly enhanced the skin penetration of caffeine and naproxen compared to aqueous control solutions. The maximum flux enhancement of caffeine was

associated with a synergistic increase in both its solubility in the stratum corneum and skin diffusivity. Enhanced skin penetration in these systems is largely driven by uptake of formulation excipients containing the active compounds into the stratum corneum. Fluxes of caffeine and naproxen absorbed into the receptor from full-thickness skin compared with epidermis were similar. Therefore, the amount of caffeine permeating the dermis and hypodermis was not affected by these structures although the stratum corneum only provided the barrier against penetration. In addition to lipids, the vesicle excipients included eucalyptol or oleic acid as penetration enhancers, and decyl polyglucoside (DPGluC) as a non-ionic surfactant. Vesicle particle sizes ranged between 135 and 158 nm and caffeine encapsulation efficiencies were between 46% and 66%. Caffeine penetration and permeation was measured using high performance liquid chromatography (HPLC). We found that niosomes, which are liposomes containing a non-ionic surfactant and transferosomes (ultraflexible vesicles) showed significantly greater penetration into the skin and permeation across the stratum corneum. Significant enhancement of caffeine penetration into hair follicles was found for transferosomes and those liposomes containing oleic acid.

The third aim was to investigate the effectiveness of our nanoemulsion formulations of caffeine and minoxidil for transfollicular delivery. Nanoemulsions were applied to full-thickness excised human abdominal skin in Franz diffusion cells for 24 h. Minoxidil concentrations in receptor fluid, tape strip extracts, follicular casts and homogenised skin extracts were analysed. The oleic acid formulation was the best at promoting minoxidil retention into the superficial skin compartments (stratum corneum and hair follicles). The eucalyptol formulation was the best for deeper penetration into and through the skin. In the second part, caffeine in nanoemulsion formulations containing OA or EU and in controls was topically applied and the amount of caffeine retained in the stratum corneum, hair follicles, in the skin and in the receptor was analysed. The hair follicles and the area around them were imaged by a LaVision Multiphoton Microscope. Oleic acid nanoemulsion showed the highest transfollicular delivery of caffeine. Less caffeine in skin layers and storage in hair follicles was found after blocking the hair follicles.

In conclusion, this project provided information to understand the mechanisms of chemical penetration enhancers on the human skin and the results of this PhD will help to improve the design of new formulations or to develop current formulations containing model drugs.

Declaration by author

This thesis is composed of my original work, and contains no material previously published or written by another person except where due reference has been made in the text. I have clearly stated the contribution by others to jointly-authored works that I have included in my thesis.

I have clearly stated the contribution of others to my thesis as a whole, including statistical assistance, survey design, data analysis, significant technical procedures, professional editorial advice, and any other original research work used or reported in my thesis. The content of my thesis is the result of work I have carried out since the commencement of my research higher degree candidature and does not include a substantial part of work that has been submitted to qualify for the award of any other degree or diploma in any university or other tertiary institution. I have clearly stated which parts of my thesis, if any, have been submitted to qualify for another award.

I acknowledge that an electronic copy of my thesis must be lodged with the University Library and, subject to the policy and procedures of The University of Queensland, the thesis be made available for research and study in accordance with the Copyright Act 1968 unless a period of embargo has been approved by the Dean of the Graduate School.

I acknowledge that copyright of all material contained in my thesis resides with the copyright holder(s) of that material. Where appropriate I have obtained copyright permission from the copyright holder to reproduce material in this thesis.

Publications during candidature

Submitted journal articles

- 1. Eman Abd**, Sarika Namjoshi, Yousuf H. Mohammed, Michael S. Roberts, Jeffrey E. Grice, Synergistic skin penetration enhancer and nanoemulsion formulations promote the human epidermal permeation of caffeine and naproxen. *Journal of Pharmaceutical Science*. (Accepted in September 2015)-
- 2. Eman Abd**, Michael S. Roberts, Jeffrey E. Grice, A comparison of the penetration and permeation of caffeine into and through human epidermis after application in various vesicle formulations. *Skin Pharmacology and Physiology*. (Accepted in September 2015)
- 3. Eman Abd**, Michael S. Roberts, Jeffrey E. Grice, The human epidermal skin permeation of solutes is determined by vehicle uptake into and effects on the stratum corneum. *American Association Pharmaceutical Scientists (AAPS)* (Submitted in October 2015)

Conference abstracts

- 1- Eman Abd**, Gregory Medley, Yousuf Mohammed, Jeffrey E. Grice, Michael S. Roberts, Development and evaluation of microemulsion formulations for transdermal delivery of caffeine. ASCEPT Annual conference, Melbourne Dec 7-11, 2013.
- 2- Eman Abd**, Gregory Medley, Yousuf Mohammed, Michael S. Roberts, Jeffrey E. Grice, Enhanced delivery of minoxidil into skin compartments using microemulsion formulations. TRI, 2014.
- 3- Eman Abd**, Gregory Medley, Yousuf Mohammed, Michael S. Roberts, Jeffrey E. Grice, Development and evaluation of nanoemulsion formulations for transdermal delivery of Naproxen, ASMR, Brisbane, 2014.
- 4- Eman Abd**, Gregory Medley, Yousuf Mohammed, Michael S. Roberts, Jeffrey E. Grice, Effect of vehicles on *in vitro* percutaneous penetration rates, PhD symposium, Sydney, 2014.
- 5- Eman Abd**, Gregory Medley, Yousuf Mohammed, Michael S. Roberts, Jeffrey E. Grice, Effect of chemical enhancers on the *in vitro* percutaneous penetration of caffeine, ASCEPT Annual conference, Melbourne Dec 7-11, 2014.
- 6- Eman Abd**, Michael S. Roberts, Jeffrey E. Grice, Follicular penetration and retention of the hydrophilic model compound caffeine is promoted by microemulsion formulations containing penetration enhancers, 6th International Postgraduate Symposium in Biomedical Sciences, UQ, Brisbane, 2015.

Publications included in this thesis

Eman Abd, Sarika Namjoshi, Yousuf H. Mohammed, Michael S. Roberts, Jeffrey E. Grice, Synergistic skin penetration enhancer and nanoemulsion formulations promote the human epidermal permeation of caffeine and naproxen. Journal of Pharmaceutical Science. (Accepted in September 2015)- **Incorporated in Chapter 4.**

Contributor	Statement of contribution
Abd, E (Candidate)	Designed experiment (80%) Conducted experiment (100%) Statistically analysed and interpreted all data (100%) Wrote the paper (70%)
Namjoshi, Sarika	Edited the paper (20%)
Mohammed, Yousuf	Edited the paper (10%)
Roberts, MS	Supervised the project Edited the paper (30%) Wrote the paper (15%)
Grice, JE	Supervised the project Designed experiment (20%) Edited the paper (40%) Wrote the paper (15%)

Eman Abd, Michael S. Roberts, Jeffrey E. Grice, A comparison of the penetration and permeation of caffeine into and through human epidermis after application in various vesicle formulations. *Skin Pharmacology and Physiology*. (Accepted in September 2015)
Incorporated as Chapter 6

Contributor	Statement of contribution
Abd, E (Candidate)	Designed experiment (80%) Conducted experiment (100%) Statistically analysed and interpreted all data (100%) Wrote the paper (70%)
Roberts, MS	Supervised the project Edited the paper (50%) Wrote the paper (15%)
Grice, JE	Supervised the project Designed experiment (20%) Edited the paper (50%) Wrote the paper (15%)

Eman Abd, Michael S. Roberts, Jeffrey E. Grice, The human epidermal skin permeation of solutes is determined by vehicle uptake into and effects on the stratum corneum. American Association Pharmaceutical Scientists (AAPS) (Submitted in October 2015) **Incorporated as Chapter 3**

Contributor	Statement of contribution
Abd, E (Candidate)	Designed experiment (80%) Conducted experiment (100%) Statistically analysed and interpreted the data (100%) Wrote the paper (70%)
Roberts, MS	Supervised the project Edited the paper (50%) Wrote the paper (15%)
Grice, JE	Supervised the project Designed experiment (20%) Edited the paper (50%) Wrote the paper (15%)

Contribution by others to the Thesis

The data collection and all data analysis for chapters 3, 4, 5 and 6 were undertaken by the PhD candidate, Eman Abd. The candidate drafted all chapters and submitted papers that are included in this thesis under the guidance of the other co-authors.

Chapter 3 was undertaken by the PhD candidate, Eman Abd. This chapter led to the soon to be submitted journal article, entitled “Exploring the effect of vehicle composition relating skin penetration maximum flux to skin solubility for different vehicles compositions” All experimental work, data analysis and drafting of this chapter were undertaken by the PhD candidate, Eman Abd. As PhD supervisors: Dr Jeffrey Grice and Prof Michael S Roberts advised with discussion and oversaw all aspects of this chapter.

The preparation and characterisations of nanoemulsions in Chapter 4 led to the submitted journal article, entitled “Synergistic skin penetration enhancer and nanoemulsion formulations promote the human epidermal permeation of caffeine and naproxen”. All experimental work, data analysis and drafting of this chapter were undertaken by the PhD candidate, Eman Abd. The names and roles of all co-authors are: Dr. Sarika Namjoshi, who helped with the revision of this chapter. Dr. Yousuf H. Mohammed, who help image the skin and advised and revised this chapter. As PhD supervisors: Dr Jeffrey Grice and Prof Michael S. Roberts oversaw all aspects of this chapter.

Chapter 5 was undertaken by the PhD candidate, Eman Abd. All experimental work, data analysis and drafting of this chapter were undertaken by the PhD candidate, Eman Abd. Dr. Washington Sanchez Jnr. assisted with the use of LaVision multiphoton microscope. Dr. Yousuf H. Mohammed helped explain the skin images. Navin Chandrakanth Chandrasekaran helped in blocking hair follicles technique. As PhD supervisors: Dr Jeffrey Grice and Prof Michael S. Roberts oversaw all aspects of this chapter.

The preparation and characterisations of vesicles in Chapter 6 led to the submitted journal article, entitled “A comparison of the penetration and permeation of caffeine into and through human epidermis after application in various vesicle formulations”. All experimental work, data analysis and drafting of this chapter were undertaken by the PhD candidate, Eman Abd. As PhD supervisors: Dr Jeffrey Grice and Prof Michael S. Roberts advised with discussion and oversaw all aspects of this chapter.

Statement of parts of the thesis submitted to qualify for the award of another degree

None

Acknowledgements

I would like to express my gratitude to Iraqi government/Ministry of Higher Education for their financial support during my study and for giving me the opportunity to study in Australia.

I would like to sincerely thank my principal supervisor, Dr. Jeffrey E. Grice who is an example of a hugely talented, innovative and dedicated researcher and a kind and determined person, his academic skills and positive energy have led me through all doubts and hardships.

My foremost thanks are directed to Professor Michael S. Roberts who, with his expertise and support, was always available to help me develop my knowledge of research strategies and provide encouragement leading to completion of this thesis.

I have greatly benefited from Dr. Gregory Medley's technical assistance and expertise in the validation of analytical assays.

I am also particularly grateful for the imaging assistance by Dr. Washington Sanchez Jnr.

My sincere thanks also go to my friends in the College of Health and Medical Technology, Baghdad, Iraq and my colleagues from the Therapeutic Research centre for their personal support.

Most importantly, I would like to express my huge gratitude to my parents especially my Dad without whom I would not be where I am now, and my life partner Haithm and my children who were always supportive and patient and encouraged me through all difficulties and challenges.

Keywords

Penetration enhancers, stratum corneum, solubility in vehicles, oleic acid, eucalyptol, transfollicular, microemulsions, vesicle systems, maximum flux, diffusivity.

Australian and New Zealand Standard Research Classifications (ANZSRC)

ANZSRC code: 110304 Dermatology, 20%

ANZSRC code: 111504 Pharmaceutical Science, 80%

Fields of Research (FoR) Classification

FoR code: 1115 Pharmacology and Pharmaceutical Sciences, 100%

Table of Contents

Chapter		Page
Chapter 1	Literature Review	1
	Enhanced skin delivery of topically applied drugs: A review	
1.1	Abstract	1
1.2	Introduction	1
1.3	Skin structure	2
1.3.1	Epidermis	2
1.3.1.1	Stratum basale	3
1.3.1.2	Stratum spinosum	3
1.3.1.3	Stratum granulosum	4
1.3.1.4	Stratum corneum	4
1.3.2	Dermis	5
1.3.3	Subcutaneous	5
1.3.4	Derivative structures of the skin (Appendages)	6
1.3.4.1	Hair	6
1.3.4.2	Sebaceous glands	6
1.3.4.3	Sweat glands	6
1.4	Barrier function	7
1.5	Routes of drug delivery via human skin	8
1.5.1	Cutaneous delivery	9
1.5.1.1	Advantages of cutaneous delivery	9
1.5.1.2	Limitations of using cutaneous delivery	10
1.5.1.3	Factors responsible for releasing a drug from a cutaneous system	10
1.5.2	Appendageal Drug Delivery'	12
1.6	Skin penetration enhancement	14
1.6.1	Chemical enhancers	14
1.6.2	Natural Enhancers	18
1.6.2.2	Terpenes	18
1.6.2.3	Fixed oils/ Fatty acids	18
1.6.3	Adverse effects of chemical and natural enhancers in skin	19
1.6.4	Other methods of enhancing skin penetration	19
1.6.4.1	Water as penetration enhancers (Effect of hydration)	19
1.6.4.2	Supersaturation	20

1.6.4.3	Physical enhancement	21
1.6.4.4	Vesicular system enhancement	21
1.7	Selection of drug models with optimal physiochemical properties for skin penetration	22
1.7.1	Molecular weight and shape	22
1.7.2	Lipophilicity	23
1.7.3	Hydrogen Bonding	23
1.8	Assessment of skin penetration	24
1.8.1	Maximum Flux (J_{max})	24
1.8.2	Drug-vehicle-skin interactions	24
1.8.3	Animal skin vs. human skin	25
1.8.4	Skin integrity	25
1.8.5	Solubility parameters	25
1.9	Colloidal delivery system	26
Chapter 2	Aims and Hypotheses	30
Chapter 3	Effect of Penetration Enhancers; Solution Studies	33
3.1	Abstract	33
3.2	Introduction	34
3.2.1	The solubility parameters concept	36
3.3.	Materials and methods	38
3.3.1	Chemicals	38
3.3.2	Sample analysis	38
3.3.3	Determination of Solubility in the vehicles (S_V)	39
3.3.4	Human skin preparation	39
3.3.5	Determination of Solubility in the stratum corneum (S_{sc})	39
3.3.6	Solvent uptake in the stratum corneum	40
3.3.7	<i>In vitro</i> permeation study	40
3.3.8	<i>In vitro</i> pretreatment permeation study	40
3.3.9	Prediction of maximum flux	41
3.3.10	Data analysis	41
3.4	Results	44
3.4.1	<i>In vitro</i> permeation of solutes across epidermal membranes	44

3.4.2	Impact of formulation on active solubility in the stratum corneum, maximum flux and derived diffusivity	48
3.4.3	Mechanism underpinning the differential enhanced uptake of actives into the epidermis	52
3.4.4	Can the permeation fluxes of actives from various vehicles be predicted by a solubility parameter approach?	56
3.4.5	Caffeine vehicle solubility	57
3.4.6	Penetration and solubility data	57
3.5	Discussion	63
3.6	Conclusions	67
Chapter 4	Synergistic skin penetration enhancer and nanoemulsion formulations promote the human epidermal permeation of caffeine and naproxen	68
4.1	Abstract	68
4.2	Introduction	69
4.3.	Materials and Methods	71
4.3.1	Preparation of Emulsions	71
4.3.2	Characterisation of emulsions	72
4.3.3	Human skin preparation	72
4.3.4	Determination of the solubility of actives in the various formulations (S_v)	73
4.3.5	Determination of solubility in the stratum corneum (S_{sc}) and solvent uptake	73
4.3.6	<i>In vitro</i> skin penetration and distribution study	73
4.3.7	Multiphoton microscopy (MPM)	74
4.3.8	HPLC analysis of caffeine and naproxen	75
4.3.9	Data analysis	75
4.3.10	Statistics	76
4.4	Results	78
4.4.1	Physical and chemical characterisation of the formulations used	78
4.4.2	<i>In vitro</i> permeation of caffeine and naproxen across epidermal membranes	79

4.4.3	Impact of formulation on active solubility in formulation, solubility in stratum corneum, maximum flux and derived diffusivity	79
4.4.4	Mechanism underpinning the differential enhanced uptake of caffeine and naproxen into the epidermis	82
4.4.5	<i>In vitro</i> permeation of caffeine and naproxen across full-thickness human skin	84
4.4.6	Multiphoton microscopy of full-thickness human skin after exposure to nanoemulsion formulations	89
4.5	Discussion	90
4.6	Conclusions	94
Chapter 5	Appendageal delivery	95
	A. Potentials of nanoemulsion formulations into delivering Minoxidil through skin appendages, stratum corneum and permeation through human skin	
	B. Investigation of the effects of nanoemulsion containing penetration enhancers on follicular penetration of hydrophilic model compound caffeine	
5.1	Abstract	95
5.2	Introduction	96
5.3.	Materials and Methods	98
5.3.1	Chemicals	98
5.3.2	Nanoemulsion formulation preparation and Characterisation	98
5.3.3	Determination of S_V and in the S_{SC}	99
5.3.4	Solvent uptake in the stratum corneum	100
5.3.5	Open hair follicles technique	100
5.3.6	Blocked hair follicles technique	100
5.3.7	<i>In vitro</i> skin penetration study	101
5.3.8	Samples analysis	102
5.3.9	Visualisation of follicles and follicular delivery	103
5.3.10	Data analysis	103
5.3.11	Statistics	104
5.4	Results	105
5.4.1	Cumulative amount of minoxidil in the receptor after 24h	105

5.4.2	Amount of minoxidil in the stratum corneum and hair follicles	106
5.4.3	Amount of minoxidil retained in the skin layers (viable epidermis and dermis) after 24h	107
5.4.4	J_{max} estimated, solubility in the stratum corneum S_{SC} and diffusivity (D^*) and S_V	107
5.4.5	Minoxidil solubility in the vehicles	108
5.4.6	Solubility in the stratum corneum and solvent uptake	108
5.4.7	Cumulative amount of caffeine in the receptor after 24h	109
5.4.8	Amount of caffeine in the stratum corneum and in the hair follicles	113
5.4.9	Amount of caffeine retained in the skin layers (viable epidermis and dermis) after 24h	114
5.4.10	Multiphoton microscopy imaging to evaluate follicular blocking technique and assess the penetration of model fluorescent dye (Acridine)	117
5.5	Discussion	117
5.6	Conclusion	122
Chapter 6	A comparison of the penetration and permeation of caffeine into and through human epidermis after application of various vesicle formulations	123
6.1	Abstract	123
6.2	Introduction	123
6.3	Materials and methods	125
6.3.1	Materials	125
6.3.2	Vesicle preparation	125
6.3.3	Vesicle characterisation	125
6.3.4	Caffeine encapsulation efficiency	125
6.3.5	Caffeine skin permeation studies	126
6.3.6	Sample analysis	126
6.3.7	Data analysis and Statistics	127
6.4	Results	127
6.4.1	Vesicle characterisation	127
6.4.2	Permeation of caffeine from vesicles and control	127
6.5	Discussion	128

6.6	Conclusion	133
Chapter 7	Conclusion and Future recommendation	134
7.1	Conclusion	134
7.1.1	Effect of Penetration Enhancers; Solution Studies	134
7.1.2	Synergistic skin penetration enhancer and nanoemulsion formulations promote the human	135
7.1.3	Appendageal delivery	136
7.1.4	A comparison of the penetration and permeation of caffeine into and through human epidermis after application in various vesicle formulations	136
7.2	Future Direction	137
List of References		138
Appendix		150

List of Figures

Chapter 1	Page
Figure 1.1	3
Figure 1.2	9
Figure 1.3	11
Figure 1.4	13
Figure 1.5	14
Figure 1.6	23
 Chapter 3	
Figure 3.1	37
Figure 3.2	45
Figure 3.3	49
Figure 3.4	50
Figure 3.5	52

Figure 3.6	Solubility in the stratum corneum (S_{SC}) versus predicted solvent uptake values from range of vehicles for A, Caffeine; B, Minoxidil; C, Lidocaine; D, Naproxen.	53
Figure 3.7	Solubility in the stratum corneum (S_{SC}) versus predicted solute uptake values from range of vehicles for A, Caffeine; B, Minoxidil; C, Lidocaine; D, Naproxen	54
Figure 3.8	Predicted versus experimental solubility in the stratum corneum (S_{SC}) from a range of vehicles for A, Caffeine; B, Minoxidil; C, Lidocaine; D, Naproxen; E, the combined dataset (Mean, n=4).	55
Figure 3.9	Log J_{max} (predicted using Hansen solubility parameters by method of Abbott) vs log J_{max} (observed) for caffeine (triangles), minoxidil (circles), lidocaine (diamonds) and naproxen (squares) applied to human epidermal membranes in different vehicles.	56
Figure 3.10	Relationship between experimentally determined caffeine solubility in each solvent (S_v) and solvent solubility parameter (δ_{total}). (The dashed line is the total solubility parameter area for caffeine)	57
Figure 3.11	Permeation profiles of caffeine through epidermal human skin after pre-treating skin for 2h with a range of t vehicles	58
Figure 3.12	Mean plot summarising the effect of Hansen solubility parameter of vehicle on enhancement of J_{max} , partition and diffusion	60
Figure 3.13	Composite of the effects of vehicle pretreatment on diffusion and partition of caffeine. (The red line is the identity line)	61
Figure 3.14	Relationship between (A) J_{max} and S_{SC} and (B) caffeine permeability coefficient (K_P) and S_{SC} .	62
 Chapter 4		
Figure 4.1	Ternary phase diagram of the oil, surfactant/co-surfactant mixture and water at ambient temperature. The dotted line in the diagram represents the nanoemulsion.	78

Figure 4.2	<i>In vitro</i> percutaneous permeation through epidermal human skin A-caffeine; B-naproxen	79
Figure 4.3	Estimated maximum fluxes for caffeine and naproxen for each of the formulations plotted against the solubility of these actives in the formulations	80
Figure 4.4	Impact of stratum corneum solubility and apparent diffusivity D^* on the maximum flux J_{max} for caffeine and naproxen. 4A. J_{max} versus stratum corneum; 4B J_{max} versus D^* .	82
Figure 4.5	Stratum corneum solubility predicted from solvent uptake for caffeine (A) and Naproxen (B). (Lin's concordance correlation coefficient of caffeine is 0.58 and naproxen is 0.93)	83
Figure 4.6	Solute solubility in vehicle and formulation uptake into stratum corneum as a function of their estimated HSP distance (R_a). A. Vehicle solubility (S_V) for caffeine (circles) and naproxen (triangles) versus the R_a between the nanoemulsion formulations and controls; B: Formulation uptake into the stratum corneum (diamonds) versus the R_a between the nanoemulsion formulations and the skin	84
Figure 4.7	<i>In vitro</i> percutaneous permeation through Full-thickness human skin A-caffeine; B-naproxen	85
Figure 4.8	A -Caffeine; B -naproxen retained in the stratum corneum and skin from nanoemulsion formulations and controls after 8h permeation from full-thickness human skin	87
Figure 4.9	structural and viability study of excised skin following the topical application of nanoemulsion formulations- explain blue and yellow fluorescence	89
 Chapter 5		
Figure 5.1	permeation profiles of minoxidil through excised human skin from nanoemulsions and control	105
Figure 5.2	Minoxidil retained in stratum corneum, hair follicles and skin layers	106
Figure 5.3	Minoxidil A - J_{max} values from all formulations versus solubility in the stratum corneum (S_{SC}) ($R^2=0.84$); B- J_{max} values from all	108

formulations versus Diffusivity (D^*) ($R^2 = 0.90$); C- Diffusivity (D^*) versus S_p ; D- S_{SC} versus S_V

Figure 5.4	S_{SC} (predicted) versus S_{SC} (measured)	109
Figure 5.5	Permeation profiles of caffeine through A- normal excised human skin; B- Excised human skin (after opening the hair follicles); C- Excised human skin (after plugging the hair follicles) from nanoemulsion formulations & controls	112
Figure 5.6	Permeation profiles of caffeine through Excised human skin A- Contribution to permeation by all the hair follicles B- Contribution to permeation by the open hair follicles from nanoemulsion formulations & controls	113
Figure 5.7	Caffeine retained in the Stratum corneum (SC) from ME formulations & controls after	115
Figure 5.8	Caffeine retained in the hair follicles after topical administration of nanoemulsion formulations & controls up to 24h	115
Figure 5.9	Caffeine retained in the viable epidermis and dermis from nanoemulsion formulations & controls after 24h	116
Figure 5.10	Skin images after applying nanoemulsion formulations and controls	121
 Chapter 6		
Figure 6.1	Permeation profiles of caffeine through excised human skin from various vesicle systems and a control	132
Figure 6.2	Caffeine recovery from the skin surface, the stratum corneum, hair follicles, residual skin and receptor solution after application of vesicles and control for 24h	133

List of Tables

Tables	Page
Chapter 1	
Table 1.1	Immune components of the skin 8
Table 1.2	Common chemical penetration enhancers (CPEs); mechanisms, safety and side effects and their features 16
Table 1.3	Nano delivery systems 27
 Chapter 3	
Table 3.1	Physicochemical properties of model compounds 38
Table 3.2	Composition of vehicles used. Concentrations (w/v) of caffeine, minoxidil, lidocaine and naproxen were ^a 3%, ^b 2%, ^c 2.5%, ^d 2%, respectively, except those marked by *, where the solutions are saturated. Vehicles containing ethanol are shaded, with those also containing penetration enhancers in darker shading. 43
Table 3.3	<i>In vitro</i> percutaneous permeation through epidermal human skin A1- caffeine with penetration enhancer vehicles, A2- caffeine with controls; B1-minoxidil with penetration enhancer vehicles, B2- minoxidil with controls; C1- lidocaine with penetration enhancer vehicles, C2- lidocaine with controls & D1- naproxen with penetration enhancer vehicles, D2- naproxen with controls 46
Table 3.4	Vehicle solubility parameters and skin parameters 59
 Chapter 4	
Table 4.1	Compositions (% w/w) of nanoemulsion formulations (C3 and C4), with penetration enhancers eucalyptol (E1 and E2) and oleic acid (O1 and O2), and control mixtures (C1 – C2). The concentration of caffeine (marked as ^c) dissolved in aqueous controls and nanoemulsions was 3% w/w, whereas a concentration of 2% w/w was used for naproxen (marked as ^N). 72

Table 4.2	Physical and chemical characterisation of the various nanoemulsion formulations and control mixtures defined in Table 1.	77
Table 4.3	Experimental data for caffeine and naproxen in different nanoemulsions without and with penetration enhancers and control vehicles. The formulations are defined in Table 1 and are nanoemulsion formulations (C3 and C4), with penetration enhancers eucalyptol (E1 and E2) and oleic acid (O1 and O2), and control mixtures (C1 – C2).	81
Table 4.4	Caffeine and naproxen permeation parameters from different vehicles though full-thickness skin C1 is 100% water, C2 is 60% ethanol/water, C3 is 25% PEG6000/water, C4 is 25% Volpo-N10 25%ethanol/50%water E nanoemulsions containing eucalyptol as oil phase, O nanoemulsions containing Oleic Acid as oil phase	86
Table 4.5	Estimated lag times and steady state flux for caffeine and naproxen from epidermal membrane and full-thickness skin.	88
 Chapter 5		
Table 5.1	Compositions and solubilities of minoxidil in selected nanoemulsion formulations (%w/w)	99
Table 5.2	Compositions of selected nanoemulsion formulations and controls (%w/w)	99
Table 5.3	Transdermal permeation parameters and pH of the minoxidil from formulations and control	106
Table 5.4	The cumulative amounts ($\mu\text{g}/\text{cm}^2$), fluxes ($\mu\text{g}/\text{cm}^2/\text{h}$) and follicular penetration ($\mu\text{g}/\text{one hair follicle}$) by follicular closing technique and open hair follicle technique using Franz diffusion cells at 24h from ME formulations and controls.	111

Table 5.5	Amount of caffeine ($\mu\text{g}/\text{cm}^2$) in different skin compartments for controls and nanoemulsion formulations.	114
-----------	---	-----

Chapter 6

Table 6.1	Liposome formulations showing excipient ratios and aqueous control composition. All formulations contained caffeine, 2% w/v.	131
Table 6.2	Vesicle systems characterisation and encapsulation efficiency.	131
Table 6.3	Permeation parameters following 24 hours application of caffeine from vesicle formulations and controls to full-thickness human skin).	132

List of Abbreviations

C_v	Initial concentration
D^*	Diffusivity
DLS	Dynamic light scattering
DPGluc	decyl polyglucoside
E	Enhancement ratio
EU	Eucalyptol
FDC	Franz diffusion cell
FTS	Full Thickness Skin
HLB	Hydrophilic lipophilic balance
HPLC	High performance liquid chromatography
J_{max}	Maximum flux
J_{ss}	Steady state flux
K_p	Permeability coefficient
K_{sc}	Partitioning coefficient
Log P	Lipophilicity
ME	Microemulsion
mg	Milligram
min	minute
mL	Milliliter
MPM	Multiphoton microscope
MW	Molecular weight
OA	Oleic acid

O/W	Oil in water
PBS	Phosphate buffer saline
PEG6000	Polyethylene glycol 6000
PDI	Polydispersity Index
Q	Cumulative amount
RI	Refractive index
SC	Stratum corneum
SD	Standard deviation
SE	Standard error
SEM	Standard error of the mean
S _F	Solubility in formulation
SLS	Sodium lauryl sulphate
S _{SC}	Solubility in the stratum corneum
S _V	Solubility in vehicle
T	Transferosomes
δ_{total}	Total solubility parameters
W/O	Water in oil microemulsion

Chapter 1

Literature Review

Enhanced skin delivery of topically applied drugs: A review

1.1 Abstract

There is substantial interest in the skin as a route of drug delivery for local or systemic effects. However, the stratum corneum forms a formidable barrier to solute penetration, limiting topical and transdermal bioavailability. Many techniques have been used to enhance the permeability of drugs and increase the penetration of drugs that are used for topical delivery. This review describes the skin structure and the various techniques that have been used to enhance drug delivery across human skin.

1.2 Introduction

The skin is the largest organ of the body; it forms a protective layer over the underlying tissues such as ligaments, muscles and internal organs, preventing exposure to exogenous particles and mechanical and radiation-induced injuries. In addition, the skin plays a role in immunity and metabolism, controls body temperature and comprises sensory nerve endings for the perception of temperature, touch, pressure and pain. Skin is made up of viable and non-viable epidermis, dermis and hypodermis (subcutaneous) layers.

Topical application of drugs has been investigated as an alternative to intravenous or parenteral routes, but transdermal delivery is frequently limited by poor drug penetrability. This low permeability can be mostly attributed to the outer layer of the skin, the stratum corneum, which serves as a rate-limiting lipophilic barrier to the uptake of exogenous chemical and biological substances and to the loss of water. This means that some drugs need penetration enhancers included in formulations to enable efficient delivery of therapeutic agents. Penetration enhancers are chemicals that reversibly reduce the barrier function of the stratum corneum, to facilitate drug delivery to and through the tissue. Ideally, they should be odourless, colourless, pharmacologically inert and chemically and physically stable.

After extensive research, the success of this technique remains limited, with many issues still to be solved. Recently, advanced formulations such as liposomes and nanoemulsions have also been used to help drugs penetrate the skin. This review describes the skin structure; routes of penetration, how drug properties affect permeation, permeation enhancement techniques and advanced formulations.

1.3 Skin structure:

The skin is the outer layer and largest organ in the body, accounting for about 16% of body weight with surface area of approximately 1.8 m² in adults (1). The skin plays an essential role for the survival of the human body in a relatively hostile environment. The most vital role is providing a physical barrier to the environment, it maintains homeostasis by limiting the loss of water, electrolytes and heat and protects against micro-organisms, toxic agents and ultraviolet radiation (2). It consists of three basic layers: the epidermis, the dermis and the subcutaneous layer. Hair, nails, sebaceous, sweat and apocrine glands are considered as skin derivatives or appendages. Even though it is structurally continuous throughout the body, skin varies in thickness according to the age of the individual and the anatomical site (3).

1.3.1 Epidermis

The epidermal layer is formed from squamous epithelium. Keratinocytes are the main cells of the epidermis that can produce the keratin protein. Protein bridges named desmosomes attach the keratinocytes and are in a constant state of moving from the deeper layers to the superficial. The separate layers of the epidermis are defined by the degree of keratinisation. The layers of the epidermis from bottom layers to the surface are the stratum basale (basal cell layer), the stratum spinosum (spinous or prickle cell layer), the stratum granulosum (granular cell layer) and the stratum corneum (horny layer) (4), (see Fig1.1). Both the stratum spinosum and stratum granulosum are occasionally mentioned as the Malpighian layer (1, 5)

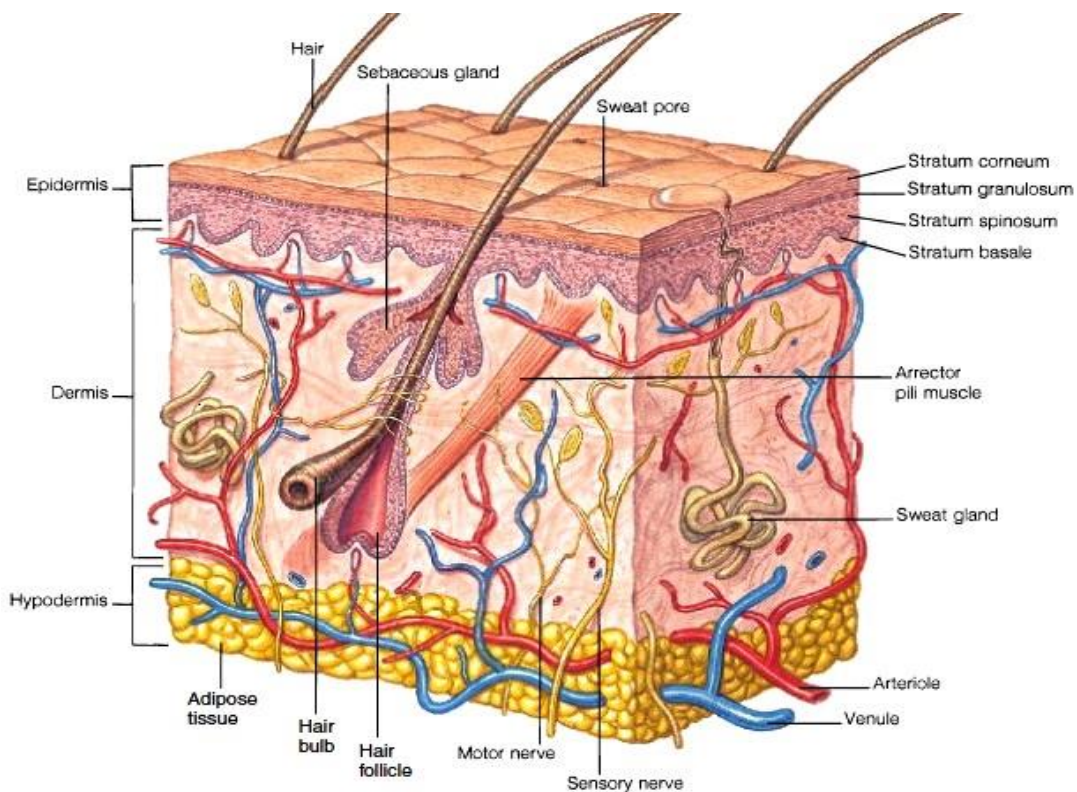


Fig1.1 Structure and Function of the Skin blog.mediligence.com

1.3.1.1 Stratum basale

The deepest layer of the epidermis which lies next to the dermis contains columnar or cuboidal cells, that are connected to the basement membrane by hemi-desmosomes (3). The nuclei of these cells is large and occupies most of the cell (3). These cells are functionally heterogeneous and can work as stem cells that divide and proliferate to remain attached to the basement membrane (6). These cells reproduce continuously by mitosis to produce daughter cells that keep the epidermis replenished. In normal human skin, the turnover and replacement of these cells takes around 30 days depending on age, area of the body and disease states (3). Keratinocytes are the predominant cells in the basal layer. The main function of keratinocytes is forming a barrier against environmental damage caused by heat, pathogenic bacteria, UV radiation and water loss. The cornified keratinocytes that form the outermost layer are constantly shed and replaced by new cells (7).

1.3.1.2 Stratum spinosum

As a result of replication and maturation of basal cells, they transfer to the outer layer of skin, firstly forming the stratum spinosum which is connected by intercellular bridges and the desmosomes (8, 9). Langerhans cells are dendritic (immune cells) of skin. They are found

throughout the epidermis but are mostly prominent in the middle of this layer. In case of skin infection, the Langerhans cells engage in and process microbial antigens to be fully functional antigen-presenting cells (10-12).

1.3.1.3 Stratum granulosum

During their migration to the surface, the cells progressively collapse and lose their nuclei and cytoplasm, so that they seem granular at this level(1). A typical feature of this layer is the presence small lamellar granules known as lamellated bodies or membrane coated granules (3). These granules are smaller than mitochondria and differ in size according to variation in species from 0.1-0.5 μm (9) or from 0.3-0.7 μm (8).

1.3.1.4 Stratum corneum

The stratum corneum results from the migration of cells from the basal layer to the skin surface by the process known as keratinisation. The final result of keratinocyte maturation is the stratum corneum, which is formed from hexagonal-shaped layers, non-viable cornified cells named corneocytes. In most skin sites, there are 10-25 layers of stacked corneocytes which are non-hydrated cells lying parallel to the skin surface (2). Every cell is enclosed by a protein envelope and filled with water-retaining keratin proteins. The form and location of the keratin proteins give strength to the stratum corneum. The thickness varies according to the physical interaction and environment, as for example, these cells are thicker on palms of the hands and soles of the feet. Moreover, the absorption of solutes through these areas is slower than other parts of the body(13). Each stratum corneum cell contains keratin (~70%) and lipid (~20%). The region between cells consists of lipid and desmosomes for corneocyte cohesion. The stratum corneum acts as a barrier to prevent the loss of internal body components such as water. The layer of corneocytes can absorb three times its mass in water if its water content falls below 10% but it no longer remains flexible and cracks. The epidermal cells take 2-3 weeks to transfer to this layer (13).

Epidermal stem cells are responsible for everyday regeneration of the different layers of the epidermis. These stem cells are found in the basal layer of the epidermis. The main functions of epidermal cells are:

- Melanocyte cells are responsible for regeneration of melanocytes, a type of pigment cell. Melanocytes produce the pigment melanin, and therefore play an important role in skin and hair follicle pigmentation. It is not yet certain where these stem cells are found in humans

- Keratinic cells play an essential role in serving to anchor the epidermis to the Basal membrane (6, 13).
- Langerhans cells have important roles in the skin's immune system. (6, 13)

Desquamation of skin cells

Desquamation is an important factor in maintaining skin integrity and smoothness of the stratum corneum. It is the process of cell shedding from the surface of the stratum corneum, and balances proliferating keratinocytes that form in the stratum basale. These cells migrate through the epidermis towards the surface in a journey that takes approximately fourteen days. The keratinocytes are denucleated during the process and corneodesmosomes are broken down to allow the cells to be shed (3).

1.3.2 Dermis

The dermis differs in thickness, from almost 0.1 -0.5 cm. It is located underneath the epidermis and is composed of a firm, supportive cell matrix. The dermis contains two layers: thin papillary layer and thicker reticular layer (1, 13). The papillary dermis lies under and connects to the epidermis. It comprises thin, free organised collagen fibres. The thicker collagen bundles are equivalent to the surface of the skin in the deeper reticular layer, and spread from the base of the papillary layer to the subcutaneous tissue. The dermis consists of fibroblasts, which create collagen, elastin and structural proteoglycans, both with immune capable mast cells and macrophages. Collagen fibres form more than 70% of the dermis, providing strength and hardness and elastin gives elasticity and flexibility whereas proteoglycans provide viscosity and hydration. The dermal vasculature, lymphatics, nervous cells and fibres are embedded in the fibrous tissue of the dermis in addition to the sweat glands, small numbers of striated muscles and hair roots. The dermis has an extensive vascular network, hair follicles, and sweat glands. Therefore, the major function of the dermis is providing nutrition and immune response to the skin. It also plays an important role in regulating the temperature, pressure and pain. Moreover, the papillary layer in the dermis provides a support system for the epidermis (1, 13).

1.3.3 Subcutaneous

The subcutaneous (hypodermis) layer is the deepest layer of the skin, and is formed from loose connective tissue and fat (50% of the body fat), which may be more than 3 cm thick on the abdomen. Its function is absorption of shock and as storage for energy in addition to its work as a heat insulator as it carries the vascular and neural systems for the skin. The

hypodermis layer is linked to the dermis by interconnecting collagen and elastin fibres in a loose arrangement, allowing flexibility and free movement of the skin over the underlying structure (3). The main cells in this layer are fibroblasts and macrophages. (1, 13).

1.3.4 Derivative structures of the skin (Appendages)

1.3.4.1 Hair

Hair is found in varying thickness over most of the body surface, with a few exceptions including the soles of the feet, palms of the hands, lips and some other areas. Every hair follicle is surrounded by germinative cells, which provide keratin and melanocytes and produce pigment. The free part of the hair above the skin surface is called the hair shaft and the part within the follicle is called the hair root, with a terminal hollow knob called the hair bulb (3). The hair shaft contains an outer cuticle, a cortex of keratinocytes and an inner medulla (1, 3) and is accompanied by arrector pili muscle that contracts the hair shaft in case of fear, emotion and cold, giving the skin “goose bumps” (1). The hair density is different in various body sites; on the forehead the hair follicles are small but high in density, while on the calf area, the density is low but the follicles are larger (14, 15).

1.3.4.2 Sebaceous glands

The sebaceous glands are derived from epidermal cells and accompany hair follicles, particularly those of the scalp, face, chest and back. These cells are not found in hairless areas. Sebaceous glands are small in children, growing and becoming active during adolescence. An oily sebum is produced from these glands by holocrine secretion, consisting of triglyceride, free fatty acids and waxes. The sebum function is to protect and lubricate the skin as well as maintain the skin pH at around 5 (13). Other functions of sebum are maintaining the epidermal permeability barrier, carrying antioxidants to the skin surface, and also regulating steroidogenesis and androgen (3, 16)

1.3.4.3 Sweat glands

Sweat glands are believed to number more than 2.5 million on the human skin surface. They are classified into apocrine and eccrine sweat glands depending on their function and shape. The apocrine gland is bigger and has ducts which empty into the hair follicles. It is found throughout the skin in most domestic animals but in humans it occurs in restricted areas only (axillae, areola and nipples, external ear canal, eyelids, inner nostrils, perianal region, and some parts of the external genitalia). The eccrine gland is the dominant form in humans and is distributed in most other areas of the body (4). Eccrine glands open directly onto the skin surface. The eccrine glands excrete watery fluid containing lactic acid, chloride, fatty

acids, urea, mucopolysaccharides and glycoproteins and are necessary for fluid and electrolytes homeostasis. Also, they secrete a dilute salt solution in case of high environmental temperature and emotional stress. Apocrine glands become active in adolescence, producing an odourless protein-rich secretion which when acted upon by skin bacteria emits a characteristic odour (1, 3).

1.4 Barrier function

stratum corneum, the result of epidermal terminal differentiation, is an important mediator of defensive function of the skin (17) and a biosensor which recognises and responds to changes in external humidity and pH. Thermoregulation is achieved by keeping a constant body temperature through alterations in blood flow in the cutaneous vascular system and sweat evaporation from the surface. UV protection is provided by the melanocytes, in the basal layer, producing melanin which absorbs UV radiation and protect the cell nuclei from DNA damage (18) .(1). Melanin particles in the epidermal inner layers form defensive shields over the keratinocyte nuclei in the outer layers, and are more regularly distributed. As well as acting as a physical barrier, skin also has an essential immunological role. It incorporates all the elements of cellular immunity, with the exception of B cells. Immune components of the skin are given in Table 1.1 (19). The skin is also working as a barrier by controlling the loss of water, electrolytes and other body components, in addition to inhibiting the entry of harmful and unwanted molecules from the external environment. This function may be attributed to the unique structure of the stratum corneum, which consists of multiple layers of nucleate, proteinaceous corneocytes embedded in an expanded, extracellular matrix of enriched lipid forming a model similar to “bricks and mortar”(20). The function of corneocytes is mechanical friction resistance which is attributed to the rigid , highly cross-linked cornified envelope (21).

Table 1.1 Immune components of the skin (19)

Defence type	Component	Immune action
Structure	Skin	Impenetrable physical barrier to most external organisms
	Blood and Lymphatic vessels	Provision of transport network for cellular defence
Cellular	Langerhans cells	Antigen presentation
	T lymphocytes	Facilitate immune reactions. Self-regulating through the action of T suppressor cells.
	Mast cells	Facilitate inflammatory skin reactions.
	Keratinocytes	Secrete inflammatory cytokines; have ability to express surface immune
Systemic molecules	Cytokines and Eicosanoids	Cytokines: cell mediation chemicals produced by components of the cellular defence system
		Eicosanoids: non-specific inflammatory Mediators produced by mast cells, Macrophages and keratinocytes. Increase the number of cellular defence facilitators in an area by binding to T cells.
	Adhesion molecules Cascade	Complement Activation of this initiates a host of destructive mechanisms, including opsonisation, lysis, chemotaxis and mast cell degranulation.
Immunogenic antigens	Major	Enables immunological recognition of Major Histocompatibility Complex (MHC)

1.5 Routes of drug delivery via human skin

When designing a topical delivery system, it is important to understand the possible penetration pathways. Drug molecules, in contact with skin, penetrate by three potential routes: directly through the stratum corneum (intercellular and transcellular) (Fig 1.2), via the sweat ducts, and through the hair follicles and sebaceous glands (the shunt or appendageal route) (Fig 1.2). The importance of the appendageal route versus transport through the stratum corneum has been debated by researchers for many years (22, 23) as its determination is complicated by the absence of suitable experimental models to allow separation of these three routes. The pilosebaceous pathway penetrating through hair

follicles may be portal for penetration of large polar molecules which have difficulty diffusing through the stratum corneum.

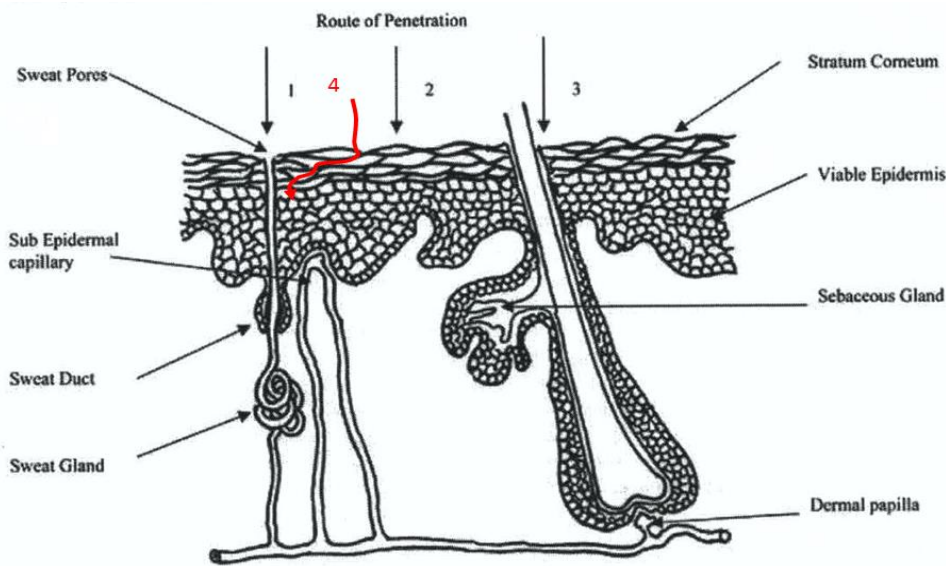


Fig 1.2 Main routes of penetration: 1. through the sweat gland; 2. directly across the stratum corneum (transcellular); 3. via the hair follicles; 4. Intercellular (modified from (24)).

1.5.1 Cutaneous delivery

Designing drug delivery systems has become a major focus of activity in the pharmaceutical industry and transdermal administration is one of the important delivery routes currently under consideration. The stratum corneum is very selective with respect to what it permits to be transported through the skin; consequently, only penetrants with particular physicochemical properties in a narrow range can pass through the skin adequately under passive conditions. This causes the variety of potential drugs that can be administered topically to be limited, which highlights the value of incorporating permeation enhancers into formulations to help in the active delivery of a larger diversity of drugs (25). The aim is to deliver active substances to targeted sites through the skin at an acceptable rate to produce the desired pharmacological effect.(26).

1.5.1.1 Advantages of cutaneous delivery

Cutaneous administration has numerous advantages and can be summarised as follows:

1. This route of administration means that the hepatic first pass metabolism and the gastrointestinal tract metabolism are avoided (27)
2. It offers an alternative pathway for patients who have oral dosing issues, such as in unconscious patients (28).
3. It is painless and convenient (29).

4. Cutaneous delivery can provide direct access to the diseased or target site such as for fungal skin disease or eczema (30).
5. It has fewer side effects related to systemic toxicity compared to other routes of administration (28, 31).
6. As the drug would normally be delivered by an external device, medication can be ceased at any point by the removal of the device. Of course, any substance that has already partitioned into the skin cannot be easily removed but only this substance can enter the body once the device is removed from the skin (26).

1.5.1.2 Limitations of using cutaneous delivery

The most obvious limitation for topical drug delivery is that the solute should be able to penetrate the skin. This means that the physicochemical properties of the drug play an important role in penetration, for example, the molecular weight should be less than 500 Da to diffuse through the stratum corneum (32), (33).

The skin is a multilaminate membrane and changes from a lipophilic material (the outer most stratum corneum) to a very aqueous internal structure (viable epidermis and dermis). Therefore, successful permeation of solutes requires molecules, which are soluble in the lipophilic environment of the stratum corneum and in the hydrophilic environment of the viable epidermis and dermis. A drug lipophilicity ($\log P$ (Octanol/Water)) should be between 1-3 in order to permeate through the variable epidermis and underlying layers successfully (34). These limitations apply only to passive delivery and the point of developing enhanced delivery systems is to circumvent the limitations.

1.5.1.3 Factors responsible for releasing a drug from a cutaneous system

The events which may occur after administration of formulation to the skin are shown in Figure 1.3. Studies of cutaneous drug delivery and transdermal absorption have demonstrated six events which are responsible for drug transfer from the system of transdermal application to the blood circulation(26):

1. Transport of drug from formulations to the stratum corneum.
2. Partitioning of drug from formulations into the stratum corneum.
3. Drug diffusion within the stratum corneum.
4. Partitioning of drug into the more aqueous epidermal tissues (Viable epidermis: VE).
5. Drug diffusion within the tissues of viable epidermis.
6. Drug absorption into the dermal and blood vessels.

Initially, the drug must be released from the vehicle followed by partitioning into the SC. Molecules will subsequently diffuse (as a result of a concentration gradient) through the SC before a further partitioning process into the viable epidermis, and further diffusion through the viable epidermis towards the dermis. Following uptake by the vasculature and lymphatic vessels in the dermis, the drug enters the systemic circulation to be distributed to tissues and organs and eventually cleared.(26, 35).

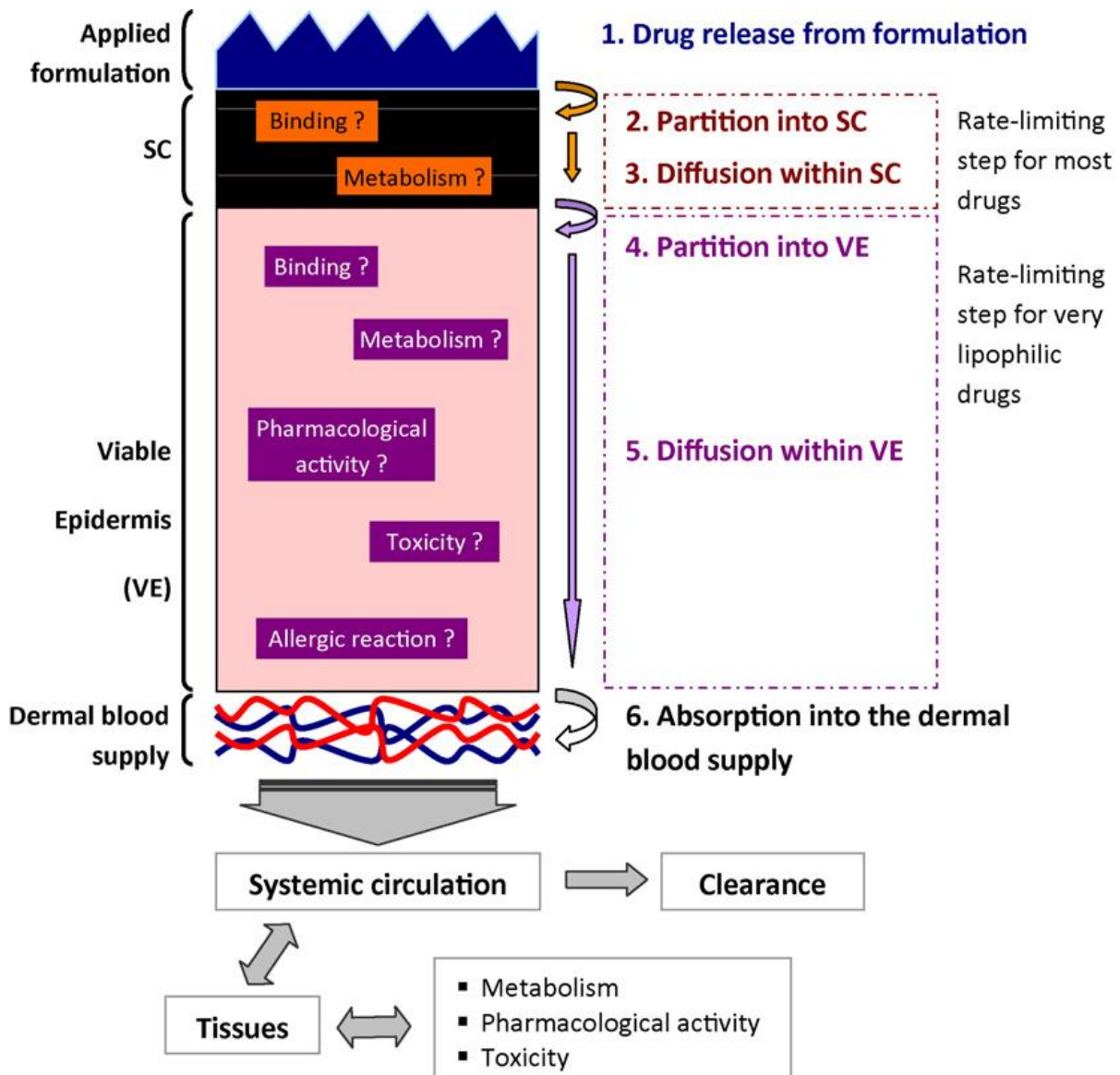


Fig 1.3 Diagrammatic representation of the drug transport into and through the skin from a topical applied formulation (36).

1.5.2 Appendageal Drug Delivery

The important role of hair follicles as penetration routes and reservoirs for topically applied substances has been validated in several animal models and in humans (37). The pilosebaceous unit describes the combined structure of the hair follicle, the adjoining arrector pili muscle and associated sebaceous gland (38), containing more than 20 various cell populations (39), which regulate different immunological, biochemical and metabolic activities.

Previously, layers of stratum corneum have been considered to be the main permeation pathway into and through the stratum corneum, while the skin appendages were supposed to play a secondary role by representing only 0.1% of the entire skin surface area (40). Further studies have concentrated on the hair follicle as a possible pathway for both systemic and localised drug delivery. Initial experiments on this idea were reviewed by Barry (41), and more contemporary methods involve fluorescence microscopy and confocal laser scanning microscopy applied to a variety of drugs in a range of vehicles. Therefore, a better understanding of the structure and function of the hair follicle may lead to more rational design of drug formulations to target follicular delivery (42). Efforts have been made to improve techniques that enhanced follicular penetration rates, in order to reach the maximum concentration of topically administration compounds in and around the hair follicle. A study by Lademann et al in 2003 suggested that large particles (e.g., 750, 1500nm) may be used to deposit high concentrations of drugs in the follicular duct, while small particles of about 40 nm especially in barrier disrupted skin, may be used to release active moieties to specific cell populations such as stem cells and multiple precursor cells (Fig1.4) (43), (44). Also for evaluation and quantification of the transfollicular process, a knowledge of variations of hair follicle parameters in various body sites is important. Different ways have been used to investigate the hair follicle as a potential follicular reservoir such as cyanoacrylate skin surface biopsy (15), (45). One aim of follicular targeting is to treat alopecia by growing new follicles bioengineered from the stem cells of patients (46).

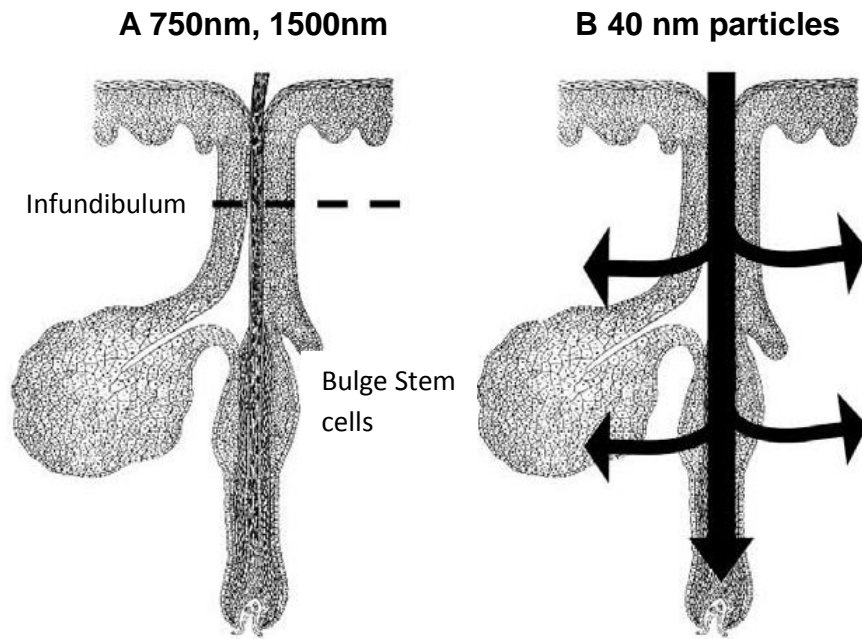


Fig 1.4 Penetration depths and capacity to penetrate the epithelium depend on the particle size (43)

1.6 Skin penetration enhancement

Substances which enhance drug diffusion through the stratum corneum and viable epidermis, are known as penetration enhancers, accelerants or promoters (47).

Extensive studies have focused on improving drug delivery through skin, by reducing the resistance of the stratum corneum to drug penetration (27). However, the main problem is in trying to improve the flux of drug through human skin. Therefore, it is essential to develop new methods or formulations that could remove the skin barrier resistance reversibly and accelerate the penetration of a drug. Numerous advances have included iontophoresis, sonophoresis, microneedle, chemicals and vesicular systems such as liposomes, transferosomes, neosomes etc. (48). Figure 1.5 shows the intercellular lipid domain of the stratum corneum as the main target of action for chemical penetration enhancers (49).

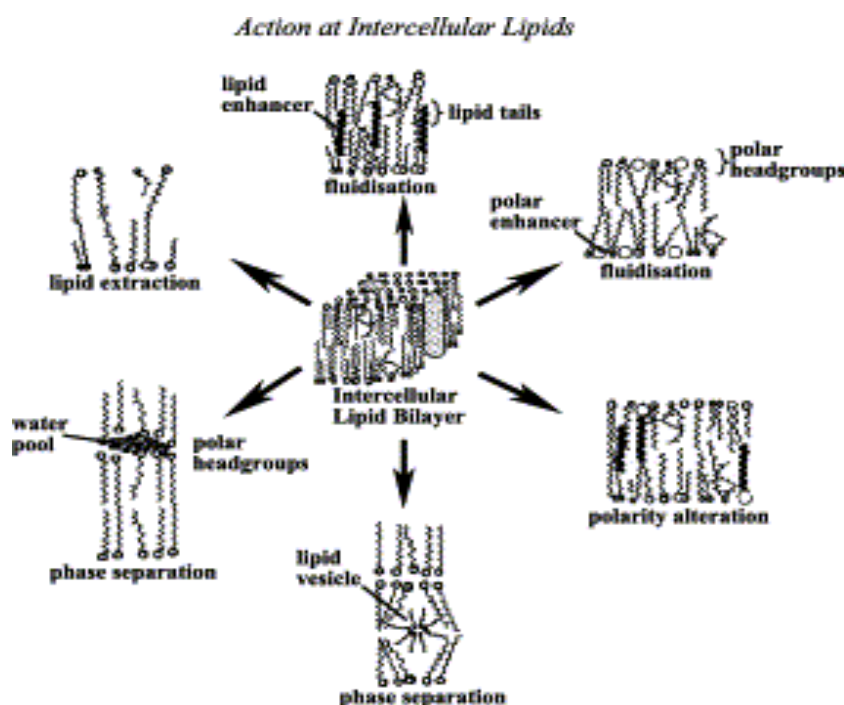


Fig.1.5 Actions of penetration enhancers within the intercellular lipid domain (49)

1.6.1 Chemical enhancers

The use of chemical penetration enhancers over other strategies has many benefits, including design flexibility with formulation chemistry. Chemical penetration enhancers should ideally be pharmacologically inert, nontoxic, non-irritant, non-allergic, odourless, tasteless, colourless, compatible with most drugs and excipients and inexpensive (49). Moreover, they should work rapidly and act unidirectionally. That is, they should allow therapeutic agents into the body while preventing the loss of endogenous material from the body. In addition, the barrier properties should return both rapidly and fully once the

enhancers are removed from the skin. Another prerequisite feature is that they should be cosmetically acceptable. A broad range of vehicles have been tested, such as alcohols and polyols (ethanol, propylene glycol); surfactants, fatty acids (oleic oil), lactams (azone), terpenes (limonene), sulfoxides (dimethyl sulfoxide) and esters (50).

Chemical enhancers work by different mechanisms:

A- Interaction with intracellular lipids. The enhancer disrupts the stratum corneum lipid organisation, making it permeable (51, 52), thereby increasing the drug diffusion coefficient. The enhancer substances jump into the bilayer, vibrating, translocating and increasing the free volume available for drug diffusion. Without accelerant, the free volume fraction is lowest (D lowest) near the bilayer interface. Many enhancers operate in this way such as azone, terpenes, fatty acid and so on. It was believed that such enhancers would penetrate into and mix homogeneously with the lipid. Nonetheless, oleic acid and terpenes pool within lipid domains at high loadings, permeable pores form, and polar molecules are allowed access to the viable epidermis (53).

B- Interaction with intracellular protein and denaturation of keratin (54). Ionic surfactant (sodium laurate sulphate (SLS)), and decylmethyl sulphoxide (DCMS) interact with keratin in corneocytes, opening up the dense protein structure and making it more permeable and consequently increasing diffusivity (51). Some molecules may also modify peptide/protein material in the bilayer domain.

C- Increasing partitioning and solubility in the stratum corneum. A large number of solvents entering the stratum corneum, change their solution properties by altering the chemical environment, and thus increase the partitioning and solubility of a molecule in the stratum corneum, for example, transcutol, ethanol and propylene glycol (24). In theory, nonsolvent enhancers that mainly act to raise drug diffusivity by lipid action mechanism, should also increase the partitioning coefficient of lipid drugs by disordering the lipid interfacial domain; they increase the free volume and make a large fraction of the bilayer available for solute partitioning (52).

Table 1.2 Common chemical penetration enhancers (CPEs); mechanisms, safety and side effects and their features (modified from (55))

Mechanism of action	Example of CPE	Safety and side effects	Features
Interaction with intracellular lipids and produce lipid disruption and fluidisation.	1-Fatty acids (FA), oleic acid (unsaturated) and Lauric acid (saturated)	-High concentration can cause skin redness and mild irritation.	-Disruption of the densely packed lipid that fill the extracellular spaces of stratum corneum and form ion pairs.
			-Increase drug solubility and partitioning.
			-Promote both lipophilic and hydrophilic drugs delivery at high concentration.
			-Previous study on hairless mouse and using hydrocortisone as a model has been found that unsaturated F.As have high enhancement potency when have been used in free form. Another study on Lauric acid and other saturated F.As, using different physicochemical properties of model drugs has shown that drug solubilisation in the vehicle increased partitioning, increased barrier disruption and solvent penetration in the presence of F.As; the mechanism differ with the adjuvant, the drug and the vehicle.
	2-Azone (1-dodecyl-azacycloheptan-2-one)	-May cause mild irritation and toxicity at low concentration	-Its Log O/W partitioning coefficient is 6.6. -Non polar, no protein interacting. -Promote penetration at low concentration (1-5%) for lipophilic and hydrophilic drugs. -It affects the fluidity of structured lipids in the intercellular channels of the skin.
	3-Terpenes such as Menthol and 1-Carvone	-FDA classified them as safe, free toxicity and has low irritancy potential.	-They are often the components of volatile oil. -They are a synergistic effect with co-solvents such as ethanol and propylene glycol. - Good penetration enhancer for both lipophilic and hydrophilic drugs. -Act by disrupting the ordered lipid structure of the stratum corneum and increase partitioning of the drug from its aqueous vehicle in the stratum corneum.

Interaction with intercellular protein (keratin), It is believed that these chemicals interact with keratin into coenocytes to alter the diffusion coefficient and increase the permeability. However, other studies claim that these compounds can also work on the various regions such as protein or peptide in the domain of the lipid to increase permeability.

1-Decylmethyl sulphoxide (DCMS)

- It acts at low concentrations, even below 0.1%.
- It accelerates polar drug more than non- polar.
- DCMS use as a solvent, altering protein conformation and thus opening up aqueous cannels and also increase lipid fluidity.
- DCMS use combination with 15% DCMS in PG or 4% in water.

2-Surfacants (Sodium laurate sulphate (SLS))

-Cause some problems such as swelling and skin irritation.

- SLS disrupt the entire membrane affecting both lipid and protein structure.
- Previous study has been shown that 0.1-1% SLS solution grossly swell the stratum corneum, uncoiling and extending alpha-keratin helices and the opening up the protein-controlled polar pathway.

3-Polymers (Dendrimers)

-No skin rotation has been reported (safe).

- These chemicals act by interacting with keratin and lipid in the stratum corneum in addition to increase the drug partitioning.

Increasing partitioning and solubility in the stratum corneum

-Alcohol (ethanol)

High concentration causes skin dehydration.

- High concentration of ethanol causes extraction lipids from stratum corneum.
- Low concentration of ethanol alters the organisation of intercellular lipids, thus increasing skin permeability.

-They act by extracting lipids from the stratum corneum and forming aqueous channels within the stratum corneum that increase permeability.

1.6.2 Natural Enhancers

While various synthetic chemicals are often employed as penetration enhancers by the pharmaceutical industry, some of these are associated with irritation and other adverse effects. Consequently, safe and effective alternative enhancers are sought and there is much interest in substances of natural origin. These offer potential advantages, such as renewable mass production from sustainable resources and lower cost, depending on the extraction process. Some examples of natural penetration enhancers are fatty acids, essential oils, including terpenes and polysaccharides (56).

1.6.2.2 Terpenes

Terpenes are components of essential oils which are derived biosynthetically from isoprene units. They are commonly used as penetration enhancers for hydrophilic and lipophilic drugs in the pharmaceutical industry and are generally regarded as safe for use on human skin. Different classes, various physicochemical features and various mechanisms of action make these compounds useful for transdermal delivery of drugs. Terpenes are classified according to the number of isoprene units (C_5H_8) in the molecule (56). It is reported that hydrocarbon terpenes are less effective enhancers for hydrophilic drugs than ketone or alcohol containing terpenes and the oxide terpenes have shown the greatest enhancement activity with hydrophilic drugs (57). Eucalyptol has been found to increase the permeation of several lipophilic drugs across hairless mouse skin (58). Some monocyclic monoterpenes such as limonene and menthol enhanced the penetration of indomethacin (59) and diazepam (60) respectively, across rat skin. Also, spectroscopic evidence has suggested that terpenes may be retained within spatial domains in the stratum corneum lipids (53).

1.6.2.3 Fixed oils/ Fatty acids

These oils are formed from an aliphatic hydrocarbon chain which may be either saturated or unsaturated and have a terminal carboxyl group. They are effective skin penetration enhancers and considered nontoxic and safe for human skin use. Examples include fish oil, fatty acids from algae and phospholipids (56). The effects of fatty acids as penetration enhancers depends on their structure, alkyl chain and degree and type of unsaturation (61). Aungst has extensively studied a range of fatty acids as penetration enhancers, and suggests that saturated alkyl chain lengths of around C10-C12 attached to the polar head group produce potent enhancers. Compared to penetration enhancers containing unsaturated compounds, the bent *cis* configuration disrupts intercellular lipid packing more

than the *trans* arrangement (62), (63). The most commonly used unsaturated fatty acid is oleic acid; it has been shown to increase the flux of many drugs such as salicylic acid 28-fold and 5-flourouacil flux 65-fold through human skin *in vitro* (64).

1.6.3 Adverse effects of chemical and natural enhancers in skin

Although the goal is to use chemical penetration enhancers that have no adverse effects, it is unlikely that chemicals that cause disruption to the organisation of the stratum corneum lipids will have no measurable side effects. Penetration enhancers may cause reversible damage or alter the physicochemical properties of the skin. One of side effects associated with penetration enhancers is skin irritancy. In addition, enhancers may work by multiple mechanisms and combinations of enhancers may induce synergistic responses. This lack of understanding causes unease, without a known mechanism or understanding the barrier repairs /restores over time. Another area that creates concern is the extrapolation of the activity of enhancers to biological effects. The effects of enhancers on biological, immunological and inflammatory cascades have received little attention.

Herbal preparations are becoming more popular and are frequently used for treatment of dermatological conditions. Hence, dermatologists need to know about their potential to cause adverse effects. A review by Ernst in 2000 (65) showed that many Chinese herbal creams were adulterated with corticosteroids. Nearly all herbal medicines are mixtures of chemicals and can cause allergic reactions and several can be responsible for photosensitisation. Several herbal medicines, in particular Ayurvedic medicines, contain arsenic or mercury that can produce skin lesions. Other common remedies that can cause dermatological side-effects include St John's Wort, kava, aloe vera, eucalyptus, camphor, henna and yohimbine. The adverse effects of herbal medicines are an important although neglected subject in treatment of skin diseases, which deserves a more systematic investigation.

1.6.4 Other methods of enhancing skin penetration

1.6.4.1 Water as penetration enhancer (Effect of hydration)

Water is the most used and safest way to increase the rate of percutaneous passage of lipophilic drugs (66). The water content of human stratum corneum is normally about 15-20% of the tissue by dry weight (54). Elevated stratum corneum hydration will swell the compact structure of the stratum corneum continuously, absorbing as much as ten times the dry weight, the water bound within the intercellular keratin, leading to a rapid increase in the

permeability and then a slow down to a steady- state diffusion (67). Hydration can be increased by occlusion with parafilm or oils, waxes as components of ointment, and water in oil emulsions which prevent transepidermal water loss (51). In occlusion, the water content in the outer membrane can increase 400% compared to tissue dry weight (57). Solid state nuclear magnetic resonance (NMR) has been used to show the movement of skin compounds in the presence of water (68). Hikima and Maibach (69) examined the ratio of fluxes and lag time for a range of solutes and concluded that hydration enhancements were independent of lipophilicity and molecular weight. These finding were consistent with the summary reported by Roberts and Walker, (70) who noted that the effects of hydration on solute penetration were equivocal, with some reporting increasing of up to ten fold for some substances, and others showing a very small effect. They commented that the major effect of hydration may be in solubility in skin lipids, citing the greater enhancement of pure glycol salicylate relative to methyl or ethyl salicylate by hydration using the human in vivo data of Wurster and Kramer (71). Bucks and Maibach (72) found that lipophilic steroids showed greater enhancement by occlusion than more polar ones.

1.6.4.2 Supersaturation

Supersaturation acts directly in the drug to increase skin permeation without alteration of stratum corneum architecture. The mechanism of enhancement is by increasing the thermodynamic activity of the drug in the vehicles. For example an increased driving force for transit out of the formulation and into and across the stratum corneum (73). Once drug concentration is increased above the saturation, the system become thermodynamically unstable and the supersaturation formulation will be typically subject to recrystallization of drug molecules and concomitant loss of the enhancing effect. Even when the stability of supersaturation formulations is improved by the use of polymers (74, 75), stability remains the limiting factor for achieving enhanced skin permeation, which can be seen only for as long as the formulations are supersaturation (75). The dependence in thermodynamic activity has been shown by Twist and Zatz (76). Silicone membrane was used to determine the diffusion of saturated parabens in different solvents. As the saturated solubility of parabens is different in these solvents, the concentration differed over two orders of magnitude. However, thermodynamic activity was constant due to continuous saturated conditions during the experiment and the same flux of paraben from all solvents was obtained (24). There are several ways to achieve supersaturation such as, heating and cooling (77), evaporation of a volatile components of the vehicle (78) or by mixing of two

solvents where the drug is significant more soluble in one solvent than the other (79) (54). Also, water can act as a solvent in the case of it being imbibed from skin into the vehicles, and the thermodynamic activity of the solute will increase (80). Many studies have reported increases in drug flux 5 to 10 times that of supersaturated solutions (75, 81). A study by Megrab et al (79) suggested that the oestradiol flux of a saturated system was increase 18-fold through human skin. However, in silastic membrane the increase was only 13-fold. They revealed that the components of the stratum corneum (fatty acids, cholesterol and ceramide etc.) may produce an antinucleating effect thus stabilising the supersaturated system.

1.6.4.3 Physical enhancement

Physical penetration enhancement transiently circumvents the normal barrier function of the skin and can permit the passage of macromolecules (82). There are different physical methods for enhancement and they share the common aim of creating pathways for molecules to penetrate. The most common strategy is iontophoresis. Iontophoresis is a process using low DC current via an electrode in contact with the drug and the skin; a grounding electrode completes the circuit. It works by two mechanisms, i) the driving electrode repels ions: ii) the flow of the current may decrease the resistance of the skin so as to increase its permeability. Another more recent method for delivery of macromolecules is microneedle-enhanced delivery (83). This technique uses tiny needle-like structures to produce pathways for macromolecules to penetrate the horny layer without breaking it. This system can enhance the permeation, up to 100,000 fold, of macromolecules across the skin (52), also offering painless delivery of drugs (84).

1.6.4.4 Vesicular system enhancement

Vesicular system enhancement uses prodrugs (85), chemical modifications (86), vascular systems or colloidal particles (87) to increase skin penetration. From these techniques, liposomes (phospholipid-based artificial vesicles), niosome (non-ionic surfactant vesicles) and transferosomes which contain phospholipids, cholesterol and edge activators-surfactant substances, such as sodium cholate, are extensively used to deliver drugs through human skin. Such systems act by one of the following mechanisms: 1- penetration of the stratum corneum by free drug or drug release from vesicles and then penetrates the skin independently. 2- Release lipids from carriers and then interact with stratum corneum lipids. 3- Improve drug uptake by skin. 4- Control drug input by different enhancement

efficiencies (82). These systems will be examined in more detail in section 1.9 which describes some specific colloidal formulations.

1.7 Selection of drug models with optimal physiochemical properties for skin penetration

Earlier studies (88, 89) found that solubility, lipid-water partition coefficient, melting point and molecular weight are significant determinants of the permeability of drugs across the skin. These studies confirm that the role of molecular weight, lipophilicity and melting point are more important than the other properties.

1.7.1 Molecular weight and shape

Several prior studies (90, 91) found that molecular size (weight, volume and radius) have an important role in determining skin permeability. Magnusson et al's (92) study of a large literature dataset has shown that molecular weight was the dominant determinant of maximum flux (Fig 1.5). Also, it has been indicated that small molecular weight drugs (preferred <500Da) can penetrate the skin more easily (93). A study in transdermal delivery claims that molecular weight has an inverse relationship with diffusivity (D) of molecules; this means that molecular weight increases exponentially when diffusivity decreases (94). However, Mitragotri suggested a logarithm for KP based on molecular radius (95)

$$D = D^0 \cdot e^{-B \cdot MW}$$

D^0 = diffusivity of molecule at zero molecular volume, B = constant.

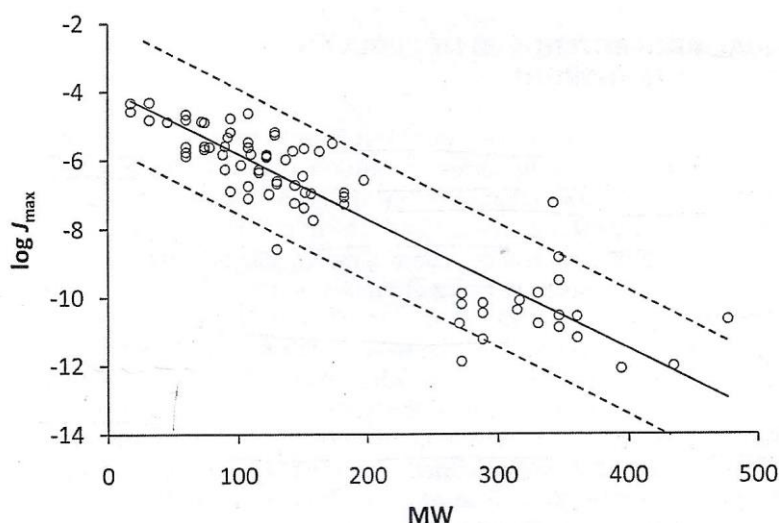


Fig 1.6 Relationship between $\log J_{\max}$ and MW for solutes from aqueous solutions that passed through human epidermal membranes (n=87). The regression line (solid line)

describes the relationship: $\log J_{\max} = -3.90 - 0.019 \text{ MW}$ ($p < 0.001$, $r^2 = 0.847$). The dashed lines show 95% confidence limits (92)

1.7.2 Lipophilicity

Previous studies claimed that drug lipophilicity is the most important determinant of skin permeation with small compounds, such as alcohols (90), and phenols (96). Scheuplein (97) found that the membrane-solvent partition coefficient of a drug was a measure of the interaction and was an essential determinant of permeability. These partitioning coefficients have been measured by partitioning between olive oil and water (97) and most frequently by octanol and water (96) as a measure of drug lipophilicity. This is expressed as the log of octanol-water partitioning coefficients, $\log K_{OW}$ or Log P . Pugh et al suggested that octanol was the better solvent for drug partitioning into the stratum corneum (98). The interaction between the drug and the lipid domain would be expected to have an important effect on drug transport (99).

1.7.3 Hydrogen Bonding

It has been reported in many studies (100), (92) as a determinant of solute skin transport, that hydrogen bonding related inversely with permeability, expressed in terms of the donor and acceptor parameters, H_d and H_a (101). Previous work (102) thought that permeability relied on the group's number of hydrogen bonding found on the molecule while recent studies (103) believed that permeability depended on mathematical treatments of each hydrogen-bonding group and where the large numbered hydrogen bonding group was found. Some reports considered that good penetration occurred with < 5 hydrogen binding sites. Studies have found that melting point also is a guide to the ability of hydrogen bonding and often permeability depends on this parameter (92), (104). Lag time is related to the type and number of hydrogen bonding groups, claiming an effect on diffusion due to solute retardation by binding to polar head groups of the stratum corneum lipid domain. When hydrogen bonding solutes bind with polar groups into the lipid bilayer, the non-hydrogen groups diffuse freely across the lipid domain (105).

From the above, it is clear that lipophilicity and molecular size are essential determinants of skin penetration as well as hydrogen bonding. A study done by Zhang et al (2009) on human epidermal penetration used phenols with Log P values of 1.8-3.54 and molecular weight and

hydrogen bonding the same; they found that the fluxes were decreased for the high lipophilic solutes which confirms the relationship between J_{max} and Log P (106).

1.8 Assessment of skin penetration

1.8.1 Maximum Flux (J_{max})

The majority of research has assessed skin permeation in terms of permeability coefficients (K_p , unit of distance/time, usually cm/h) from simple solutions, including aqueous solutions (88, 99). Nonetheless, other studies have used maximum (or more correctly, saturated) flux (J_{max} , units of amount/area/time). J_{max} describes the rate of penetration through a membrane from saturated solutions or pure substances and as such, should theoretically be independent of the vehicle (67, 107). On the other hand, K_p is dependent upon the vehicle in which the penetrant is dissolved. Therefore, J_{max} allows a comparison to be made between permeation data that may have been obtained under different vehicle conditions (108). Also, the importance of using J_{max} is that it is an invariant in the thermodynamic activity of the permeation process, while K_p , relies on formulation applied to the skin (106).

1.8.2 Drug-vehicle-skin interactions

Any approach with topical delivery should start with consideration of the stratum corneum and as mentioned in this review that the transport of molecules throughout the skin is a complex phenomenon including chemical, physical and biological interactions. Higuchi was the first one to progress equation about the relationship between thermodynamic activity and skin absorption from ointments and creams (104). Barry has considered on relating numerous models with percutaneous absorption from binary vehicles (105) and he has defined the solute-vehicle–skin interaction depending on the theoretical model described by Poulsen (2). First theory is, the ideal case when neither SC solubility nor diffusivity is affected by either the vehicle or the drug. The maximum solubility of the drug in this vehicle, produced release from that vehicle is not diffusion limited. High effect may be achieved by adding other drugs with the similar action to the solvent system. Secondly (105), a vehicle or solute leads to increase in drug solubility in the SC. For example, a study by Kadir et al (106) suggested that addition of paraffin oil to propionic acid solutions increased the flux of either theophylline or adenosine by enhancing the flux of propionic acid into the skin and accelerating the partitioning of the solutes in the modified skin barrier. There are many agents which can enhance or retard skin penetration. For instance, Azone analogue N-0915 has been identified as a penetration retarder, for which the mode of action is believed to be

an increase in the order of the SC lipids (107). Also, when the solubility of solute in the vehicle increase, the flux should decline due to reduction in skin/vehicle partitioning coefficient. There are many factors effect drug-vehicle-skin interaction relationship such as, the applied area, type of the vehicle (induce hydration to the SC or not), solubility of the solute in the vehicle, concentration of the solute in the vehicle, length time of contact application and the condition of skin itself (the outer SC intact or not) (108). Understanding barrier characteristic of the skin, can help understanding the mechanism of vehicles and drugs on skin for optimized the design of formulations with solutes from the drug-vehicle-skin interaction point of view.

1.8.3 Animal skin vs. human skin

Human skin is clearly the best choice but is not always readily available. Otherwise, pig skin can be used because it shares vital permeation features with human skin (109). Rat skin is 2 to 10 times more permeable than human skin (110) which may result in an overestimation of dermal absorption. Mouse, guinea pig or rabbit skins also have reduced barrier function compared to human skin (57, 111). The use of cultured or reconstructed skin models is under development and those systems are not yet recommended for *in vitro* testing on the basis of their inadequate barrier function (112).

1.8.4 Skin integrity

Barrier integrity is essential for skin penetration experiments, and should therefore be measured. This is achieved by either measuring the penetration of a marker molecule, such as tritiated water, caffeine or sucrose, or by physical methods, such as determination of Transepidermal water loss (TEWL) or Transcutaneous Electrical Resistance (TER).

1.8.5 Solubility parameters

Solubility parameters are useful to describe features of materials, such as compatibility, miscibility and adsorption. Solubility parameter values for various excipients allow forecasting of the magnitude of interactions between the compounds of formulation in addition to the stability of a product. The term solubility parameter is connected to cohesive energy density (CED), which indicates the energy of vaporisation per unit volume (113) and is important to the pharmaceutical material scientist as it determines physicochemical properties such as solubility and melting point of the solutes and excipients.

$$\delta = (\text{CED})^{1/2} = \left[\frac{\Delta H - RT}{V_m} \right]^{1/2} = \left[\frac{\Delta E}{V_m} \right]^{1/2} \quad (1)$$

Where δ is the solubility parameter, R the gas constant, T the temperature, ΔH the enthalpy of vaporisation, V_m the molar volume, and ΔE is the free energy of vaporisation. The solubility parameter defined by Eq. (1) is named Hildebrand solubility parameter or Hildebrand parameters (114). The supposed Hansen solubility parameter (HSP) is an extension of the Hildebrand solubility parameter to polar and hydrogen bonding systems(115). Hansen expected that cohesive energy could be measured as a sum of contributions from dispersive (E_d), polar (E_p) and hydrogen bonding (E_h) interactions (113, 115-117).

$$E_{coh} = E_d + E_p + E_h \quad (2)$$

And the total solubility parameter (δ_T) is expressed as

$$\delta^2_T = \delta^2_d + \delta^2_p + \delta^2_h \quad (3)$$

Where δ_d , δ_p , and δ_h represent the dispersive, polar and hydrogen bonding, respectively. According to Hansen's interpretation, it can be expected that for the spontaneous mixing process between liquids, the values of HSP compounds for one liquid should be close to the other liquid. Various approaches can be used for estimating solubility parameters. The solubility parameter can be found from energy of evaporation for volatile materials and, by using Eq. (1), this only gives total solubility parameter not Hansen solubility parameters. For low- or non-volatile compounds, measuring the solubility parameter straight from the energy of evaporation, and comparing it to liquids, is impossible. The HSP can be used to describe relationships among all kinds of organic and inorganic substances. and they have been applied to many practical and industrial issues (118).

1.9 Colloidal delivery system

New nano-delivery systems such as emulsions, lipogels, rigid or flexible liposomes and so on are being assessed for their ability to provide improved delivery of therapeutic, prophylactic and diagnostic agents (119). Active ingredients in these nano-sized systems, such as phospholipids, fatty acids, surfactants, etc., are combined to accelerate penetration across the skin leading to more rapid absorption of the drug. While some of the older

chemical enhancers caused skin irritation (120), more recent systems using emulsions and liposomes are more biocompatible (121). In addition to the components of the vehicle, it is worth remembering that frequently a simple alteration in properties, such as pH, viscosity, water or surfactant content in an emulsion, the relative amount of oil, droplet size; ionic nature or the method of preparation may affect skin absorption. Table 1.3 provides some examples of advanced formulations.

Table 1.3 Nano delivery systems (122).

Technique	Principle	Deliverables
Nano emulsion or micro emulsion	System of water, oil and an amphiphile, which forms a single optically isotropic solution	Plasmid DNA, Ketoprofen, amorphine, oestradiol and lidocaine
Liposomes	Vesicles formed by one or multiple lipid bilayers made of mixture of phospholipids	Cosmetics, antibiotics and vaccine adjuvants
Niosomes	Mixture of non-ionic surfactants, cholesterol and phospholipids	Tretinoin, peptide drugs and zidovudine
Ethosomes	Increase skin penetration by increasing the elasticity of the lipidic vesicle, contain up to 20-45% of ethanol	5-ALA(Aminoolevulinic acid), salbutamol, finasteride and anti-HIV therapy
Transferosomes	Phospholipids with surfactants, that acts to provide vesicle elasticity and deformability	Vaccines, 5-fluorouracil, IL-2
SECosomes or nanosomes	Mixture of surfactants, ethanol, cholesterol	siRNA
SLN(solid lipid nanoparticles)	Produced with one single solid lipid and surfactant , with perfect crystalline lattice	CoQ-10, glucocorticoids, minoxidil and oxybenzone
NLC(nanostructured lipid carriers)	Produced with liquid and solid lipid and surfactants, with distorted crystalline lattice	Targeted tumour delivery, phospholipaseA2 inhibitors, benzocaine, lidocaine and psoriasis treatment
Polymeric nanoparticles	Consist of micro and nano spheres or capsules developed to control the release of the entrapped drug	Chlorhexidine, indomethacin, melatonin and poorly soluble drugs

Microemulsions are clear, thermodynamically stable, isotropic liquid mixtures of oil, water and surfactants, often in combination with a co-surfactant, with droplet sizes typically in the 10-100 nm range. They may be a water in oil (W/O) type, with water dispersed in a continuous oil phase; oil in water (O/W), with the oil phase dispersed in a continuous

aqueous phase; or bi-continuous (121),(123). Multi-phase systems such as W/O/W or O/W/O are also possible. In all kinds of emulsions, the interface is stabilised by a proper combination of surfactants with or without co-surfactants. The choice of oils and surfactants for an emulsion system for topical delivery is limited by their potential irritation and toxicity.

A significant difference between macro-emulsions and micro- or nanoemulsions is that macro-emulsions are unstable thermodynamically and phase separation will eventually occur. In addition, the macroemulsion droplet size will increase with time. Furthermore, the larger droplet size in macroemulsions makes them cloudy, unlike the clear liquids formed with the micro or nano-sized droplets. Whereas, macroemulsions require the input of energy for preparation, microemulsions do not, because they are created spontaneously when their components are brought into contact (121). While, nanoemulsions need Low or high energy methods, in high energy methods, large disruption forces are provided by the use of mechanical devices such as ultrasonicators, microfurdisers and high pressure homogenizers which produce small droplet size. In low energy, no external force is provided, instead it makes use of intrinsic physiological properties of the system for production of nanoemulsions (124). Finally, macro-emulsions are more viscous than micro- or nanoemulsions (121). Nanoemulsions combined some of the important requirements of a liquid delivery system, such as thermodynamic instability, ease of formation, high viscosity and small droplet size (125). They can be given orally, topically or nasally as an aerosol for direct administration into the lungs (125). Characterisation of a microemulsion may be done by assessing viscosity (126, 127) conductivity (127), NMR spectra (128) and dynamic light scattering (DLS) (129). Benefits of topical nanoemulsions include avoidance of hepatic metabolism, simple and convenient administration methods and immediate removal if necessary (125). Nanoemulsions work by different mechanisms. For instance, denaturation of intercellular proteins causes swelling and increased skin hydration (49), modification of lipid bilayers reduces resistance to penetration (49) and changing the solvent properties of the stratum corneum modify solute partitioning (49).

Liposomes are enclosed spherical vehicles that are organised in one or several concentric phospholipidic bilayer/s with an aqueous core (130). The liposomal membrane is mainly supported by edge activators, a type of surfactant, which destabilise the lipid bilayer of the liposomes and increase the elasticity bilayer at the same time (131). Researchers believe that the mechanism of action of liposomes on skin is by either forming a thin lipid film on the skin surface or increasing the total lipid content of the skin by forming a liquid crystalline on the uppermost skin layer (132). There are many types of liposomes such as niosome (non-

ionic surfactant) and transferosomes (phospholipid and surfactants) (133). The presence of surfactant will increase the elasticity of the lipid bilayer (134). El Maghraby et al in 2006 reported that flexible liposomes are more effective in transdermal drug delivery (135). It is reported that surfactants (edge activators) are able to impart deformability to the nano-carrier which permits improved transcutaneous delivery of drugs (136). Liposomes are able to exert various functions after topical administration (135). They are able to improve drug deposition within the skin at the action site where the aim is to decrease systemic absorption and thus reduce side effects. They also are able to produce targeted delivery to skin appendages as well as having potential for transepidermal delivery (135).

Chapter 2

2.1 Aims and Hypotheses

My PhD project is entitled “Targeted skin delivery of topically applied drugs by optimised formulation design”. Each of the three aims is detailed below.

Aim 1

A) To gain mechanistic understanding of the factors that drive skin permeation rates: Effect of vehicle composition.

Hypothesis

The skin permeation flux of solutes should be identical unless the vehicle has affected the skin.

B) To determine if enhanced solute permeation is due to combinations of increased solubility of the compounds in the stratum corneum and increased diffusivity in the skin

In this study, we examined how skin penetration fluxes are affected by vehicles reported to interact with the skin barrier to various degrees. We compared *in vitro* penetration fluxes (J_{max}) and solubilities in the vehicles (S_v) and stratum corneum (S_{SC}) for caffeine, minoxidil, lidocaine and naproxen from various solvent vehicles (with or without penetration enhancers) to evaluate vehicle effects on permeability parameters. To separate and quantify this effect, we also examined the relationship between maximum fluxes, solubility of solute into the stratum corneum with the solubility parameters of the solvents. We also examined whether the solvent of solutes uptake into the stratum corneum related to the solubility of the solutes in the stratum corneum. Further study was done with caffeine to determine the relationship between skin parameters and solubility parameters after pretreatment of skin with a range of vehicles for 2 h.

Aim 2

To investigate the efficacy of incorporating penetration enhancers into advanced formulations (e.g. flexible liposomes, microemulsions) for enhanced skin penetration / permeation of model compounds.

Hypothesis

Targeted delivery of topically applied drugs to skin compartments, including hair follicles, can be achieved by design of an optimised drug delivery system.

The second aim was to investigate the efficacy of incorporating penetration enhancers into advanced formulations (e.g. flexible liposomes and microemulsions) on the skin permeation of model compounds. I prepared and characterised nanoemulsion formulations with caffeine (hydrophilic model) and naproxen (lipophilic model), using oleic acid and eucalyptol as combined oil phases / penetration enhancers. The nanoemulsions were evaluated according to their particle size, conductivity, viscosity and refractive index. Permeation through epidermal membrane and full-thickness excised human skin was measured for caffeine and naproxen. Evaluations were also undertaken to prove that the maximum flux of the compounds may be enhanced by either increasing its solubility in stratum corneum lipid components or by increasing the diffusivity of the solutes in the stratum corneum. The amount of caffeine and naproxen in receptor fluid, extracts of tape strips (20 times) and skin was quantified using high performance liquid chromatography (HPLC). The effect of nanoemulsion formulation on the skin and the delivery route was determined using Multiphoton microscopy (MPM). I also prepared and characterised liposomes, transferosomes and neosomes with caffeine using oleic acid, eucalyptol and decyl glucoside as combined edge activators. The liposomes were evaluated according to their particle size, zeta potential, and dispersity index and drug efficiency. Permeation through full-thickness excised human skin, retention in the stratum corneum and in the skin was measured for caffeine. All samples were analysed using HPLC.

Aim 3

To investigate the effects of penetration enhancers on follicular penetration of model compounds.

Hypothesis

Hair follicles are pertinent and efficient penetration pathways and reservoirs for topically applied chemicals/drugs

This study aimed to develop substances which can be topically applied and able to penetrate into hair follicles. In this aim, we have tested the penetration of model drugs (caffeine and minoxidil) into hair follicles, using the same nanoemulsion and liposome formulations used

in Aim 2. For follicular localisation of drug molecules, we have been measured the amount of drug that penetrates into the follicle by a technique available in our lab called follicular casting (a non-invasive method). We examined targeted delivery of solute molecules specifically to hair follicles, and the difference between normal, open and block hair follicles in permeation using solution and nanoemulsion formulations. We also imaged the penetration depth of Acriflavine (a dye) into the hair follicles and the area around the hair follicles.

Chapter 3

Effect of Penetration Enhancers; Solution Studies

A- The impact of chemical penetration enhancers on permeation of solutes through human epidermal membranes *in vitro*: Mechanistic investigations

B- The effect of vehicle pretreatment on the flux, retention and diffusion of topically applied caffeine *in vitro*: understanding the relationship between solvent and solute penetration using human skin.

3.1 Abstract

This study aimed to explore the mechanism by which skin permeation fluxes are affected by a range of vehicles reported to interact with the skin barrier to different degrees. We compared *in vitro* penetration fluxes (J_{max}) and solubilities in the vehicles (S_v) and stratum corneum (S_{SC}) for caffeine, minoxidil, lidocaine and naproxen of various solvent vehicles to evaluate the vehicle effects on permeability parameters. Solutions of four drugs with log P ranging from -0.07 (caffeine) to 3.18 (naproxen) were dissolved in a range of vehicles and applied to heat separated human epidermal membranes in Franz diffusion cells. The vehicles either contained substances known to enhance skin penetration (e.g., ethanol, oleic acid, eucalyptol, sodium lauryl sulphate) or were known to have no effect on skin. We measured the solubility of these solutes in the vehicles (S_v) and in the stratum corneum (S_{SC}). We also examined whether the solubility of the solutes in the stratum corneum was determined by the uptake of solvent, in which the solutes were dissolved, into the stratum corneum. For the pretreatment study, the flux of caffeine was measured over 8 h through heat-separated human epidermis pretreated for 2 h with water, 20, 40, 60% ethanol/water and 5% oleic acid (OA), 5% eucalyptol (EU) or 1% SLS in 60% ethanol, mineral oil (MO) and microemulsions with eucalyptol or silicone oil as the oil phase. Enhancement was greater after pretreatment with vehicles containing penetration enhancers (oleic acid and eucalyptol in 60% ethanol and in the eucalyptol microemulsion). For vehicles that had no effect on the skin, the J_{max} values were the same, regardless of the S_v . Similarly, there was a linear relationship between J_{max} and S_{SC} for these vehicles, whereas vehicles containing penetration enhancers caused deviations from linearity. The treatment study indicates that

the solubility model has a good correlation between the predicted S_{SC} and measured S_{SC} for caffeine, minoxidil and lidocaine. It provides a linear shape with $R^2= 0.8, 0.7, 0.8$, respectively. However, we could not find the same correlation with naproxen. There was significant enhancement following pretreatment with 40% and 60% ethanol vehicles relative to controls (water and 20% ethanol, MO and silicone oil). The enhancement rate was related to Hanson solubility parameters.

We conclude that the solubility of a solute in the skin can be correlated to its solubility in the vehicle and the amount of vehicle absorbed by the stratum corneum. This study observed that changes in both diffusivity and solubility of solute (caffeine) in the stratum corneum can be affected by vehicle absorption in the skin.

3.2 Introduction

Topical administration products account for an increasingly significant percentage of solute delivery candidate compounds under clinical evaluation (106). To be useful, topical products must provide efficient delivery of actives to either the systemic circulation or to the skin, but for most substances, the uppermost layer of the skin, the stratum corneum presents a substantial barrier to their penetration. However, the barrier may often be overcome to meet therapeutic or cosmetic goals by judiciously designed delivery systems (137), taking into account the active's potency, its physicochemical properties and the properties of the vehicle and its interaction with the skin.

In this study we investigated some of the factors that influence the penetration and permeation of topically applied substances through skin and sought to relate the observed permeation fluxes to the physicochemical properties of the actives and the vehicles, as well as the various active-vehicle, active-skin and vehicle-skin interactions that occurred. Techniques previously applied to relate drug flux to solute-skin, solute-vehicle, and vehicle-skin interactions include maximum flux studies, (64, 96), and relating the membrane fluxes to solute uptake in the stratum corneum (138). The maximum or saturation flux (J_{max}) is defined as that occurring when a solute is applied to the skin in a saturated solution. The important of J_{max} is that for a given solute, it is an invariant in the thermodynamic description of the permeation process (106). By definition, if neither the vehicle nor the solute affect the membrane, the same maximum flux will be observed for the solute from a range of vehicles regardless of its concentration in them (138). For example, Twist and Zatz (139) found that methyl paraben had the same flux from a range of saturated solutions in different vehicles

applied to inert polydimethylsiloxane membranes that were not affected by the vehicles (139). Physicochemical properties including molecular size, melting point, lipophilicity, solubility and hydrogen bonding acceptor ability have been considered to be important in determining permeation flux (89, 140).

Maximum flux is determined by the solubility of the drug in the stratum corneum (S_{SC}) according to the equation:

$$J_{max} = D^* \cdot S_{SC} = D^* \cdot K_{SC} S_V$$

Where D^* is the diffusivity, S_{SC} is the solubility in the stratum corneum, K_{SC} is the epidermal permeability coefficient and S_V is the solubility in the vehicles (138). Inspection of Equation indicates that the maximum flux of a solute through the stratum corneum can be enhanced by three mechanisms; (a) increasing the diffusivity of the solute in the stratum corneum; (b) affecting the partitioning between the stratum corneum lipids and other stratum corneum components; (c) increasing its solubility in the stratum corneum lipids (141). Accordingly, skin absorption depends upon the physicochemical properties of the solutes (69), so that lipophilic compounds penetrate more easily than hydrophilic compounds and lower MW more easily than high MW (69). As well, the vehicle is a key factor in determining the efficacy of transdermal drug delivery systems. Two main mechanisms are thought to govern the effect of vehicles on the skin permeability of solutes; firstly, the force driving the drug into the skin is due to thermodynamic activity of the solute in the vehicle (142) and secondly, the skin barrier properties may be modified by interaction with the skin's lipid and keratin components (142).

Several technological advances have been made in the recent decades to overcome the stratum corneum barrier and thereby deliver therapeutic substances accurately to their skin target sites in sufficient quantities (82). One approach is to use chemical penetration enhancers (27). These can act by various mechanisms, such as promoting supersaturation in the vehicle, leading to an enhanced partitioning into stratum corneum (75), interaction with intercellular lipids causing organisation disruption and thereby raising their fluidity, extraction of stratum corneum lipids (143) or interaction with intercellular protein and denaturation of keratin (64, 82). While it is well recognised that appropriately chosen vehicles can enhance skin penetration (144), there appear to be limited studies examining the effect of vehicles on the maximum flux of solutes across the skin.

In this study, we sought to explore the impact of various solution compositions on the skin permeation of some model drugs. We compared *in vitro* maximum penetration fluxes (J_{max}) and solubilities in the vehicles (S_v) and in the stratum corneum (S_{SC}) of four drugs (caffeine, minoxidil, lidocaine and naproxen) having a range of lipophilicities (log P -0.07, 1.24, 2.44, and 3.18, respectively). We used a range of solvent vehicles that were hypothesised to affect the skin to differing degrees to evaluate vehicle effects on permeability parameters.

3.2.1 The solubility parameters concept

An understanding the interaction of between topically applied formulations and the skin barrier is crucial for tailoring effective skin delivery. The equilibrium between solute solubility in the vehicles, and in the skin and the complex interaction that may occur between different components of the system will determine the targeting of topical solutes to the stratum corneum, epidermis and deeper tissues (98, 104). Solubility parameters have been used as tools to predict the adhesive and cohesive properties of materials and in particular have been used to model and predict the permeation of topically applied substances (145). The solubility parameter concept was developed by Hildebrand (146, 147), who assumed that the solubility of the compounds rely on the cohesive energy, the square root of cohesive pressure is Hildebrand's solubility parameter, δ :

$$\delta = \sqrt{C} = \sqrt{\Delta H_v - RT \div V_m} \quad (1)$$

Where ΔH_v is the heat of vaporisation, R is the gas constant, T is absolute temperature, and V_m is the molar volume of the solvent. Frequently, the RT term is ignored because it accounts for only 5-10% of the evaporation heat (145). If the solubility parameter of the vehicle and the drug are similar, it is likely that the drug is soluble in the vehicle. This model is an experimental development of the rule of "like dissolve like" (145). Hansen proposed a model to extend Hildebrand's model to polar and hydrogen binding systems and defined the solubility parameter as:

$$\delta_t^2 = \delta_d^2 + \delta_p^2 + \delta_h^2 \quad (2)$$

Where δ_t is the total or three dimensional solubility parameter, δ_d the dispersive, δ_p the polar term and δ_h the hydrogen binding (115, 116, 148). The Hansen model describes solvents as points in three dimensional space and the solute as a sphere of solubility (Fig 1). If the solvent point is within the solute volume space, the solute is dissolved by the solvent and if the solvent points are located outside the space volume, the solvent does not dissolve the

solute (148). Furthermore, Hansen (116) developed the solubility parameter equation to express the distance (Ra), between two materials:

$$(R_a)^2 = 4 (\delta_{D2} - \delta_{D1})^2 + (\delta_{P2} - \delta_{P1})^2 + (\delta_{H2} - \delta_{H1})^2 \quad (3)$$

Equation 3 was improved from plots of experimental values where the constant “4” more accurately represented the solubility data by encompassing the “good” solvents (148). Various approaches to quantify solvent-solute and solvent-skin interaction using the solubility parameter have been suggested (δ). The first attempt to characterise human skin with the HSP was made visually using psoriasis scales of swelling when immersed for prolonged time in different solvents (114). An extensive study has been done on permeation through viable human skin that allowed placement of the solvents into groups according to actual permeation rates (115). In the second part of this study (B: pretreatment) we explored the use of HSPs in the particular solute-vehicle, solute-skin and vehicle skin interaction. We used a hydrophilic model solute (caffeine) and a range of vehicles with differing HSPs. Heat separated epidermal membrane was pretreated for 2 h with the chosen vehicle and an aqueous solution of caffeine was applied for 8 h. Flux and drug retained in the epidermis after the experiment was measured to determine the effect of the vehicle on the skin parameters.

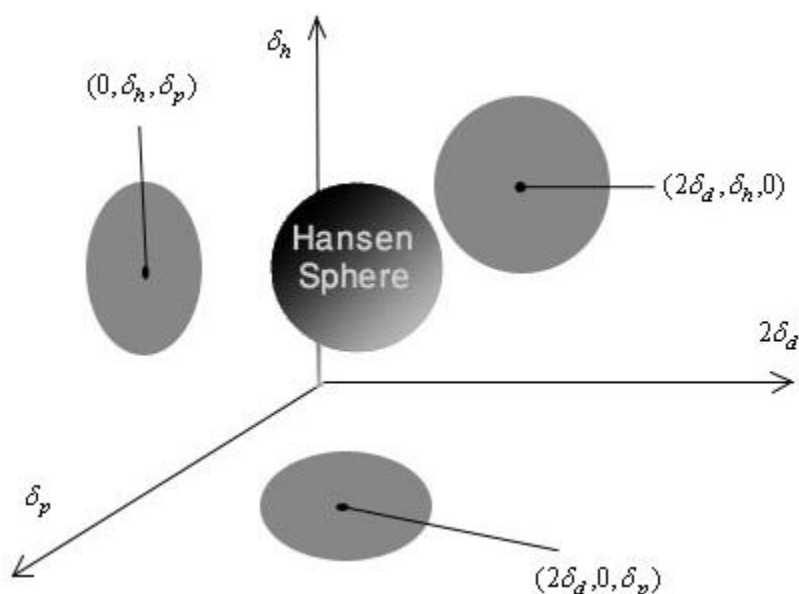


Figure 3.1 Hansen sphere in schematic form (145) (Copyright ©2011; Steven Abbott, Charles Hansen and Hiroshi Yamamoto)

3.3 Materials and methods

3.3.1 Chemicals

Caffeine, naproxen, minoxidil, lidocaine, ethanol, OA, EU, polyethylene glycol 400 (PEG400) and polyethylene glycol 6000 (PEG6000) were purchased from Sigma-Aldrich Pty. Ltd. (Sydney, Australia). MO was purchased from Galtex (Australia, Ltd), Glycerol from Ajax (a division of Naplex industries, Australia Pty. Ltd), Polyoxyl-20 Oleyl ether (Volpo-N20) was purchased from CRODA (Croda Europe Ltd, United Kingdom) and Polyoxyl 10 Oleyl ether (Volpo-N10, also known as Brij96v) from UNIQEMA (Wilton, United Kingdom). All chromatography reagents were analytical reagent grade.

The physicochemical properties of the model compounds are shown in Table 3.1.

Table 3.1. Physicochemical properties of model compounds [Molecular weight (MW g/mol); Lipophilicity (Log P); Melting point (MP °C); Molar volume (MV), Solubility in aqueous solution (S_{aq} mg/L); Dissociation constant (pKa)]

Compound	MW ^a	Log P ^a	MP ^a	MV ^b	S_{aq}	pKa ^a
Caffeine	194.19	-0.07	238	151.8	21600	14
Minoxidil	209.25	1.24	248	214.6	2200	4.61
Lidocaine	234.34	2.44	68.5	89.7	4100	7.9
Naproxen	230.26	3.18	153	142.6	15.9	4.2

^aChemIDplus advanced-chemical information with searchable synonyms, structure, formulas <http://chem.sis.nlm.nih.gov/chemidplus/>

^bHSPiP program (Steven Abbott of Steven Abbott TCNF Ltd; ©2011 Steven Abbott and Johann Wiechers)

3.3.2 Sample analysis

All samples were analysed using a High Performance Liquid Chromatography (HPLC) system consisting of Shimadzu SIL-20 a HT, CBM-20A system controller, a SPD-20A detector, LC-20AD a pump and an auto injector. Samples were separated isocratically on a Phenomenex Luna 5µm, C18 (150 x 4.6 mm) column using aqueous buffers containing

acetonitrile. Caffeine, minoxidil, lidocaine and naproxen were detected at 273, 281, 210 and 230 nm respectively.

3.3.3 Determination of Solubility in the vehicles (S_V)

S_V was determined in saturated solutions of the compounds in each vehicle (see Table 3 A-D). An excess amount of the compound was added to 5 ml of the vehicle and the samples were incubated in a water bath at 32°C for 24 h, with continuous magnetic stirring. The samples were then centrifuged at 4000 rpm for 15 min and the supernatants were analysed by validated HPLC methods, after appropriate dilution where necessary.

3.3.4 Human skin preparation

Human epidermal membranes were prepared from abdominal full-thickness skin using heat separation (149). The skin was provided by a female donor (aged 57) following an elective surgical procedure, with ethical approval granted by the University of Queensland Human Research Ethics Committee (Approval No. 2008001342). The epidermal membranes were stored at -20°C until use.

3.3.5 Determination of Solubility in the stratum corneum (S_{SC})

The stratum corneum was prepared from epidermal sheets by trypsin digestion (149). The full-thickness skin was immersed in water at 60°C for 1 min, allowing the epidermis to be teased off the dermis. The epidermis was floated overnight on a solution of 0.01% trypsin in phosphate buffer saline at 37°C. The viable epidermis was scraped off using cotton buds and the remaining stratum corneum membrane was rinsed several times with distilled water. The isolated stratum corneum sheets were placed flat on aluminium foil and stored at -20°C until use.

Discs of stratum corneum (4 replicates for each sample) were weighed before using. They were then equilibrated in a saturated solution 1 mL of each solute at 32°C for 24 h, according to established methods (150). At the end of incubation period, the stratum corneum was removed and blotted dry. It was extracted with 1 mL 70% ethanol/water for another 24 h, at the same temperature used for equilibrium (32°C). The S_{SC} was determined from the amount of recovered model compound in the extraction fluid, measured by HPLC.

3.3.6 Solvent uptake in the stratum corneum

The total solvent uptake into the stratum corneum was determined from the weight difference of a piece of the dry stratum corneum (about 0.6mg) soaked in individual solvents (1 mL) for 24 h at 35°C. The stratum corneum pieces were wiped three times with Kimwipe tissues before being weighed again.

3.3 7 *In vitro* permeation study

The epidermis has cut into discs and mounted stratum corneum side uppermost in horizontal glass Franz type static diffusion cells, with 4 replicates for each vehicle. The cells had an exposed surface area of 1.33 cm² and a receptor volume of approximately 3.4mL. To assess the integrity of the epidermis, the donor and receptor chambers were filled with PBS (phosphate buffered saline pH 7.4) and the cells equilibrated for 30 min before measuring transepidermal electrical resistance with a standard multimeter. Skin samples with resistance less than 20 kΩ were considered damaged and were discarded (151). Donor and receptor chambers were then emptied and the receptor refilled with PBS. The diffusion cells were placed in a Perspex holder in a water bath, to maintain the receptor phase temperature at 35°C, and the receptors were constantly stirred with magnetic fleas (152).

The formulations (see Table 3.2) were applied to the skin at an infinite dose of 1 mL and the donor chamber was covered with a glass cover slip to minimise evaporation from the donor phase. Samples of receptor phase (200 µL) were removed at regular time points over the next 8 h and replaced with same amount of fresh PBS. All samples were analysed using HPLC.

3.3.8 *In vitro* pretreatment permeation study

The epidermis was cut into discs and mounted in horizontal glass Franz type static diffusion cells, with 4 replicates for each vehicle. Receptor compartment was filled with phosphate-buffered saline (pH7.4), maintained at 35°C in water bath. The donor doses (1 mL) of the vehicles were added to the skin and left for 2 h., covered with glass cover slip to minimise evaporation. Before application of caffeine, the excess vehicles were removed and the skin surface washed three times with water before applying 1 mL of water containing 3% caffeine. Samples of receptor phase (200 µL) were removed at regular time points over the next 8 h

and replaced with same amount of fresh PBS. All samples were analysed using a HPLC system.

3.3.9 Prediction of maximum flux

The method used the software package HSPiP generously supplied by Stephen Abbott (153) based on melting point and molar volume of the solute. The experimental temperature and the HSPs of the solute and the stratum corneum was used to predict J_{max} . The HSP distance (Ra) can be related to the mutual solubility of two substances and is given by:

$$Ra = [4(\delta_{D1} - \delta_{D2})^2 + (\delta_{P1} - \delta_{P2})^2 + (\delta_{H1} - \delta_{H2})^2]^{1/2} \quad (4)$$

Where δ_D , δ_P and δ_H are the dispersion, polar and hydrogen-bonding HSPs of the interacting substances.

This method relies solely on the properties of the solute and the interaction between it and the skin. No account is taken for the effect of the vehicle on the skin.

3.3.10 Data analysis

The cumulative amount penetrating per skin surface area (Q , $\mu\text{g}/\text{cm}^2$) was plotted against time (h). The steady state flux J_{SS} ($\mu\text{g}/\text{cm}^2/\text{h}$) was derived from the slope of the linear portion of the cumulative amount (Q) versus time (t) plot.

J_{max} , applicable to saturated solutions, is derived from the experimental steady state flux by correcting for the actual solubility in the vehicle (106). (Equation 5)

$$J_{max} = J_{SS} \cdot S_v / C_v \quad (5)$$

Where S_v is the solubility in the vehicle and C_v is the experimental vehicle concentration used.

The diffusivity of solutes in the skin divided by path length (D^*) was calculated from equation 6:

$$D^* = J_{max} / S_{sc} \quad (6)$$

The Partitioning of solute in the stratum corneum (K_{sc}) was calculated from equation 7:

$$K_{sc} = SC \text{ density} * S_{sc} / C_v \quad (7)$$

The permeability coefficient (K_p) of caffeine was calculated from equation 8

$$K_p = J_{ss} / C_v \quad (8)$$

Total solubility parameters (3D) for each of the solvents were estimated by formulating efficacy software (JW solution B.V., The Netherlands). The solubility parameter for human skin was taken from the Hanson Handbook (148).

Data were analysed by one-way analysis of variance (ANOVA) with post-hoc comparisons (Tukey in Graph pad); $P < 0.05$ was considered to be significant.

Table 3.2. Composition of vehicles used.

Caffeine^a	Minoxidil^b	Lidocaine^c	Naproxen^d
		mineral oil	
100% water		100% water *	
25% PEG 6000 /water	35% PEG6000/water	25% PEG6000/water	40% PEG6000/water
35% PEG 6000/water	50% PEG6000/water	50% PEG6000/water	50% PEG6000/water
50% PEG 6000/water	75% PEG6000/water	75% PEG6000/water	75% PEG6000/water
90% PEG 6000/water			
20% glycerol/water *	20% glycerol/water *		
3% V20/water *	3% V20/water *		5% V20/water *
25% PEG400/water *		30% PEG400/water *	5% V20/30% PEG400/water*
20% ethanol/water			
40% ethanol/water			
60% ethanol/water	60% ethanol/water	60% ethanol/ water	60% ethanol/water
60% ethanol/water/5% V20			60% ethanol/water/5% V20
			25% ethanol/water/25% V10/
60% ethanol/water/ 5% EU	60% ethanol/water/5% EU	60% ethanol/water/5% EU	60% ethanol/water/5% EU
60% ethanol/water/3% OA	60% ethanol/water/3% OA	60% ethanol/ water /3% OA	60% ethanol/ water /3% OA
60% ethanol/water/1%SLS	60% ethanol/water/1%SLS	60% ethanol/water/1%SLS	60% ethanol/water/1%SLS

Concentrations (w/v) of caffeine, minoxidil, lidocaine and naproxen were ^a3%, ^b2%, ^c2.5%, ^d2%, respectively, except those marked by *, where the solutions are saturated. Vehicles containing ethanol are shaded, with those also containing penetration enhancers in a darker shading.

3.4 Results

3.4.1 *In vitro* permeation of solutes across epidermal membranes

Figure 3.2 shows drug permeation through human epidermal membranes generally reaching a steady state by 2-4 h. The estimated steady state and maximum fluxes (J_{max} , determined from Equation 5) for all solutes are summarised in Table 3.3 (A-D). Vehicles containing EU, OA and SLS, all generally regarded as skin penetration enhancers, affected permeation fluxes to varying extents. EU and OE significantly increased the flux of caffeine, minoxidil and naproxen compared to all vehicles lacking penetration enhancers. There were no significant differences in the presence of SLS ($P>0.05$, $n=4$). On the other hand, the highest J_{max} for lidocaine came from EU and SLS.

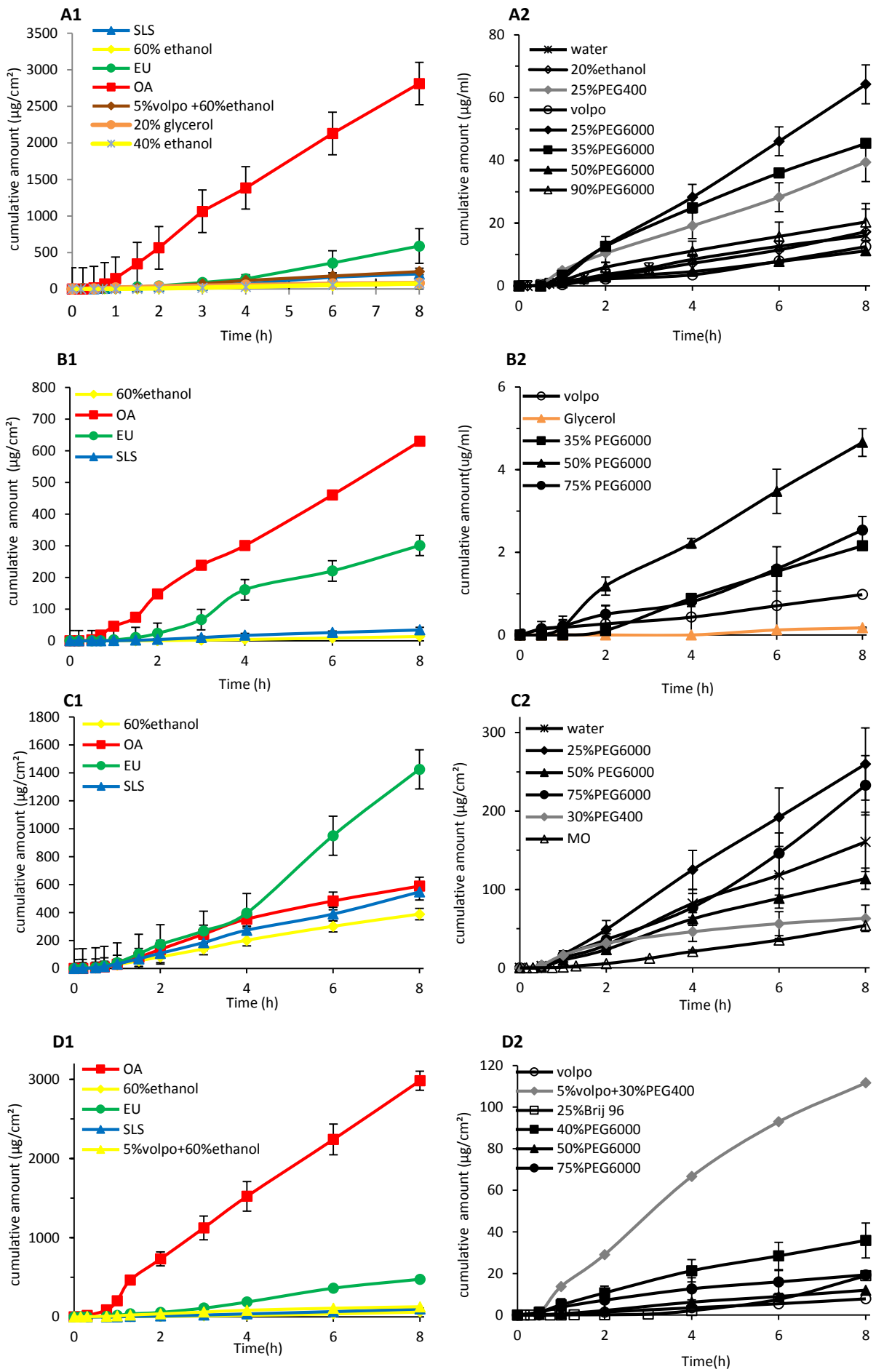


Figure 3.2 *In vitro* percutaneous permeation through epidermal human skin: A1- caffeine with penetration enhancer vehicles, A2- caffeine with controls; B1-minoxidil with penetration enhancer vehicles, B2- minoxidil with controls; C1- lidocaine with penetration enhancer vehicles, C2- lidocaine with controls; and D1- naproxen with penetration enhancer vehicles, D2- naproxen with controls (Mean± SEM, n=4).

Symbols: Black, inert controls; Red, oleic acid (OA); Green, eucalyptol (EU); Blue, sodium lauryl sulphate (SLS); Yellow, ethanol vehicles; Orange, glycerol; Grey, 5% volpo in 30% PEG400/water.

Table 3.3.

A: Caffeine

Vehicle	% Active	S_v (mg/cm ³)	J_{ss} (µg/cm ² /h)	J_{max} (µg/cm ² /h)	S_{sc} (mg/cm ³)	D^* (x10 ⁴ cm/h)
H ₂ O 100%	3	31.3±1	2.1±.16	2.2±06	21.6±2.6	1.0
H ₂ O / 25% PEG6000	3	98.5±8.2	2±2.0	6.5±3.7	98.2±0.3	0.7
H ₂ O / 35% PEG6000	3	85.2±5.2	3.5±1.8	6.7±3.7	68.2±0.3	0.2
H ₂ O / 50% PEG6000	3	57.4±9.5	1.1±.16	2.1±0.9	49.5±0.3	0.3
H ₂ O / 90% PEG6000	3	17.9±0.4	2.1±1.6	1.2±0.7	60.2±0.3	0.2
H ₂ O / 20% glycerol	Sat'd	48.1±4.5	10.5±4.0	35.0±11.6	22.9±16.2	15.3
H ₂ O / 3% V10	Sat'd	69.4±7.8	1.6±1.4	5.3±5.0	51.9±25.7	1.0
H ₂ O / 25% PEG400	Sat'd	72.8±6.7	4.7±3.0	15.5±13.0	17.5±8.3	8.8
ethanol 20% / H ₂ O	3	48.0±1.0	2.4±0.5	3.8±1.4	39.5±9.0	1.0
ethanol 40% / H ₂ O	3	71.9±1.7	11.8±3.0	28.3±8.0	54.5±24.5	5.2
60% ethanol/H ₂ O/5% V10	3	54.6±0.6	33.9±3.5	61.8±6.5	105.5±9.9	5.9
60% ethanol/ H ₂ O	3	81.5±1.1	9.4±.48	25.6±2.5	151.9±34.4	1.7
60% ethanol/ H ₂ O /1%SLS	3	74.8±1	18.1±8.8	45.2±6.0	100.9±23.5	4.5
60% ethanol/ H ₂ O / 5% EU	3	98.3±7.3	310.0±10.4	1015.8±28.9*	254.5±66.0	39.9
60% ethanol/ H ₂ O /3% OA	3	56.0±2.5	368.2±17.0	692.6±24.0*	155.9±44.7	44.4

(Mean ± 95% confidence intervals, n=4)

B: Minoxidil

Vehicles	% Active	S_v (mg/cm ³)	J_{ss} (µg/cm ² /h)	J_{max} (µg/cm ² /h)	S_{sc} (mg/cm ³)	D^* (x10 ⁴) cm/h)
35% PEG6000/water	2	15.5±2.3	0.4±0.1	0.3±0.1	13.2±0.4	0.2
50% PEG6000/water	2	39.0±0.9	0.3±0.1	0.3±0.1	12.3±4.2	0.5
75% PEG6000/water	2	73.0±1.2	0.3±0.0	0.3±0.1	15.5±0.4	0.2
20%glycerol/water	Sat'd	5.9±0.1	0.1±0.1	0.1±0.1	4.6±1.0	0.3
3%Volpo+water	Sat'd	21.6±1.2	0.1±0.1	0.1±0.1	5.3±0.6	0.2
60% ethanol/water	2	34.7±2.7	2.2±1.4	3.7±1.5	44.0±5.3	0.5
60% ethanol/water/1%SLS	2	51.4±0.7	7.8±4.7	20.0±12.2	62.6±10.4	3.2
60% ethanol/water/5% EU	2	56.0±0.6	4.3±2.2	101.6±6.2*	68.7±4.7	14.8
60% ethanol/water/3% OA	2	71.4±8.7	9.3±26.4	332.96±54.2*	133.8±8.6	24.9

(Mean ± 95% confidence intervals, n=4)

C: Lidocaine

Vehicles	% Active	S_v (mg/cm ³)	J_{ss} (µg/cm ² /h)	J_{max} (µg/cm ² /h)	S_{sc} (mg/cm ³)	D^* (x10 ⁴) cm/h)
mineral oil	2.5	44.9±2.3	7.6±0.4	7.6±0.4	29.9±4.7	2.5
100% water	sat'd	7.2±0.7	21.5±12.0	6.1±2.9	11.6±2.7	5.3
25% PEG6000/water	2.5	23.3±0.2	33.0±9.3	15.4±11.1	69.3±3.8	2.2
50% PEG6000/water	2.5	47.7±3.0	14.9±3.2	14.2±12.7	49.2±2.7	2.9
75% PEG6000/water	2.5	94.9±4.2	26.3±14.0	11.4±18.7	48.7±2.8	2.3
30% PEG400/water	sat'd	67.1±10.7	5.6±2.7	8.2±2.8	19.0±0.4	4.3
60% ethanol/ water	2.5	47.9±0.4	38.4±8.5	73.5±16.3	97.1±12.4	7.6
60% ethanol/water/1%SLS	2.5	97.4±21.0	71.9±11.4	280.3±39.4	114.1±22.5	21.7
60% ethanol/ water /5% EU	2.5	64.0±6.8	185.8±17.2	475.7±41.3	133.7±27.6	33.4
60% ethanol/ water /3% OA	2.5	62.8±13.0	72.2±28.7	181.4±64.2	107.4±11.6	15.0

(Mean ± 95% confidence intervals, n=4)

D: Naproxen

Vehicles	% Active	S_v (mg/cm ³)	J_{ss} (µg/cm ² /h)	J_{max} (µg/cm ² /h)	S_{sc} (mg/cm ³)	D^* (x10 ⁴) cm/h)
40% PEG6000/ H ₂ O	2	45.5±11.7	3.4±1.4	3.5±0.8	9.6±3.5	3.7
50% PEG6000/ H ₂ O	2	66.8±5.6	2.0±0.1	5.6±0.7	12.0±4.0	4.6
75% PEG6000/ H ₂ O	2	84.2±11.4	2.0±0.1	5.1±2.8	16.6±7.0	3.1
5% volpo/ H ₂ O	Sat'd	15.1±11.9	2.3±1.3	2.3±2.0	3.5±0.2	6.2
5%volpo/30%PEG400/H ₂ O	Sat'd	76.6±8.0	13.4±7.0	13.7±6.6	26.0±0.9	5.2
Ethanol/V10/H ₂ O (1/1/2)	2	25.9±6.9	4.1±0.9	5.3±1.4	9.5±1.6	5.6
60% ethanol/ H ₂ O /5% V10	2	51.9±0.7	14.5±1.2	37.7±3.2	37.8±2.4	9.9
60% ethanol/ H ₂ O	2	50.9±1.1	9.2±1.5	23.4±3.9	18.3±5.0	12.8
60% ethanol/ H ₂ O / 1%SLS	2	55.3±16.0	14.8±2.4	41.0±6.6	23.9±9.0	17.1
60% ethanol/ H ₂ O / 5% EU	2	20.7±14.6	72.5±7.0	74.9±12.3	38.7±1.2	11.7
60% ethanol/ H ₂ O /3% OA	2	23.9±12.0	373.3±20.5	446.3±37.9	55.6±1.8	80.2

(Mean ± 95% confidence intervals, n=4)

3.4.2 Impact of formulation on active solubility in the stratum corneum, maximum flux and derived diffusivity

To investigate some of the determinants of increased flux in these vehicles, we examined the relationships between some of the parameters in Table 3.3 (A-D). As shown in Figure 3.3 (A-D), although there were considerable differences in vehicle solubility (S_v), J_{max} was independent of S_v , for all control vehicles. Particularly those containing ethanol and may alter the properties of the skin barrier those Figure 3.3E shows J_{max} enhancement for vehicles containing ethanol, EU, OA and SLS, expressed as a ratio:

J_{max} / J_{max} (50% PEG6000 control).

The greatest enhancement was seen with EU and OA, predominantly with the more hydrophilic solutes, caffeine and minoxidil.

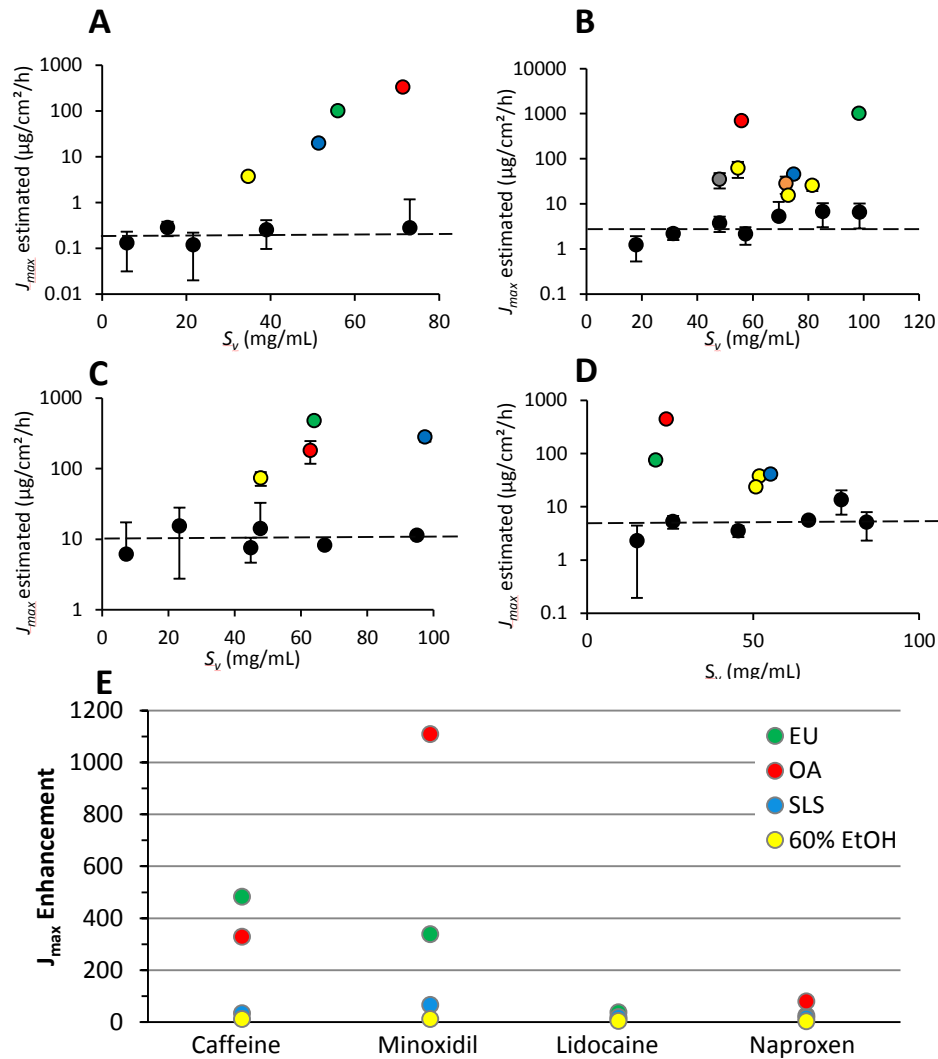


Figure 3.3. A-D, J_{max} versus solubility in the vehicles (S_v). A, Caffeine; B, Minoxidil; C, Lidocaine; D, Naproxen.

The dashed lines represent the mean of the control values. E: J_{max} enhancement ratio compared to control (50%PEG6000/water) for selected vehicles. (Mean \pm 95% confidence intervals, n=4)

Symbols: Black, inert controls; Red, oleic acid (OA); Green, eucalyptol (EU); Blue, sodium lauryl sulphate (SLS); Yellow, ethanol vehicles; Orange, glycerol; Grey, 5% volpo in 30% PEG400/water.

As expected for vehicles that do not alter the properties of the skin, there was little variation in diffusivity (D^*) amongst the control solutions for all four solutes (see Fig. 3.4A-D). Figure 3.4E shows D^* enhancement for vehicles containing ethanol, EU, OA and SLS, expressed as a ratio: D^* / D^* (50% PEG6000 control). The greatest enhancement in diffusivity was again seen with caffeine and minoxidil, applied in the EU and OA vehicles. Smaller effects were seen with SLS on caffeine diffusivity and with OA on naproxen.

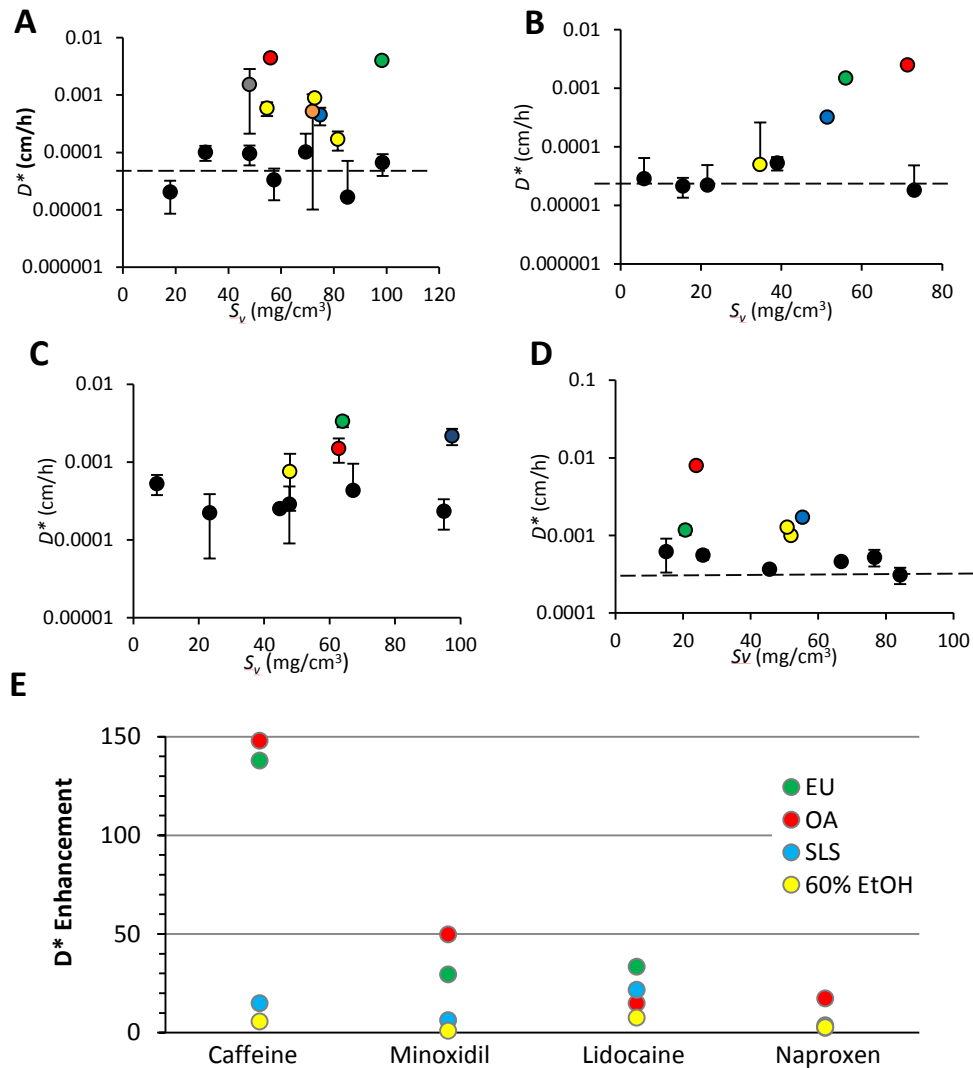


Figure 3.4. A-D, Effective diffusivity, D^* ($= D/h$) versus solubility in the vehicles (S_v). A, Caffeine; B, Minoxidil; C, Lidocaine; D, Naproxen.

The dashed lines represent the mean of the control values. E: D^* enhancement ratio compared to control (50%PEG6000/water) for selected vehicles. (Mean \pm SEM, n=4)

Symbols: Black, inert controls; Red, oleic acid (OA); Green, eucalyptol (EU); Blue, sodium lauryl sulphate (SLS); Yellow, ethanol vehicles; Orange, glycerol; Grey, 5% volpo in 30% PEG400/water.

We next explored the relationships between maximum flux and solubility in the stratum corneum. Rearranging Equation 6, we obtain $J_{max} = S_{SC} \cdot D^*$, indicating that if D^* is constant, there should be a linear relationship between J_{max} and S_{SC} (with a slope of D^* , or D/h). We have already seen that for our control vehicles, there was a minimal variation in D^* . Figure 3.5 illustrates the observed linear relationships between J_{max} and S_{SC} for each solute and the control vehicle, with R^2 values ranging from 0.67 to 0.88. Vehicles containing ethanol and penetration enhancers show elevated J_{max} values that do not fit the relationships seen with the control vehicles, reflecting the effects on diffusivity seen in Figure 3.5.

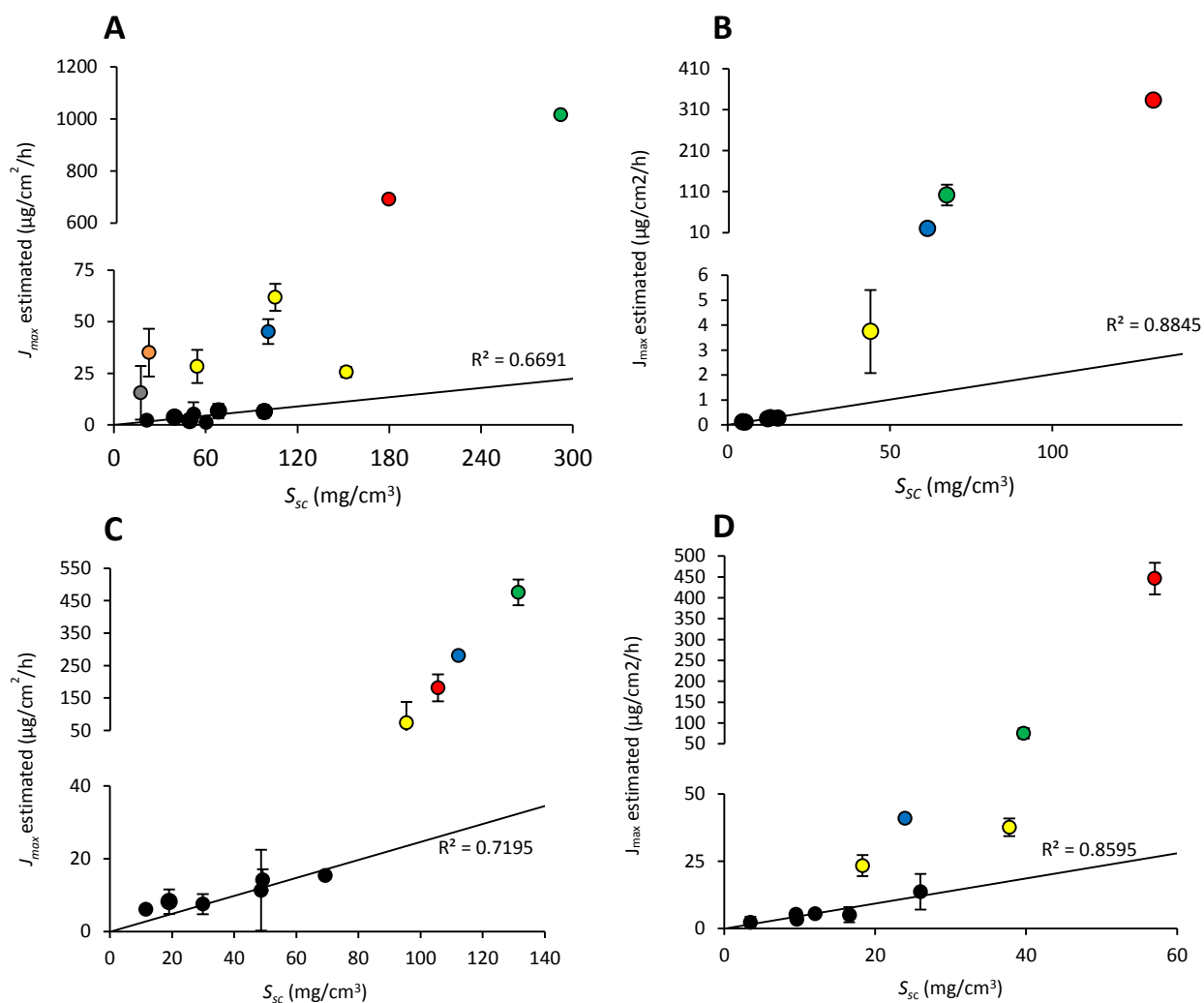


Figure 3.5 J_{max} versus solubility in the stratum corneum, S_{sc} for A, Caffeine; B, Minoxidil; C, Lidocaine; D, Naproxen (Mean \pm SEM, $n=4$).

Symbols: Black, inert controls; Red, oleic acid (OA); Green, eucalyptol (EU); Blue, sodium lauryl sulphate (SLS); Yellow, ethanol vehicles; Orange, glycerol; Grey, 5% volpo in 30% PEG400/water.

3.4.3 Mechanism underpinning the differential enhanced uptake of actives into the epidermis

We investigated the hypothesis that stratum corneum solubility was related to the amount of vehicle taken up by the membrane, carrying with it an amount of solute determined by its solubility in the vehicle. Vehicle uptake into the stratum corneum was determined by measuring the weight of pieces of stratum corneum before and after incubation in the various vehicles. Solute uptake was then estimated from this and the measured solubility of the

solutes in each vehicle (S_V). The relationships between solute solubility in the stratum corneum from each vehicle (S_{SC}) and the vehicle uptake or solute uptake are shown in Figures 3.6 and 3.7, respectively. There was a good correlation for both parameters with all compounds, with the exception of naproxen uptake, where the values for the EU and OA vehicles were seen as outliers.

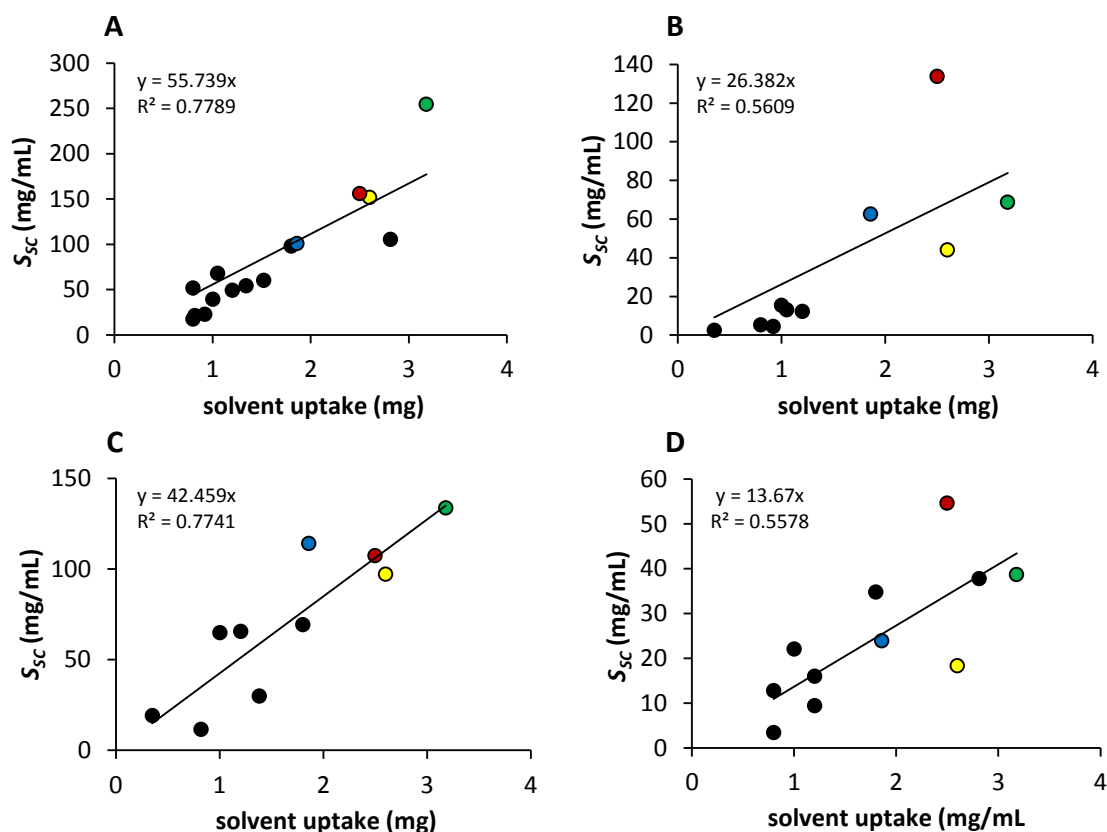


Figure 3.6 Solubility in the stratum corneum (S_{SC}) versus predicted solvent uptake values from a range of vehicles (Mean, $n=4$) for A, Caffeine; B, Minoxidil; C, Lidocaine; D, Naproxen.

Symbols: Black, inert controls; Red, oleic acid (OA); Green, eucalyptol (EU); Blue, sodium lauryl sulphate (SLS); Yellow, ethanol vehicle; Orange, glycerol; Grey, 5% volpo in 30% PEG400/water.

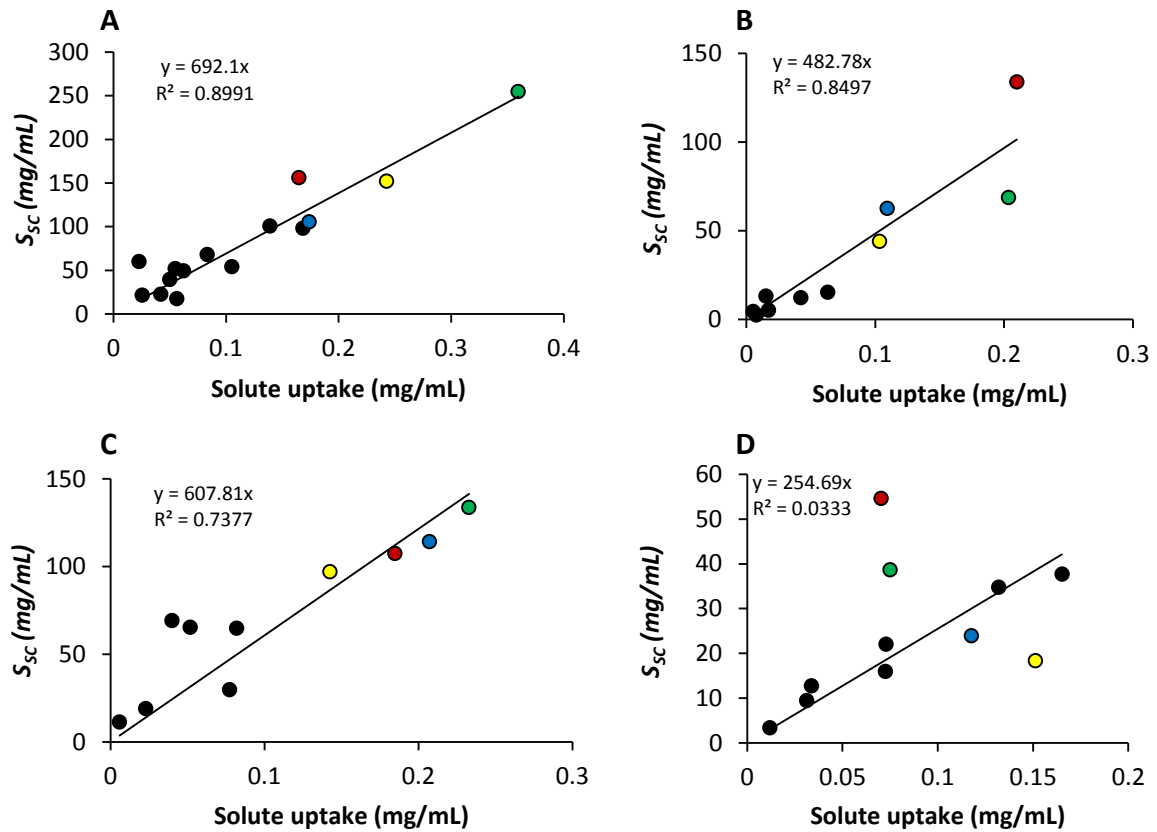


Figure 3.7. Solubility in the stratum corneum (S_{SC}) versus predicted solute uptake values from range of vehicles for A, Caffeine; B, Minoxidil; C, Lidocaine; D, Naproxen (Mean, $n=4$). *Symbols:* Black, inert controls; Red, oleic acid (OA); Green, eucalyptol (EU); Blue, sodium lauryl sulphate (SLS); Yellow, ethanol vehicle; Orange, glycerol; Grey, 5% volpo in 30% PEG400/water.

To predict stratum corneum solubility of the solutes, an optimal regression was found when it was assumed that all the dissolved solute in the vehicle was taken up into the stratum corneum as defined by:

$$S_{SC}(\text{predicted}) = S_{SC}(\text{skin, control}) + S_v * V_{up}/V_{SC} \quad (9)$$

Where V_{up} is the volume of vehicle taken up, V_{SC} is the measured volume of the stratum corneum used, and

$$S_{SC}(\text{skin, control}) = S_{SC}(\text{control, observed}) - S_v(\text{control}) * V_{up}(\text{control}) / V_{SC} \quad (10)$$

Predicted versus experimental S_{SC} plots are shown in Figure 3.8. Good correlations were seen for caffeine, minoxidil and lidocaine, with R^2 values of 0.81, 0.80 and 0.84 respectively, and 0.69 for the combined dataset of all actives. The correlation for naproxen was poor ($R^2 = 0.02$). Equation 9 under predicted S_{SC} in each case, as shown by most of the points falling below the line of identity. The underproduction is also indicated by values of Lin's

concordance correlation coefficients of 0.65, 0.86, 0.72, 0.42 and 0.73 for caffeine, minoxidil, lidocaine, naproxen and the combined dataset, respectively.

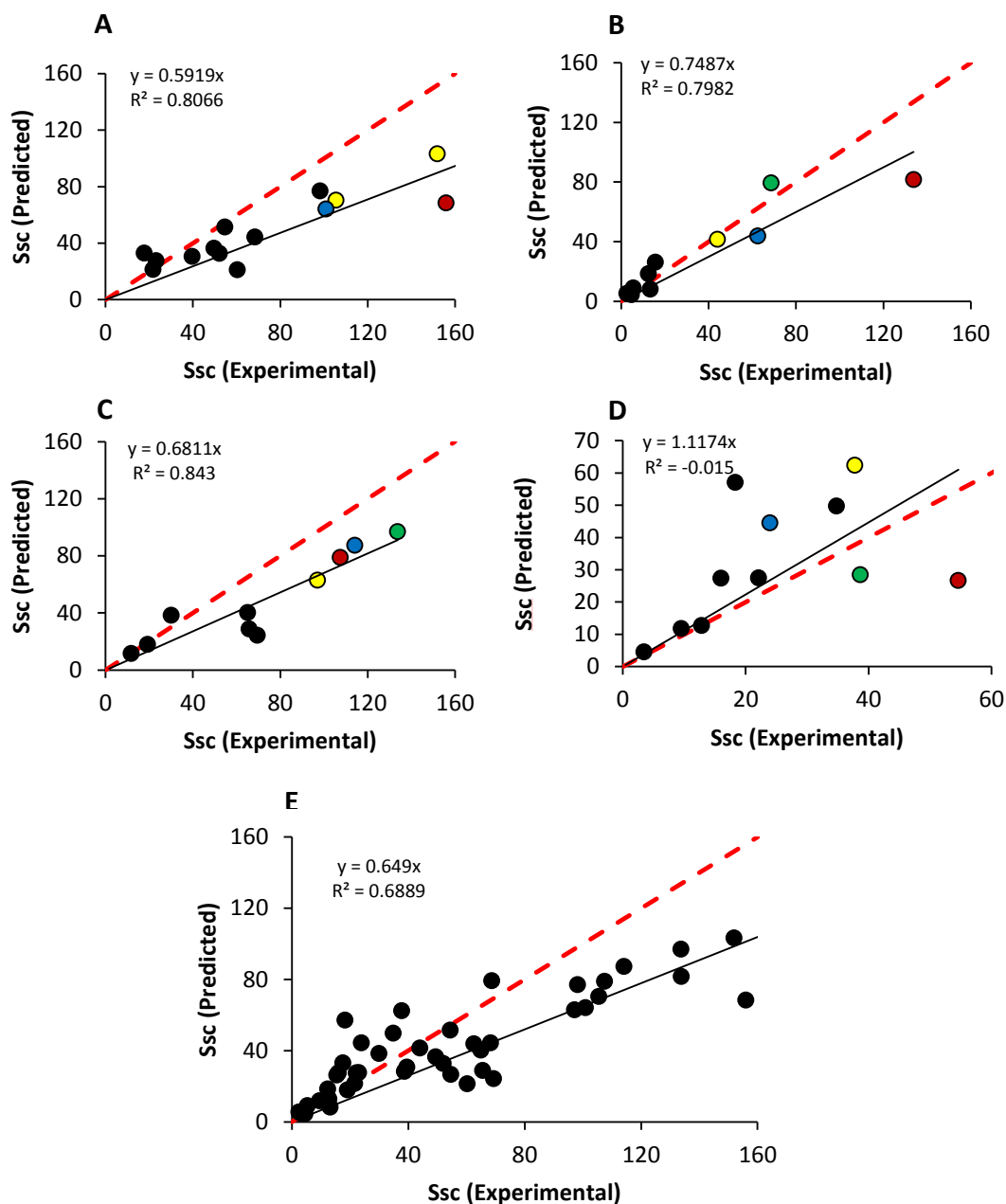


Figure 3.8. Predicted versus experimental solubility in the stratum corneum (S_{SC}) from a range of vehicles for A, Caffeine; B, Minoxidil; C, Lidocaine; D, Naproxen; E, the combined dataset (Mean, $n=4$).

Symbols: Black, inert controls; Red, oleic acid (OA); Green, eucalyptol (EU); Blue, sodium lauryl sulphate (SLS); Yellow, ethanol vehicles; Orange, glycerol; Grey, 5% volpo in 30% PEG400/water. The red dotted line is the line of identity.

3.4.4 Can the permeation fluxes of actives from various vehicles be predicted by a solubility parameter approach?

We used a method based on physicochemical properties of the solutes and the HSP interaction between the solute and the skin to predict J_{max} . This method takes no account of the properties of the vehicle or its effect on the skin. For the inert control vehicle (50% PEG-6000/water) there was a good correlation ($R^2=0.9439$) between predicted and observed $\log J_{max}$ for the four solutes (Fig. 3.9, white symbols). The regression line approximated the line of identity, with a Lin's concordance correlation coefficient of 0.9007. Minoxidil applied in the control vehicle 50% PEG-6000/water (white circle) appears to be an outlier, with a smaller observed flux than predicted.

Figure 3.9 also shows a comparison between the control vehicle and the vehicles containing 60% ethanol and the penetration enhancers EU, OA and SLS. The increased fluxes observed with these enhancing vehicles were not matched by the predicted values, supporting the view that the vehicles have modified the epidermal barrier.

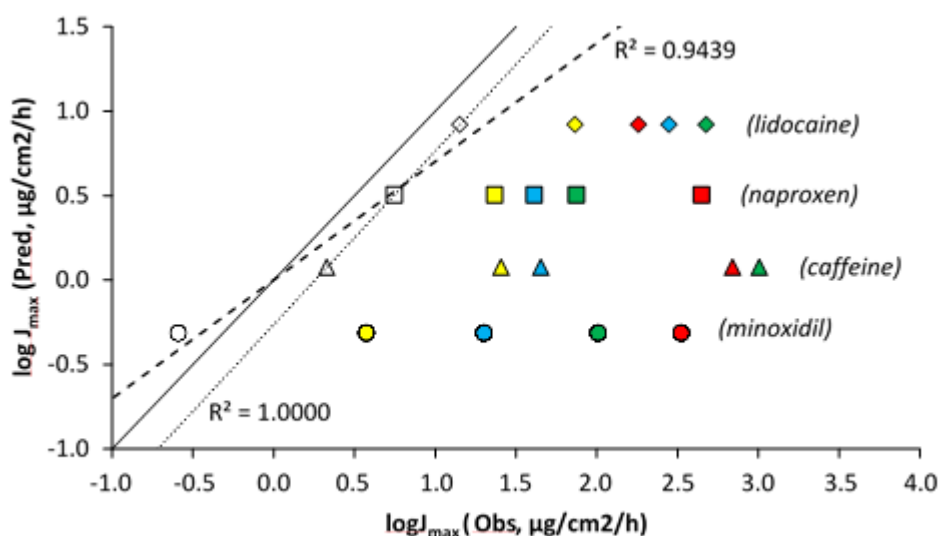


Figure 3.9. $\log J_{max}$ (predicted using Hansen solubility parameters by method of Abbott) vs $\log J_{max}$ (observed) for caffeine (triangles), minoxidil (circles), lidocaine (diamonds) and naproxen (squares) applied to human epidermal membranes in different vehicles.

Vehicles are 50% PEG6000/water (control, white symbols), 60% ethanol/water (yellow), 60% ethanol/water/1% SLS (blue), 60% ethanol/water/3% OA (red), 60% ethanol/water/5% Eucalyptol (green).

3.4.5 Caffeine vehicle solubility

The solubility of caffeine in a range of solvents (S_v) (16.6-47.8) is shown in Table 3.4. Figure 3.10 shows that with the particular solvents chosen for this study, a better relationship between solubility and δ_v was seen when the S_v increased as the solubility parameter for the vehicle approached that of caffeine. ($\delta_{total}=25$). This study agrees with a study done by Cross in 2001 on silicone membrane with hydrocortisone (104) when they claimed that the best relationship between solubility and δ_{total} may not be linear.

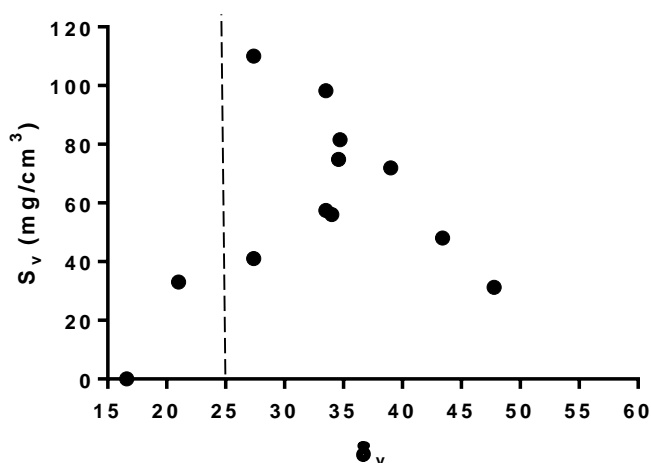


Figure 3.10. Relationship between experimentally determined caffeine solubility in each solvent (S_v) and solvent solubility parameter (δ_v). (The dashed line is the total solubility parameter area for caffeine.)

3.4 6 Penetration and solubility data

In vitro permeability of caffeine through excised human skin was examined after pretreatment with different vehicles for 2 h. Fig 3.11 shows that drug permeation generally reaches a steady state in 1-2 h, allowing a steady state flux to be established.

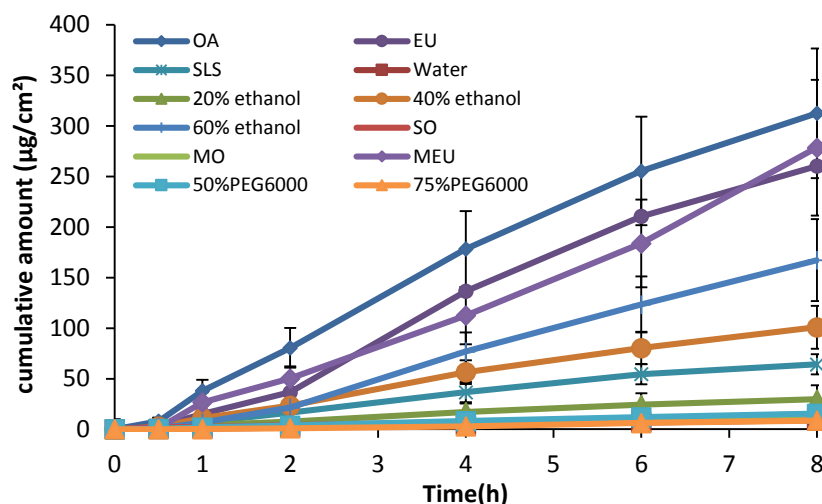


Figure 3.11 Permeation profiles of caffeine through epidermal human skin after pre-treating skin for 2 h with a range of vehicles (**Mean \pm sd, n=3**).

OA (oleic acid in 60%ethanol/water); EU (eucalyptol in 60%ethanol/water); SLS (sodium lauryl sulphate in 60%ethanol/water); MO (mineral oil); SO (silicone oil), MEU (Eucalyptol/Volpo-N10/water/ethanol).

The estimated permeation parameters for all solutes are summarised in Table 3.4. OA and EU formulations and SLS significantly increased the flux of caffeine through the epidermal human skin compared to the other vehicles. In fact, these reported the highest J_{max} for caffeine. There were no significant differences in the presence of 60% ethanol ($P < 0.05$, mean \pm SD, n=4). Generally, the effect of the Eucalyptol/Volpo-N10/water/ethanol (MEU) vehicle on the diffusivity (D^* , determined from Equation 6), of caffeine seems to be larger than those on D^* with other vehicles (Table 3.4). The effect of the penetration enhancer vehicles (EU, OA, SLS and 60% ethanol/water) on the partitioning (K_{sc} determined from Equation 8), of caffeine seems to be larger than those on K_{sc} for other vehicles (Table 3.4) The effect of pretreatment vehicles on caffeine flux is summarised in the Table 3.4.

Table 3.4 Vehicle solubility parameters and skin parameters

Formula code	Vehicles	δ_v	S_v (mg/mL)	J_{max} ($\mu\text{g}/\text{cm}^2/\text{h}$)	S_{sc} (mg/cm^3)	D^* (cm/h)	K_{sc}
Water	100% water	47.8	31.3	1.2	21.6	0.6	0.7
50%PEG6000	50% PEG6000/water	33.5	57.4	2.0	49.5	0.4	1.6
75%PEG6000	75%PEG6000/water	27.4	41.0	1.3	54.4	0.2	1.8
20% ethanol	20%ethanol/water	43.4	48.0	1.8	39.5	0.5	1.3
40% ethanol	40%ethanol/water	39.0	71.9	10.7	54.5	1.9	1.8
60% ethanol	60%ethanol/water	34.7	81.5	18.3	151.0	1.2	5.0
OA	60%ethanol/water + 5%OA	34.0	56.0	40.3	156.	2.6	5.2
EU	60%ethanol/water + 5% EU	33.5	98.3	38.9	254.6	1.5	8.5
SLS	60%ethanol/water + 1% SLS	34.6	74.8	20.1	100.9	2.0	3.4
MO	Mineral oil	16.6	0.4	0.002	0.4	-	-
SO	50% Silicone/volpo/water/ethanol	21.0	33.7	2.1	47.7	0.4	1.6
MEU	Eucalyptol/Volpo- N10/water/ethanol	27.4	110.0	37.2	35.5	10.2	1.2

Enhancement ratio of the flux was greatest after pretreatment with the penetration enhancer vehicles. However, the flux was not enhanced to the same extent (Fig 3.12). Also, the enhancement partitioning ratio of caffeine into the stratum corneum is generally higher for OA and EU solutions (Fig 3.12).

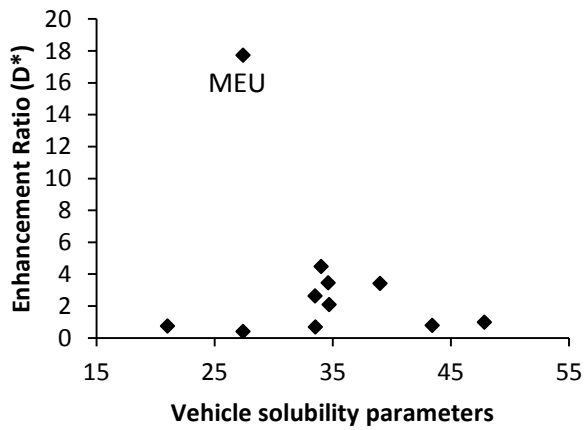
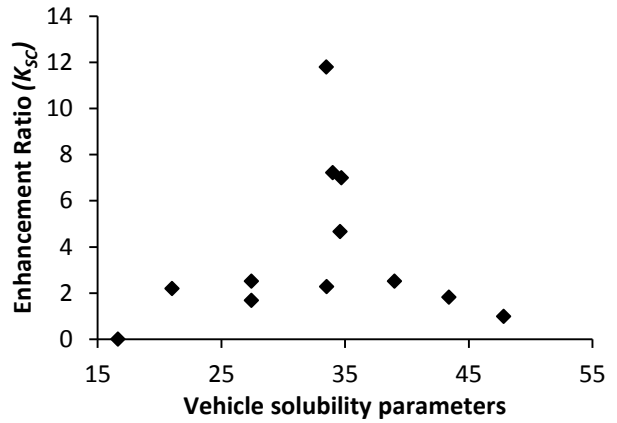
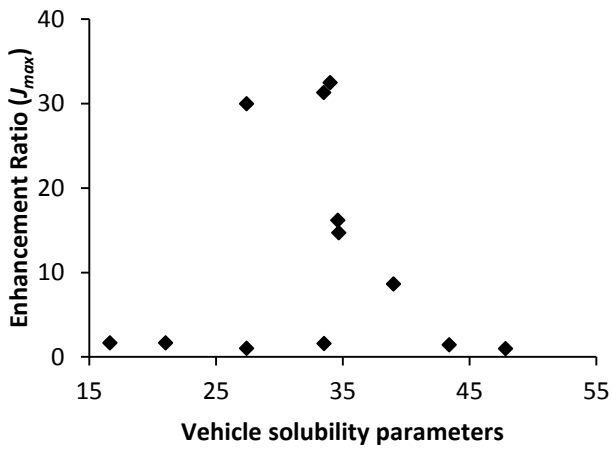


Figure 3.12 Mean plot summarising the effect of Hansen solubility parameter of vehicle on enhancement of J_{max} , partition and diffusion.

MEU (eucalyptol, Volpo-N10, ethanol and water).

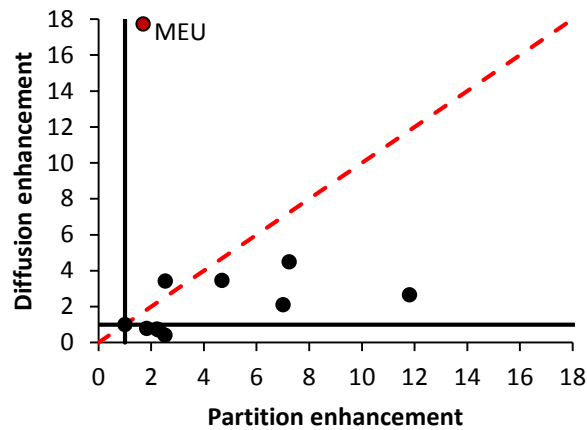


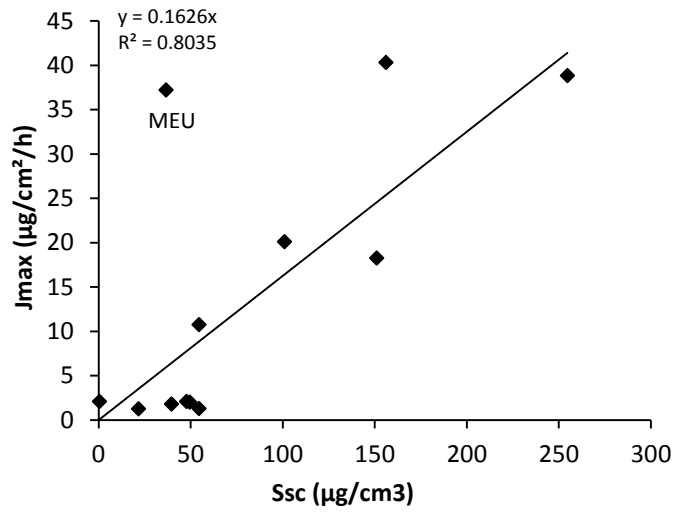
Figure 3.13 Composite of the effects of vehicle pretreatment on diffusion and partition of caffeine. (The red line is the identity line).

MEU (eucalyptol, Volpo-N10, ethanol and water).

Figure 3.13 is the composite plot for caffeine with all vehicles. The line of identity suggests that the enhancement mechanism is an increase into the partition of the epidermis.

The J_{max} and S_{SC} of caffeine from each vehicle in the δ_v range (16-48) are shown in Figure 3.14. A linear relationship, found between J_{max} and S_{SC} $R^2=0.80$, can be seen when all points are considered. Also a linear relationship was found between the caffeine permeability coefficient (K_P) and S_{SC} $R^2=0.80$ (Fig 3.14B).

A



B

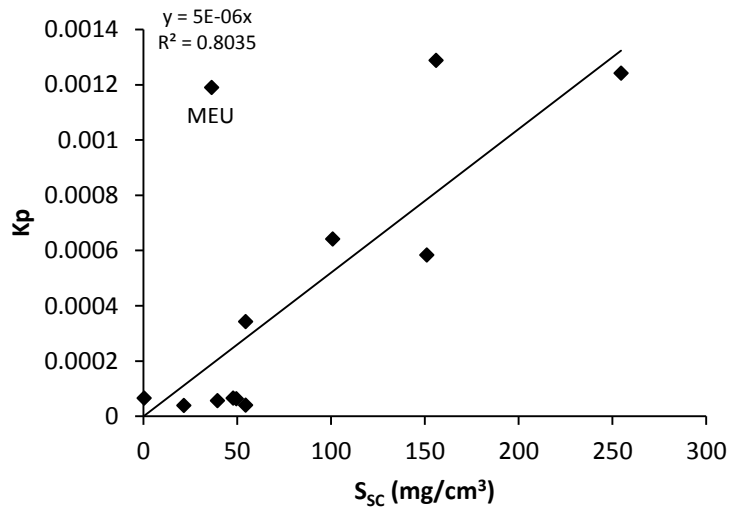


Figure 3.14 Relationship between (A) J_{max} and S_{sc} and (B) caffeine permeability coefficient (K_p) and S_{sc} .

MEU (eucalyptol, Volpo-N10, ethanol and water).

3.5 Discussion

This work has revealed marked differences in the epidermal permeation of solutes using different solution vehicles, some of which contained excipients that were hypothesised to alter the properties of skin. This was demonstrated by differences in solute uptake into the stratum corneum, permeation maximum flux and derived diffusivity. Interpretation of our results adds to our mechanistic understanding on how vehicles effect the penetration of different solutes. Our findings of selective permeation enhancement can be understood in terms of three mechanisms: i) alterations in the solubility of the drug in the applied vehicle, ii) uptake of the vehicle carrying the active compounds into the stratum corneum, and iii) changes in the properties of the stratum corneum membrane, such as fluidisation of the lipid bilayers.

In this work, we estimated the solute maximum (or saturated) fluxes (J_{max}) as a measure of skin permeation rates. It has long been recognised that maximum flux is independent of the vehicle and dependent solely on the thermodynamic activity of the solute in the vehicle, provided the vehicle or solute does not alter the properties of the membrane (154). This concept was initially highlighted in the work of Twist and Zatz (155), who showed the same flux for methyl paraben across synthetic membranes, regardless of its solubility in a range of different vehicles. More recently, we published similar findings on the epidermal permeation of a group of phenols with similar molecular weights but different log P values (106-108). Our results for the control solutions here are consistent with these findings in that similar low values for J_{max} were found for each control solutions not affecting skin permeability across a range of vehicle solubilities. In contrast, the J_{max} values seen with the enhancer solutions and to some extent, ethanol/water, are much higher than the controls, indicating that these vehicles have altered the properties of the stratum corneum.

An interesting result from this work was the predominant effect on J_{max} and D^* seen with the more hydrophilic solutes, caffeine and minoxidil, compared to lidocaine and naproxen. This suggests that flux increases in these compounds are driven by increased diffusivity. It is well recognised that diffusivity is independent of solute lipophilicity when the vehicle does not alter the properties of the stratum corneum (107, 141). However, this may not be the case when the vehicle does affect the stratum corneum. For example, we (107) recently showed enhanced diffusivity for the more hydrophilic phenols applied to epidermal membranes in isopropyl myristate (IPM), a vehicle that has a high affinity for the skin and can disrupt stratum corneum lipid arrangements (156). The diffusivity-driven increases in caffeine permeation seen here, particularly with the EU vehicle, were consistent with previous work

showing increased diffusivity of the polar compound 5-FU with EU enhancers, which was explained in terms of disruption of stratum corneum lipids (157). Skin permeation of the lipophilic compound tamoxifen has also been shown to be enhanced by terpenes, due to enhanced partitioning into the stratum corneum (158). Williams and Barry (159) suggested that generally, partitioning plays a greater role in enhancement of more lipophilic substances.

The relationship between stratum corneum solubility and solute maximum flux and the recognition that the stratum corneum solubility depends upon both solvent and solute uptake into the stratum corneum were key findings in this work. Firstly, our results, showing good linear relationships between J_{max} and solubility in the stratum corneum for the control vehicles but not for the vehicles that affected the skin, are consistent with our previous findings (106-108). This supports the concept that dual mechanisms for permeation enhancement, stratum corneum solubility and diffusion, may be acting in varying degrees in these systems. The observed correlations between stratum corneum solubility and solute or solvent uptake prompted us to hypothesise that the solvent acts as a carrier to draw solute into the stratum corneum. Interestingly, the points for the penetration enhancer vehicles generally follow the same linear regression lines as those for the controls in Figures 3.6 and 3.7, whereas they do not in Figure 3.5. This suggests that enhanced fluxes for these compounds may be mainly driven by diffusivity rather than stratum corneum solubility.

Polyethylene glycols (PEGs) are used in a great variety of cosmetic applications because of their solubility and viscosity properties and because of their low toxicity (160). Based on available data, the PEGs with a wide molecular weight range (200 to 10000) are safe for use in cosmetic products (160). It was clear from our results that PEG6000 vehicles were inert and did not penetrate skin, as would be expected for a compound of such a high molecular weight. The vehicles containing EU, OA and SLS also contained 60% ethanol, while some of the other vehicles had 20%, 40% and 60% ethanol/water. Generally, the responses with ethanol/water solutions alone were less than those with the enhancers. The influence of ethanol in aqueous solutions in the transport of hydrophilic and lipophilic drugs has been investigated and it has been suggested that ethanol has no or little effect in penetration at low levels. However, at higher concentrations, it can cause extraction of lipids (57, 161-163), which is consistent with our results. Pershing et al. found that ethanol enhances the flux of oestradiol across human skin without affecting diffusion, while increasing the solubility of drug in the membrane (164). This work also found that 60% ethanol/water with caffeine, minoxidil and lidocaine had little effect on diffusivity but

increased the solubility of these solutes in the stratum corneum. Ethanol is a volatile solvent and evaporation can lead to increased drug concentration and a greater driving force for permeation (45, 57, 165), although this is unlikely to have occurred in our infinite dose experiments here.

We attempted to use solubility parameters to predict solute maximum fluxes and from this to distinguish between vehicles that do or do not affect the skin. The prediction depends entirely on the properties of the solute (molar volume, melting point), the HSPs of the solute and the skin and the experimental temperature. It therefore applies only to inert vehicles that have no effect on the skin. Deviations of observed fluxes from the predicted values could be attributed, in part, to skin effects. The plot of predicted versus observed J_{max} values for a typical inert vehicle that was used for all solutes (50% PEG-6000/water) showed excellent correlation and concordance. It was noted that J_{max} for minoxidil was over-predicted by the solubility parameter method. The pKa of minoxidil is 4.61 and we believe that at the pH at which the experiment was performed, the compound was substantially ionised, leading to a lower than expected experimental flux. A better fit to the predicted correlation line would be obtained if the minoxidil point was adjusted to account for the degree of ionisation. As expected, given that the HSP prediction of J_{max} takes no account of vehicle effects on the skin, there were significant deviations from predicted values seen for the four vehicles shown in Figure 3.9. The 60% ethanol/water and the ethanol/water/SLS vehicles showed the least deviation, as seen above. We also applied a published regression based on a large literature database (89) to predict J_{max} (data not shown). This used solute properties (log P, molecular weight and melting point) and once again, took no account of vehicle-skin interactions. The resulting correlation between predicted and observed J_{max} values was almost identical to that obtained with the HSP prediction, but with a poorer correlation coefficient (0.7344). Recently, Riviere reported a quantitative structure permeability model to predict *in vitro* permeation of some ectoparasiticides through porcine and canine skin that accounted for both the physicochemical properties of the penetrant and the formulation components (166).

For the pretreatment study, the principal goals were to find the relationship between total solubility parameters, solute, solvents and skin. The important finding in this work is the parabolic relationship between enhancement ratio for J_{max} , K_{SC} , S_V and δ_V for the vehicles which interacted with skin and straight line in vehicles which did not interact with skin (inert) such as water and PEG6000 vehicles. The treatment result with the caffeine showed a linear relationship between J_{max} , and S_{SC} ; the same finding has been shown with pretreatment

results. The effect of vehicles on flux is summarised in mean effect plot (Fig 3.12 and Table 3.4). Enhancement is generally higher for OA, EU and eucalyptol vehicle MEU. It is noted that Hansen 2007 (148) considered the stratum corneum to have 30 (total solubility δ_v) implying that vehicles with a value close to this should mix easily with the skin and have maximal enhancement properties. This is seen in the present study, which shows that any vehicle in the range close to 30 will penetrate the barrier effectively. This hypothesis is in accordance with the similarity in enhancement values for most vehicles. After recognising that J_{max} was increased by vehicle pretreatment, we proceeded to separate it into its partition and diffusion components. Vehicles can strongly effect permeation through the stratum corneum barrier by altering the partitioning coefficient between the vehicles and the membrane (K_{SC}) and or solute diffusion (D^*) within the membrane (167). The K_{SC} is a kinetic effect that could be related to structural effects such as alterations to the stratum corneum cells structure. As mentioned earlier, if the vehicle has no effect on the skin, the J_{max} of a given solute appears to be independent of vehicles for saturated solutions. This has been noted experimentally (168), (107) for many vehicles. However, the ones known as penetration enhancers are either entering the skin to change partitioning and diffusion or removing the skin components. The partitioning coefficient K_{SC} was determined experimentally as described, so the apparent diffusivity D^* could be found indirectly from J_{SS}/K_{SC} . The main effects plots for K_{SC} and D^* are shown in Figure 3.12. Generally the effects of a vehicle on K_{SC} seem to be similar to those on D^* , but trend with respect to δ_v can be seen. Water, MO, PEG6000 vehicles, silicone oil and 20% ethanol/water as expected have no effect on any of the three factors J_{max} , K_{SC} and D^* .

Figure 3.13 is a line of identity, so it is apparent that the effect of vehicles on partitioning is more than on diffusion, suggesting that the enhancement mechanism includes a high increase in the thermodynamic (partition). These results agree with Rosado et al's (167) finding that the enhancement mechanism includes a greater increase in the thermodynamic (partition) than in the kinetic (diffusion). The maximum flux of compounds was increased by increasing the solubility of these compounds in the stratum corneum lipids (Table 3.4). A linear relationship found between J_{max} and S_{SC} , $r^2=0.80$, could be seen when all points were considered (Fig 3.14A). A linear relationship was found between caffeine permeability coefficient (K_p) and S_{SC} $r^2=0.80$ (Fig 3.14B). In future, expansion of the HSP or other approaches to account for vehicle-skin interactions would be valuable to provide more realistic predictions that can be generally applied.

3.6 Conclusions

This study has shown that the permeation of caffeine, minoxidil, lidocaine and naproxen were selectively enhanced by vehicles containing specific excipients that were hypothesised to alter the properties of skin (OA, EU, SLS and ethanol). The greatest effects were seen on flux and diffusivity by the EU and OA vehicles on the more hydrophilic compounds, caffeine and minoxidil. Enhancements in stratum corneum solubility were predicted by experimentally determined uptake of solvent and solute. We conclude that enhanced solute fluxes are mainly driven by increased diffusivity in the stratum corneum, likely to be due to greater lipid fluidisation caused by the enhancers. In the pretreatment study, there was enhancement of caffeine flux following penetration enhancer vehicles pretreatment of heat separated epidermis. Enhancement could be related to HSPs of the vehicle. Calibration of the solute flux and its solubility in the stratum corneum data is a simple novel plotting procedure that separated and quantified the effects of the vehicle on solute partition and diffusion. The treatment and pretreatment results indicate that mainly, enhancement is related to an increase in partition into skin with an increase in diffusivity. The diffusivity was obtained for all compounds and was unaffected by the inert control vehicles (controls) supporting the notion that J_{max} is determined by stratum corneum solubilities and not diffusivity.

Chapter 4

Synergistic skin penetration enhancer and nanoemulsion formulations promote the human epidermal permeation of caffeine and naproxen

4.1 Abstract

Targeted delivery of topically applied drugs to various skin compartments, including hair follicles, can be achieved by designing an optimised drug delivery system. One of the many ways of enhancing delivery through the skin is by formulation optimisation. They are considered as novel alternatives to conventional transdermal delivery systems and the main reasons include simplicity of the formulation process, stability of the system and a high potential in pharmaceutical applications. Nanoemulsions, a formulation, act as efficient vehicles for topical drug delivery mainly due to their potential of providing enhanced solubility and improved bioavailability. The aim of this study is to assess delivery of caffeine, a model hydrophilic compound and Naproxen, a model lipophilic compound across human epidermal and full-thickness skin, utilising nanoemulsion formulations containing oleic acid (OA) and eucalyptol (EU) as oil phases. Evaluations were also undertaken to prove that the maximum flux of the compounds may be enhanced by either increasing their solubility in the stratum corneum lipid component or by increasing the diffusivity of the solutes in the stratum corneum. Two oil-in-water (O/W) nanoemulsion formulations containing caffeine and naproxen (3% and 2% w/w, respectively) with OA or EU as oil phases were prepared. The proportion of the surfactant, co-surfactant and aqueous phase was selected through the construction of a pseudo-ternary phase diagram. The formed systems were characterised using particle size, measurement of electrical conductivity, viscosity and refractive index. Nanoemulsions and controls consisting of 3% w/w caffeine in water (C1), 60% ethanol/water (C2), or 50% PEG₆₀₀₀/water (C3); 2% naproxen in 60% ethanol/water (C2) or 25% ethanol, 25% volpo-N10 and 50% water (C4) were applied to epidermal and excised full-thickness human abdominal skin in Franz diffusion cells (n=4) for 8 h. The stratum corneum distribution of the chosen model drugs was studied using the tape-stripping technique. The amount of caffeine and naproxen in receptor fluid, extracts of tape strips (20 times) and skin was quantified using HPLC. The effect of the nanoemulsion formulation on the skin and the delivery route was determined using Multiphoton microscopy (MPM). The results depicted that both O/W nanoemulsions significantly enhanced the delivery of caffeine that permeated across as well as was retained in the skin as compared to the controls. The rate of penetration of naproxen through the skin (epidermis and full-thickness skin) (flux) as well as

the amount retained in the skin were significantly greater than for all the controls ($p < 0.005$) for both O/W nanoemulsions, whereas no significant differences in flux and skin retention between the EU and OA nanoemulsions was observed. For Naproxen, it was found that the maximum flux was related to the stratum corneum solubility of the nanoemulsion formulation and the amount of vehicle absorbed into the stratum corneum, as well as the amount of naproxen dissolved in that absorbed vehicle. Caffeine maximum flux enhancement was found to be associated with increased skin diffusivity. These relationships were reflected in the uptake of active compound into the stratum corneum, carried with the vehicle being taken up. Also, estimated diffusivity appeared to be vehicle independent. Images of nanoemulsion treated skin showed altered stratum corneum barrier structure. In the case of caffeine, the transdermal flux from EU formulations was higher than OA nanoemulsions but the amount retained in the stratum corneum and skin were not significantly different for these formulations. In conclusion, both the nanoemulsion systems in this study significantly enhanced penetration of caffeine and naproxen. The possible cause of enhancement may be due to alterations in the stratum corneum barrier structure due to the presence of EU and OA as penetration enhancers in the formulation. Further work is needed, directed at applying theoretical principles based on HSPs to design formulations for improved targeting of specific skin layers.

4.2 Introduction

Percutaneous absorption offers an attractive non-invasive route of administration for local topical or systemic effects of substances but is limited by the skin's inherent barrier to penetration of any exogenous material. It is well established that the uppermost layer of the skin, the stratum corneum, is the main barrier to such penetration but can be overcome to meet therapeutic and cosmetic goals by prudent considerations of the active's potency, physicochemical properties, formulation and delivery systems (169). Formulation approaches include optimisation, use of pro-drugs and incorporation of chemical or biological modifiers to transiently reduce stratum corneum barrier function. The range of delivery systems in current use include: topical products, transdermal patches, physical methods such as microneedles and heat as well as other technologies, including iontophoresis, sonophoresis, radiofrequency and laser ablation(169).

Microemulsions, defined as single phase and thermodynamically stable isotropic systems composed of water, oil and amphiphilic molecules (170), are attractive systems for enhancing drug delivery to the skin because of their ease of formulation, thermodynamic

stability and solubilisation(171). They are capable of incorporating and enhancing the skin delivery of both hydrophilic and lipophilic drugs (172, 173) and are considered to be more stable than conventional emulsions because of their small droplet sizes preventing phase separation. Moreover, small droplet size provides better adherence to membranes, leading to more efficient transport of drug molecules in a controlled fashion (174, 175).

Micro- and nanoemulsions may be categorised into three main types: water in oil (W/O), bicontinuous and O/W though a mixture of oil, water and surfactants will be able to generate a variety of structures and phases (173, 176, 177). When similar amounts of oil and water are used, the structures formed are not well characterised and are assumed to be continuous (178). While micro- and nanoemulsion formation depends on the capacity of the surfactant system to decrease the surface tension, in practice almost all surfactants require the presence of additional co-surfactants. Excipients such as short- or long-chain alcohols or polyglycerol derivatives have been used to achieve low surface tension. Addition of a co-surfactant reduces the interfacial tension as well as the critical micelle concentration. The correct selection of components is the main factor to be considered when formulating microemulsions for topical or transdermal delivery (179). Micro- and nanoemulsions may enhance topical and transdermal delivery mainly by increasing the solubilisation capacity for hydrophilic and lipophilic compounds, maintaining constant supply of the drug from the internal to the external phase and thus keeping the external phase saturated and promoting skin absorption. The formulation ingredients such as the oil, surfactants, co-surfactants and penetration enhancers may increase drug diffusion by enhancing partitioning through the skin. Also, the low interfacial tension required for micro- and nanoemulsion formations may be responsible for the excellent wetting properties, which ensures surface contact between the membrane and the vehicle (180). In addition to their favourable permeation enhancement properties, micro- and nanoemulsions may also reduce skin irritancy of certain excipients. For example, an aqueous solution containing 20% propylene glycol was shown to cause irritation, but the same concentration of propylene glycol used as a co-surfactant in microemulsion formulations did not (181).

The components of the oil phase in a microemulsion may include penetration enhancers such as lecithin, hydrophilic terpenes such as EU or unsaturated fatty acids such as OA to enhance the permeation of the active through the skin without causing local irritation (182, 183). Studies suggest that these penetration enhancers may cause disruption of the stratum corneum lipid organisation thus increasing the fluidity and decreasing diffusion resistance to solutes (182, 184). In this study OA and EU were selected as the penetration enhancers.

The objective of this study was to investigate the synergy of using skin penetration enhancers in nanoemulsions on human epidermal permeation for a model hydrophilic compound (caffeine; log P, -0.07) and a lipophilic compound (naproxen; log P, 3.18). OA and EU were the penetration enhancers studied. Each formulation was characterised in terms of its physical and chemical properties, including deriving their apparent solubility parameters. We then carried out *in vitro* human epidermal permeability studies in Franz diffusion cells and evaluated the permeation of caffeine and naproxen from nanoemulsions, formulated with skin penetration enhancers as the oil phase, and various control solutions. As described in our previous work (108, 185), we also estimated for each active ingredient its saturated flux, solubility in the stratum corneum and diffusivity as well as quantifying the extent of formulation uptake into the stratum corneum. These were then used to investigate the mechanism by which the nanoemulsions facilitated an enhanced permeation of the active ingredient across the human epidermis. We also examined the effects of these microemulsions on the full-thickness skin.

4.3. Materials and Methods

Caffeine, naproxen, ethanol, oleic acid (OA), eucalyptol (EU), were purchased from Sigma-Aldrich Pty. Ltd. (Sydney, Australia). Volpo-N10 was obtained from Umigema (Witton Centre, Witton Redcar TS10 4RF, UK). All chromatography reagents were analytical grade.

4.3.1 Preparation of Emulsions

Volpo-N10 (surfactant) was dissolved in ethanol (co-surfactant) in a 1:1 ratio. The resulting mixture was then mixed with the oil phase, OA or EU (oil) in a 0.6:1:1 ratio followed by gentle mixing with phosphate buffered saline (PBS). The resulting nanoemulsions were clear at room temperature. Caffeine and naproxen were dissolved in the nanoemulsions and control solutions at 3% w/w and 2% w/w, respectively. A pseudo-ternary phase diagram was constructed using the water titration method. At the weight ratio of 1:1 the highest amount of water was solubilised in the system. The O/(S/Co-S) mixture was diluted drop wise with PBS under moderate agitation. The samples were classified as nanoemulsions when they appeared as clear liquids. The compositions of emulsions and control solutions made are shown in Table 4.1.

Table 4.1 Compositions (% w/w) of nanoemulsions formulations (C3 and C4), with penetration enhancers eucalyptol (E1 and E2) and oleic acid (O1 and O2), and control mixtures (C1 – C2). The concentration of caffeine (marked as ^C) dissolved in aqueous controls and nanoemulsions was 3% w/w, whereas a concentration of 2% w/w was used for naproxen (marked as ^N).

	Water	Ethanol	PEG-6000	Volpo-N10	Eucalyptol	Oleic Acid
C1^C	100	-	-	-	-	-
C2^{C,N}	40	60	-	-	-	-
C3^C	75	-	25	-	-	-
C4^N	50	25	-	25	-	-
E1^{C,N}	30.97	26.55	-	26.55	15.93	-
E2^{C,N}	36.59	24.39	-	24.39	14.63	-
O1^{C,N}	30.97	26.55	-	26.55	-	15.93
O2^{C,N}	36.59	24.39	-	24.39	-	14.63

4.3.2 Characterisation of emulsions

The droplet size distributions, refractive indices and electrical conductivities of the emulsions were determined at ambient temperature using dynamic light scattering (Zetasizer Nano ZS, Malvern Instruments, Ltd, Malvern, UK), on a RFM34 refractometer (Bellingham & Stanley, UK) and a Digitor multimeter (DSE, Australia), respectively. Electrical conductivity measurement enables identification of the continuous phase of the emulsion, with O/W emulsions being conductive, while W/O emulsions are not. The viscosity of the emulsion formulations was measured using a U-tube viscometer at 25°C. All determinations were done with three replicates.

4.3.3 Human skin preparation

Skin samples were obtained with informed consent from female patients undergoing elective abdominoplasty, and approval from The University of Queensland Human Research Ethics Committee (HREC Approval no. 2008001342). The procedures were conducted in compliance with guidelines of the National Health and Medical Research Council of Australia. Full-thickness skin was prepared by removal of subcutaneous fat by blunt

dissection. Heat separation was used to separate epidermal membranes from full-thickness skin, by immersing it in water at 60°C for 1 min, to allow the epidermis to be teased away from the dermis (186). Stratum corneum was prepared from the epidermal membranes by trypsin digestion (187). The epidermis was floated overnight on a solution of 0.01% trypsin in PBS at 37°C. The digested viable epidermis was gently scraped off with cotton buds and the remaining stratum corneum membrane was rinsed several times with distilled water. The isolated stratum corneum membranes were dried with absorbent paper and placed flat between parafilm sheets covered with aluminium foil. All skin membranes were stored frozen at -20°C until use.

4.3.4 Determination of the solubility of actives in the various formulations (S_v)

The solubility of caffeine and naproxen in each formulation (S_v) was determined by adding caffeine or naproxen to 5 mL of each nanoemulsion or control solution until an excess amount remained. The samples were then incubated in a water bath at 32°C for 24 h with continuous agitation and centrifuged at 4700 rpm for 10 minutes. The supernatant was withdrawn and diluted to accurately quantify the amount of each compound by HPLC.

4.3.5 Determination of solubility in the stratum corneum (S_{sc}) and solvent uptake

To determine the stratum corneum solubilities of caffeine and naproxen from the various vehicles, pre-weighed discs of stratum corneum (4 replicates for each compound) were incubated in 1 mL saturated solutions of each compound in the various vehicles at 32°C for 24 h (187). At the end of the incubation period, the stratum corneum discs were removed and blotted dry and further incubated with 1 mL of 70% ethanol/water for 24 h at 32°C to enable complete extraction of the solutes. S_{sc} was determined from the amount recovered in the extraction fluid measured by HPLC divided by the thickness and area of the stratum corneum (185). The total solvent uptake into the stratum corneum was determined from the weight differences of the dry pieces of the stratum corneum (about 0.7mg) soaked in each formulation (1mL) for 24 h at 32°C. The stratum corneum pieces were wiped three times with Kimwipe tissues before being weighed again.

4.3.6 *In vitro* skin penetration and distribution study

In vitro skin permeation studies were performed with epidermal skin in Franz diffusion cells with an effective diffusion area of 1.33cm² and an approximate receptor chamber capacity of 3.4 mL. The skin was cut into discs and mounted between the donor and receptor

compartment of the Franz cell with the stratum corneum side facing the donor chamber. The receptor compartment containing PBS (pH 7.4) was immersed in a water bath at $35\pm 0.5^{\circ}\text{C}$. The donor solution consisted of 1 mL of the nanoemulsions or control formulations, containing either 3% w/w caffeine or 2% w/w naproxen. The donor compartment was covered with parafilm to prevent evaporation. At pre-determined time points, 200 μL of the receptor phase was withdrawn and replaced with an equal volume of fresh PBS.

In vitro skin absorption studies were performed with full-thickness human abdominal skin in Franz diffusion cells as described previously. The skin was cut into discs and mounted in between the donor and receptor compartment of the Franz cell with the stratum corneum side facing the donor chamber. The receptor compartment containing PBS (pH 7.4) was immersed in a water bath at $35\pm 0.5^{\circ}\text{C}$. The donor solution consisted of 1 mL of nanoemulsion formulations (with 3% and 2% w/w of caffeine and naproxen, respectively) or control formulations. The donor compartment was covered with parafilm to prevent evaporation. At pre-determined time points, 200 μL of the receptor phase was withdrawn and replaced with an equal volume of fresh PBS over the duration of the study. The caffeine and naproxen content in the samples was determined using HPLC. On completion of the diffusion studies, the donor remaining at the end was withdrawn and the skin in each cell was wiped with a cotton bud to remove any formulation. This was followed by tape stripping (20 tape strips) to separate the stratum corneum from the epidermis by application of adhesive tape (D-Squame tapes, CuDerm Corp., TX) to the exposed skin surface for about 5 seconds. Tapes were placed in separate scintillation vials, soaked overnight with 2 mL methanol with constant shaking. The amount of absorbed material in the stratum corneum was determined by HPLC. The amounts in the first tape were not included, as this represents surface material. Subsequent to tape stripping, the remaining skin was sliced into small sections; homogenised and soaked overnight with 2 mL methanol under constant shaking. The caffeine and naproxen content in these samples was then determined by HPLC.

4.3.7 Multiphoton microscopy (MPM)

Multiphoton microscopy (MPM) was used to assess the effect of these formulations in the stratum corneum. A DermaInspect system (JenLab GmbH, Jena, Germany), coupled to an ultra-short-pulsed, mode-locked, 80-MHz Titanium Sapphire laser (Mai Tai, Spectra Physics, Mountain View, California, USA) was used to image the skin. Full-thickness abdominal skin was mounted in Franz diffusion cells and an infinite dose of formulation 2 of EU and OA was applied. Samples of untreated skin were used as controls. After 8 h, the

Franz diffusion cells were dismantled and the skin was rinsed gently with water and blotted dry with a tissue. It was then placed on a microscope slide and protected with a cover slip (108). Images were captured by two photon excitation at 740 nm. The skin was imaged at four depths, from the superficial surface, corresponding to the *stratum corneum* (~5-10 μm), *stratum granulosum* (SG; ~15-20 μm), *stratum spinosum* (SS; 25-30 μm) and *stratum basale* (SB; 35-40 μm). Keratinocyte morphology was used to confirm each of these layers.

4.3.8 HPLC analysis of caffeine and naproxen

Caffeine and naproxen in solution and extracts from various matrices were analysed by a sensitive and rapid HPLC. The HPLC system consisted of a Shimadzu SIL-20 a HT, CBM-20A system controller, a SPD-20A detector, LC-20AD a pump and an auto injector. Isocratic separation of both caffeine and naproxen was achieved on a Phenomenex Luna 5 μm , C18 (150 x 4.6 mm) column. For caffeine analysis, elution was performed at ambient temperature with a mobile phase of 95% water, 2% acetonitrile, 2% tetrahydrofuran and 0.5% acetic acid at a flow rate of 1 mL/min. Detection wavelength was 273nm. For naproxen the mobile phase consisted of 35% water, 45% acetonitrile, 20% methanol and 0.3% acetic acid at a flow rate of 0.7 mL/min. The detection wavelength was 230 nm.

4.3.9 Data analysis

The cumulative amount (Q , $\mu\text{g}/\text{cm}^2$) of caffeine and naproxen penetrating through an area of 1.3 cm^2 was plotted against time (t). The steady state flux J_{SS} ($\mu\text{g}/\text{cm}^2/\text{h}$) was determined from the slope of the linear portion of the cumulative amount (Q) versus time t plot.

The maximum flux (J_{max}) that would be applicable to saturated solutions can be estimated from the experimental steady state flux corrected for the known solubility in the formulation by Equation 2 (185)

$$J_{max} = J_{SS} \cdot S_V / C_V \quad (1)$$

Where S_V is the solubility of the formulation and C_V is the experimental concentration used.

The diffusivity of solute in the skin divided by path length (D^*) was calculated from the maximum flux and the solubility of the active compound in the stratum corneum according to Equation 2 (185).

$$D^* = J_{max} / S_{sc} \quad (2)$$

Where S_{sc} is the experimentally determined solubility of the solute in the stratum corneum.

HSPs (δ_D , δ_P , δ_H) for formulation excipients, solvents and active compounds were obtained from the software package HSPiP (JW solutions B.V, the Netherlands). The total solubility parameters were also obtained from HSPiP, according to the formula:

$$\delta_{total}^2 = \delta_D^2 + \delta_P^2 + \delta_H^2 \quad (3)$$

Values of the solubility parameters for human skin ($\delta_D=17$, $\delta_P=8$ and $\delta_H=8$) were taken from *Hansen Solubility Parameters: A User's Handbook* (148) and used with the reported solubility parameters for caffeine ($\delta_D=19.5$, $\delta_P=10.1$ and $\delta_H=13.0$) and naproxen ($\delta_D=18.9$, $\delta_P=4.3$ and $\delta_H=9.9$) to estimate the HSP distance (R_a), a measure of the similarity between two materials:

$$Ra = [4(\delta_{D1} - \delta_{D2})^2 + (\delta_{P1} - \delta_{P2})^2 + (\delta_{H1} - \delta_{H2})^2]^{1/2} \quad (4)$$

4.3.10 Statistics

All experiments were analysed by one-way analysis of variance (ANOVA) with post-hoc comparisons (Tukey) using GraphPad Prism 6 (GraphPad Software Inc. La Jolla, CA92037, USA); $p < 0.05$ was considered to be significant.

Comparisons were made between the nanoemulsion formulations, with and without enhancers, and controls as well as between the different nanoemulsion formulations for the cumulative amount permeated at different time points and the amount of caffeine and naproxen recovered following skin extraction. A result was considered significant when $p < 0.05$.

Table 4.2 Physical and chemical characterisation of the various of nanoemulsion formulations and control mixtures defined in Table 1.

Physical and Chemical Properties	Formulations								
	Control mixtures		Nanoemulsion formulations		Nanoemulsion formulations with eucalyptol		Nanoemulsion formulations with oleic acid		
	C1 ^C	C2 ^{C,N}	C3 ^C	C4 ^N	E1 ^{C,N}	E2 ^{C,N}	O1 ^{C,N}	O2 ^{C,N}	
Appearance	Clear	Clear	Clear	Clear	Clear	Clear	Clear	Clear	
Viscosity (cp)	0.96	2.65	22.20	25.40	13.7±4.5	15.1±4.0	23.0±4.7	28.3±4.5	
Conductivity (µS)	0.21	1.15	0.12	1.05	87.5±2.2	91.3±3.9	80.8±8.2	84.5±10.1	
Refractive Index	1.33	1.36	1.32	1.34	1.38	1.37	1.38	1.37	
Emulsion droplet size (nm)	-	-	-	-	29.6±3.1	19.5±1.3	8.0±0.5	12.4±0.1	
Hansen Solubility Parameters (MPa)^{1/2}	δ_D	15.5	15.4	16.7	15	15.3	15.3	15.3	15.3
	δ_P	16	11.9	13.6	11.9	9.4	9.3	9.4	10
	δ_H	42.3	28.7	25.7	28.4	20.7	22.5	21.2	22.9
	δ_{Total}	47.8	34.7	33.5	34.3	27.4	28.8	27.8	29.3
(HSP dist)^a		43.2	26.3	29.1	20.7	15.8	17.3	14.8	16.8
Molar volume (MV)		18	30.8	35.9	30.9	43.3	38.9	44.2	39.5

^aHSP distances (Ra) of mixtures calculated from Equation 4 below, using software package HSPiP.

4.4 Results

4.4.1 Physical and chemical characterisation of the formulations used

Table 4.2 summarises the physical and chemical properties of the various formulations used in this study. In general, all formulations were clear and had a low viscosity. As one example, shown in Figure 4.1, the nanoemulsions area in the pseudo-ternary phase diagram with a 1:1 w/w ratio of Volpo-N10 to ethanol is in a region with a surfactant concentration between 80% and 40%. In this region, a high amount of water can be solubilised without causing phase separation and is characterised by transparency and higher viscosity. In contrast, in other regions of the phase diagram, a turbid emulsion is seen. Figure 4.1 also shows that the proportion of the ternary diagram existing as the nanoemulsion increases as the amount of water increases and the concentration of surfactant / co-surfactant mixture decreases.

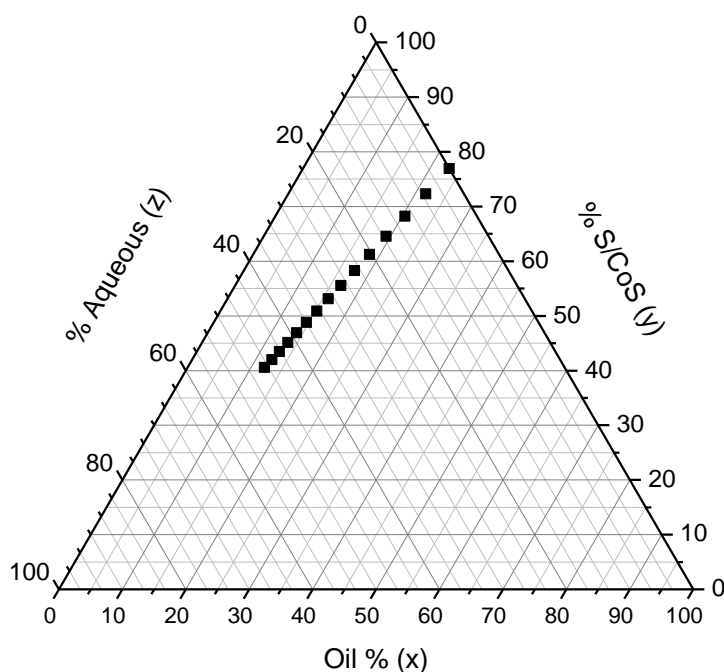


Figure 4.1. Ternary phase diagram of the oil, surfactant/co-surfactant mixture and water at ambient temperature. The dotted line in the diagram represents the nanoemulsion.

Table 4.2 also shows the viscosity, conductivity, refractive index and, where appropriate, nanoemulsion droplet size. However, it is apparent that, consistent with OA's surface active properties, the droplets from the nanoemulsions containing OA are smaller than those of EU. Further, all nanoemulsions had mean droplet sizes < 100 nm, indicating that they should be regarded as being nanoemulsions, and high conductivities, consistent with them being oil in water (O/W) nanoemulsions. Also, included in Table 4.2 are the estimated solubility parameters and "average" molar volume for each of the formulations studied. It

evident that the various solubility parameters are in the general order: water>nanoemulsions>nanoemulsions containing penetration enhancers.

4.4.2 *In vitro* permeation of caffeine and naproxen across epidermal membranes

Figure 4.2A shows the cumulative amount ($\mu\text{g}/\text{cm}^2$) of caffeine that penetrated across epidermal membranes versus time for nanoemulsions and controls for this study. Penetration from nanoemulsions containing skin penetration enhancers was greater than from control vehicles. The corresponding cumulative amount versus time profiles for naproxen are shown in Figure 4.2B, where similar but greater penetration occurs from nanoemulsions compared to controls. For both caffeine and naproxen, the ethanol/water solution promoted a greater epidermal penetration than the other control solutions.

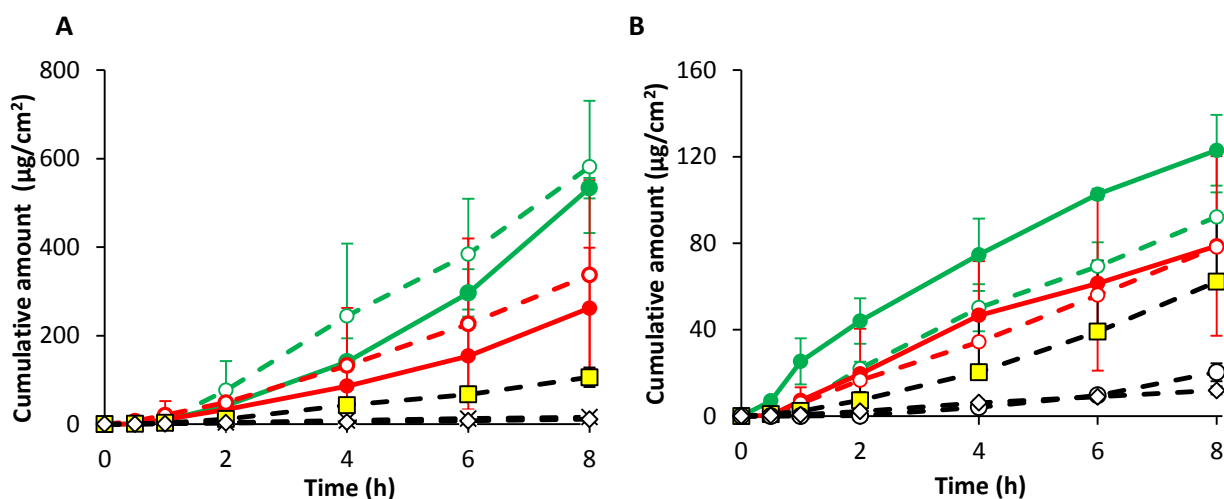


Figure 4.2. *In vitro* percutaneous permeation through epidermal human skin A-caffeine; B-naproxen (E1, green solid lines; E2, green dashed lines; O1, red solid lines; O2, red dashed lines; C1 (water), crosses; C2 (60% EtOH/water), yellow squares; C3 (50% PEG6000/water), diamonds and C4 (Volpo-N10/EtOH/water), circles).

4.4.3 Impact of formulation on active solubility in formulation, solubility in stratum corneum, maximum flux and derived diffusivity

Table 4.3 shows the estimated active solubility in formulation, solubility in stratum corneum, maximum flux calculated from steady state flux using Equation 1 and diffusivity per path length D^* derived from the maximum flux and stratum corneum solubility using equation 2. It is apparent that both caffeine and naproxen have a much higher solubility in nanoemulsion formulations containing enhancers than in controls. Indeed, the solubility of caffeine in water was much less than the corresponding values with the other controls and with the emulsions;

naproxen had a higher solubility in the nanoemulsions than in the controls. Pronounced enhancements in caffeine and naproxen maximum fluxes were evident for the aqueous ethanolic solution and the various emulsion formulations containing enhancers, the enhancement being between one and two orders of magnitude greater than the controls (Figure 4.3). It is apparent that the solubility of caffeine in the stratum corneum after application of various emulsion formulations containing enhancers is modest, whereas the derived D^* for these formulations increases by one or two orders of magnitude. It is thus apparent that the marked formulation enhancement in caffeine penetration arises from the enhancers reducing the diffusion resistance for caffeine permeation. In contrast, the solubility of naproxen in the stratum corneum after application of various emulsion formulations containing enhancers is about one order of magnitude greater than the controls, whereas the derived D^* is not greatly different from the slight enhanced D^* seen for an aqueous ethanolic formulation.

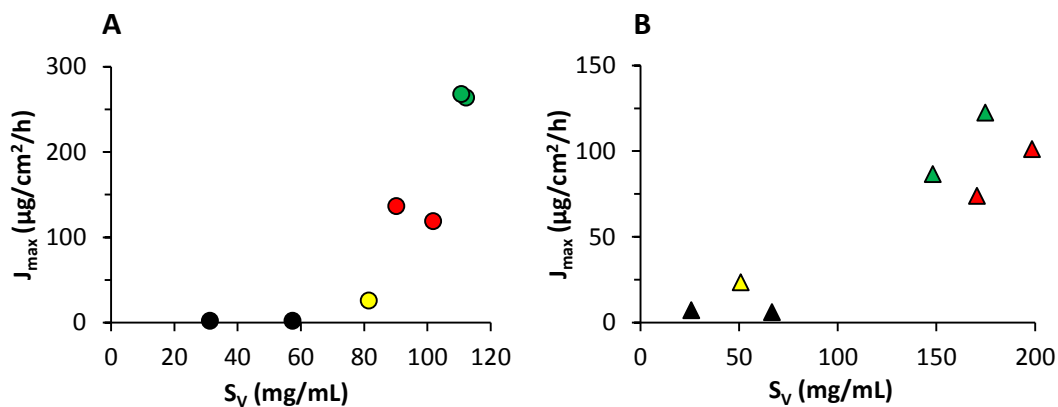


Figure 4.3. Estimated maximum fluxes for caffeine and naproxen for each of the formulations plotted against the solubility of these actives in the formulations. Circles, caffeine; Triangles, naproxen. Black symbols - controls (solutions in water and 25% PEG6000/water for caffeine, 25% PEG6000/water and Volpo-N10/EtOH/water for naproxen); Yellow symbols - 60% EtOH/water; Red symbols - nanoemulsions containing oleic acid; Green symbols - nanoemulsions containing eucalyptol

Table 4.3 Experimental data for caffeine and naproxen in different nanoemulsions without and with penetration enhancers and control vehicles. (Mean \pm SD).

Formulation	Active							
	Caffeine				Naproxen			
	S_v (mg/mL)	J_{max} ($\mu\text{g}/\text{cm}^2/\text{h}$)	S_{sc} ($\mu\text{g}/\text{mL}$)	D^* (cm/h *1E4)	S_v (mg/mL)	J_{max} ($\mu\text{g}/\text{cm}^2/\text{h}$)	S_{sc} ($\mu\text{g}/\text{mL}$)	D^* ($\times 10^4$ cm/h)
C1	31.3 \pm 1.2	2.2 \pm 0.8	21.6 \pm 2.2	1.0 \pm 0.4	-	-	-	-
C2	81.5 \pm 13.4	25.6 \pm 3.1	151.0 \pm 37.7	1.7 \pm 0.2	50.9 \pm 1.4	23.4 \pm 4.8	18.3 \pm 6.1	12.8 \pm 2.6
C3	57.4 \pm 10.1	2.5 \pm 0.7	49.4 \pm 14.2	0.5 \pm 0.1	66.8 \pm 1.9	6.2 \pm 0.3	16.0 \pm 1.8	3.9 \pm 0.2
C4	-	-	-	-	25.9 \pm 1.5	7.3 \pm 2.7	9.5 \pm 1.7	7.7 \pm 2.9
EU1	112.3 \pm 8.5	263.6 \pm 1.2	38.2 \pm 15.3	69.1 \pm 0.3	174.9 \pm 8.3	122.4 \pm 27.1	101.8 \pm 22.4	12.0 \pm 2.7
EU2	110.8 \pm 9.5	267.7 \pm 24.0	36.5 \pm 4.1	73.3 \pm 6.6	148.1 \pm 5.1	86.6 \pm 8.9	114.0 \pm 35.1	7.6 \pm 0.8
OA1	101.8 \pm 2.2	118.8 \pm 57.3	52.4 \pm 3.9	22.7 \pm 11.0	198.5 \pm 0.4	101.2 \pm 41.7	113.8 \pm 66.7	8.9 \pm 3.7
OA2	90.2 \pm 8.1	136.4 \pm 95.2	64.4 \pm 20.6	21.2 \pm 14.8	170.6 \pm 3.3	74.0 \pm 2.3	95.9 \pm 58.2	7.7 \pm 0.2

The formulations are defined in Table 1 and are nanoemulsion formulations (C3 and C4), with penetration enhancers eucalyptol (EU1 and EU2) and oleic acid (OA1 and OA2), and control mixtures (C1 – C2).

The different mechanisms of enhancement for the nanoemulsions with enhancers for caffeine and naproxen are more clearly shown in Figure 4.4. In Figure 4.4A it is evident that the J_{max} for naproxen is correlated with its solubility in the stratum corneum S_{SC} whereas, as shown in Figure 4.4B, caffeine is better related to its altered diffusivity D^* associated with the various formulations.

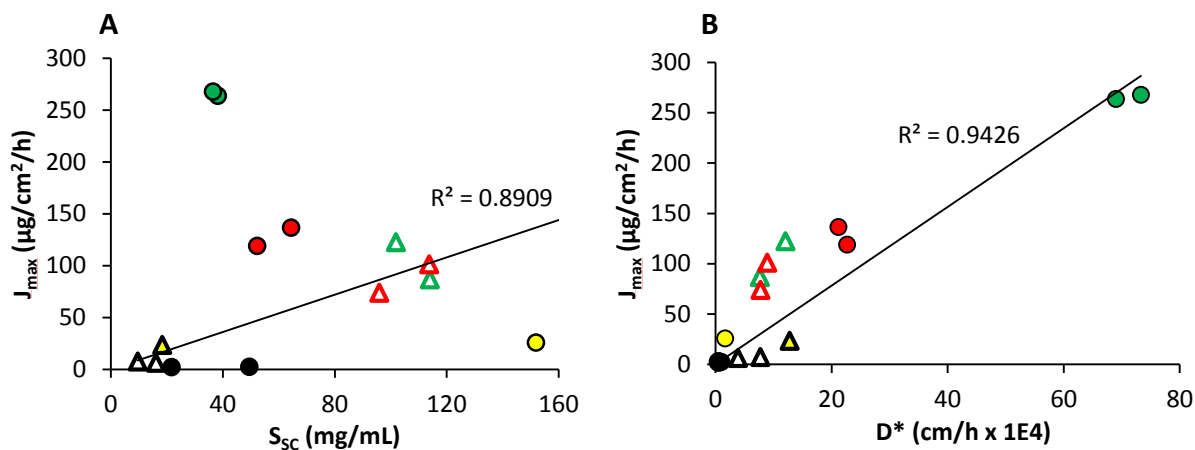


Figure 4.4 Impact of stratum corneum solubility and apparent diffusivity D^* on the maximum flux J_{max} for caffeine and naproxen. A. J_{max} versus stratum corneum; B. J_{max} versus D^* . Circles, caffeine; Triangles, naproxen. Black symbols - controls (solutions in water and 25% PEG6000/water for caffeine, 25% PEG6000/water and Volpo-N10/EtOH/water for naproxen); Yellow symbols - 60% EtOH/water; Red symbols - nanoemulsions containing oleic acid; Green symbols - nanoemulsions containing eucalyptol. The trend line for naproxen is shown. It is evident from Figure A that J_{max} is more dependent on stratum corneum solubility for naproxen, whereas in Figure B J_{max} is better related to D^* for caffeine.

4.4.4 Mechanism underpinning the differential enhanced uptake of caffeine and naproxen into the epidermis

Figure 4.5 shows that the enhanced solubility in the stratum corneum from the various formulations could be related to the uptake of both caffeine and vehicle into the stratum corneum. An optimal regression was found when it was assumed that all the dissolved solute in the vehicle was taken up into the stratum corneum as defined by:

$$S_{SC}(\text{predicted}) = S_{SC}(\text{skin, control}) + S_V(\text{vehicle}) * V_{up} / V_{SC}$$

Where V_{up} is solvent uptake and V_{SC} is the volume of the stratum corneum. $S_{SC}(\text{skin, control})$ represents the solute in the stratum corneum, derived from the experimental data for a control solution:

$$S_{SC}(\text{skin, control}) = S_{SC}(\text{exp, control}) - S_f(\text{exp, control}) * V_{up}(\text{control}) / V_{SC}$$

An excellent S_{SC} (predicted) versus S_{SC} (experimental) is evident for naproxen ($R^2=0.84$) but not for caffeine ($R^2=0.48$).

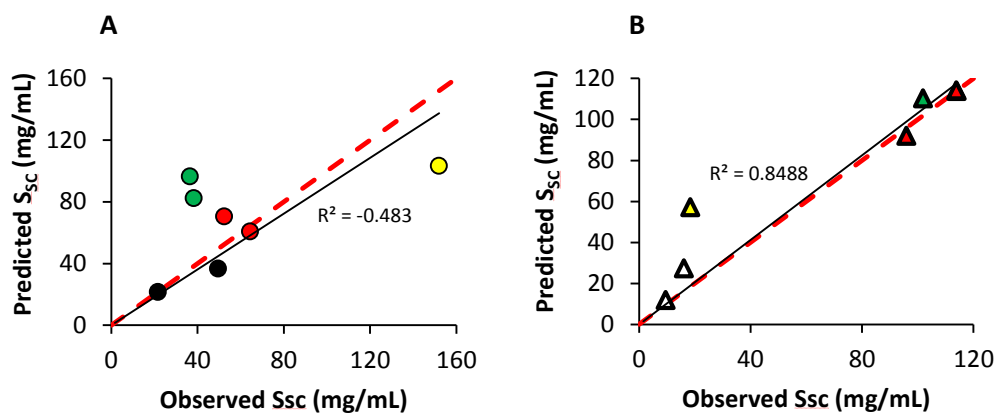


Figure 4.5. Stratum corneum solubility predicted from solvent uptake for caffeine (A) and naproxen (B). (Lin’s concordance correlation coefficient for caffeine is 0.58 and for naproxen is 0.93.) Black symbols, control solutions in water and 25% PEG6000/water for caffeine, 25% PEG6000/water and Volpo-N10/EtOH/water for naproxen); Yellow symbols, 60% EtOH/water; Red symbols - nanoemulsions containing oleic acid; Green symbols - nanoemulsions containing eucalyptol.

Can the solubility of the actives in various formulations and the uptake of formulations into stratum corneum be predicted by the solubility parameter approach?

Figure 4.6 shows the relationships between the solubility of solutes in formulations, uptake of formulations into stratum corneum and stratum corneum solubility as a function of the HSP distance (R_a). Figure 4.6A shows that the experimental solubilities of caffeine and naproxen in the various vehicles were highest when R_a was lowest and when the solutes and nanoemulsions were most similar in their various solubility parameters. Figure 4.6B shows that solvent uptake into the stratum corneum is also greatest for these formulations when R_a is lowest, i.e. formulations which are most similar to the stratum corneum in their various solubility parameters.

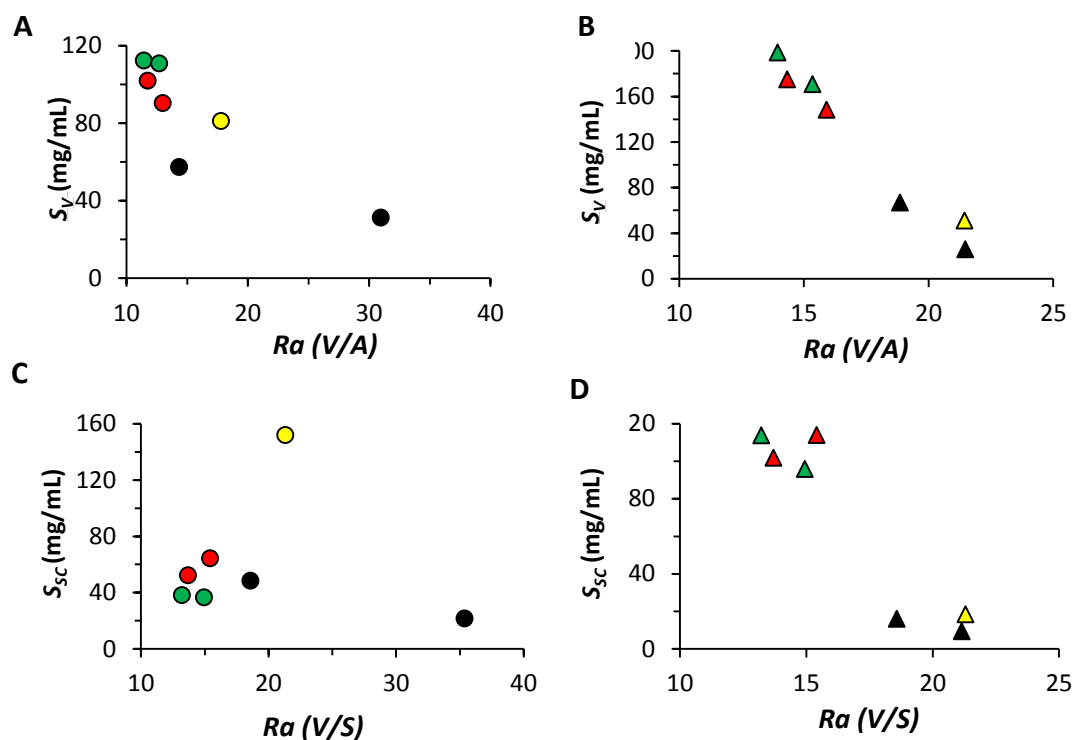


Figure 4.6. Solute solubility in vehicle and formulation uptake into stratum corneum as a function of their estimated HSP distance (Ra). **A & B.** Vehicle solubility (S_V) for caffeine (circles) and naproxen (triangles) respectively versus the Ra between the nanoemulsion formulations and controls; **C & D:** Formulation uptake into the stratum corneum for caffeine (circles) and naproxen (triangles) respectively versus the Ra between the nanoemulsion formulations and the skin. Black symbols - controls (solutions in water and 25% PEG6000/water for caffeine, 25% PEG6000/water and Volpo-N10/EtOH/water for naproxen); Yellow symbols - 60% EtOH/water; Green symbols - nanoemulsions containing eucalyptol; Red symbols - nanoemulsions containing oleic acid.

4.4.5 In vitro permeation of caffeine and naproxen across full-thickness human skin

The cumulative amount of caffeine and naproxen penetrated through full-thickness human skin ($\mu\text{g}/\text{cm}^2$) was plotted as a function of time (h) and the slope yielded the pseudo steady-state flux J_{SS} ($\mu\text{g}/\text{cm}^2/\text{h}$). The permeability coefficient K_p (cm/h) was calculated from equation 1. After 8 h exposure, the amount of caffeine delivered into the receptor from the microemulsion formulations was significantly higher than controls ($P < 0.05$), Fig 4.7.

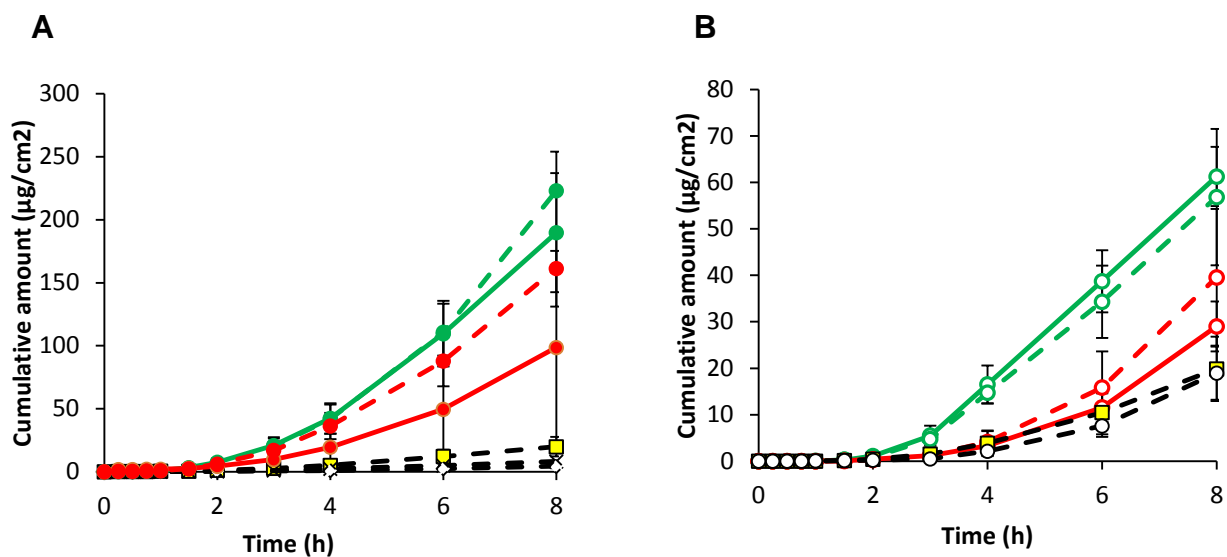


Figure 4.7. *In vitro* percutaneous permeation through full-thickness human skin; A-caffeine; B-naproxen (E1 (Eucalyptol 1 - green solid lines); E2 (Eucalyptol 2 - green dashed lines; O1 Oleic acid 1 - red solid lines; O2 (Oleic acid - red dashed lines; C1 (water -, crosses; C2 (60% EtOH/water - yellow squares; C3 (50% PEG6000/water - diamonds and C4 (Volpo-N10/EtOH/water - circles).

The calculated flux and permeability coefficient from O/W microemulsions for both systems (OA and EU) was 10-fold higher (36.8 and 56 $\mu\text{g}/\text{cm}^2/\text{h}$, respectively) than controls (C1, C2 and C3) (1.7, 4.6 and 1.2 $\mu\text{g}/\text{cm}^2/\text{h}$, respectively) in the case of caffeine; and 2- to 3- fold (11.9 and 11.3 $\mu\text{g}/\text{cm}^2/\text{h}$ OA and EU, respectively) higher than controls (C2, C4) (4.7 and 5.5 $\mu\text{g}/\text{cm}^2/\text{h}$, respectively) for naproxen.

Table 4.4. Caffeine and naproxen permeation parameters for different vehicles through full-thickness skin (Mean \pm SD, n=4)

Formulation	K_p (cm/h *1E4)		J_{max} (μ g/cm ² /h)		D^* ($\times 10^4$ cm/h)	
	Caffeine	Naproxen	Caffeine	Naproxen	Caffeine	Naproxen
C1	0.5 \pm 0.1	-	1.5 \pm 0.3	-	0.7 \pm 0.7	-
C2	1.2 \pm 0.3	1.4 \pm 0.3	10.0 \pm 3.0	7.3 \pm 2.8	0.7 \pm 0.2	4.0 \pm 1.5
C3	0.3 \pm 0.1	-	1.8 \pm 0.7	-	0.4 \pm 0.1	-
C4	-	1.6 \pm 0.1		4.2 \pm 1.5		4.5 \pm 1.6
E1	11.4 \pm 2.8	5.2 \pm 0.5	127.9\pm31.4	90.8 \pm 8.9	33.5\pm8.2	8.9 \pm 0.8
E2	12.0 \pm 2.1	4.8 \pm 1.0	132.5\pm26.5	71.1 \pm 8.8	36.3\pm7.2	6.2 \pm 1.4
O1	6.9 \pm 4.3	2.4 \pm 0.4	69.8\pm21.8	47.0 \pm 8.3	13.3\pm4.0	4.1 \pm 0.7
O2	9.6 \pm 1.6	3.3 \pm 1.0	86.9\pm15.0	55.7 \pm 18.2	13.5\pm2.0	5.8 \pm 2.2

C1 is 100% water, C2 is 60% ethanol/water, C3 is 25% PEG6000/water, and C4 is 25% Volpo-N10 25% ethanol/50% water

EU nanoemulsions containing eucalyptol as oil phase, OA nanoemulsions containing Oleic Acid as oil phase

Figure 4.8 shows that more caffeine was promoted from nanoemulsion formulations into skin and stratum corneum than from the controls and that the amount permeating from these formulations was greater for caffeine than for naproxen. However, the same pattern not seen for lipophilic drug naproxen. Also, a significant difference ($P < 0.05$) was found in the amount of caffeine retained in the stratum corneum when compared between nanoemulsions and controls (C1 & C3). No differences were found between nanoemulsion formulations for caffeine and naproxen. Unexpectedly, high naproxen levels were retained in the stratum corneum from control C2 (60% ethanol/water) solution. We are not sure why this occurred but it could be due to enhanced partitioning of actives into the stratum corneum caused by ethanol.

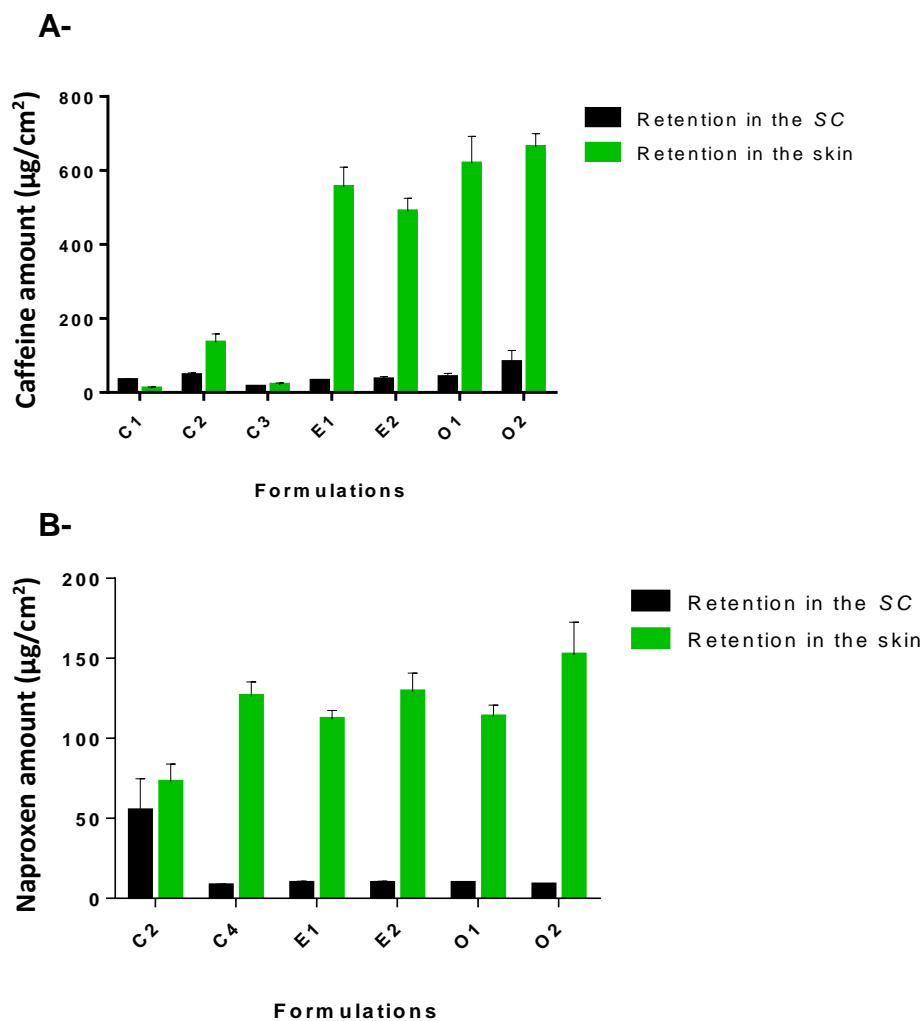


Fig 4.8 A-Caffeine; B-naproxen retained in the stratum corneum (SC) and skin from nanoemulsion formulations and controls after 8 h permeation in full-thickness human skin (Mean \pm SEM, n=4)

Table 4.5 shows the lag time for full-thickness skin is higher than for epidermal membrane for both caffeine and naproxen and from all nanoemulsion formulations and controls. It also shows that the caffeine flux of nanoemulsion formulations from epidermal membranes was significantly higher than the flux from full-thickness skin ($P < 0.05$). The naproxen epidermal flux was slightly higher than full-thickness skin but was not significant.

Table 4.5 Estimated lag times and steady state flux for caffeine and naproxen in epidermal membrane and full-thickness skin.

Formulation	Lag time (h)		JSS ($\mu\text{g}/\text{cm}^2/\text{h}$)	
	FTS	Epi	FTS	Epi
Caffeine				
C1	4	2.5	1.4 \pm 0.3	2.1 \pm 0.6
C2	3	2	3.7 \pm 1.1	9.4 \pm 0.9
C3	4	3	0.9 \pm 0.1	1.3 \pm 0.4
E1	2.5	1	34.2 \pm 8.6	70.4 \pm 0.3
E2	2.5	1	35.9 \pm 6.3	72.5 \pm 6.2
O1	2.5	1	20.6 \pm 2.0	35.0 \pm 19.6
O2	2.5	1	28.9 \pm 5.8	45.4 \pm 10.5
Naproxen				
C2	3	1.5	2.9 \pm 0.8	9.2 \pm 1.5
C3	-	2	-	1.9 \pm 0.1
C4	4	2	3.3 \pm 1.2	5.7 \pm 1.7
E1	3	0.5	10.4 \pm 1.0	14.0 \pm 3.6
E2	3	0.5	9.6 \pm 2.3	11.7 \pm 1.1
O1	3	0.5	4.7 \pm 0.8	10.2 \pm 4.8
O2	3	0.5	6.5 \pm 2.0	8.7 \pm 0.3

4.4.6 Multiphoton microscopy of full-thickness human skin after exposure to nanoemulsion formulations

MPM images of human full-thickness skin exposed to the formulations and corresponding control samples (untreated) are shown in Figure 4.9. The pseudo-coloured images (40X) have been recreated from normalised average endogenous autofluorescence lifetime of NADPH and FAD. The images are coloured from shorter lifetime (blue) to longer lifetimes (red). An area (2cm²) of skin pre-treated with the formulations for 8 h was imaged using the Derma Inspect multiphoton tomography system. We observed a change in stratum corneum morphology compared to the control skin. The hollowing of the cellular regions (Figure 4.9- white arrow) can be attributed to the action of nanoemulsion on the stratum corneum lipids. In addition, an increase in the thickness of the viable epidermis was observed. The visible layers could be observed for a greater depth. In the case of the oleic acid formulation the total depth of the epidermis was 100 μm ; this is nearly twice the generally observed thickness of epidermis. However, when metabolic analysis of the NADPH and FAD lifetimes was conducted on the viable layers, no change was observed. The treated skin and the control skin were both found to have a comparable average lifetime (t_m). (188, 189)

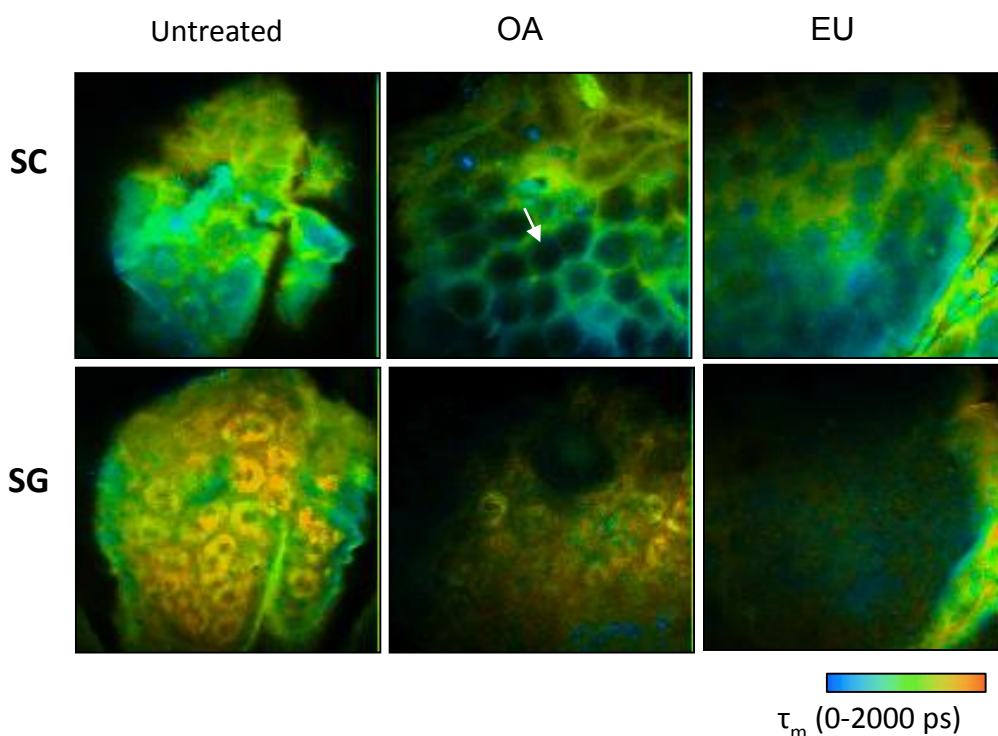


Fig 4.9 Structural and viability study of excised skin following the topical application of nanoemulsion formulations-. SC = stratum corneum; SG = stratum granulosum; OA = nanoemulsions with oleic acid; EU = nanoemulsions with eucalyptol

4.5 Discussion

This work has demonstrated that the skin permeation of caffeine and naproxen is markedly enhanced using nanoemulsion formulations containing the penetration enhancers, OA and EU, in comparison to the controls. These results are consistent with those previously reported for skin permeation of hydrophilic and lipophilic drugs using microemulsion formulations (190). A key question we also addressed was how the nanoemulsions with the penetration enhancers promoted skin penetration. It is evident that the nanoemulsions made in this study worked by three mechanisms, which may or may not be working in concert to give a synergistic effect: i) an enhanced solubility of the drug in the applied vehicle, ii) uptake of the vehicle carrying the drug into the stratum corneum, and iii) alteration of the properties of the stratum corneum membrane, for example by fluidisation of the stratum corneum lipids.

The combinations of surfactants and oils used in our emulsions enabled the vehicle solubility of both caffeine and naproxen to be increased more than any single solvent solution or solvent mixture used in this study as controls (Table 4.3). The 3- to 4-fold increase in solubility of the water soluble compound caffeine in the nanoemulsions compared to the aqueous solution is most likely reflecting the process of micellar solubilisation (191). The nanoemulsion induced enhanced solubility was even more evident with the lipophilic naproxen, with a 6- to 8-fold solubility enhancement seen when compared to the complex co-solvent mixture containing Volpo-N10 and ethanol (25.9 mg/mL). The findings are consistent with the general view that solubilisation is even more pronounced for lipophilic compounds (192). The nanoemulsions were also associated with excellent stratum corneum solubility, particularly in the case of the more lipophilic naproxen (Table 4.3). Further, both EU and OA are known to disrupt the stratum corneum by multiple mechanisms, including dissolution of stratum corneum lipids (193).

To clarify that there had been a nanoemulsion induced permeation enhancement for caffeine and naproxen, we estimated the solute maximum (or saturated) fluxes (J_{max}). The use of maximum flux enables the potential enhancement caused by the nanoemulsions to be defined as it is now well recognised that maximum flux is independent of the vehicle and dependent solely on the thermodynamic activity of the solute in the vehicle, provided the vehicle or solute does not alter the properties of the membrane (106, 154). This concept was initially highlighted by the work of Twist and Zatz (155), who showed the same flux for methyl paraben across synthetic membranes, regardless of its solubility in a range of different vehicles. Our results for the control solutions are consistent with these findings in that a similar low value for J_{max} for both caffeine and naproxen was found for each control

solution not affecting skin permeability across a range of vehicle solubilities. In contrast, the J_{max} values seen with nanoemulsions and to some extent, ethanol/water, are much higher than the controls (Figure 4.3), consistent with their enhancement of skin permeability and suggesting that these vehicles have altered the properties of the stratum corneum. The penetration enhancer, EU, had a much greater effect on J_{max} than OA for the hydrophilic drug caffeine; a differentiation not seen with the lipophilic naproxen.

In order to understand the mechanisms by which the solutions and nanoemulsions had acted as permeation enhancers, we also estimated the underlying J_{max} determinants of stratum corneum solubility and stratum corneum diffusivity. Ethanol, used as a co-surfactant in these nanoemulsions, has been shown to extract stratum corneum lipids and perturb barrier function by improving the permeation of more hydrophilic drugs such as caffeine through skin by partitioning between the vehicle and stratum corneum. Peltola et al also reported enhanced transdermal delivery of the lipophilic steroid oestradiol from microemulsions containing ethanol as a co-surfactant (194), with which our findings are consistent. Interestingly, ethanol has been reported to act synergistically with terpenes to enhance penetration of both hydrophilic and lipophilic drugs (195, 196). The increased ethanol content in the 60% ethanol/water mixture however, was likely to have a greater effect on the skin, particularly on the extraction of skin lipids. This would have a larger impact on the partitioning of the hydrophilic caffeine, compared to the lipophilic naproxen, accounting for the much greater enhancement of S_{sc} seen with caffeine.

Table 4.3 showed that the stratum corneum solubility of naproxen was enhanced by the nanoemulsions much more than that for caffeine (range, 96-114 mg/mL compared to 36-64 mg/mL) and that this increased stratum corneum solubility was, in turn, associated with an enhanced flux (Figure 4.4). In contrast, there was no such clear relationship seen with caffeine (Figure 4.4). On the other hand, the apparent linear relationship between effective diffusivity in the epidermal membrane and J_{max} for caffeine (Figure 4.4) suggests that the nanoemulsion formulations may have modified the stratum corneum lipids (157). In contrast, the J_{max} for naproxen appears to not have been increased by alterations in the stratum corneum diffusivity. In general, diffusivity will be independent of solute lipophilicity for those vehicles that do not affect the stratum corneum (107, 197). However, when the vehicle does affect the stratum corneum, there may be varying impacts for different types of solutes. We have found, for instance, an increased diffusivity for the more hydrophilic phenol compounds such as isopropyl myristate (IPM) relative to more lipophilic phenols. IPM has a high affinity for skin and can disrupt the lipid bilayer regions of the stratum corneum intercellular matrix.

Its stratum corneum diffusivity enhancement was most pronounced for moderately hydrophilic compounds like methyl paraben (log P 1.95) and 4-propoxyphenol (log P 2.34) and so may be anticipated to also affect caffeine (log P -0.07), consistent with the nanoemulsion enhancement of its diffusivity seen in this work. Interestingly, we also observed a reduced diffusivity for the more lipophilic phenols (above log P of about 3.0) from IPM (107), consistent with our findings with naproxen. Our findings of diffusivity-mediated caffeine flux increases, that were particularly evident in the nanoemulsions containing EU, are consistent with previous work showing increased diffusivity of the polar compound 5-FU with terpene enhancers, including EU (157). In that work, the terpenes were not considered to act by increasing stratum corneum solubility but by disruption of the stratum corneum lipids to enhance diffusivity. On the other hand, in other work, OA had only a moderate diffusion-enhancing effect compared to the terpene d-limonene for solutes with a range of lipophilicities (198), analogous to our findings. Terpenes have also been shown to enhance the permeation of a lipophilic compound, tamoxifen, by enhancing its partitioning into the stratum corneum (199). Williams and Barry (159) observed that in general, partitioning may play a greater role in enhancement of more lipophilic substances. Another contribution to enhanced flux seen with the nanoemulsions could come from an increase in surface area coverage, due to distribution of the drug in the nanoemulsion droplets to aid in the transfer of the active compounds from the formulation to the stratum corneum (184, 194).

A key finding in this work is that the nanoemulsion enhanced stratum corneum solubility is due to the uptake of solute dissolved in the formulation and this, in turn, depends on the solubilities of the solutes in the formulations and formulation uptake into the stratum corneum. We did explore for any the relationships between the solubilities of the active compounds in the various formulations and in the stratum corneum after application of the formulations with the HSP distance for the nanoemulsions and actives (Figure 4.6). Our conclusion is that the data are consistent with the adage of “like dissolves like” in that the highest solubility in the formulations and the uptake of formulations into the stratum corneum corresponded to the lowest HSP distance. The findings appear to be consistent with the general principles enunciated by Abbott et al (153). Further studies using an expanded range of vehicles and actives may allow predictive algorithms to be generated.

The caffeine and naproxen permeation of full-thickness skin and epidermis layers was measured. Epidermal membrane had, as expected, higher permeability of caffeine and naproxen as flux than the full-thickness skin. However, fluxes of caffeine and naproxen absorbed into the receptor from full-thickness skin compared with epidermis were similar. A study by Cross et al found that the ratio of fluxes of salicylate into the receptor from their

formulations remained constant in full-thickness skin and epidermis and they suggested that the dermis constitutes a similar barrier to the diffusion of active ingredients from their formulations (200). Therefore, the presence of dermis and hypodermis did not affect the permeation amount of caffeine and the stratum corneum was just limiting the rate of barrier against penetration. These results are similar to other results obtained from a study done in 2008 on caffeine (201).

The amount of caffeine and naproxen retained in the stratum corneum was measured by tape stripping to correlate solubility of solute in the formulations to that in the stratum corneum. We found that the solubility of nanoemulsion formulations containing caffeine and naproxen in the stratum corneum followed the same trend as that obtained from tape stripping (amount of caffeine and naproxen retained in the stratum corneum). It was seen (Table 4.4) that the highest permeability of naproxen was obtained from OA and EU nanoemulsion formulations, which may be due to high solubility of naproxen in the stratum corneum from these formulations compared with controls. Naoui et al found significant differences in the amount of caffeine stored in the stratum corneum (202). It was previously claimed that diffusional resistance in the dermal matrix could significantly decrease the permeability of lipophilic solutes (203). As shown in Table 4.5, this effect is evident for both caffeine and naproxen in this study with the greatest reduction in flux and diffusion seen for caffeine.

Our microscopic evaluation of the skin concurs with the lipid dissolution hypothesis. As described in the results, the dissolution of stratum corneum lipids was evident after 8 h of treatment with the emulsions. Walker and Hadgraft found that the use of oleic acid as a penetration enhancer disrupted the intercellular lipid arrangement of the stratum corneum (188). A study using a EU nanoemulsion with curcumin (log P 3.2) as a model penetrant showed similar changes to those observed in our work (189). Their histological images comparing a PBS control and the terpene nanoemulsion showed keratin fragmentation and disruption of the lipid bilayers after 24 h microemulsion treatment of full-thickness pig ear skin.

4.6 Conclusions

In conclusion, the nanoemulsion systems in this study significantly enhanced the human epidermal permeation of caffeine and naproxen. Both a nanoemulsion increase in stratum corneum solubility and in diffusivity could be shown as the key mechanisms for this increase with the enhanced solubility arising from solute being carried into the stratum corneum with the formulation. Analysis of these data using solubility parameters suggests that “like dissolves like” is the key adage determining solute solubility in the formulations, uptake of the formulations into the stratum corneum and then the stratum corneum solubility. Our results comparing the responses in epidermal membrane full-thickness skin highlight the additional behavior provided by the dermis in the permeation of both hydrophilic and lipophilic solutes.

Chapter 5

Appendageal delivery

A. Potential of nanoemulsion formulations for delivery of Minoxidil through skin appendages, stratum corneum and permeation through human skin.

B. Investigation of the effects of nanoemulsions containing penetration enhancers on follicular penetration of the hydrophilic model compound caffeine.

5.1 Abstract

Hair follicles are pertinent and efficient penetration pathways and reservoirs for topically applied chemicals/drugs. Penetration enhancers can also be incorporated as the oil phase of microemulsions to further enhance drug delivery. Penetration enhancers are used to reduce the skin barrier by physically and chemically altering its properties. Enhanced minoxidil delivery, targeted to receptors localised within hair follicles, aims to promote hair growth. We aimed to compare the permeation of minoxidil into and through excised human skin using different nanoemulsion formulations, compared to a simple solution control. A further aim was to prove that maximum flux of solutes can be enhanced by increasing its solubility in stratum corneum lipid components and increasing the diffusivity of the solute in the stratum corneum. Oil in water (O/W) nanoemulsions containing 2% minoxidil and either oleic acid (OA) or eucalyptol (EU) as oil phase were prepared and characterised. Nanoemulsions and control (C - 2% minoxidil in 60% ethanol/water) were applied to full-thickness excised human abdominal skin in Franz diffusion cells (n=4) for 24 h. Minoxidil concentrations in receptor fluid (through the skin), tape strip extracts (stratum corneum retention), follicular casts (hair follicle retention) and homogenised skin extracts (deeper skin retention) were analysed by high performance liquid chromatography (HPLC). Minoxidil penetration through and into skin was greater for all nanoemulsions compared to the control. The OA formulation was the best at promoting minoxidil retention into the superficial skin compartments (stratum corneum and hair follicles). The EU formulation was best for deeper penetration into and through the skin. We also found that maximum flux was related to formulations and was dependent on stratum corneum solubilities for minoxidil. These solubilities, in turn, depended on the amount of vehicle absorbed into the stratum corneum and the amount of minoxidil dissolved in that absorbed formulation.

The second aim of this study was to investigate the effectiveness of our nanoemulsion formulations for follicular delivery of caffeine. In excised human full-thickness skin, hair follicles were opened by tape stripping, blocked with a microdrop of super glue and acriflavine (for visualisation), or left untreated. Caffeine in nanoemulsion formulations containing OA or EU and in controls was topically applied. Caffeine retention in the stratum corneum, hair follicles and the skin, as well as penetration through the skin after 24 h was determined. Separately, acriflavine was applied to the skin and imaged in the follicles and surrounding area by multiphoton microscopy

Nanoemulsions caused significant increases in caffeine permeation through untreated skin, compared to controls (16- and 25-fold for OA and EU, respectively), with the follicular route contributing 18% of caffeine permeation for the OA nanoemulsion and 24% for EU. When follicles were opened, the respective contributions rose to 32% and 43%. The nanoemulsions also promoted caffeine retention in the follicles, with 11- and 15-fold increases with OA and EU, respectively. Imaging showed cellular uptake of acriflavine around the opened follicle, but not in the untreated follicle with OA, suggested that OA was unable to penetrate the sebum barrier around the follicle. This study demonstrated effective delivery of a hydrophilic model drug into and through hair follicles and showed that the follicles and surrounding regions may be targeted by optimised formulations for specific treatment.

O/W nanoemulsions containing OA or EU enhanced transdermal delivery of minoxidil. OA appeared to promote stratum corneum and follicular delivery more than EU. This study has also suggested that OA and EU nanoemulsions containing caffeine as a hydrophilic model drug appeared to be convenient to be used in the transfollicular penetration. Improved follicular targeting has implications for acne treatment and vaccine delivery to adjacent antigen-presenting cells.

5.2 Introduction

The knowledge of the permeation process is essential for improving and optimising skin transport solutes and cosmetics. Even though the stratum corneum is commonly known as the most important barrier to transdermal absorption, it is also regarded as the main route for penetration. Recently, researchers have suggested, in addition to percutaneous absorption, hair follicles and sebaceous glands may contribute significantly to topical or transdermal delivery (204). Previously, the actual importance of the transfollicular route had been overlooked based on the fact that the hair follicle orifices occupy only approximately

0.1% of the total skin surface area (205). Nonetheless, hair follicles are a pocket within the epidermis extending deep into the dermis, providing a much greater area for absorption below the surface of skin. Follicular density has major effects on penetration. Shelley and Melton observed the appearance of tiny multiperifollicular wheals on hairy human skin after topical administration of epinephrine and histamine phosphate in propylene glycol. There was no response in areas with less hair density, thus, suggesting follicular contribution (206). Also, studies by a number of researchers have shown higher absorption rates in skin areas with higher follicle density (207), (208). Previous studies of the transfollicular route were mostly qualitative and histological studies depended on stain and dye localisation within the hair follicle. For instance, Mackee et al (209) were amongst the first to study the role of the hair follicles in topical drug delivery. There have been substantial studies on the effect of vehicles and drugs on the transfollicular route but it seems the physicochemical features of the solute itself may influence the final transport of the solutes within the skin. Many theoretical considerations of the follicular route have been suggested. Theoretical consideration of the transfollicular or shunt pathway was first considered by Scheuplein (210). Shunt-mediated diffusion of charged dye was observed. Transient diffusion depended upon conditions, considered to be either transdermal or transfollicular (210). These examples of transient percutaneous absorption apply only to solution dosage forms, and can not necessarily be extended to other topical vehicles (204). Particle size may greatly influence targeted delivery into hair follicles (205), (211) and different particle sizes may be used to aim at various depths in the follicular duct. It has been suggested that 750 nm and 1500 nm polystyrene particles can penetrate to the end of a hair follicle (44). However, it has been also reported that 750 and 1500 nm particles were not able to enter the cells after topical administration, although 40 nm particles did enter (212). Lademann et al (15) identified body-region-dependent hair follicle features varying in follicular size and follicular distribution. Furthermore, it has been reported that solutes enter from active hair follicles only and that inactive or closed hair follicles produce sebum and prevent the growth of hair. Consequently, open orifices are obtained by mechanical peeling before applying the substances (213). The variation in the stratum corneum thickness in different body areas has been the most important reason for the varying rates of absorption.

Nanoemulsions are a modern approach to carrying drugs acting as new delivery system due to their high solubilisation and the possibility of managing delivery rates of drugs. Mostly, these advanced formulations have been used topically. It is believed that drug permeation rates from nanoemulsions are significantly higher than from other formulations such as conventional emulsions and vehicles because the nanoemulsions combine several

enhancing components (202). Nanoemulsions are a dispersed system of oil, water, surfactant and co-surfactant. The mixture of oil, water and surfactant could form a wide range of phases or structures, which can be discerned microscopically. The physicochemical properties of nanoemulsions influence the delivery of a drug to the skin and many hypotheses have been put forward. One of these theories claimed that contact of the drug with the skin could be improved by low interfacial tension between oil and water (176). The bioavailability of the drug increases due to the low interfacial tension and the fluctuating oil-water interface, which enhances material movement between lipophilic and hydrophilic domains of the nanoemulsion and the stratum corneum (202).

The aim of this study was to determine the influence of an oil-in-water droplets nanoemulsion on the permeation of minoxidil as a moderate lipophilic drug ($\log P$ 1.24) in hair follicles, stratum corneum, other skin layers and in receptor samples after 24 h. Minoxidil was the drug to be loaded into the nanoemulsions that contained EU and OA (oil), Volpo-N10 (non-ionic surfactant) and ethanol (co-surfactant). The second aim of the present study was to investigate the transfollicular delivery enhancement of caffeine using the same nanoemulsion formulations. Differential tape stripping was performed followed by cyanoacrylate skin surface biopsies to determine the amount of caffeine in the hair follicles. Follicular closing and opening technique in human skin was also performed to determine the penetration of caffeine through hair follicles. Skin was also imaged using a LaVision multiphoton microscope to see permeation into hair follicles and the area around the hair follicles.

5.3. Materials and Methods

5.3.1 Chemicals

Caffeine, minoxidil, ethanol, OA and EU, were purchased from Sigma-Aldrich Pty. Ltd. (Sydney, Australia). Volpo-N10 was obtained from Umiqema (Witton Centre, Witton Redcar TS10 4RF, UK). All chromatography reagents were analytical grade.

5.3.2 Nanoemulsion formulation preparation and Characterisation

Volpo-N10 (surfactant) was dissolved in ethanol (co-surfactant) in a 1:1 ratio. The resulting mixture was then mixed with the oil phase, OA or EU (oil) in a 0.6:1:1 ratio followed by gentle mixing with phosphate buffered saline (PBS). The resulting nanoemulsion was clear at room temperature. Minoxidil and caffeine were dissolved in selected nanoemulsions at 2% and

3% w/w, respectively. The characterisation methods are described in Chapter 5. The compositions of emulsions and control solutions are shown in Table 5.1 and 5.2.

Table 5.1 Compositions and solubilities of minoxidil in selected nanoemulsion formulations and control (%w/w)

Formulation	Compositions
C	2% minoxidil in 60% ethanol
M1 ^E	2% minoxidil + 15.93% EU+53.10% Volpo-N10/ethanol+30.97% water
M2 ^E	2% minoxidil + 14.63% EU+ 48.78% Volpo-N10/ethanol+ 36.59% water
M3 ^O	2% minoxidil + 15.93% OA+53.10% Volpo-N10/ethanol+30.97% water
M4 ^O	2% minoxidil + 14.63% OA+ 48.78% Volpo-N10/ethanol+ 36.59% water

Table 5.2 Compositions of selected nanoemulsion formulations and controls (%w/w)

Formulation	Compositions
C1	3% caffeine in water
C2	3% caffeine in 25% PEG6000/water
M ^O	3% caffeine + 14.63% OA+ 48.78% Volpo-N10/ethanol+ 36.59% water
M ^E	3% caffeine + 14.63% EU+ 48.78% Volpo-N10/ethanol+ 36.59% water

5.3.3 Determination of S_V and the solubility in the stratum corneum S_{Sc}

Solubility in the formulation (S_V) was determined by adding minoxidil to 5 mL of each nanoemulsion or control solution until an excess amount remained. The samples were then incubated in a water bath at 32°C for 24 h with continuous agitation and centrifuged at 4700 rpm for 10 minutes. The supernatant was withdrawn and diluted to accurately quantify the amount of each compound by HPLC.

The stratum corneum was prepared from epidermal sheets by trypsin digestion (149), then stored frozen at -20°C until use. Circles of stratum corneum (4 replicates for each formulation) were weighed before use. They were then equilibrated in a saturated solution 1mL of each formulation at 32°C for 24 h, according to established methods (150). At the

end of the incubation period, the stratum corneum was removed and blotted dry. Then it was extracted using 1 mL 70% ethanol/water for another 24 h, at the same temperature used for equilibrium (32°C). The solubility in the stratum corneum (S_{SC}) was determined from the amount of recovered model compound in the extraction fluid, measured by HPLC, divided by the area (1.33cm) and the thickness (0.02cm) of the stratum corneum.

5.3.4 Solvent uptake in the stratum corneum

The total solvent uptake into the stratum corneum was determined from the weight difference of piece of the dry stratum corneum (about 0.7mg) soaked in individual formulations (1mL) for 24 h at 32°C. The stratum corneum pieces wiped three times with Kimwipe tissues before weighing again.

5.3.5 Open hair follicles technique

A cyanoacrylate skin surface biopsy was used to open the hair follicles; a drop of ethyl cyanoacrylate, (Loctite Super glue) was placed on the skin and covered with a glass slide under slight pressure as described by Lademann 2000 (214). After 5 min, the cyanoacrylate polymerised and the slide was removed with one quick movement to open the hair follicles.

5.3.6 Blocked hair follicle technique

Our group has developed a method to plug the hair follicles on excised skin to evaluate their contribution in permeability across the skin. Accordingly, all hair follicles in a marked region were carefully identified under the ZEISS microscope (Stemi 2000-C). The plugging procedure involved applying 0.1µL acriflavine solution (dissolved in milliQ water) to form a globule around the follicle and subsequently 0.1µL of ethyl cyanoacrylate, (Loctite Super glue) (Henkel, Ohio, USA) was added on top of it. The polar monomers of cyanoacrylate polymerise when they come in contact with the water molecules in the presence of acriflavine dye. This dye-sensitised polymerisation forms long and strong chains, thus plugging the skin and hair follicle.

5.3.7 *In vitro* skin penetration study

In the first part, 2% minoxidil was totally solubilised in formulations that have high concentrations of water (e.g., O/W). Therefore, two concentrations of nanoemulsion formulations were chosen for OA and EU and control in minoxidil (Table 5.1). *In vitro* skin absorption studies were performed on a Franz diffusion cell with an effective diffusion area of 1.33 cm² and 3.4 mL receptor chamber capacity using full-thickness human abdominal skin. The skin was cut into circular pieces and mounted in a Franz diffusion cell between donor and receptor compartment, the stratum corneum side was facing the donor chamber and the dermal side was facing the receptor chamber. The receptor contained PBS buffer (pH 7.4) at 35°C. 1 mL of nanoemulsion formulation or control formulation was added to the donor. The donor was wrapped with parafilm after addition of the nanoemulsions to prevent water evaporation. After 30min, 60min, 90min, 2h, 3h, 4h, 6h, 8h and 24h, 200 µL of the receptor was withdrawn and replaced with the same amount of fresh PBS buffer. The samples were analysed by HPLC. After Franz diffusion studies were completed, skin in each cell was wiped with cotton buds to remove any remaining formulation and then subjected to tape stripping (20 times) which involved by application of adhesive tape (D-Squame tapes, CuDerm Corp., TX) to the exposed skin surface for about 5 second, and then the tape was carefully removed. The tapes were placed into separate vials and soaked overnight with 2 mL methanol before analysis by HPLC. The amount of absorbed material in the tapes was determined, representing material deposited within the stratum corneum.

Follicular casting followed tape stripping; one drop of superglue was placed on a microscope slide. Then, the slide was pressed onto the surface of the stripped skin with light pressure for 15 min. After that, the slide was peeled carefully from the skin. The superglue was dissolved by rubbing with acetone-soaked cotton buds (four times), the cotton buds were soaked overnight in 2 mL methanol and then were analysed by HPLC.

After follicular casting, the skin was chopped into small pieces, homogenised and soaked overnight in 2 mL methanol under constant shaking and at room temperature before being analysed by HPLC.

Part 2 of study, the full-thickness skin (FTS) was cut into discs and divided into three groups (open hair follicles, plugged hair follicles and normal skin), then mounted in horizontal glass Franz type static diffusion cells, stratum corneum side uppermost, with 3 replicates for each formulation. The Franz diffusion cells had an exposed surface area of 1.33 cm² and a receptor volume of approximately 3.4 mL. The formulations (see Table 5.2) were applied to

the skin at an infinite dose of 1 mL and the donor chamber was covered with a glass cover slip to minimise evaporation from the donor phase. Samples of receptor phase (200 µL) were removed at regular time points over the next 24 h and replaced with the same amount of fresh PBS. All samples were analysed using HPLC.

After Franz diffusion studies were completed, the skin in each cell was wiped with cotton buds to remove any remaining formulation and then subjected to tape stripping (20 times) which involved application of adhesive tape (D-Squame tapes, CuDerm Corp., TX), to the exposed skin surface for about 5 second, and then carefully removed. The tapes were placed into separate vials and soaked overnight with 2 mL methanol before being analysed by HPLC. Results for the first tape are discarded, as this represents surface deposited material only.

Follicular casting followed tape stripping. One drop of superglue was placed on a microscope slide. Then, the slide was pressed onto the surface of the stripped skin with light pressure for 15 min. After that, the slide was peeled carefully from the skin. The superglue was then dissolved by rubbing with acetone–soaked cotton buds (four times). The cotton buds were soaked overnight in 2 mL methanol and then analysed by HPLC.

After follicular casting, skin was chopped into small pieces, homogenised and soaked overnight with 2 mL methanol under constant shaking before being analysed by HPLC.

5.3.8 Sample analysis

Minoxidil and caffeine in the receptor fluid, stratum corneum, hair follicles and skin layers were analysed and validated by sensitive and rapid HPLC. The HPLC system consisted of a Shimadzu SIL-20 a HT, CBM-20A system controller, a SPD-20A detector, LC-20AD a pump and an auto injector. Isocratic separation was performed on a Phenomenex Luna C18 5µ (150×4.6 mm) column. The mobile phase of minoxidil (60% of 0.01M sodium dihydrogen phosphate [Na₂H₂PO₄] buffer, 40% acetonitrile v/v containing 2.5 mM sodium dodecyl sulphate [SDS] (adjusted to pH 3) was pumped across the system at 1mL/min flow rate. Minoxidil and its internal standard (propyl paraben) were detected at 281 nm. The caffeine in the skin and receiver compartments were assayed by HPLC using the same conditions as described in Chapters 3 and 4.

5.3.9 Visualisation of follicles and follicular delivery

The LaVision Microscope (LaVision BioTec GmbH, Germany) was used to assess the effect of these formulations in hair follicles and the area around hair follicles. The Multiphoton system coupled to an ultra-short-pulsed Titanium Sapphire laser (Mai Tai, Spectra Physics, Mountain View, California, USA) was used to image the skin. Full-thickness abdominal skin (3 replicates) were mounted in Franz diffusion cells and a finite dose of acriflavine in the formulations containing EU, OA and control (water) was applied. Samples of untreated skin were used as controls. After 24 h, the cells were dismantled and the skin was rinsed gently with water and blotted dry with a tissue. It was then placed directly on a microscope slide. Images were captured by two photon excitation at 740 nm. A 100 μm Z- stack was captured with a 5 μm step size totalling 20 images. The skin was imaged through to capture different depths, from the superficial surface, corresponding to the stratum corneum (SC; ~5-10 μm), stratum granulosum (SG; ~15-20 μm), *stratum spinosum* (SS; 25-30 μm) and *stratum basale* (SB; 35-40 μm). Keratinocyte morphology was used to confirm each of these layers. Image analysis was done using Image J (Wayne Rasband, National Institutes of Health, USA).

5.3.10 Data analysis

The cumulative amount (Q , $\mu\text{g}/\text{cm}^2$) of minoxidil and caffeine penetrating through an area of 1.3 cm^2 was plotted against time (h). The steady state flux, J_{ss} ($\mu\text{g}/\text{cm}^2/\text{h}$), was determined from the slope of the linear portion of the cumulative amount (Q) versus time plot.

The maximum flux (J_{max}) that would be applicable to saturated solutions can be estimated from the experimental steady state flux corrected for the known solubility in the formulation by Equation 1 (185)

$$J_{max} = J_{ss} \cdot S_V / C_V \quad \text{Equation (1)}$$

Where S_V is the solubility in the formulation and C_V is the experimental concentration used.

The permeability coefficient K_P (cmh^{-1}) was calculated by Equation 2 below which is derived from Fick's 1st law of diffusion (215).

$$K_P = J_{ss} / C_V \quad \text{Equation (2)}$$

Where C_V is the initial concentration of the model compound in the donor.

The apparent diffusivity of solute in the skin divided by path length (D^*) was calculated from the maximum flux and the solubility of the active compound in the *stratum corneum* according to Equation 3 (185).

$$D^* = J_{max} / S_{sc} \quad \text{Equation (3)}$$

Where S_{sc} is the experimentally determined solubility of the solute in the stratum corneum.

Hansen solubility parameters (HSPs) (δ_D , δ_P , δ_H) for formulation excipients, solvents and active compounds were obtained from the software package HSPiP (JW solutions B.V., The Netherlands). The total solubility parameters were also obtained from HSPiP, according to the formula:

$$\delta_{total}^2 = \delta_D^2 + \delta_P^2 + \delta_H^2 \quad \text{Equation (4)}$$

The cumulative amount, fluxes and transfollicular penetration per one hair follicle in the receiving solutions were calculated by the following equations which have been mentioned below:

$$\text{Cumulative amounts } (\mu\text{g}/\text{cm}^2) = \frac{FA \text{ open} - FA \text{ block}}{1.33}$$

$$\text{Transfollicular penetration per one HF } (\mu\text{g}/\text{one HF}) = \frac{(FA \text{ open} - FA \text{ block})}{\text{number of HF}}$$

Where FA open was the caffeine amount in the open system, FA block was the caffeine amount in the block system and HF was the hair follicle.

5.3.11 Statistics

All experiments were analysed by one-way analysis of variance (ANOVA) with post-hoc comparisons (Tukey) using GraphPad Prism 6 (GraphPad Software Inc. La Jolla, CA92037, USA); $P < 0.05$ was considered to be significant.

5.4 Results

5.4.1 Cumulative amount of minoxidil in the receptor after 24h

The cumulative amount of minoxidil penetrating the full-thickness human skin from formulations and controls are shown in Figure 5.1. The cumulative amount of minoxidil penetrating through human skin ($\mu\text{g}/\text{cm}^2$) was plotted as a function of time (h) and the slope yielded the pseudo steady-state flux, J_{SS} ($\mu\text{g}/\text{cm}^2/\text{h}$) (Table 5.3). The permeability coefficient K_P (cm/h) was calculated (Table 5.3). After 24 h exposure, the permeation of minoxidil delivered into the receptor from the nanoemulsion was significantly higher than the control ($P < 0.05$). The highest permeation was seen with the formulation containing EU as the oil phase. However, all formulations were significantly higher than controls and there were no significant differences between OA and EU nanoemulsion formulations in the amount of minoxidil permeation after 24 h.

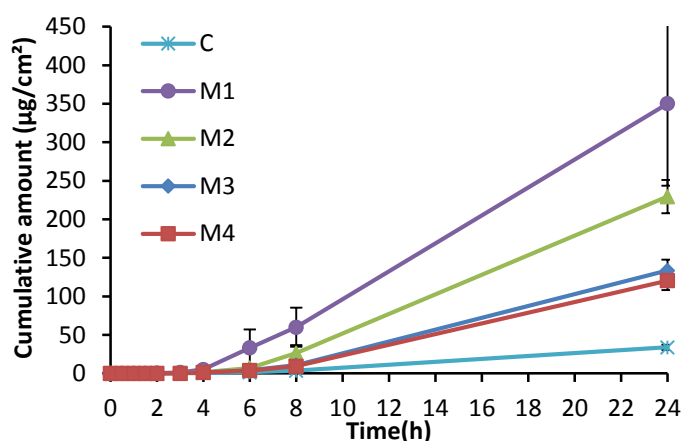


Figure 5.1 Permeation profiles of minoxidil through excised human skin from nanoemulsions and controls (**Mean \pm SD, n=4**)

Table 5.3 Transdermal permeation parameters and pH of the minoxidil from formulations and control (**Mean \pm SD, n=4**)

Formulation	J_{SS} ($\mu\text{g}/\text{cm}^2/\text{h}$)	$Kp \times 10^4$ (cm^2/h)	J_{max} ($\mu\text{g}/\text{cm}^2/\text{h}$)	D^* ($\times 10^4 \text{ cm}^2/\text{h}$)	S_V (mg/mL)	S_{SC} (mg/mL)	pH
C	1.9 \pm 0.1	0.9 \pm 0.0	3.3 \pm 0.2	0.8 \pm 0.0	34.7 \pm 2.7	44.3 \pm 4.6	7.2
M1 ^E	18.1 \pm 2.3	9.1 \pm 1.1	188.4 \pm 23.4	13.8 \pm 0.1	207.8 \pm 1.6	136.1 \pm 16.9	7.1
M2 ^E	12.7 \pm 1.9	6.3 \pm 0.1	179.9 \pm 27.1	12.5 \pm 1.8	283.4 \pm 2.3	143.9 \pm 13.4	7.2
M3 ^O	6.2 \pm 1.9	3.1 \pm 1.3	42.6 \pm 12.9	5.7 \pm 2.4	137.3 \pm 1.1	74.2 \pm 8.0	5.4
M4 ^O	6.9 \pm 1.2	3.5 \pm 0.5	52.8 \pm 9.0	7.0 \pm 1.2	152.1 \pm 1.3	75.1 \pm 5.7	5.9

5.4.2 Amount of minoxidil in the stratum corneum and hair follicles

The effect of nanoemulsion formulations on minoxidil penetration into the stratum corneum was assessed by tape stripping, is shown in Figure 5.2. Application of M1^E M2^E, M3^O, resulted in more minoxidil being recovered in the stratum corneum than from control and M4^O. The minoxidil recovered from follicular casting is also shown in Figure 5.2; more minoxidil was retained from the appendages after application of the formulation containing OA than EU, although both were higher than the control which contained 60% ethanol. However, the differences between these formulations (OA, EU) failed to reach statistical significance.

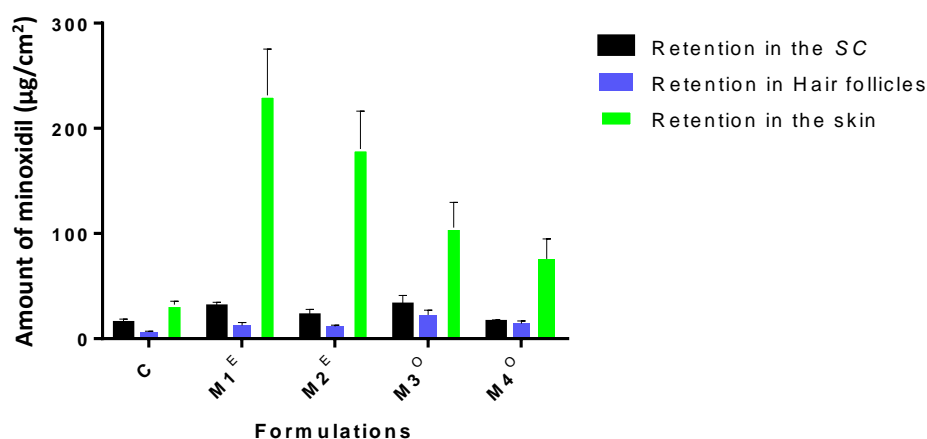


Figure 5.2 Minoxidil retained in stratum corneum, hair follicles and skin layers (**Mean \pm SD, n=4**)

5.4.3 Amount of minoxidil retained in the skin layers (viable epidermis and dermis) after 24h

The amount of minoxidil retained in the skin after 24 h from nanoemulsion formulations and control is showed in Figure 5.2. Minoxidil retained in the skin from nanoemulsion formulations were significantly higher than control and were in this order $M1^E > M2^E > M3^O > M4^O$, the same pattern as receptor.

5.4.4 J_{max} estimated, solubility in the stratum corneum S_{SC} and diffusivity (D^*) and S_V

Maximum flux (calculated from steady state flux using Equation 1), permeability coefficient K_P (calculated from Equation 2) and the apparent diffusivity D^* (diffusivity divided by path length, from Equation 3) are shown in Table 5.3 (caffeine). Significantly enhanced fluxes were observed for minoxidil with the nanoemulsions compared to the control. Apparent diffusivity was also enhanced with the nanoemulsions

To elucidate the mechanisms by which maximum flux was enhanced in these formulations, we examined the relationships between J_{max} and some determinants of this parameter. As seen in Figure 5.3A, the stratum corneum solubility of minoxidil was enhanced by the nanoemulsions much more than that of the control (range, 34.7-283 mg/mL). Moreover, minoxidil increased stratum corneum solubility, which was associated with an enhanced flux. Figure 5.3B shows a clear relationship between effective diffusivity in the membrane and J_{max} , indicating that the nanoemulsion formulations have affected the epidermis so that diffusivity also has become a major determinant for J_{max} for this drug.

In addition, minoxidil has shown no relationship between S_{SC} and solubility in formulations (S_V) for all nanoemulsion formulations (Fig 5.3C).

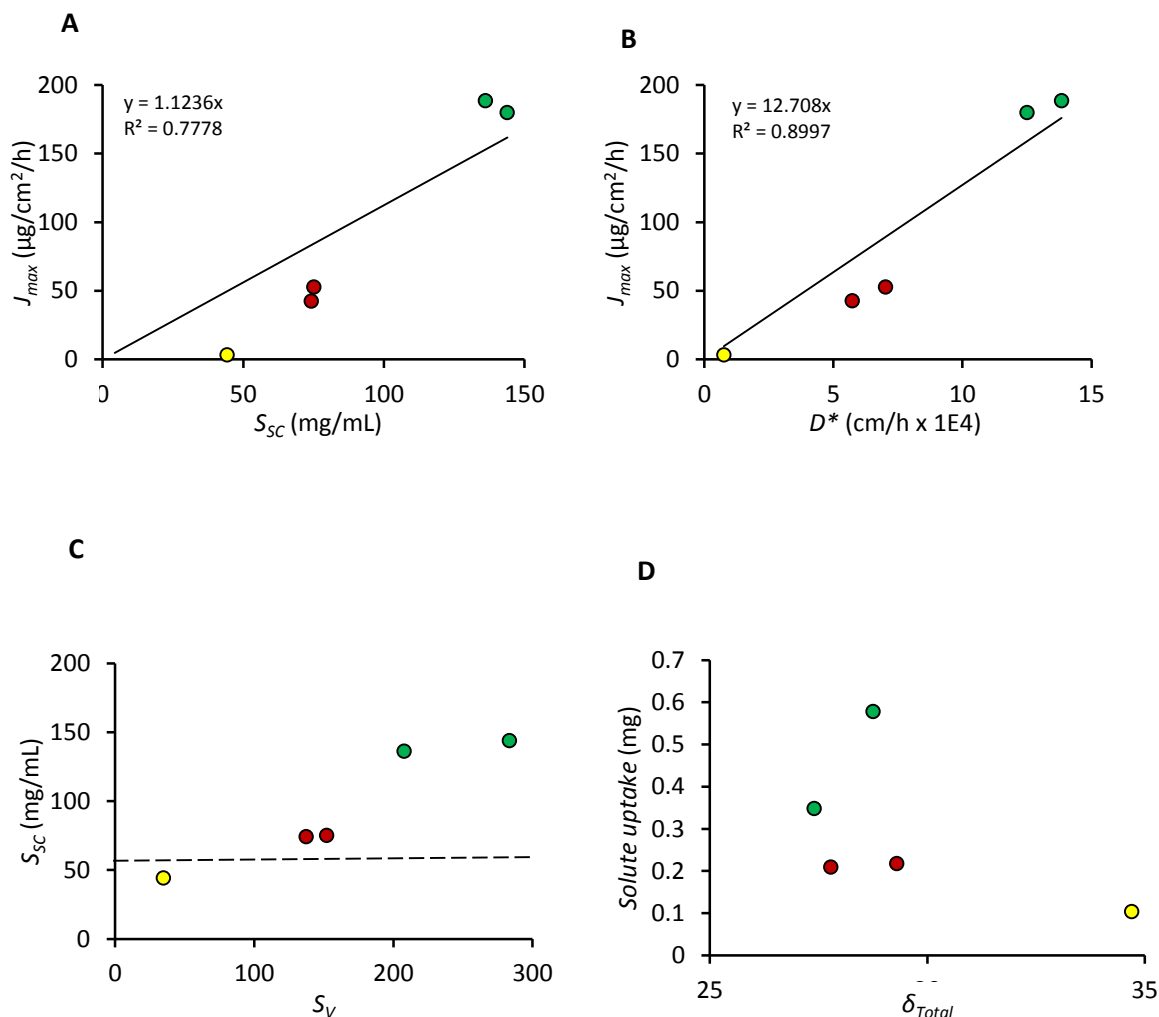


Figure 5.3 Minoxidil A - J_{max} values for all formulations versus solubility in the stratum corneum (S_{sc}) ($R^2=0.77$); B- J_{max} values for all formulations versus Diffusivity (D^*) ($R^2=0.89$); C- Solubility in the stratum corneum versus S_v ; D- Solute uptake versus total solubility parameters (yellow circle is control (60% ethanol/water), red is OA formulations and green is EU formulations).

5.4.5 Minoxidil solubility in the vehicles

The solubility of minoxidil in the formulations is also shown in Table 5.3. The solubility of minoxidil in the control (60% ethanol/water) was much less than in the corresponding values of the nanoemulsions. EU tended to enhance the stratum corneum solubility of minoxidil more than OA did.

5.4.6 Solubility in the stratum corneum and solvent uptake.

The solubility of caffeine in the stratum corneum for each of the different vehicles is shown in Table 5.3. There were significant differences between the stratum corneum solubilities of

minoxidil in the nanoemulsion vehicles compared to the control solution. We investigated the possibility that the stratum corneum solubility was determined by the uptake of the vehicle into the membrane, carrying solute with it. We explored whether vehicle uptake into the stratum corneum was related to the properties of the vehicle. Figure 5.3D shows solute uptake into the stratum corneum plotted against the total solubility parameter of the vehicle (δ_{total}); we found that solvent uptake into the stratum corneum is greatest for those formulations where the total solubility parameter is lowest (Fig 5.3D).

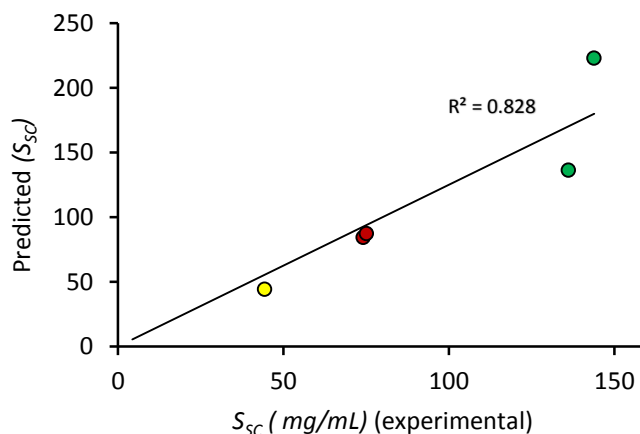


Figure 5.4 S_{SC} (predicted) versus S_{SC} (measured) (yellow circle is control (60% ethanol/water), red is OA nanoemulsion and green is EU nanoemulsion)

We also attempted to predict solubility in the stratum corneum from solvent uptake (Fig 6.4), by assuming the solute was taken up by the stratum corneum partitions into a skin compartment from the vehicle, using the equation:

$$S_{SC}(\text{predicted}) = S_{SC}(\text{skin, control}) + S_V(\text{vehicle}) * V_{up} / V_{SC}$$

Where V_{up} is solvent uptake and V_{SC} is the volume of the stratum corneum. S_{SC} (skin, control) represents the solute in the skin compartment, derived from the experimental data for a control solution:

$$S_{SC}(\text{skin, control}) = S_{SC}(\text{exp, control}) - S_V(\text{exp, control}) * V_{up}(\text{control}) / V_{SC}$$

Where S_{SC} (predicted) was plotted against S_{SC} (experimental) versus experiment stratum corneum (Figure 5.4); a good relationship was found with minoxidil ($R^2=0.82$).

5.4.7 Cumulative amount of caffeine in the receptor after 24 h

Two nanoemulsion formulations containing OA and EU as the oil phase and as penetration enhancers have been characterised and tested in a previous study and have been used in

the present study (Table 5.2). The cumulative amount of caffeine penetrating the full-thickness human skin from open, normal and block hair follicles from these formulations and controls are shown in Figure 5.5A-C. The cumulative amount of caffeine penetrating through human skin ($\mu\text{g}/\text{cm}^2$) was plotted as a function of time (h) and the slope yielded the pseudo steady-state flux J_{ss} ($\mu\text{g}/\text{cm}^2/\text{h}$) (Table 5.4). After 24 h exposure, the permeation of caffeine delivered into the receptor from the nanoemulsions was significantly higher than the controls ($P < 0.05$). The highest permeation was seen from the open hair follicles Fig 5.5B. However, there were no significant differences between open and normal hair follicles in the amount of caffeine permeating after 24 h (Fig 5.5A&B).

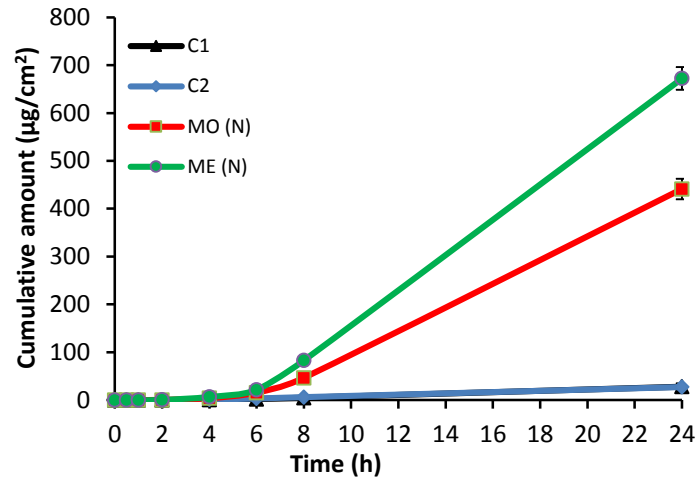
The caffeine flux from nanoemulsion formulation systems was higher than the controls. The caffeine flux from open hair follicles (OHF) was higher than from normal hair follicles (NHF) and block hair follicles (BHF) from ME formulation systems. The transfollicular penetration of caffeine from nanoemulsion formulations was also calculated and found to be higher than controls (Fig 5.6A&B) (Table 5.4). Also, the transfollicular flux was higher for nanoemulsions relative to controls (Table 5.4).

Table 5.4 The cumulative amounts ($\mu\text{g}/\text{cm}^2$), fluxes ($\mu\text{g}/\text{cm}^2/\text{h}$) and follicular penetration ($\mu\text{g}/\text{one hair follicle}$) by follicular closing technique and open hair follicle technique using Franz diffusion cells for 24 h from nanoemulsion formulations and controls.)

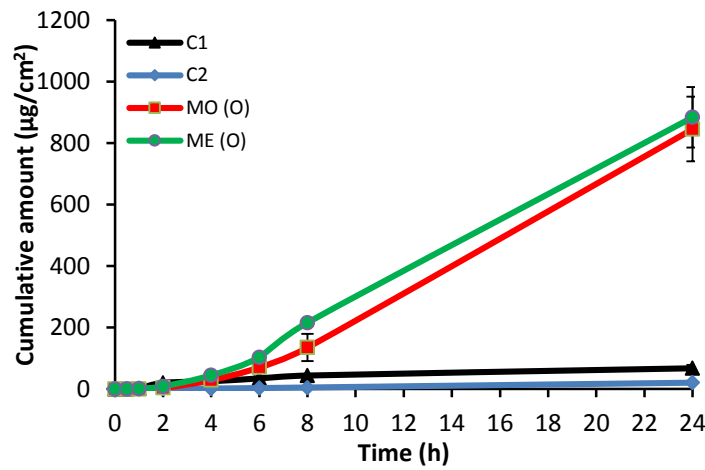
Formulations	C1	C2	M ^o	M ^E
Cumulative amount ($\mu\text{g}/\text{cm}^2$) (NHF)	28.2±7	27.3±2.8	441.4±21.5	672.5±23.8
Cumulative amount ($\mu\text{g}/\text{cm}^2$) (OHF)	67.5±10	20.6±2.6	845.9±105	884.2±98
Cumulative amount ($\mu\text{g}/\text{cm}^2$) (BHF)	21.3±1.4	16.6±3.4	362.7±27	510.2±9.4
Cumulative amount ($\mu\text{g}/\text{cm}^2$) (N-BHF)	12.2	14.9	168.7	288.9
Cumulative amount ($\mu\text{g}/\text{cm}^2$) (O-BHF)	51.5	8.3	573.2	500.6
Transfollicular per one HF (N-BHF)	1.7	2.1	24.1	41.3
Transfollicular per one HF (O-BHF)	7.4	1.6	81.9	71.5
Flux (NHF)	0.6±1	1.3±0.1	21.4±1	32.6±1
Flux (OHF)	2.5 ±0.1	0.1±0.01	40.1±4.5	41.2±5
Flux (BHF)	1.1±0.02	0.9±0.1	17.6±1.3	24.7±0.4
Flux (N-BHF)	0.6	0.7	8.7	15
Flux (O-BHF)	1.1	0.3	27.9	22.7
Flux- Transfollicular per one HF (N-BHF)	0.1	0.9	1.2	2.1
Flux- Transfollicular per one HF (O-BHF)	0.2	0.04	4	3.2

HF = hair follicle; NHF = normal hair follicle, OHF = open hair follicle, BHF = blocked hair follicle (Mean±SEM, n=3); N-BHF = Contribution to permeation by all the hair follicles; O-BHF = Contribution to permeation by the open hair follicles.

A-



B-



C-

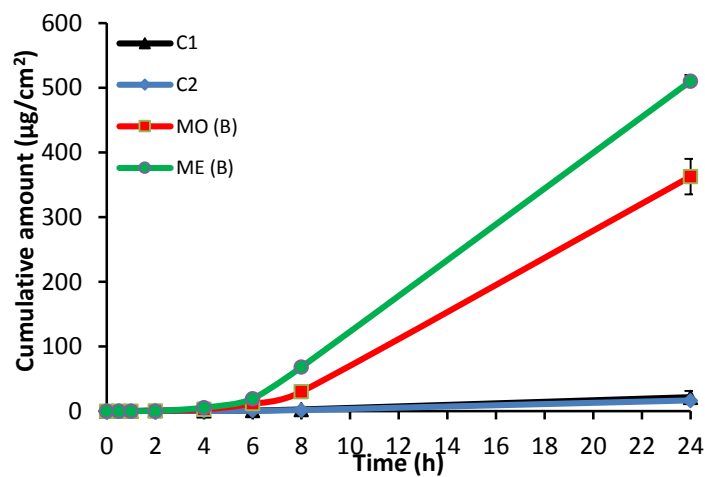
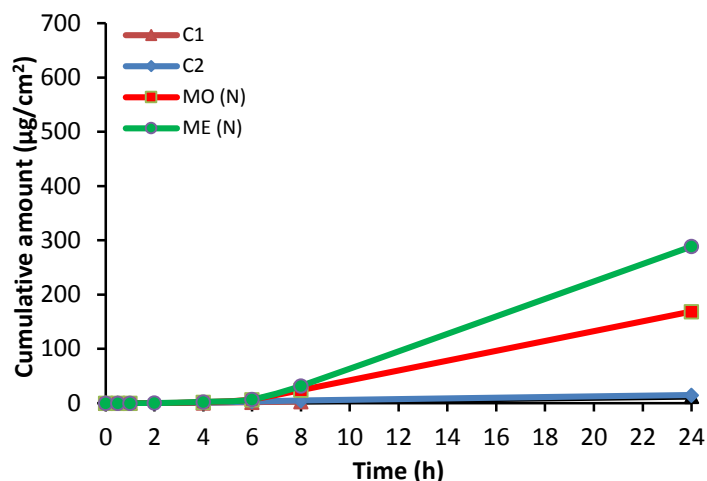


Figure 5.5 Permeation profiles of caffeine through: A- normal excised human skin; B- Excised human skin (after opening the hair follicles); C- Excised human skin (after plugging the hair follicles) from nanoemulsion formulations and controls (Mean \pm SEM, n=3). MO (Nanoemulsion with oleic acid); ME (Nanoemulsion with eucalyptol); B (Blocked hair follicles).

A-



B-

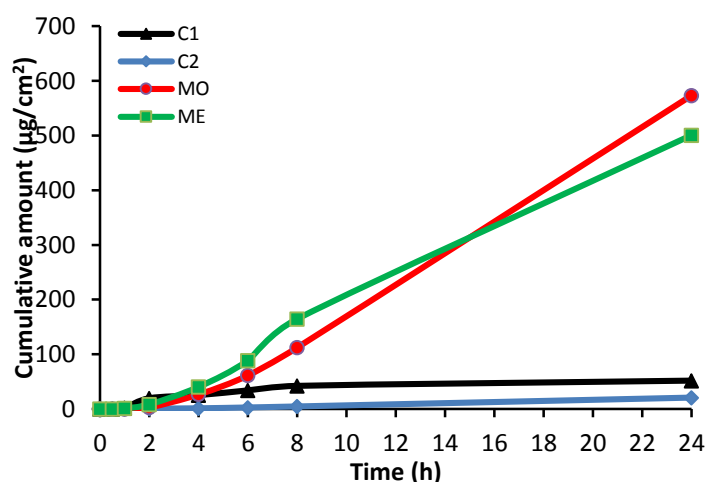


Figure 5.6 Permeation profiles of caffeine through excised human skin: A- Contribution to permeation by all the hair follicles; B- Contribution to permeation by the open hair follicles from nanoemulsion formulations and controls (Mean \pm SEM, n=3).

MO (Nanoemulsion with oleic acid); ME (Nanoemulsion with eucalyptol); N (Normal hair follicles).

5.4.8 Amount of caffeine in the stratum corneum and in the hair follicles

The effect of nanoemulsion formulations and controls from different techniques on caffeine penetration into the stratum corneum, which has been assessed by tape stripping, is shown in Figure 5.7 and Table 5.5. More caffeine has been recovered from the stratum corneum from nanoemulsions than from controls and similar pattern for both controls and nanoemulsions from all techniques.

Recovery of caffeine from follicular casting is shown in Figure 5.8 and Table 5.5; the amount of caffeine recovered from skin layers after application of formulations containing OA and EU was slightly higher than for controls. However, the amount of caffeine recovered from appendages after application of formulations containing EU and OA and controls from blocked hair follicles was lower than for other tests (open and normal hair follicles).

5.4.9 Amount of caffeine retained in the skin layers (viable epidermis and dermis) after 24 h

The amount of caffeine retained in the skin after 24 h from nanoemulsion formulations and control and from open, normal and blocked hair follicles are shown in Figure 5.9 and Table 5.5. The amount of caffeine retained in the skin from nanoemulsion formulations was significantly higher than controls and almost same for all tests (NHF, OHF, and BHF).

Table 5.5 Amount of caffeine ($\mu\text{g}/\text{cm}^2$) in different skin compartments for controls and nanoemulsion formulations.

Formulations	Retention in the stratum corneum			Retention in the HF			Retention in the Skin		
	NHF	BHF	OHF	NHF	BHF	OHF	NHF	BHF	OHF
C1	52.4±5	49.6±5	52.8±3	7.7±2	4.5±1	4.8±1	63.1±12	39.4±6	30.9±4
C2	39.5±3	35.8±6	30.7±2	1.5±0	3.8±1	4.2±1	58.8±13	25.9±6	41.0±11
M^o	113.2±15	128.2±18	115.0±30	12.5±1	12.1±1	15.6±3	623.5±49	713.3±83	724.2±50
M^f	108.7±24	111.3±10	95.2±15	14.0±2	8.5±2	14.1±1	874.0±58	868.1±48	886.0±150

HF = hair follicle; NHF = normal hair follicle, OHF = open hair follicle, BHF = blocked hair follicle (Mean±SEM, n=3).

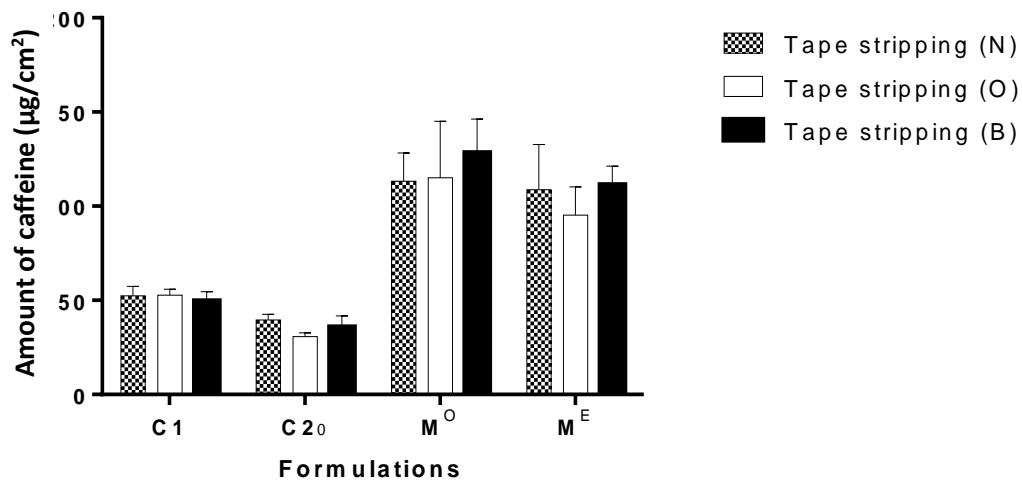


Figure 5.7 Caffeine retained in the stratum corneum from nanoemulsion formulations and controls after 24 h (**Mean ± SEM, n=3**)

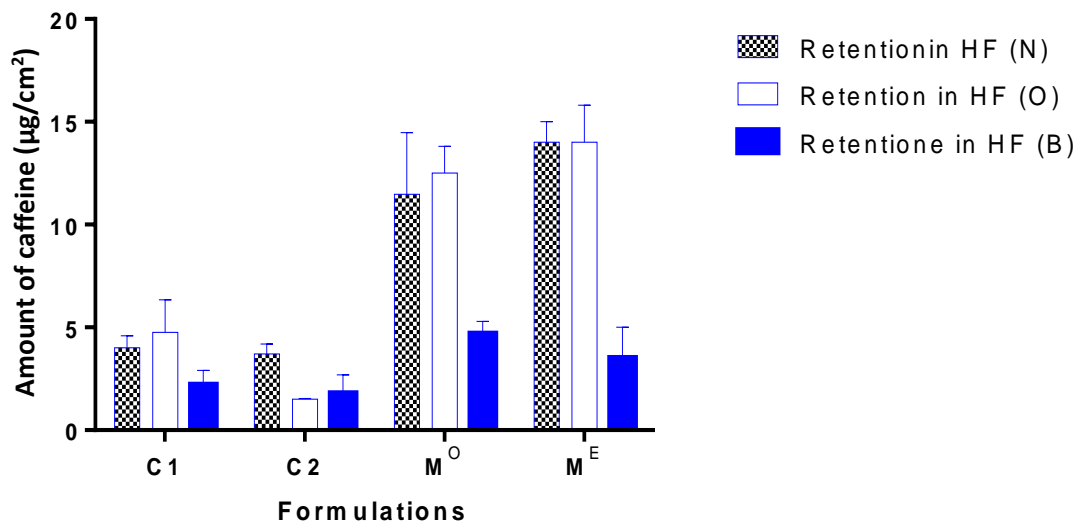


Figure 5.8 Caffeine retained in the hair follicles after topical administration of nanoemulsion formulations & controls up to 24 h (**Mean ± SEM, n=3**)

N = normal hair follicle, O = open hair follicle, B = blocked hair follicle

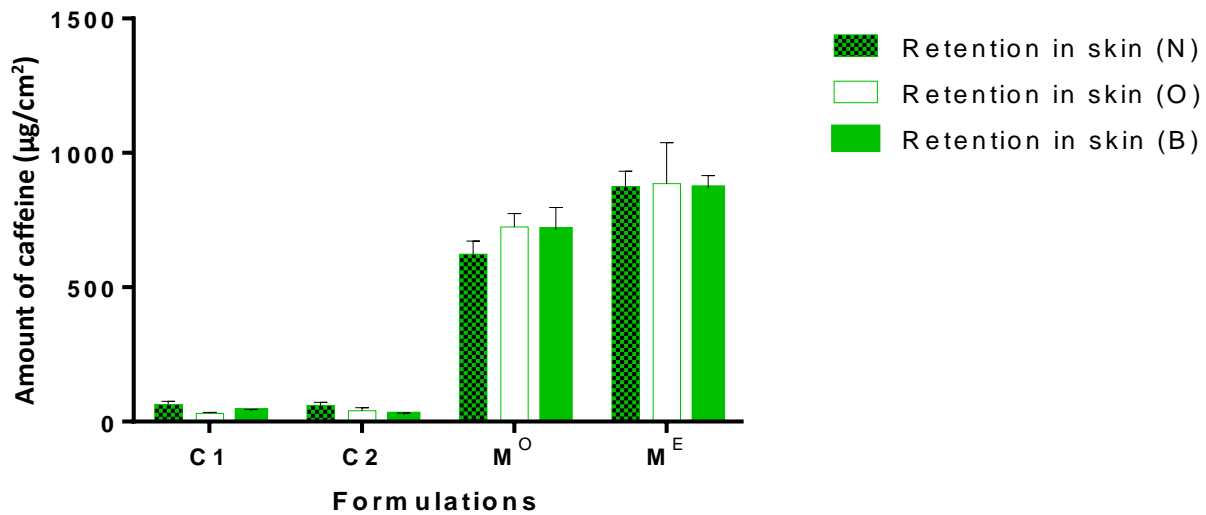


Figure 5.9 Caffeine retained in the viable epidermis and dermis from nanoemulsion formulations and controls after 24 h (**Mean ± SEM, n=3**)

N = normal hair follicle, O = open hair follicle, B = blocked hair follicle

5.4.10 Multiphoton microscopy imaging to evaluate follicular blocking technique and assess the penetration of model fluorescent dye (Acriflavine)

Figure 5.10 illustrates representative images of normal, open and blocked follicles. When the area around the follicle was imaged, both open hair follicles and normal hair follicles showed cellular uptake of acriflavine in the viable layers. The EU nanoemulsion showed uptake of acriflavine when follicles were unmodified while the OA nanoemulsion showed acriflavine uptake into the viable cells with the follicles being opened. However, when the follicles were blocked no visible uptake of acriflavine was seen in the viable cells from either of the emulsions or the control.

5.5. Discussion

Nanoemulsions are composed of non-ionic surfactant (Volpo-N10) which is nontoxic and two types of oil (OA and EU) which are themselves penetration enhancers (188, 216-218). In order to assess the effect of these nanoemulsion formulations of minoxidil on the accumulation and permeation through the skin, an *in vitro* study was carried out using full-thickness human skin and Franz diffusion cells. The results of this study were similar to a study done by Grice et al in 2010, in which they found that the minoxidil recovery from appendages was of the same order as the cumulative amount of minoxidil penetrating through the skin (45). In the current work, it was found that at early on in the experiments the effect of formulations were similar to that of the control, but a change occurred after 4 h similar to the Grice et al finding, and also similar to another study by Patois et al in 2011, which showed that minoxidil penetrated excised pig skin after 6 h, suggesting that the dermis has a longer lag time for penetration in the receiver (219). Our results showed that after 24 h only a small amount of minoxidil reached the receptor fluid. In 2011, Mura et al also found that only small amount of minoxidil reached the epidermis after 8 h (220). The pH value of skin is between 4.2 – 6.1, applied formulations outside of these pH values may lead to skin damage (219). For the nanoemulsion formulations having EU as oil phase, the pH was around 7.2 and the ionisation of minoxidil may have contributed to a high skin accumulative profile from this formulation as the skin has a positive charge. However, the pH of nanoemulsions with OA are at skin range (~5.4); these results are similar to Padois et al findings (219). This study used ethanol as a co-surfactant and also the control contained 60% ethanol, therefore evaporation of the solvent could increase the viscosity of the vehicles and reduce the solubility of minoxidil in the skin and thermodynamic activity of the drug in the vehicles, (especially the control) and permeation (221) (222). Incorporation of minoxidil

in O/W nanoemulsion formulations increased the penetration drug flux significantly (3- to 9-fold), compared with the control (Table 5.3), and these results are consistent with other results that have been done to evaluate the transdermal delivery of several hydrophilic and lipophilic drugs from nanoemulsion formulations (223). The mechanism for this increase is due to increased solubility of these solutes in the stratum corneum (S_{SC}) and also by increased D^* across the skin (Table 5.3). Our study also focused on the relationship between J_{max} and S_{SC} , D^* . A unique finding in this work is the linear relationship between J_{max} and S_{SC} and D^* from all formulations (Figure 5.3A&B). Similarly, Zhang et al showed a linear relationship between J_{max} and S_{SC} for phenolic compounds (108). OA and EU are well known penetration enhancers. It is believed that OA provides high permeation due to its *cis* double bond at C_9 which causes a kink in the alkyl chain and disrupts the skin lipid (224). Although skin lipid is also disrupted by the nanoemulsion and shows enhanced penetration, it acts as a solution (224). This could be contributed to a low percentage of enhancing chemicals compared to the percentage in other formulations. So, the compounds of the vehicle are as important as the structure of the vehicle (225). EU is believed to act by changing intercellular lipid, disrupting the lipid structure organisation and increasing fluidisation which leads to increased diffusivity of the drug (159). A study done by Obata et al in 1991 (226) suggested that ethanol combined with relatively hydrophilic terpenes such as EU have a much greater enhancing effect than lipophilic terpenes. It is also claimed that polar terpenes such as EU could provide better enhancement for hydrophilic drugs than hydrocarbon terpenes such as R-(+)-limonene (227, 228). In our study nanoemulsion formulations with EU gave the highest permeation of minoxidil: these results are consistent with the microemulsion results conducted with curcumin by Liu et al (2010). They reported that terpenes have a different mechanism to enhance transdermal drug delivery: the first possibility proposed was that EU enters the skin as a monomer to increase the solubility of drug in the skin, increases the partitioning of drug in the skin and creates high drug concentration in the upper layers of the skin (189). Our study agrees with this mechanism as the solubility of minoxidil from EU nanoemulsions has a higher solubility in the stratum corneum than that of OA formulations. Another mechanism depended on the direct drug transfer from nanoemulsion droplets to the stratum corneum (189).

We showed in Figure 5.3D that the solute uptake into the stratum corneum was associated with the HSPs of the vehicles. This suggests that the vehicle acts as a carrier for the solute into the stratum corneum.

We also examined whether the uptake solvent of solutes into the stratum corneum may be related to the solubility of the solutes in the stratum corneum. Figure 5.4 suggests that our

solubility model has good correlation between the predicted S_{sc} and measured S_{sc} for minoxidil, as it provides a linear shape with ($r^2= 0.82$). This supports the hypothesis that the enhanced minoxidil permeation in this study is mainly due to an increased solubility of the compounds in the skin (modified stratum corneum solubility). The model here is to induce the idea that the solubility of a solute in the skin can be correlated to its solubility in the formulations and the amount of vehicle absorbed by the stratum corneum: our finding is supported by Zhang et al (108).

In the second part of the study, the penetration of substances into the skin occurred by two main ways; the transfollicular and transepidermal (transcellular and intercellular) penetration routes (229). This study used the normal hair follicles, opened hair follicles and blocked hair follicles skin system. The penetration across open hair follicles presented two methods of penetration, the transfollicular and transepidermal, while, the blocked hair follicles presented only the transepidermal route. The different flux between open, and blocked hair follicles skin was determined as the transfollicular penetration flux.

The caffeine loaded nanoemulsions were investigated for penetration in stratum corneum and in hair follicles of human skin. A study by Ogiso et al in 2002 suggested that hair follicles play an important role in penetration and reservoir processes (230). Cyanoacrylate skin surface biopsy was performed to investigate the transfollicular drug delivery (Fig 5.5) as this method provides selective qualitative and quantitative penetration of topically applied drugs into the hair follicles (15). The amount of caffeine permeating the stratum corneum was removed using tape stripping. Then, the follicular contents were removed by cyanoacrylate skin surface biopsy. The caffeine permeating the rest of the skin was measured by mincing and extracting the stripped skin. The transfollicular flux from nanoemulsion formulations was higher than from controls. A study by Bhatia et al in 2013 on adapalene penetration in porcine ear skin suggested that increased water content in the nanoemulsions, increased the amount of drug in the stratum corneum and in the hair follicle (231). As the nanoemulsion formulations in the study are O/W nanoemulsions, the finding of this study was consistent with Bhatia et al's findings. The mechanism of permeation enhancement with ME formulations may be because of increase partitioning and diffusion of caffeine into the stratum corneum. Hair follicles provide an attractive site in dermatology and can act as long term reservoirs for topical application (232), whereas, drugs located in the uppermost cell layers of the stratum corneum, are continuously depleted because of the physiological process of desquamation (231), which suggest, that the stratum corneum provides only a short term reservoir function. Drug depletion in hair follicles occurs primarily through the

slow process of sebum production and hair growth (14), (233). Colloidal systems such as microemulsions have demonstrated good potential for targeting hair follicles. The present study indicates that nanoemulsions with penetration enhancers (OA and EU), not only increase the permeation through the stratum corneum, but also demonstrate optimal penetration into the hair follicles. The flux of caffeine in the stratum corneum increased from $2.5 (\mu\text{g}/\text{cm}^2) \pm 0.1$ in control (C1) to $40 (\mu\text{g}/\text{cm}^2) \pm 4.5$ with OA and $41 (\mu\text{g}/\text{cm}^2) \pm 5$ in EU nanoemulsions and the penetration in the hair follicles also increased from $0.2 (\mu\text{g}/\text{cm}^2)$ in control (C1) to 4 and $3.2 (\mu\text{g}/\text{cm}^2)$ with M^O and M^E , respectively. Therefore, nanoemulsions were able to penetrate the hair follicle and increased the transfollicular caffeine penetration. Faster absorption of caffeine was detected after 24 h when the hair follicles were open. Otberg et al (234) conducted a similar study on caffeine *in vivo* and found that artificial blocking of hair follicles led to passage through the interfollicular epidermis and its lipid domain only and possibly through sweat glands. Blocking hair follicles led to prolonged time for caffeine to penetrate the skin (234). The same study suggested that hair follicles can be an important route for chemical compounds. This study also finds that hair follicles should not be ignored in the development and optimisation of topically applied drugs and cosmetics. The present study was only with caffeine, which is a model hydrophilic compound. The novel follicular plugging method we developed was very effective in visualisation of the blocked follicles both under the optical microscope while plugging and also allowed multiphoton imaging to evaluate the penetration into and around the hair follicles. The increase in observed acriflavine penetration was similar to the increase in caffeine penetration from the Franz cell studies. Acriflavine stained the nuclei of the cells consistent with other unpublished studies conducted. As with the follicular casting studies where the amount of caffeine present in the hair follicle was calculated, we imaged the area of the hair follicle and the skin around the hair follicle and observed a large amount of acriflavine (hydrophilic model compound) present in the follicle and sweat glands. We also observed that when the follicles were blocked off by the cyanoacrylate and acriflavine blocking procedure, the intercellular area of viable layer cells seemed to have taken up some of the acriflavine delivered through the OA nanoemulsion. However, the staining was unlike the nuclear staining observed previously and was more localised around the cells. Further studies will be needed to further understand this interesting observation and also to evaluate the effect of hair follicles on percutaneous penetration of other compounds with different physicochemical properties.

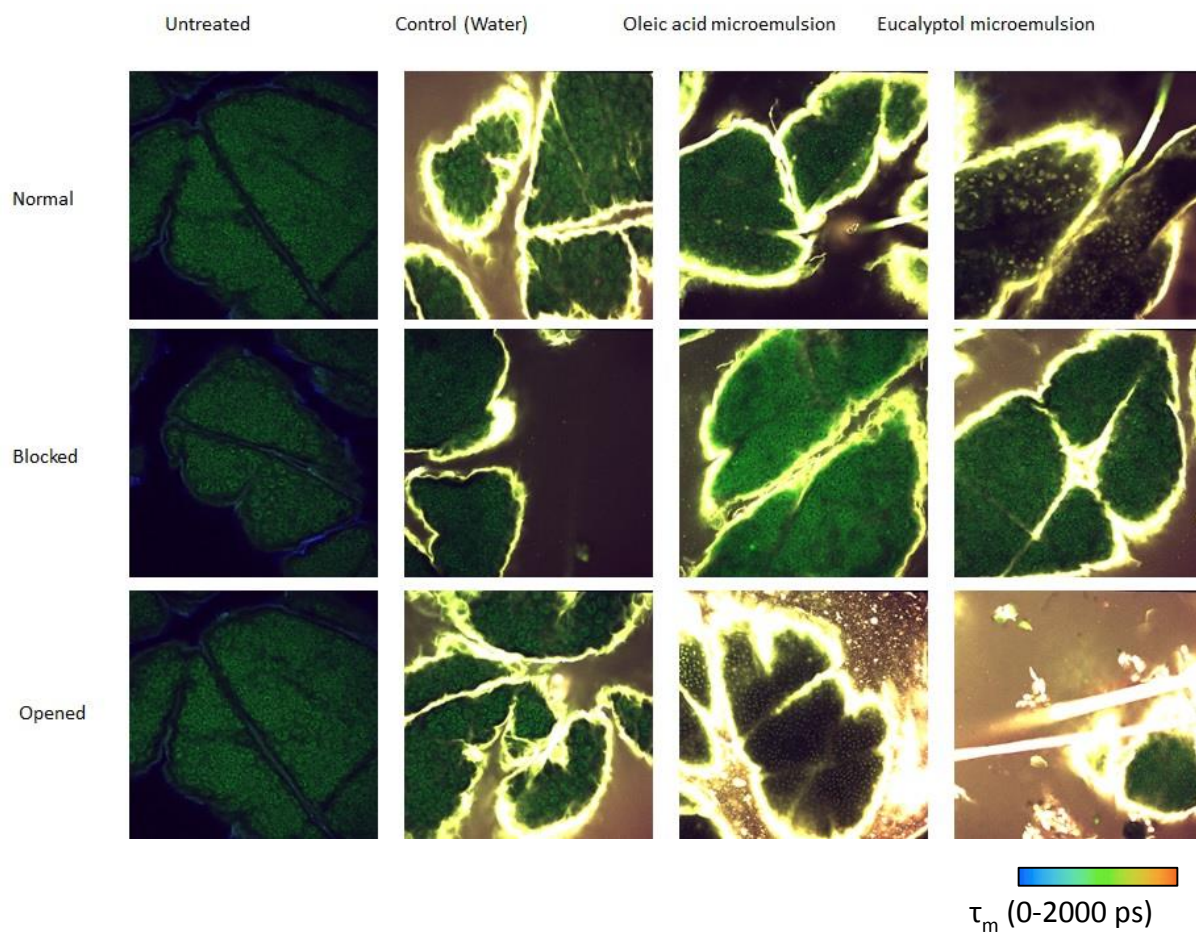


Figure 5.10 Skin images after applying nanoemulsion formulations and controls.

5.6 Conclusion

In short, from these results for minoxidil transdermal penetration, we found that O/W nanoemulsions containing OA and EU as oil phase and penetration enhancers were highly effective *in vitro*. The transdermal flux of minoxidil increased 3~ 9-fold in contrast to the control. Moreover, transport by the appendages can be a valuable route for minoxidil. The mechanism of penetration from these formulations is by increasing the partitioning and diffusivity of minoxidil in the stratum corneum. The results obtained from the transfollicular study demonstrate that nanoemulsion formulations are not only promising vehicles for transdermal delivery but also transfollicular delivery of the hydrophilic drug caffeine. The imaging results from the skin confirm this finding that the hydrophilic model penetrated the hair follicles. Therefore, further study of these advanced formulations and their mechanism of action is needed in order to find suitable and safe formulations for transdermal and transfollicular delivery of different lipophilicity drugs.

Chapter 6

A comparison of the penetration and permeation of caffeine into and through human epidermis after application of various vesicle formulations

6.1 Abstract

A range of vesicles is now widely used to carry various solutes into and through the epidermis. These usually have the active solute encapsulated within and may be modified to confer flexibility and skin penetration enhancement. Here, we compared the ability of five different vesicle systems to deliver a model hydrophilic drug, caffeine, into and through excised human skin. In addition to lipids, the vesicle excipients included eucalyptol (EU) or oleic acid (OA) as penetration enhancers, and decyl polyglucoside (DPGluc) as a non-ionic surfactant. Vesicle particle sizes ranged between 135 and 158 nm and caffeine encapsulation efficiencies were between 46% and 66%. Caffeine penetration and permeation was measured using HPLC. We found that niosomes, which are liposomes containing a non-ionic surfactant and transferosomes (ultraflexible vesicles) showed significantly greater penetration into the skin and permeation across the stratum corneum. Significant enhancement of caffeine penetration into hair follicles was found for transferosomes and those liposomes containing OA.

We conclude that targeted delivery of the hydrophilic drug, caffeine, into the skin compartments can be modified using optimised vesicular formulations.

6.2 Introduction

Topical drug delivery offers specific benefits over other administrative routes for local action but the barrier nature of the skin presents a major obstacle for many drugs delivered into and through it (235). Chemical strategies to reduce the effect of the barrier include the use of penetration enhancers, such as OA or octyl salicylate, and the use of more advanced colloidal systems such as microemulsions, solid lipid nanoparticles and nanostructured lipid carriers. Liposomes are hollow spheres comprising phospholipid and an aqueous phase. Hydrophilic drugs may be inserted in the aqueous compartment while lipophilic drugs can be sequestered in the phospholipid. Many excipients including lipids, surfactants and solvents have been added to improve the stability or other structural features of liposomes (236). Cholesterol tends to make the liposome membrane less permeable by filling up holes or disruptions (236). Jacobs et al (237) speculated that liposomes may either form a thin

lipid film on the surface of the skin, so that water loss is retarded, or combine with intercellular skin lipids to form liquid-crystalline matrices in the uppermost skin layers.

Various forms of liposomes exist. Transferosomes are defined as vesicular particles composed of phospholipids and surfactants such that the inner aqueous compartments are surrounded by a highly elastic and adaptable lipid bilayer (238). They are metastable, making them able to enter pores smaller than their size (239). They present a more flexible transport system with improved vesicular stability and the potential to be used with diverse active components (240). The flexibility is contributed in part to their relatively high membrane hydrophilicity, which gives the membrane the ability to swell more than, for example, conventional liposomes. Like liposomes, transferosomes are unilamellar or multilamellar structures (241) and contain a surfactant as an edge activator (242, 243). Niosomes are uni- or multi-lamellar spheroidal structures containing a mixture of cholesterol and non-ionic surfactants such as alkyl ethers, esters or amides (221, 244). They have been assessed as an alternative drug delivery system compared to conventional liposomes.

Niosomes offer higher physical and chemical stability (245) and a great variety of surfactant choice (246). It is claimed that for topical applications, niosomes can increase the time of drug residence in the stratum corneum and epidermis whilst decreasing drug systemic absorption (246). Another study observed structural changes in the lipid interstitial spaces of the stratum corneum after exposure of the skin to niosomes and suggested that these changes may be responsible for the resultant enhanced penetration (247).

Skin appendages provide an alternative route for drug penetration through the skin. Pertinent to drug penetration via hair follicles, the follicular infundibulum provides an increase in the surface area, acting as a reservoir, and represents, at the lower end, an interruption of the stratum corneum barrier (248). Some studies have focused on direct targeting of hair follicles, such as with compounds for acne and alopecia therapies. Many attempts have been made to measure substances retained in the hair follicles after topical administration of model compounds such as dyes (249) and nanoparticles (213); however, little has been done with therapeutic agents and this subject requires further investigation (250).

This study aimed to investigate the feasibility of vesicle (liposome, transferosome and niosome) structure to improve the delivery of the hydrophilic drug caffeine into appendages, stratum corneum and through human skin. Differential stripping (40) or tape stripping is a useful technique that allows measurement of the amount of solute retained in the stratum

corneum and of the amount of follicular retention by follicular casting. In order to target a particular skin site after topical application, the formulation of caffeine was manipulated. Liposome, transferosome and niosome formulations were prepared by the thin film-hydration (TFH) method using DLPC and cholesterol (as lipid) and OA, EU, or DPGLuc as edge activators.

6.3 Materials and Methods

6.3.1 Materials

Caffeine, OA, EU, ethanol, cholesterol, dilauroyl L- α -phosphatidylcholine (DLPC, CAS # 18194-25-7) were obtained from Sigma-Aldrich Pty. Ltd. (Sydney, Australia). DPGLuc (sold as Oramix NS 10) was obtained from SEPPIC SA (France). All chemicals and solvents were of analytical grade.

6.3.2 Vesicle preparation

Six different vesicles were prepared, with excipient mixtures as shown in Table 6.1. For all vesicles, the excipients were mixed in a rotary flask in the ratios shown, followed by glass beads (4 g) and chloroform (3 mL) treatments. Once the lipids were dissolved, the solvent was gradually evaporated on a rotary evaporator at 30°C until a lipid film formed on the wall of the flask. The flask was set aside for 2 h to eliminate residual chloroform, after which the lipid film was stirred with 2 mL caffeine solution (2% in water) for 2 h at 30°C. The liposome suspensions were extruded through a polycarbonate membrane with pore size 100 nm using the Liposofast extruder (AVESTIN, Inc., Ottawa, Canada). Thirty-one cycles of extrusion were performed for each vesicle type.

6.3.3 Vesicle characterisation

The average particle diameter, polydispersity index (PDI) and zeta potential of the vesicles were measured with a Zetasizer Nano ZS (Malvern Instruments, Ltd, Malvern UK). Each sample was measured three times and the mean value was calculated.

6.3.4 Caffeine encapsulation efficiency

To separate the non-encapsulated drug, the vesicle suspensions were centrifuged at 14000 rpm for 30 min at room temperature. The amounts of caffeine in the supernatant and also in

the clear solution were analysed by high performance chromatography (HPLC). Drug encapsulation efficiency (EE%) was calculated as: $EE\% = 100 \times \text{mass of incorporated drug} / \text{total mass in vesicle preparation}$.

6.3.5 Caffeine skin permeation studies

Permeation studies using full-thickness human abdominal skin were performed in Franz diffusion cells with an effective diffusion area of 1.33 cm² and a 3.4 mL receptor chamber volume. The skin was provided by a female donor following elective surgery, with ethical approval granted by The University of Queensland Human Research Ethics Committee (Approval No. 2008001342). The skin was cut into discs and mounted in Franz diffusion cells with the stratum corneum side facing upwards. The receptor contained PBS buffer (pH 7.4) at 35°C. A volume of 160 µL of the vesicle formulations and the control solution was applied to the surface of the skin and the donor chamber was covered in parafilm for the duration of the experiment to inhibit water evaporation. Several times over a 24 h period, 200 µL of the receptor was withdrawn and replaced with the same amount of fresh PBS buffer. After 24 h, the sample was taken, the cells dismantled and the skin in each cell was wiped with cotton buds to remove any remaining formulation. Up to 20 tape strips were then taken from each skin sample (D-Squame tapes, CuDerm Corp., TX). The tapes were placed into separate vials and mixed overnight with 2 mL methanol to extract the caffeine removed from the stratum corneum by the tapes. Follicular casting was performed after tape stripping. One drop of superglue (LOCTITE®, Henkel Australia) was placed on a microscope slide and pressed onto the surface of the stripped skin with light pressure for 15 min. The slide was peeled carefully from the skin and the superglue containing caffeine sampled from the follicles was dissolved by rubbing four times with acetone-soaked cotton buds. The cotton buds were mixed overnight with 2 mL methanol. After follicular casting, the skin was chopped into small pieces, homogenised and mixed overnight with 2 mL methanol. Receptor fluid and extracts from tapes, casts and skin were analysed by HPLC.

6.3.6 Sample analysis

Caffeine was analysed by a sensitive and rapid HPLC method. The HPLC system consisted of a Shimadzu SIL-20 a HT, CBM-20A system controller, a SPD-20A detector, LC-20AD a pump and an auto injector. Isocratic separation was performed on a Phenomenex Luna C18 5µ (150×4.6 mm) column using 95% water, 2% acetonitrile, 2% tetrahydrofuran and 0.5%

acetic acid as the mobile phase, at a flow rate of 1 mL/min. Caffeine was detected at 273 nm.

6.3.7 Data analysis and Statistics

The cumulative amount ($\mu\text{g}/\text{cm}^2$) penetrating per skin surface area was plotted against time (h). The steady state flux J_{SS} ($\mu\text{g}/\text{cm}^2/\text{h}$) was derived from the slope of the linear portion of the cumulative amount versus time (t) plot.

All data were analysed by one-way analysis of variance (ANOVA) with post-hoc comparisons (Tukey) using GraphPad Prism 6 (GraphPad Software Inc. La Jolla, CA92037, USA); $P < 0.05$ was considered to be significant.

6.4 Results

6.4.1 Vesicle characterisation

Particle size, polydispersity indices (PDI), zeta-potentials and caffeine encapsulation efficiencies of all vesicles are presented in Table 6.2. As shown by the low PDI values, all vesicles had a narrow size distribution. The high negative zeta potential values for both niosomes and the liposomes containing OA indicate that these materials, in particular, would be stable in suspension. The encapsulation efficiencies were relatively similar across the five vesicle types.

6.4.2 Permeation of caffeine from vesicles and control

The cumulative amounts of caffeine penetrating full-thickness human skin from each of the test formulations over 24 h are shown in Figure 6.1 and overall steady-state fluxes calculated from these plots are shown in Table 6.3. Niosomes and transferosomes had significantly greater fluxes than other formulations, as indicated.

Other skin permeation parameters for caffeine from the six applications are illustrated in Table 6.3 and Figure 6.2. Penetration of caffeine into the receptor was significantly enhanced from the niosomes (N), compared to the aqueous control solution (C) and the liposomes (L, LEU, LOA) and from the transferosomes (T), compared to control (C) and the basic liposomes (L). In addition, total skin penetration (stratum corneum, hair follicles, residual skin and receptor solution) was significantly enhanced by niosomes compared to

control (C) and the basic liposomes (L). Caffeine recovered from hair follicles after transferosome application was 50% more abundant than with LOA and more than twice that seen in all other formulations, although the differences did not reach statistical significance ($P=0.10$, T vs. C). Similarly, stratum corneum and skin retention were enhanced with the advanced formulations (niosomes, transferosomes and to a lesser extent, the liposomes containing penetration enhancers EU and OA) but differences did not reach statistical significance.

6.5 Discussion

The nano size range of the vesicles used in this study (128-158 nm) makes them suitable for topical delivery. We (251) and others (252) have shown that by decreasing the vesicle size, the penetration of the encapsulated drug into deeper skin layers can be enhanced. Further reductions in vesicle size could be achieved by extrusion through smaller membranes, particularly with ultraflexible materials such as transferosomes and SECosomes (251). In addition to the narrow range of nano sizes in our series of vesicles, the individual vesicles were shown to be homogeneous, as indicated by the low PDI values (0.05 to 0.15). However, given this homogeneity in particle size seen across the range of vesicle formulations, it is likely that factors other than particle size contributed to the observed differences in caffeine flux and retention in skin compartments (Table 6.3, Figs. 6.1 and 6.2). Regarding the zeta potential, LOA, N possessed a negative surface charge (Table 6.2) while LEU, T and L dispersion possessed a neutral charge, indicating that the incorporation of edge activators into liposomes had an important influence on their surface charge.

The encapsulation efficiencies seen here (46–66%) compare well with 30% found by Budai and coworkers (253) for solid lipid nanocarriers based on soy or egg lecithin. Because caffeine $\log p$ is -0.07 ($K_{OW} = 0.85$) it is reasonably soluble in both water and lipophilic solvents. Therefore, it is able to enter both hydrophilic and lipophilic regions of the vascular structure (254). The caffeine encapsulation efficiency was highest in the liposomes containing EU. This may be due to the relatively hydrophilic nature of EU which results in low permeability of vesicles.

Optimised vesicular systems can exert different functions upon topical delivery (255). They can improve drug deposition in the skin at the site of action, with the additional goal of decreasing systemic absorption and thus minimising adverse effects (133). They may also provide targeted delivery to skin appendages. In an attempt to find a vesicular formulation

for topical delivery of caffeine, vesicular systems were formulated using OA, EU and decyl polyglucoside (DPGluc) as edge activators. OA and EU are well known penetration enhancers (256). DPGluc is a low irritant, non-ionic surfactant that is commonly used in pharmaceutical and cosmetic formulations and can form vesicles including niosomes in combination with appropriate amounts of cholesterol (257).

In this work, all formulations were able to achieve sustained delivery of caffeine into and through the skin over 24 h, with no depletion of the donor material. As a percentage of the total applied drug dose, total caffeine delivery ranged from 6.6% and 7.4% for the aqueous solution and the conventional liposomes, up to 14.9% and 16.0% for the transferosomes and niosomes, respectively. The greatest flux was seen for transferosomes and niosomes, with apparent flux increases between 12 and 24 h for these formulations. Interestingly, these were the vesicles containing DPGluc as edge activators. This hydrophilic surfactant has also been shown to act as a penetration enhancer for dermal delivery of tretinoin when incorporated into liposomes (258), while other non-ionic surfactants cause similarly enhanced permeation fluxes, for example, with lidocaine (259). A relatively constant flux after about 8 h was seen with the other formulations, including the liposomes containing EU and OA. Given the relatively moderate enhancement of caffeine penetration seen with these latter vesicles, it seems likely that their actions as penetration enhancers in those formulations were not important factors. The combined functions of surfactant edge activator and penetration enhancer would appear to explain the relative enhancement seen with DPGluc. While their work relates to the more lipophilic oestradiol, it is interesting to compare the findings of El Maghraby et al (260), where greater penetration was seen with surfactant-containing liposomes than with OA as a penetration enhancer alone. The authors suggested that liposomes increased oestradiol permeation by mechanisms that are additional to penetration enhancing effects.

The niosomes and transferosomes also showed greater skin retention than other formulations. In particular, penetration into hair follicles from transferosomes appeared to be enhanced. The ultradeformable nature of these vesicles may allow them to gain access to these appendages more readily. Motwani et al (261) suggested that polar drugs delivered from vehicles which are poorly miscible with sebum will have little chance to reach deeper parts of the hair follicles. On the other hand, lipophilic vehicles may assist the transport of drugs dissolved in the oil phase and into the pilosebaceous units (244). Therefore, enhancement of follicular penetration would rely on the solubility of drug in the formulation and the compatibility of the formulation with the lipid environment of the sebum (261).

One way in which the non-ionic surfactant could enhance solute transfer from vesicles into the skin could be to assist in absorption and fusion of the vesicle to the skin surface. This could maximise the ability of the vesicle to structurally modify the barrier properties of the skin, allowing the solute to pass more readily from its encapsulated environment into the intercellular regions of the stratum corneum. Studies (132, 262, 263) conclude that: a) absorption and fusion of niosomes and transferosomes into the surface of skin will enhance drug permeation; b) the vesicles act as penetration enhancers to reduce the barrier properties of the stratum corneum; and c) the lipid bilayers of niosomes act as a rate limiting membrane barrier of solutes (264). The possible mechanism for liposome and niosome formulations is structural modification of the stratum corneum. For transferosomes, both phospholipid (DLPC) and non-ionic surfactant (e.g.,DPGluc) can act as penetration enhancers, which are valuable for increasing the penetration of many drugs. These results suggest that the mechanism of drug transport across skin depends on the compositions of the vesicle formulation and the solute used.

Table 6.1. Liposome formulations showing excipient ratios and aqueous control composition. All formulations contained caffeine, 2% w/v.

Name	Description	Composition
C	Aqueous control solution	100% Water
L	Conventional liposome	DLPC:cholesterol 35:7
LEU	Conventional liposome + eucalyptol	DLPC:Eucalyptol:cholesterol 35:7:7
LOA	Conventional liposome + oleic acid	DLPC:Oleic acid: cholesterol 35:7:7
T	Modified liposome → Transferosome	DLPC:DPGluc:cholesterol 35:7:7
N	Modified liposome → Niosome	DPGluc:cholesterol 35:735:7

Table 6.2. Vesicle system characterisation and encapsulation efficiency (mean ± SD)

Formula	Vesicle size (nm)	PDI	Zeta potential	Encapsulation efficiency %
L (liposomes)	137.1±1.3	0.06±0.03	2.3±0.7	48
LEU (liposomes + EU)	142.3±2.3	0.10±0.01	-9.5. ±0.5	66
LOA (liposomes + OA)	128.4±1.9	0.08±0.02	-51.0±2.7	50
T (transferosomes)	158.3±4.0	0.14±0.04	-18.3±0.2	47
N (niosomes)	135.2±2.3	0.15±0.02	-42.6±2.4	46

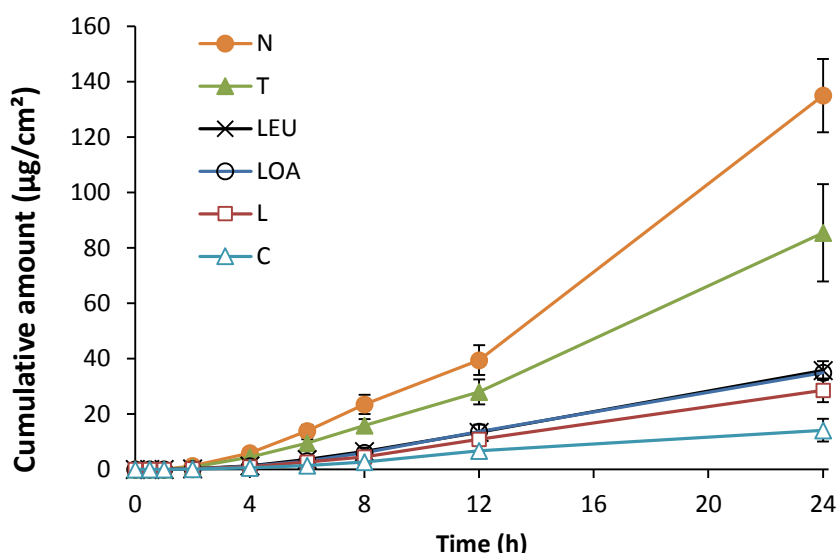


Figure 6.1. Permeation profiles of caffeine through excised human skin from various vesicle systems and a control; (Mean \pm SEM, n=4).

Table 6.3 Permeation parameters following 24 h application of caffeine from vesicle formulations and controls to full-thickness human skin (Mean \pm SD, n=4).

Formula	J_{ss} ($\mu\text{g}/\text{cm}^2/\text{h}$)	SC retention ($\mu\text{g}/\text{cm}^2$)	Hair follicles ($\mu\text{g}/\text{cm}^2$)	Skin retention ($\mu\text{g}/\text{cm}^2$)	Receptor @ 24h($\mu\text{g}/\text{cm}^2$)	Total ($\mu\text{g}/\text{cm}^2$)
C (Control)	0.7 \pm 0.2	17.3 \pm 4.2	0.8 \pm 0.2	48.4 \pm 7.8	14.2 \pm 4.1	80.7 \pm 12.4
L (liposomes)	1.4 \pm 0.4	24.7 \pm 4.1	1.7 \pm 0.4	51.7 \pm 12.7	28.7 \pm 4.3	106.7 \pm 20.5
LEU (liposomes + EU)	1.8 \pm 0.7	32.8 \pm 5.1	1.6 \pm 0.4	95.7 \pm 11.0	35.8 \pm 15.8	166.0 \pm 26.8
LOA (liposomes + OA)	1.7 \pm 0.2	39.4 \pm 6.4	3.5 \pm 0.7	93.5 \pm 7.8	34.9 \pm 3.3	147.9 \pm 30.7
T (transferosomes)	4.1\pm0.8*	66.4 \pm 25.9	5.3 \pm 3.3	85.7 \pm 28.5	85.5\pm20.3*	242.9 \pm 77.6
N (niosomes)	6.6\pm0.6**	70.7 \pm 28.9	2.2 \pm 0.5	103.4 \pm 7.8	135.0\pm13.3**	285.3\pm50.8*

The total shown is the sum of retention in the stratum corneum (SC), hair follicles, residual skin and receptor penetration.

Significant differences (1-way ANOVA/Tukey): *versus Control solution (C) and Liposomes (L); **versus Control solution (C), Liposomes (L), Liposomes +EU (LEU), Liposomes + OA (LOA)

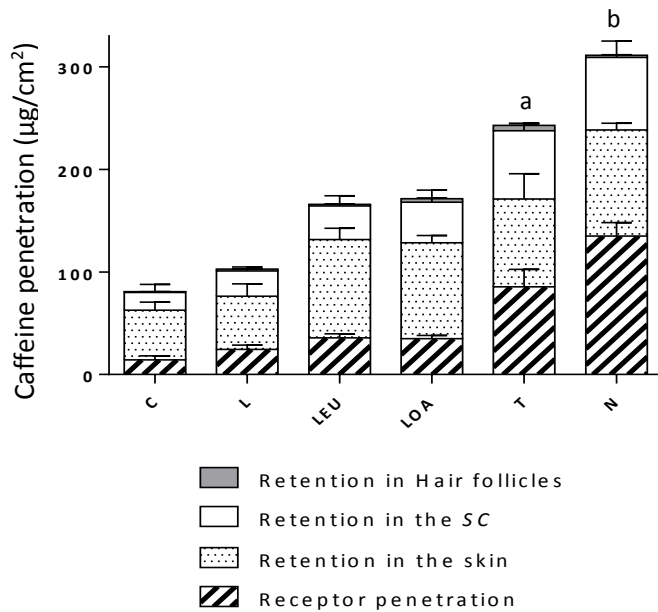


Figure 6.2. Caffeine recovery from the stratum corneum (SC), hair follicles, residual skin and receptor solution after application of vesicles and control for 24h (Mean \pm SEM, n=4).
^aAmount in receptor at 24 h; Transfersomes > Control solution (C) and Liposomes (L);
^bAmount in receptor and total penetration at 24 h; Niosomes > Control solution (C), L = Liposomes, LEU = Liposomes +EU, LOA = Liposomes + OA. (1-way ANOVA / Tukey)

6.6 Conclusion

The *in vitro* permeation of caffeine from vesicles with different compositions of penetration enhancers and non-ionic surfactants have been studied and evaluated. Incorporating the non-ionic surfactant DPGLuc into liposomes enhanced skin penetration of caffeine more than the penetration enhancers OA and EU. The results suggest that fusion of the vesicles with the lipid of the stratum corneum and direct transfer of solute from the vesicle formulations to the skin may contribute to the mechanism of drug permeation enhancement by transfersomes and niosomes. The overall results indicate that the presence of penetration enhancers in the vesicle components is not the important operating factor.

Chapter 7

Conclusion and Future Directions

Skin delivery offers many benefits over conventional routes of administration. However, the barrier nature of the stratum corneum presents an important issue for many drugs to be delivered into and through the skin (2). Hence, many strategies have been used to overcome the skin barrier. Penetration enhancers have been claimed to improve drug delivery and can be used as oil phase or edge activators in advanced formulations such as microemulsions and liposomes. This thesis started with using penetration enhancers with simple solutions to explore the relationship between skin penetration maximum flux to the skin solubility for different vehicle compositions. Then, I extended this approach by incorporating these penetration enhancers into advanced formulations (microemulsions and vesicle systems) to investigate their effect on skin permeation of model compounds. The third aim was to investigate the effect of these penetration enhancers on follicular penetration of model compounds.

7.1 Conclusion

7.1.1 Effect of Penetration Enhancers; Solution Studies

This study has shown that the permeation of caffeine, minoxidil, lidocaine and naproxen were enhanced by specific vehicles that interacted with the skin (OA, EU, SLS and ethanol). The greatest effects were seen on flux and diffusivity by the EU and OA vehicles on the more hydrophilic compounds, caffeine and minoxidil. Enhancements in stratum corneum solubility were predicted by experimentally determined uptake of solvent and solute. We concluded that enhanced solute fluxes were mainly driven by increased diffusivity in the stratum corneum, likely to be due to greater lipid fluidisation caused by the enhancers. Much evidence in the literature suggests that vehicles can act by promoting partitioning of the skin. The solubilities in the stratum corneum depend on the amount of vehicle absorbed in the stratum corneum and the amount of solutes dissolved in the vehicles.

In the pretreatment study, there was enhancement of caffeine flux following pretreatment with penetration enhancer vehicles of the heat separated epidermis. Enhancement could be related to Hanson solubility parameters of the vehicle. Calibration of the solute flux and its solubility in the stratum corneum data is a simple novel plotting procedure that separated and quantified the effects of the vehicle on solute partition and diffusion. The treatment and pretreatment results indicate that enhancement is related mainly to an increase in partition

into the skin with an increase in diffusivity. The diffusivity obtained for all compounds, was unaffected by the inert control vehicles (controls) supporting the notion that J_{max} is determined by stratum corneum solubilities and not diffusivity. More investigations are needed to understand the behaviours of different types of actives, and vehicles on the skin to design a cosmetic and dermatological product with high strength and fewer side effects.

7.1.2 Synergistic skin penetration enhancer and nanoemulsion formulations promote the human epidermal permeation of caffeine and naproxen

Nanoemulsions can be formed from different aqueous, surfactants, co-surfactants and oil components. They are commercially feasible, simple and convenient vehicles to enhance delivery of hydrophilic and lipophilic compounds with few side effects. The objective of this study was to investigate the effect of nanoemulsions on improving the skin delivery of a model hydrophilic (caffeine) and a lipophilic compound (naproxen). The nanoemulsions were formulated with oleic acid (OA) and eucalyptol (EU) as penetration enhancers for both caffeine and naproxen. Extensive physicochemical characterisation was undertaken to evaluate the characteristics of the nanoemulsion systems generated. Evaluations were also undertaken to understand the mechanism through which these systems enhance drug delivery across skin. Similar to Zhang et al (108), we examined the maximum flux, solubility in stratum corneum lipid components and diffusivity of both the model compounds, which have different lipophilicity (caffeine -0.07 and naproxen 3.18) from saturated solutions. A study was done on full-thickness skin and epidermal membranes. Our nanoemulsions were characterised by their transparency, small size and low viscosity. Both the microemulsion systems in this study significantly enhanced penetration of caffeine and naproxen. The possible cause of enhancement may be due to alterations in the stratum corneum barrier structure due in turn to the presence of EU and OA as penetration enhancers in the formulation. The mechanism of action of these penetration enhancers depends on the lipophilicity of the solute, with effects mediated by changes in diffusion being important for the hydrophilic caffeine and effects on stratum corneum solubility being the major determinant for the lipophilic drug naproxen. Nanoemulsions are promising vehicles to use for systemic delivery, controlled release and improved bioavailability. More investigation will allow the elucidation of mechanisms of nanoemulsion delivery into skin.

7.1.3 Appendageal delivery

A series of studies by the Lademann group has emphasised that hair follicles represent a highly relevant and efficient penetration pathway and reservoir for topically applied substances. The work in Chapter 6 has assessed the transepidermal and transfollicular penetration flux and retention in the hair follicles, stratum corneum and in the skin for different formulations and two actives. In the first part dealing with minoxidil penetration, we found that O/W nanoemulsions containing OA and EU as combined oil phase and penetration enhancers were highly effective *in vitro* with the transdermal flux of minoxidil increasing 3 to 9- fold over the control. The mechanism of penetration from these formulations is by increasing the partitioning and diffusivity of minoxidil in the stratum corneum. In the second part of this work dealing with transfollicular penetration, storage of caffeine in the hair follicles as well as retention in the stratum corneum and skin after 24 h application of selected nanoemulsions and controls was studied. The results showed that the permeation of caffeine delivered into the receptor from nanoemulsions was significantly higher than for controls. The highest permeation was seen in the open hair follicles (OHF). The caffeine flux from these OHF was higher than from the untreated and blocked hair follicles. The transfollicular flux was higher from nanoemulsions relative to controls. Also, the amount of caffeine recovered from appendages after application of formulations containing EU and OA and controls from blocked hair follicles was lower than that from open and normal hair follicles. These results demonstrate that nanoemulsion formulations are promising vehicles for transfollicular delivery of the hydrophilic drug caffeine. More understanding of the hair follicle structure and function will allow the design of improved formulations for follicular delivery. More investigation is required to understand the influence of the physicochemical properties of the penetrant and the vehicle on follicular targeting.

7.1.4 A comparison of the penetration and permeation of caffeine into and through human epidermis after application of various vesicle formulations

Vesicle systems are widely applicable for topical administration. They can improve drug penetration into the desired skin site, with the aim of reducing systemic absorption and side effects. In addition, they are promising candidates for follicular delivery. The aim of this study was to investigate the effect of vesicle-encapsulation of a model hydrophilic drug, caffeine on its skin delivery. The *in vitro* permeation of caffeine from vesicles with different compositions of penetration enhancers and a non-ionic surfactant was studied. Vehicles that incorporated the non-ionic surfactant decyl polyglucoside (DPGluc) caused greater skin

penetration of caffeine than those containing either OA or EU as penetration enhancers. The results suggest that fusion of the vesicles with the lipid of the stratum corneum and direct transfer of solute from the vesicle formulations to the skin may contribute to the mechanism of drug permeation enhancement by transferosomes and niosomes. The overall results indicate that the presence of penetration enhancers in the vesicle components is not the important operating factor. Further investigation will be carried out in ongoing studies with fluorescently labelled liposomes.

7.2 Future Direction

Current Hansen solubility parameter models for predicting solubility and solute maximum flux consider only the properties of the solute and either the vehicle or the skin. In future this should be extended to take account of solute-vehicle, solute-skin and vehicle-skin interaction, analogous to current attempts to develop quality structure–property relationships (QSPR) models to account for formulation effects.

The formulations developed for enhanced permeation of model drugs in this thesis should be extended and applied to therapeutic and diagnostic agents, many of which are macromolecules, peptides or oligonucleotides. For example, targeted delivery of substances for regional treatment or early detection of melanoma or other skin cancers is a promising area of application.

The imaging techniques used to show alteration in stratum corneum morphological properties following delivery of nanoemulsions to excised human skin need to be developed further to allow quantitation of actual drug delivery to targeted skin sites.

List of References

1. Bensouilah J, and Buck P. *Aromadermatology: aromatherapy in the treatment and care of common skin conditions*. Abingdon: Radcliffe Publishing; 2006.
2. Barry BW. *Dermatological formulations: percutaneous absorption*. Informa Health Care; 1983.
3. Monteiro-Riviere NA. 1 Structure and Function of Skin. *Toxicology of the Skin*. 2010:1.
4. Montagna W. *The Structure and Function of Skin 3E*. Elsevier; 2012.
5. Brown MB, Martin GP, Jones SA, and Akomeah FK. Dermal and Transdermal Drug Delivery Systems: Current and Future Prospects. *Drug Delivery*. 2006;13(3):175-87.
6. Lavker RM, and Sun T-T. Heterogeneity in epidermal basal keratinocytes: morphological and functional correlations. *Science*. 1982;215(4537):1239-41.
7. Gilbert SF. The epidermis and the origin of cutaneous structures. 2000.
8. Fluhr JW, Mao-Qiang M, Brown BE, Wertz PW, Crumrine D, Sundberg JP, Feingold KR, and Elias PM. Glycerol regulates stratum corneum hydration in sebaceous gland deficient (asebia) mice. *Journal of Investigative Dermatology*. 2003;120(5):728-37.
9. Zaiou M, and Gallo RL. Cathelicidins, essential gene-encoded mammalian antibiotics. *Journal of molecular medicine*. 2002;80(9):549-61.
10. Aiba S, and Katz SI. Phenotypic and functional characteristics of in vivo-activated Langerhans cells. *The Journal of Immunology*. 1990;145(9):2791-6.
11. Teunissen M. Dynamic nature and function of epidermal langerhans cells in vivo and in vitro: a review, with emphasis on human Langerhans cells. *The Histochemical journal*. 1992;24(10):697-716.
12. Potten CS, and Allen TD. A model implicating the Langerhans cell in keratinocyte proliferation control. *Differentiation*. 1976;5(1):43-7.
13. Walters KA, and Roberts MS. In: Walters KA ed. *Dermatological and Transdermal Formulations*. New York: Marcel Dekker, Inc.; 2002:1-39.
14. Lademann J, Richter H, Schaefer UF, Blume-Peytavi U, Teichmann A, Otberg N, and Sterry W. Hair Follicles – A Long-Term Reservoir for Drug Delivery. *Skin Pharmacology and Physiology*. 2006;19(4):232-6.
15. Otberg N, Richter H, Schaefer H, Blume-Peytavi U, Sterry W, and Lademann J. Variations of hair follicle size and distribution in different body sites. *J Invest Dermatol*. 2004;122(1):14-9.
16. Ro BI, and Dawson TL. The role of sebaceous gland activity and scalp microfloral metabolism in the etiology of seborrheic dermatitis and dandruff. *The journal of investigative dermatology Symposium proceedings / the Society for Investigative Dermatology, Inc [and] European Society for Dermatological Research*. 2005;10(3):194-7.
17. Elias PM. Stratum corneum defensive functions: an integrated view. *Journal of General Internal Medicine*. 2005;20(5):183-200.
18. Gilchrist BA, Eller MS, Geller AC, and Yaar M. The Pathogenesis of Melanoma Induced by Ultraviolet Radiation. *New England Journal of Medicine*. 1999;340(17):1341-8.
19. Gawkrödger DJ. *Dermatology*. Edinburgh: Churchill Livingstone; 2002.
20. Elias PM. Epidermal lipids, barrier function, and desquamation. *Journal of Investigative Dermatology*. 1983;80(S44-9).
21. Roop D. Defects in the barrier. *Science*. 1995;267(5197):474-5.
22. Sloan KB. *Prodrugs: topical and ocular drug delivery*. New York: Dekker; 1992.
23. Bronaugh RL, and Maibach HI. *Percutaneous absorption: drugs, cosmetics, mechanisms, methodology*. Boca Raton: Taylor and Francis; 2005.
24. Benson HAE. Transdermal Drug Delivery: Penetration Enhancement Techniques. *Current Drug Delivery*. 2005;2(1):23-33.
25. Fox LT, Gerber M, Du Plessis J, and Hamman JH. Transdermal Drug Delivery Enhancement by Compounds of Natural Origin. *Molecules*. 2011;16(12):10507-40.
26. Richard H. G, Jonathan H, and Daniel A. B. Transdermal drug delivery and cutaneous metabolism. *Xenobiotica*. 1987;17(3):325-43.

27. Barry BW. Mode of action of penetration enhancers in human skin. *Journal of Controlled Release*. 1987;6(1):85-97.
28. Kornick CA, Santiago-Palma J, Moryl N, Payne R, and Obbens EA. Benefit-risk assessment of transdermal fentanyl for the treatment of chronic pain. *Drug Safety*. 2003;26(13):951-73.
29. Cleary GW. In: Shah VP, and Maibach HI eds. *Topical Drug Bioavailability, Bioequivalence and Penetration*. New York: Plenum Press; 1993:17-68.
30. Long C. In: Walters KA ed. *Dermatological and transdermal formulations*. New York: Marcel Dekker; 2002:41-60.
31. Cramer MP, and Saks SR. Translating safety, efficacy and compliance into economic value for controlled release dosage forms. *Pharmacoeconomics*. 1994;5(482-504).
32. Bos JD, and Meinardi MM. The 500 Dalton rule for skin penetration of chemical compounds and drugs. *Exp Dermatol*. 2002;9(165-9).
33. Steinstrasser I, and Merkle HP. Dermal metabolism of topically applied drugs: pathways and models reconsidered. *Pharm Acta Helv*. 1995;70(3-24).
34. Yano T, Negakawa. A., Tsuji. M., and Noda.K. Skin permeability of various non-steroidal anti-inflammatory drugs in man. *Life Sci*. 1986;39(1043-50).
35. Majhi PR, and Moulik SP. Physicochemical Studies on Biological Macro- and Microemulsions VI : Mixing Behaviors of Eucalyptus Oil, Water and Polyoxyethylene Sorbitan Monolaurate (Tween 20) Assisted by n-Butanol or Cinnamic Alcohol. *Journal of Dispersion Science and Technology*. 1999;20(5):1407-27.
36. Lane ME. Skin penetration enhancers. *International Journal of Pharmaceutics*. 2013;447(1-2):12-21.
37. Illel B, and Schaefer H. Transfollicular percutaneous absorption. Skin model for quantitative studies. *Acta Derm Venereol*. 1987;68(5):427-30.
38. Meidan VM, Bonner MC, and Michniak BB. Transfollicular drug delivery—is it a reality? *International journal of pharmaceutics*. 2005;306(1):1-14.
39. Vogt A, and Blume-Peytavi U. Die Biologie des menschlichen Haarfollikels. *Der Hautarzt; Zeitschrift fur Dermatologie, Venerologie, und verwandte Gebiete*. 2003;54(8):692-8.
40. Teichmann A, Jacobi U, Ossadnik M, Richter H, Koch S, Sterry W, and Lademann J. Differential Stripping: Determination of the Amount of Topically Applied Substances Penetrated into the Hair Follicles. *Journal of General Internal Medicine*. 2005;20(5):264-9.
41. Barry BW. Drug delivery routes in skin: a novel approach. *Adv Drug Deliv Rev*. 2002;54(Supplement):S31-S40.
42. Schaefer H, and Lademann J. The Role of Follicular Penetration. *Skin Pharmacology and Physiology*. 2001;14(Suppl. 1):23-7.
43. Knorr F, Lademann J, Patzelt A, Sterry W, Blume-Peytavi U, and Vogt A. Follicular transport route – Research progress and future perspectives. *European Journal of Pharmaceutics and Biopharmaceutics*. 2009;71(2):173-80.
44. Toll R, Jacobi U, Richter H, Lademann J, Schaefer H, and Blume-Peytavi U. Penetration profile of microspheres in follicular targeting of terminal hair follicles. *J Invest Dermatol*. 2004;123(1):168-76.
45. Grice JE, Ciotti S, Weiner N, Lockwood P, Cross SE, and Roberts MS. Relative uptake of minoxidil into appendages and stratum corneum and permeation through human skin in vitro. *Journal of Pharmaceutical Sciences*. 2010;99(2):712-8.
46. Stenn KS, and Cotsarelis G. Bioengineering the hair follicle: fringe benefits of stem cell technology. *Current opinion in biotechnology*. 2005;16(5):493-7.
47. Pfister WR, and Hsieh DS. Permeation enhancers compatible with transdermal drug delivery systems. Part I: selection and formulation considerations. *Medical device technology*. 1989;1(5):48-55.
48. Walker RB, and Smith EW. The role of percutaneous penetration enhancers. *Advanced Drug Delivery Reviews*. 1996;18(3):295-301.
49. Williams AC, and Barry BW. Penetration enhancers. *Advanced Drug Delivery Reviews*. 2004;56(5):603-18.
50. Santus GC, and Baker RW. Transdermal enhancer patent literature. *Journal of controlled Release*. 1993;25(1):1-20.

51. Patel HJ, Trivedi DG, Bhandari AK, and Shah DA. Penetration enhancers for transdermal drug delivery system: A review. *IJPI's Journal of Pharmaceutics and Cosmetology*. 2011;1(2):67-80.
52. Barry BW. Novel mechanisms and devices to enable successful transdermal drug delivery. *Eur J Pharm Sci*. 2001;14(2):101-14.
53. Cornwell PA, Barry BW, Bouwstra JA, and Gooris GS. Modes of action of terpene penetration enhancers in human skin; differential scanning calorimetry, small-angle X-ray diffraction and enhancer uptake studies. *International Journal of Pharmaceutics*. 1996;127(1):9-26.
54. Bharkatiya M, and Nema RK. Skin penetration enhancement techniques. *Journal of Young Pharmacists*. 2009;1(2):110-5.
55. Danyi; Q, and Howard HXaMI. Chemical enhancements of transdermal drug delivery systems: Advantages and Challenges-part 1. *Transdermal*. 2010:5-11.
56. Fox LT, Gerber M, Plessis JD, and Hamman JH. Transdermal Drug Delivery Enhancement by Compounds of Natural Origin. *molecules*. 2011;16(12):10507-40.
57. Williams AC, and Barry BW. Penetration enhancers. *Advanced Drug Delivery Reviews*. 2012;64, Supplement(0):128-37.
58. Zupan JA. In: Merck & Co I ed. *Google Patents*. 1983.
59. Okabe H, Takayama K, Ogura A, and Nagai T. Effect of limonene and related compounds on the percutaneous absorption of indomethacin. *Drug design and delivery*. 1989;4(4):313-21.
60. Hori M, Satoh S, Maibach HI, and Guy RH. Enhancement of propranolol hydrochloride and diazepam skin absorption in vitro: effect of enhancer lipophilicity. *Journal of Pharmaceutical Sciences*. 1991;80(1):32-5.
61. Ibrahim SA, and Li SK. Efficiency of Fatty Acids as Chemical Penetration Enhancers: Mechanisms and Structure Enhancement Relationship. *Pharm Res*. 2010;27(1):115-25.
62. Aungst BJ. Structure/effect studies of fatty acid isomers as skin penetration enhancers and skin irritants. *Pharm Res*. 1989;6(3):244-7.
63. Aungst BJ, Rogers NJ, and Shefter E. Enhancement of naloxone penetration through human skin in vitro using fatty acids, fatty alcohols, surfactants, sulfoxides and amides. *International Journal of Pharmaceutics*. 1986;33(1):225-34.
64. Goodman M, and Barry BW. Lipid-protein-partitioning (LPP) theory of skin enhancer activity: finite dose technique. *International Journal of Pharmaceutics*. 1989;57(1):29-40.
65. Ernst E. Adverse effects of herbal drugs in dermatology. *British Journal of Dermatology*. 2000;143(5):923-9.
66. Idson B. Hydration and percutaneous absorption. *Current Problems in Dermatology*. 1978;7(132-41).
67. Roberts MS, Cross SE, and Pellett MA. In: Walters KA ed. *Dermatological and Transdermal Formulations*. New York: Marcel Dekker; 2002:89-196.
68. Wiedmann TS. Influence of hydration on epidermal tissue. *Journal of Pharmaceutical Sciences*. 1988;77(12):1037-41.
69. Hikima T, and Maibach H. Skin Penetration Flux and Lag-Time of Steroids Across Hydrated and Dehydrated Human Skin in Vitro. *Biological & Pharmaceutical Bulletin*. 2006;29(11):2270-3.
70. Walters KA, and Hadgraft J. *Pharmaceutical skin penetration enhancement*. Informa Health Care; 1993.
71. Wurster DE, and Kramer SF. Investigation of some factors influencing percutaneous absorption. *Journal of pharmaceutical sciences*. 1961;50(4):288-93.
72. Bucks D, Maibach HI, and Guy R. Occlusion does not uniformly enhance penetration in vivo. *DRUGS AND THE PHARMACEUTICAL SCIENCES*. 2005;155(65).
73. Higuchi T. Physical Chemical analysis of Percutaneous Absorption Process from Creams and Ointments. *J Soc Cosmet Chem*. 1960;11(85-97).
74. Megrab NA, Williams AC, and Barry BW. Oestradiol permeation across human skin, silastic and snake skin membranes: The effects of ethanol/water co-solvent systems. *International Journal of Pharmaceutics*. 1995;116(1):101-12.
75. Pellett MA, Roberts MS, and Hadgraft J. Supersaturated solutions evaluated with an in vitro stratum corneum tape stripping technique. *International Journal of Pharmaceutics*. 1997;151(1):91-8.

76. Twist JN, and Zatz JL. A model for alcohol-enhanced permeation through polydimethylsiloxane membranes. *Journal of Pharmaceutical Sciences*. 1990;79(1):28-31.
77. Henmi T, Fujii M, Kikuchi K, Yamanobe N, and Matsumoto M. Application of an Oily Gel Formed by Hydrogenated Soybean Phospholipids as a Percutaneous Absorption-Type Ointment Base. *CHEMICAL & PHARMACEUTICAL BULLETIN*. 1994;42(3):651-4_1.
78. Chia-Ming C, Flynn GL, Weiner ND, and Szpunar GJ. Bioavailability assessment of topical delivery systems: effect of vehicle evaporation upon in vitro delivery of minoxidil from solution formulations. *International journal of pharmaceuticals*. 1989;55(2):229-36.
79. Megrab NA, Williams A, and Barry B. Oestradiol permeation through human skin and silastic membrane: effects of propylene glycol and supersaturation. *Journal of controlled release*. 1995;36(3):277-94.
80. Kemken J, Ziegler A, and Müller B. Influence of Supersaturation on the Pharmacodynamic Effect of Bupranolol After Dermal Administration Using Microemulsions as Vehicle. *Pharm Res*. 1992;9(4):554-8.
81. Dias MMR, Raghavan SL, Pellett MA, and Hadgraft J. The effect of β -cyclodextrins on the permeation of diclofenac from supersaturated solutions. *International Journal of Pharmaceutics*. 2003;263(1):173-81.
82. Thong HY, Zhai H, and Maibach HI. Percutaneous Penetration Enhancers: An Overview. *Skin Pharmacology and Physiology*. 2007;20(6):272-82.
83. Prausnitz MR. Microneedles for transdermal drug delivery. *Advanced drug delivery reviews*. 2004;56(5):581-7.
84. Sivamani RK, Stoeber B, Wu GC, Zhai H, Liepmann D, and Maibach H. Clinical microneedle injection of methyl nicotinate: stratum corneum penetration. *Skin Research and Technology*. 2005;11(2):152-6.
85. Sloan KB, and Bodor N. Hydroxymethyl and acyloxymethyl prodrugs of theophylline: enhanced delivery of polar drugs through skin. *International Journal of Pharmaceutics*. 1982;12(4):299-313.
86. Choi H-K, Flynn GL, and Amidon GL. Transdermal delivery of bioactive peptides: the effect of n-decylmethyl sulfoxide, pH, and inhibitors on enkephalin metabolism and transport. *Pharm Res*. 1990;7(11):1099-106.
87. Mezei M, and Gulasekharan V. Liposomes-a selective drug delivery system for the topical route of administration I. Lotion dosage form. *Life Sci*. 1980;26(18):1473-7.
88. Roberts MS, Cross SE, Pellett MA, and Walters KA. In: Walters KA ed. *Dermatological and Transdermal Formulations*. New York: Marcel Dekker; 2002:89-196.
89. Milewski M, and Stinchcomb AL. Estimation of Maximum Transdermal Flux of Nonionized Xenobiotics from Basic Physicochemical Determinants. *Molecular pharmaceutics*. 2012.
90. Lien EJ, and Tong GL. Physicochemical properties and percutaneous absorption of drugs. *J Soc Cosmet Chem*. 1973;24(371-84).
91. Lian G, Chen L, and Han L. An evaluation of mathematical models for predicting skin permeability. *Journal of Pharmaceutical Sciences*. 2008;97(1):584-98.
92. Magnusson BM, Anissimov YG, Cross SE, and Roberts MS. Molecular size as the main determinant of solute maximum flux across the skin. *Journal of Investigative Dermatology*. 2004;122(4):993-9.
93. Guy RH, and Hadgraft J. *Selection of drug candidates for transdermal drug delivery*. Marcel Dekker, New York; 1989.
94. Kasting GB, Smith RL, and Cooper E. Effect of lipid solubility and molecular size on percutaneous absorption. *Skin pharmacokinetics*. 1987;1(138-53).
95. Mitragotri S. A theoretical analysis of permeation of small hydrophobic solutes across the stratum corneum based on scaled particle theory. *Journal of Pharmaceutical Sciences*. 2002;91(3):744-52.
96. Roberts MS, Anderson RA, and Swarbrick J. Permeability of human epidermis to phenolic compounds. *Journal of Pharmacy and Pharmacology*. 1977;29(1):677-83.
97. Scheuplein RJ. Mechanism of percutaneous adsorption. *Journal of investigative Dermatology*. 1965;45(5):334-46.

98. Pugh WJ, Roberts MS, and Hadgraft J. Epidermal permeability — Penetrant structure relationships: 3. The effect of hydrogen bonding interactions and molecular size on diffusion across the stratum corneum. *International Journal of Pharmaceutics*. 1996;138(2):149-56.
99. Potts RO, and Guy RH. Predicting skin permeability. *Pharm Res*. 1992;9(5):663-9.
100. Anderson BD, and Raykar PV. Solute structure-permeability relationships in human stratum corneum. *J Invest Dermatol*. 1989;93(2):280-6.
101. Potts RO, and Guy RH. A predictive algorithm for skin permeability: the effects of molecular size and hydrogen bond activity. *Pharm Res*. 1995;12(11):1628-33.
102. Roberts MS, Anderson RA, Swarbrick J, and Moore DE. The percutaneous absorption of phenolic compounds: the mechanism of diffusion across the stratum corneum. *Journal of Pharmacy and Pharmacology*. 1978;30(1):486-90.
103. Roberts MS, Pugh WJ, and Hadgraft J. Epidermal permeability: penetrant structure relationships. 2. The effect of H-bonding groups in penetrants on their diffusion through the stratum corneum. *International Journal of Pharmaceutics*. 1996;132(1-2):23-32.
104. Cross SE, Pugh WJ, Hadgraft J, and Roberts MS. Probing the Effect of Vehicles on Topical Delivery: Understanding the Basic Relationship Between Solvent and Solute Penetration Using Silicone Membranes. *Pharm Res*. 2001;18(7):999-1005.
105. du Plessis J, Pugh WJ, Judefeind A, and Hadgraft J. Physico-chemical determinants of dermal drug delivery: effects of the number and substitution pattern of polar groups. *European journal of pharmaceutical sciences*. 2002;16(3):107-12.
106. Zhang Q, Grice JE, Li P, Jepps OG, Wang GJ, and Roberts MS. Skin solubility determines maximum transepidermal flux for similar size molecules. *Pharm Res*. 2009;26(8):1974-85.
107. Zhang Q, Li P, Liu D, and Roberts MS. Effect of vehicles on the maximum transepidermal flux of similar size phenolic compounds. *Pharm Res*. 2013;30(1):32-40.
108. Zhang Q, Li P, and Roberts MS. Maximum transepidermal flux for similar size phenolic compounds is enhanced by solvent uptake into the skin. *Journal of controlled release : official journal of the Controlled Release Society*. 2011;154(1):50-7.
109. Bartek MJ, Labudde JA, and Maibach HI. Skin permeability in vivo: comparison in rat, rabbit, pig and man. *Journal of Investigative Dermatology*. 1972;58(3):114-23.
110. Ross JH, Dong MH, and Krieger RI. Conservatism in Pesticide Exposure Assessment. *Regulatory Toxicology and Pharmacology*. 2000;31(1):53-8.
111. Bond JR, and Barry BW. Limitations of hairless mouse skin as a model for in vitro permeation studies through human skin: hydration damage. *Journal of investigative dermatology*. 1988;90(4):486-9.
112. Coquette A, Berna N, Poumay Y, and Pittelkow MR. In: Kydonieus AF, and Wille JJ eds. *Biochemical Modulation of Skin Reactions: Transdermals, Topicals, Cosmetics*. New York: CRC Press; 2000:125-43.
113. Hancock BC, York P, and Rowe RC. The use of solubility parameters in pharmaceutical dosage form design. *International Journal of Pharmaceutics*. 1997;148(1):1-21.
114. Hildebrand JH, and Scott RL. *The solubility of non electrolytes* New York: Reinhold Publishing Corp.; 1950.
115. Hansen CM. *The three dimensional solubility parameter and solvent diffusion co efficient*. Copenhagen: Danish Technical Press; 1967.
116. Hansen CM. The three-dimensional solubility parameter-key to paint component affinities: I. solvents, plasticizers, polymers, and resins. II. Dyes, emulsifiers, mutual solubility and compatibility, and pigments. III. Independent calculation of the parameter components. *Journal of Paint Technology*. 1967;39(505-10).
117. Abbott S. An integrated approach to optimizing skin delivery of cosmetic and pharmaceutical actives. *International journal of cosmetic science*. 2012;34(3):217-22.
118. Hansen CM. The universality of the solubility parameter. *Industrial & engineering chemistry product research and development*. 1969;8(1):2-11.
119. Šentjurc M, Kristl J, and Abramović Z. Transport of liposome-entrapped substances into skin as measured by electron paramagnetic resonance oximetry in vivo. *Methods in enzymology*. 2004;387(267-87).

120. Abramovic Z, Sustarsic U, Teskac K, Sentjurc M, and Kristl J. Influence of nanosized delivery systems with benzyl nicotinate and penetration enhancers on skin oxygenation. *Int J Pharm.* 2008;359(1-2):220-7.
121. Azeem A, Khan ZI, Aqil M, Ahmad FJ, Khar RK, and Talegaonkar S. Microemulsions as a Surrogate Carrier for Dermal Drug Delivery. *Drug Dev Ind Pharm.* 2009;35(5):525-47.
122. Leite-Silva VR, de Almeida MM, Fradin A, Grice JE, and Roberts MS. Delivery of drugs applied topically to the skin. *Expert Review of Dermatology.* 2012;7(4):383-97.
123. Salerno C, Carlucci AM, and Bregni C. Study of in vitro drug release and percutaneous absorption of fluconazole from topical dosage forms. *AAPS PharmSciTech.* 2010;11(2):986-93.
124. Setya S, Talegonkar S, and Razdan B. Nanoemulsions: Formulation methods and stability aspects. *World J Pharm Pharm Sci.* 2014;3(2214-28).
125. Kogan A, and Garti N. Microemulsions as transdermal drug delivery vehicles. *Advances in colloid and interface science.* 2006;123(369-85).
126. Djordjevic L, Primorac M, Stupar M, and Krajisnik D. Characterization of caprylocaproyl macrogolglycerides based microemulsion drug delivery vehicles for an amphiphilic drug. *International Journal of Pharmaceutics.* 2004;271(1-2):11-9.
127. Bennett KE, Hatfield JC, Davis HT, Macosko CW, and Scriven LE. In: Robb ID ed. *Microemulsions.* Springer US; 1982:65-84.
128. Andersson M, and Löfroth J-E. Small particles of a heparin/chitosan complex prepared from a pharmaceutically acceptable microemulsion. *International Journal of Pharmaceutics.* 2003;257(1-2):305-9.
129. Kang BK, Chon SK, Kim SH, Jeong SY, Kim MS, Cho SH, Lee HB, and Khang G. Controlled release of paclitaxel from microemulsion containing PLGA and evaluation of anti-tumor activity in vitro and in vivo. *International Journal of Pharmaceutics.* 2004;286(1-2):147-56.
130. Pham TT, Jaafar-Maalej C, Charcosset C, and Fessi H. Liposome and niosome preparation using a membrane contactor for scale-up. *Colloids and Surfaces B: Biointerfaces.* 2012;94(0):15-21.
131. Chen J, Lu W-L, Gu W, Lu S-S, Chen Z-P, and Cai B-C. Skin permeation behavior of elastic liposomes: role of formulation ingredients. *Expert Opinion on Drug Delivery.* 2013;10(6):845-56.
132. Schreier H, and Bouwstra J. Liposomes and niosomes as topical drug carriers: dermal and transdermal drug delivery. *Journal of Controlled Release.* 1994;30(1):1-15.
133. El Maghraby GM, Barry BW, and Williams AC. Liposomes and skin: From drug delivery to model membranes. *European Journal of Pharmaceutical Sciences.* 2008;34(4-5):203-22.
134. El Maghraby GMM, Williams AC, and Barry BW. Interactions of surfactants (edge activators) and skin penetration enhancers with liposomes. *International Journal of Pharmaceutics.* 2004;276(1):143-61.
135. El Maghraby GMM, Williams AC, and Barry BW. Can drug-bearing liposomes penetrate intact skin? *Journal of Pharmacy and Pharmacology.* 2006;58(4):415-29.
136. Cevc G. Transfersomes, liposomes and other lipid suspensions on the skin: permeation enhancement, vesicle penetration, and transdermal drug delivery. *Critical Reviews™ in Therapeutic Drug Carrier Systems.* 1996;13(3-4).
137. Pastore MN, Kalia YN, Horstmann M, and Roberts MS. Transdermal patches: history, development and pharmacology. *British journal of pharmacology.* 2015;172(9):2179-209.
138. Michaels AS, Chandrasekaran SK, and Shaw JE. Drug permeation through human skin: Theory and invitro experimental measurement. *AIChE Journal.* 1975;21(5):985-96.
139. Twist J, and Zatz J. Influence of solvents on paraben permeation through idealized skin model membranes. *J Soc Cosmet Chem.* 1986;37(6):429-44.
140. Magnusson BM, Anissimov YG, Cross SE, and Roberts MS. Molecular size as the main determinant of solute maximum flux across the skin. *The Journal of Investigative Dermatology.* 2004;122(4):993-9.
141. Tojo K, Chiang CC, and Chien YW. Drug permeation across the skin: Effect of penetrant hydrophilicity. *Journal of Pharmaceutical Sciences.* 1987;76(2):123-6.
142. Hatanaka T, Shimoyama M, Sugibayashi K, and Morimoto Y. Effect of vehicle on the skin permeability of drugs: polyethylene glycol 400-water and ethanol-water binary solvents. *Journal of Controlled Release.* 1993;23(3):247-60.

143. Dias M, Hadgraft J, and Lane ME. Influence of membrane–solvent–solute interactions on solute permeation in skin. *International Journal of Pharmaceutics*. 2007;340(1–2):65-70.
144. Rosado C, Cross SE, Pugh WJ, Roberts MS, and Hadgraft J. Effect of vehicle pretreatment on the flux, retention, and diffusion of topically applied penetrants in vitro. *Pharm Res*. 2003;20(9):1502-7.
145. Gharagheizi F, Sattari M, and Angaji MT. Effect of Calculation Method on Values of Hansen Solubility Parameters of Polymers. *Polymer Bulletin*. 2006;57(3):377-84.
146. Hildebrand JH, and Scott RL. *Regular solutions*. Prentice-Hall; 1962.
147. Hildebrand JH, Prausnitz JM, and Scott RL. *Regular and Related Solutions. The Solubility of Gases, Liquids, and Solids*. 1970.
148. Hansen CM. *Hansen Solubility Parameters: A User's Handbook*. 2007.
149. Kligman AM, and Christophers E. Preparation of isolated sheets of human stratum corneum. *Archives of dermatology*. 1963;88(6):702-5.
150. Anderson RA, Triggs EJ, and Roberts MS. The percutaneous absorption of phenolic compounds. 3. Evaluation of permeability through human stratum corneum using a desorption technique. *Aust J Pharm Sci*. 1976;5(107-10).
151. Mitragotri S. In Situ Determination of Partition and Diffusion Coefficients in the Lipid Bilayers of Stratum Corneum. *Pharm Res*. 2000;17(8):1026-9.
152. Franz J, Thomas. Percutaneous absorption. on the relevance of in vitro data. *J Investig Dermatol*. 1975;64(3):190-5.
153. Abbott S, Hansen CM, Yamamoto H, and Valpey RS. In: Abbott S ed.: Hansen-Solubility.com; 2013.
154. Barry BW, Harrison SM, and Dugard PH. Correlation of thermodynamic activity and vapour diffusion through human skin for the model compound, benzyl alcohol. *The Journal of pharmacy and pharmacology*. 1985;37(2):84-90.
155. Twist JN, and Zatz JL. Influence of Solvents on Paraben Permeation through Idealized Skin Model Membranes. *Journal of the Society of Cosmetic Chemists*. 1986;37(6):429-44.
156. Brinkmann I, and Müller-Goymann CC. Role of Isopropyl Myristate, Isopropyl Alcohol and a Combination of Both in Hydrocortisone Permeation across the Human Stratum corneum. *Skin Pharmacology and Physiology*. 2003;16(6):393-404.
157. Williams AC, and Barry BW. Terpenes and the Lipid–Protein–Partitioning Theory of Skin Penetration Enhancement. *Pharm Res*. 1991;8(1):17-24.
158. Gao S, and Singh J. In vitro percutaneous absorption enhancement of a lipophilic drug tamoxifen by terpenes. *Journal of Controlled Release*. 1998;51(2–3):193-9.
159. Williams AC, and Barry BW. The enhancement index concept applied to terpene penetration enhancers for human skin and model lipophilic (oestradiol) and hydrophilic (5-fluorouracil) drugs. *International Journal of Pharmaceutics*. 1991;74(2–3):157-68.
160. Fruijtier-Pöllloth C. Safety assessment on polyethylene glycols (PEGs) and their derivatives as used in cosmetic products. *Toxicology*. 2005;214(1):1-38.
161. Ghanem A-H, Mahmoud H, Higuchi WI, Liu P, and Good WR. The effects of ethanol on the transport of lipophilic and polar permeants across hairless mouse skin: Methods/validation of a novel approach. *International Journal of Pharmaceutics*. 1992;78(1–3):137-56.
162. Kim D-D, Kim JL, and Chien YW. Mutual hairless rat skin permeation-enhancing effect of ethanol/water system and oleic acid. *Journal of Pharmaceutical Sciences*. 1996;85(11):1191-5.
163. Obata Y, Takayama K, Maitani Y, Machida Y, and Nagai T. Effect of ethanol on skin permeation of nonionized and ionized diclofenac. *International Journal of Pharmaceutics*. 1993;89(3):191-8.
164. Pershing LK, Silver BS, Krueger GG, Shah VP, and Skelley JP. Feasibility of Measuring the Bioavailability of Topical Betamethasone Dipropionate in Commercial Formulations Using Drug Content in Skin and a Skin Blanching Bioassay. *Pharm Res*. 1992;9(1):45-51.
165. Pershing LK, Lambert LD, and Knutson K. Mechanism of ethanol-enhanced estradiol permeation across human skin in vivo. *Pharm Res*. 1990;7(2):170-5.
166. Riviere JE, Brooks JD, Collard WT, Deng J, de Rose G, Mahabir SP, Merritt DA, and Marchiondo AA. Prediction of formulation effects on dermal absorption of topically applied ectoparasiticides dosed in vitro on canine and porcine skin using a mixture-adjusted quantitative structure permeability relationship. *Journal of veterinary pharmacology and therapeutics*. 2014;37(5):435-44.

167. Rosado C, Cross S, Pugh WJ, Roberts M, and Hadgraft J. Effect of Vehicle Pretreatment on the Flux, Retention, and Diffusion of Topically Applied Penetrants in Vitro. *Pharm Res.* 2003;20(9):1502-7.
168. Twist JNaZ, J. L. Influence of solvents on paraben permeation through idealized skin model membranes *Journal of the Society of Cosmetic Chemists.* 1968;37(6):429-44
169. Pastore MN, Kalia YN, Horstmann M, and Roberts MS. Transdermal patches: history, development and pharmacology. *British Journal of Pharmacology.* 2015;172(9):2179-209.
170. Danielsson I, and Lindman B. The definition of microemulsion. *Colloids and Surfaces.* 1981;3(4):391-2.
171. Naoui W, Bolzinger M-A, Fenet B, Pelletier J, Valour J-P, Kalfat R, and Chevalier Y. Microemulsion Microstructure Influences the Skin Delivery of an Hydrophilic Drug. *Pharm Res.* 2011;28(7):1683-95.
172. Azeem A, Khan ZI, Aqil M, Ahmad FJ, Khar RK, and Talegaonkar S. Microemulsions as a surrogate carrier for dermal drug delivery. *Drug development and industrial pharmacy.* 2009;35(5):525-47.
173. Talegaonkar S, Azeem A, Ahmad FJ, Khar RK, Pathan SA, and Khan ZI. Microemulsions: a novel approach to enhanced drug delivery. *Recent patents on drug delivery & formulation.* 2008;2(3):238-57.
174. Lindman B, Shinoda K, Olsson U, Anderson D, Karlström G, and Wennerström H. On the demonstration of bicontinuous structures in microemulsions. *Colloids and Surfaces.* 1989;38(1):205-24.
175. Shinoda K, and Lindman B. Organized surfactant systems: microemulsions. *Langmuir.* 1987;3(2):135-49.
176. Kreilgaard M. Influence of microemulsions on cutaneous drug delivery. *Advanced Drug Delivery Reviews.* 2002;54(Supplement):S77-S98.
177. Santos P, Watkinson A, Hadgraft J, and Lane M. Application of microemulsions in dermal and transdermal drug delivery. *Skin Pharmacology and Physiology.* 2007;21(5):246-59.
178. Lawrence MJ. Surfactant systems: their use in drug delivery. *Chemical Society Reviews.* 1994;23(6):417-24.
179. Zulauf M, and Eicke HF. Inverted micelles and microemulsions in the ternary system water/aerosol-OT/isooctane as studied by photon correlation spectroscopy. *Journal of Physical Chemistry.* 1979;83(4):480-6.
180. Carlfors J, Blute I, and Schmidt V. Lidocaine in microemulsion-a dermal delivery system. *Journal of dispersion science and technology.* 1991;12(5-6):467-82.
181. Chen H, Chang X, Weng T, Zhao X, Gao Z, Yang Y, Xu H, and Yang X. A study of microemulsion systems for transdermal delivery of triptolide. *Journal of Controlled Release.* 2004;98(3):427-36.
182. Golden GM, McKie JE, and Potts RO. Role of stratum corneum lipid fluidity in transdermal drug flux. *Journal of Pharmaceutical Sciences.* 1987;76(1):25-8.
183. Kreilgaard M, Pedersen EJ, and Jaroszewski JW. NMR characterisation and transdermal drug delivery potential of microemulsion systems. *Journal of Controlled Release.* 2000;69(3):421-33.
184. El Maghraby GM. Transdermal delivery of hydrocortisone from eucalyptus oil microemulsion: Effects of cosurfactants. *International Journal of Pharmaceutics.* 2008;355(1-2):285-92.
185. Zhang Q, Grice JE, Li P, Jepps OG, Wang GJ, and Roberts MS. Skin solubility determines maximum transepidermal flux for similar size molecules. *Pharm Res.* 2009;26(8):1974-85.
186. Kligman AM, and Christophers E. Preparation of Isolated Sheets of Human Stratum Corneum. *Arch Dermatol.* 1963;88(702-5).
187. Anderson R, Triggs E, and Roberts M. The percutaneous absorption of phenolic compounds. 3. Evaluation of permeability through human stratum corneum using a desorption technique. *Aust J Pharm Sci.* 1976;5(107-10).
188. Walker M, and Hadgraft J. Oleic acid — a membrane “fluidiser” or fluid within the membrane? *International Journal of Pharmaceutics.* 1991;71(1-2):R1-R4.
189. Liu C-H, and Chang F-Y. Development and Characterization of Eucalyptol Microemulsions for Topic Delivery of Curcumin. *Pharmaceutical Society of Japan.* 2010;59 (2):172—8
190. Lee P, Langer R, and Shastri VP. Novel Microemulsion Enhancer Formulation for Simultaneous Transdermal Delivery of Hydrophilic and Hydrophobic Drugs. *Pharm Res.* 2003;20(2):264-9.

191. Zhao X, Liu JP, Zhang X, and Li Y. Enhancement of transdermal delivery of theophylline using microemulsion vehicle. *International Journal of Pharmaceutics*. 2006;327(1–2):58-64.
192. Gursoy RN, and Benita S. Self-emulsifying drug delivery systems (SEDDS) for improved oral delivery of lipophilic drugs. *Biomedicine & Pharmacotherapy*. 2004;58(3):173-82.
193. Cal K, Janicki S, and Sznitowska M. In vitro studies on penetration of terpenes from matrix-type transdermal systems through human skin. *International Journal of Pharmaceutics*. 2001;224(1–2):81-8.
194. Peltola S, Saarinen-Savolainen P, Kiesvaara J, Suhonen TM, and Urtti A. Microemulsions for topical delivery of estradiol. *International Journal of Pharmaceutics*. 2003;254(2):99-107.
195. Kobayashi D, Matsuzawa T, Sugibayashi K, Morimoto Y, Kobayashi M, and Kimura M. Feasibility of use of several cardiovascular agents in transdermal therapeutic systems with l-menthol-ethanol system on hairless rat and human skin. *Biol Pharm Bull*. 1993;16(3):254-8.
196. Obata Y, Takayama K, Machida Y, and Nagai T. Combined effect of cyclic monoterpenes and ethanol on percutaneous absorption of diclofenac sodium. *Drug Des Discov*. 1991;8(2):137 - 44.
197. Tojo K, Chiang CC, and Chien YW. Drug permeation across the skin: effect of penetrant hydrophilicity. *J Pharm Sci*. 1987;76(2):123-6.
198. Koyama Y, Bando H, Yamashita F, Takakura Y, Sezaki H, and Hashida M. Comparative analysis of percutaneous absorption enhancement by d-limonene and oleic acid based on a skin diffusion model. *Pharm Res*. 1994;11(3):377-83.
199. Gao S, and Singh J. In vitro percutaneous absorption enhancement of a lipophilic drug tamoxifen by terpenes. *Journal of controlled release : official journal of the Controlled Release Society*. 1998;51(2-3):193-9.
200. Cross SE, Anderson C, and Roberts MS. Topical penetration of commercial salicylate esters and salts using human isolated skin and clinical microdialysis studies. *British Journal of Clinical Pharmacology*. 1998;46(1):29-35.
201. Bolzinger MA, Briançon S, Pelletier J, Fessi H, and Chevalier Y. Percutaneous release of caffeine from microemulsion, emulsion and gel dosage forms. *European Journal of Pharmaceutics and Biopharmaceutics*. 2008;68(2):446-51.
202. Naoui W, Bolzinger M-A, Fenet B, Pelletier J, Valour J-P, Kalfat R, and Chevalier Y. Microemulsion Microstructure Influences the Skin Delivery of an Hydrophilic Drug. *Pharm Res*. 2011;28(7):1683-95.
203. Koch RL, Palicharla P, and Groves MJ. Diffusion of [2-14C] diazepam across isolated hairless mouse stratum corneum/epidermal tissues. *Journal of Investigative Dermatology*. 1988;90(3):317-9.
204. Lauer A, Lieb L, Ramachandran C, Flynn G, and Weiner N. Transfollicular Drug Delivery. *Pharm Res*. 1995;12(2):179-86.
205. Schaefer H, Watts F, Brod J, and Illel B. Follicular penetration. *Prediction of Percutaneous Penetration Methods, Measurements, Modelling*. 1990;163(732).
206. Shelley WB, and Melton FM. Factors Accelerating the Penetration of Histamine Through Normal Intact Human Skin1. *The Journal of Investigative Dermatology*. 1949;13(2):61-71.
207. Feldmann RJ, and Maibach HI. Regional variation in percutaneous penetration of 14C Cortisol in Man1. *Journal of Investigative Dermatology*. 1967;48(2):181-3.
208. Tenjarla SN, Kasina R, Puranajoti P, Omar MS, and Harris WT. Synthesis and evaluation of N-acetylprolinatate esters—novel skin penetration enhancers. *International journal of pharmaceutics*. 1999;192(2):147-58.
209. Mackee GM, Sulzberger MB, Herrmann F, and Baer RL. Histologic Studies on Percutaneous Penetration with Special Reference to the Effect of Vehicles12. *The Journal of Investigative Dermatology*. 1945;6(1):43-61.
210. Scheuplein RJ. Mechanism of percutaneous absorption. *Journal of Investigative Dermatology*. 1967;48(1):79-88.
211. Rolland A, Wagner N, Chatelus A, Shroot B, and Schaefer H. Site-specific drug delivery to pilosebaceous structures using polymeric microspheres. *Pharm Res*. 1993;10(12):1738-44.
212. Vogt A, Combadiere B, Hadam S, Stieler KM, Lademann J, Schaefer H, Autran B, Sterry W, and Blume-Peytavi U. 40 nm, but not 750 or 1,500 nm, nanoparticles enter epidermal CD1a+ cells after transcutaneous application on human skin. *J Invest Dermatol*. 2006;126(6):1316-22.

213. Lademann J, Knorr F, Richter H, Blume-Peytavi U, Vogt A, Antoniou C, Sterry W, and Patzelt A. Hair Follicles – An Efficient Storage and Penetration Pathway for Topically Applied Substances. *Skin Pharmacology and Physiology*. 2008;21(3):150-5.
214. Lademann J, Otberg N, Richter H, Weigmann H, Lindemann U, Schaefer H, and Sterry W. Investigation of follicular penetration of topically applied substances. *Skin pharmacology and applied skin physiology*. 2000;14(17-22).
215. Panigrahi L, Pattnaik S, and Ghosal SK. The effect of pH and organic ester penetration enhancers on skin permeation kinetics of terbutaline sulfate from pseudolatex-type transdermal delivery systems through mouse and human cadaver skins. *AAPS PharmSciTech*. 2005;6(2):E167-E73.
216. Touitou E, Godin B, Karl Y, Bujanover S, and Becker Y. Oleic acid, a skin penetration enhancer, affects Langerhans cells and corneocytes. *Journal of Controlled Release*. 2002;80(1-3):1-7.
217. Biruss B, Kählig H, and Valenta C. Evaluation of an eucalyptus oil containing topical drug delivery system for selected steroid hormones. *International Journal of Pharmaceutics*. 2007;328(2):142-51.
218. Ongpipattanakul B, Burnette RR, Potts RO, and Francoeur ML. Evidence that Oleic Acid Exists in a Separate Phase Within Stratum Corneum Lipids. *Pharm Res*. 1991;8(3):350-4.
219. Padois K, Cantiéni C, Bertholle V, Bardel C, Pirot F, and Falson F. Solid lipid nanoparticles suspension versus commercial solutions for dermal delivery of minoxidil. *International Journal of Pharmaceutics*. 2011;416(1):300-4.
220. Mura S, Manconi M, Valenti D, Sinico C, Vila AO, and Fadda AM. Transcutol containing vesicles for topical delivery of minoxidil. *Journal of Drug Targeting*. 2011;19(3):189-96.
221. Balakrishnan P, Shanmugam S, Lee WS, Lee WM, Kim JO, Oh DH, Kim D-D, Kim JS, Yoo BK, Choi H-G, et al. Formulation and in vitro assessment of minoxidil niosomes for enhanced skin delivery. *International Journal of Pharmaceutics*. 2009;377(1-2):1-8.
222. Mura S, Pirot F, Manconi M, Falson F, and Fadda AM. Liposomes and niosomes as potential carriers for dermal delivery of minoxidil. *Journal of Drug Targeting*. 2007;15(2):101-8.
223. Lee PJ, Langer R, and Shastri VP. Novel Microemulsion Enhancer Formulation for Simultaneous Transdermal Delivery of Hydrophilic and Hydrophobic Drugs. *Pharm Res*. 2003;20(2):264-9.
224. Osborne DW, Ward AJI, and O'Neill KJ. Microemulsions as topical drug delivery vehicles: in-vitro transdermal studies of a model hydrophilic drug. *Journal of Pharmacy and Pharmacology*. 1991;43(6):451-4.
225. Feldman Y, Kozlovich N, Nir I, Garti N, Archipov V, Idiyatullin Z, Zuev Y, and Fedotov V. Mechanism of Transport of Charge Carriers in the Sodium Bis(2-ethylhexyl) Sulfosuccinate–Water–Decane Microemulsion near the Percolation Temperature Threshold. *The Journal of Physical Chemistry*. 1996;100(9):3745-8.
226. Obata Y, Takayama K, Machida Y, and Nagai T. Combined effect of cyclic monoterpenes and ethanol on percutaneous absorption of diclofenac sodium. *Drug design and discovery*. 1991;8(2):137-44.
227. El-Kattan AF, Asbill CS, and Michniak BB. The effect of terpene enhancer lipophilicity on the percutaneous permeation of hydrocortisone formulated in HPMC gel systems. *International Journal of Pharmaceutics*. 2000;198(2):179-89.
228. Okabe H, Takayama K, Ogura A, and Nagai T. Effect of limonene and related compounds on the percutaneous absorption of indomethacin. *Drug Des Deliv*. 1989;4(4):313-21.
229. Grams YY. Leiden University, Faculty of Mathematics & Natural Sciences, Leiden-Amsterdam Center for Drug Research; 2005.
230. Ogiso T, Shiraki T, Okajima K, Tanino T, Iwaki M, and Wada T. Transfollicular drug delivery: penetration of drugs through human scalp skin and comparison of penetration between scalp and abdominal skins in vitro. *Journal of Drug Targeting*. 2002;10(5):369-78.
231. Bhatia G, Zhou Y, and Banga AK. Adapalene microemulsion for transfollicular drug delivery. *Journal of Pharmaceutical Sciences*. 2013;102(8):2622-31.
232. Konrádssdóttir F, Ogmundsdóttir H, Sigurdsson V, and Loftsson T. Drug targeting to the hair follicles: a cyclodextrin-based drug delivery. *AAPS PharmSciTech*. 2009;10(1):266-9.
233. Weigmann HJ, Lademann J, Schanzer S, Lindemann U, Von Pelchrzim R, Schaefer H, Sterry W, and Shah V. Correlation of the local distribution of topically applied substances inside the stratum

- corneum determined by tape-stripping to differences in bioavailability. *Skin pharmacology and applied skin physiology*. 2000;14(98-102).
234. Otberg N, Patzelt A, Rasulev U, Hagemeister T, Linscheid M, Sinkgraven R, Sterry W, and Lademann J. The role of hair follicles in the percutaneous absorption of caffeine. *Br J Clin Pharmacol*. 2008;65(4):488-92.
 235. Barry BW. *Dermatological formulations: percutaneous absorption*. New York: Marcel Dekker; 1983:127-280.
 236. Sharma VK, Sarwa KK, and Mazumder B. Fluidity enhancement: a critical factor for performance of liposomal transdermal drug delivery system. *Journal of Liposome Research*. 2014;24(2):83-9.
 237. Jacobs M, Martin GP, and Marriott C. Effects of Phosphatidylcholine on the Topical Bioavailability of Corticosteroids Assessed by the Human Skin Blanching Assay. *Journal of Pharmacy and Pharmacology*. 1988;40(12):829-33.
 238. Jain S, Jain P, Umamaheshwari R, and Jain N. Transfersomes-a novel vesicular carrier for enhanced transdermal delivery: development, characterization, and performance evaluation. *Drug development and industrial pharmacy*. 2003;29(9):1013-26.
 239. Cevc G, Gebauer D, Stieber J, Schätzlein A, and Blume G. Ultraflexible vesicles, Transfersomes, have an extremely low pore penetration resistance and transport therapeutic amounts of insulin across the intact mammalian skin. *Biochimica et Biophysica Acta (BBA) - Biomembranes*. 1998;1368(2):201-15.
 240. Gupta A, Aggarwal G, Singla S, and Arora R. Transfersomes: A Novel Vesicular Carrier for Enhanced Transdermal Delivery of Sertraline: Development, Characterization, and Performance Evaluation. *Scientia Pharmaceutica*. 2012;80(4):1061-80.
 241. Fang J-Y, Hong C-T, Chiu W-T, and Wang Y-Y. Effect of liposomes and niosomes on skin permeation of enoxacin. *International Journal of Pharmaceutics*. 2001;219(1-2):61-72.
 242. Cevc G, Schätzlein A, and Blume G. Transdermal drug carriers: basic properties, optimization and transfer efficiency in the case of epicutaneously applied peptides. *Journal of Controlled Release*. 1995;36(1):3-16.
 243. Paul A, Cevc G, and Bachhawat B. Transdermal immunisation with an integral membrane component, gap junction protein, by means of ultradeformable drug carriers, transfersomes. *Vaccine*. 1998;16(2):188-95.
 244. Manosroi A, Wongtrakul P, Manosroi J, Sakai H, Sugawara F, Yuasa M, and Abe M. Characterization of vesicles prepared with various non-ionic surfactants mixed with cholesterol. *Colloids and Surfaces B: Biointerfaces*. 2003;30(1):129-38.
 245. Vora B, Khopade AJ, and Jain NK. Proniosome based transdermal delivery of levonorgestrel for effective contraception. *Journal of Controlled Release*. 1998;54(2):149-65.
 246. Manconi M, Sinico C, Valenti D, Lai F, and Fadda AM. Niosomes as carriers for tretinoin: III. A study into the in vitro cutaneous delivery of vesicle-incorporated tretinoin. *International Journal of Pharmaceutics*. 2006;311(1-2):11-9.
 247. Hofland HEJ, van der Geest R, Bodde HE, Junginger HE, and Bouwstra JA. Estradiol Permeation from Nonionic Surfactant Vesicles Through Human Stratum Corneum in Vitro. *Pharm Res*. 1994;11(5):659-64.
 248. Blume-Peytavi U, and Vogt A. Human hair follicle: reservoir function and selective targeting. *British Journal of Dermatology*. 2011;165(13-7).
 249. Grams YY, and Bouwstra JA. Penetration and distribution of three lipophilic probes in vitro in human skin focusing on the hair follicle. *Journal of controlled release*. 2002;83(2):253-62.
 250. Herkenne C, Alberti I, Naik A, Kalia YN, Mathy F-X, Pr eat V, and Guy RH. In vivo methods for the assessment of topical drug bioavailability. *Pharm Res*. 2008;25(1):87-103.
 251. Geusens B, Van Gele M, Braat S, De Smedt SC, Stuart MCA, Prow TW, Sanchez W, Roberts MS, Sanders NN, and Lambert J. Flexible Nanosomes (SECosomes) Enable Efficient siRNA Delivery in Cultured Primary Skin Cells and in the Viable Epidermis of Ex Vivo Human Skin. *Adv Funct Mater*. 2010;20(23):4077-90.
 252. Verma DD, and Fahr A. Synergistic penetration enhancement effect of ethanol and phospholipids on the topical delivery of cyclosporin A. *Journal of Controlled Release*. 2004;97(1):55-66.

253. Budai L, Kaszas N, Grof P, Lenti K, Maghami K, Antal I, Klebovich I, Petrikovics I, and Budai M. Liposomes for topical use: a physico-chemical comparison of vesicles prepared from egg or soy lecithin. *Sci Pharm*. 2013;81(4):1151-66.
254. Fadda AM, Baroli BM, Maccioni AM, Sinico C, Valenti D, and Alhaique F. Phospholipid-detergent systems: effects of polysorbates on the release of liposomal caffeine. *Il Farmaco*. 1998;53(10-11):650-4.
255. El Maghraby GM, Williams AC, and Barry BW. Can drug-bearing liposomes penetrate intact skin? *The Journal of pharmacy and pharmacology*. 2006;58(4):415-29.
256. Williams AC, and Barry BW. Skin absorption enhancers. *Crit Rev Ther Drug Carrier Syst*. 1992;9(3-4):305-53.
257. Manconi M, Sinico C, Valenti D, Lai F, and Fadda AM. Niosomes as carriers for tretinoin. III. A study into the in vitro cutaneous delivery of vesicle-incorporated tretinoin. *Int J Pharm*. 2006;311(1-2):11-9.
258. Manconi M, Sinico C, Caddeo C, Vila AO, Valenti D, and Fadda AM. Penetration enhancer containing vesicles as carriers for dermal delivery of tretinoin. *Int J Pharm*. 2011;412(1-2):37-46.
259. Sarpotdar PP, and Zatz JL. Evaluation of penetration enhancement of lidocaine by nonionic surfactants through hairless mouse skin in vitro. *Journal of Pharmaceutical Sciences*. 1986;75(2):176-81.
260. El Maghraby GMM, Williams AC, and Barry BW. Skin delivery of oestradiol from lipid vesicles: importance of liposome structure. *International Journal of Pharmaceutics*. 2000;204(1-2):159-69.
261. Motwani MR, and Rhein LD. Influence of vehicles on the phase transitions of. *J Cosmet Sci*. 2002;53(35-42).
262. El Maghraby GM, Williams AC, and Barry BW. Skin delivery of 5-fluorouracil from ultradeformable and standard liposomes in-vitro. *The Journal of pharmacy and pharmacology*. 2001;53(8):1069-77.
263. Uchegbu IF, and Vyas SP. Non-ionic surfactant based vesicles (niosomes) in drug delivery. *International Journal of Pharmaceutics*. 1998;172(1-2):33-70.
264. Alsarra IA, Bosela AA, Ahmed SM, and Mahrous GM. Proniosomes as a drug carrier for transdermal delivery of ketorolac. *European journal of pharmaceutics and biopharmaceutics : official journal of Arbeitsgemeinschaft fur Pharmazeutische Verfahrenstechnik eV*. 2005;59(3):485-90.
265. Namjoshi S, Caccetta R, Edwards J, and Benson HA. Liquid chromatography assay for 5-aminolevulinic acid: Application to in vitro assessment of skin penetration via Dermaportation. *Journal of Chromatography B*. 2007;852(1):49-55.
266. Dept of Health and Human Services FaDAF, Center for Drug Evaluation and Research (CDER), Center for Biologics Evaluation and Research (CBER). Guidance for Industry: Q2B Validation of Analytical Procedures: Methodology. <http://www.fda.gov/downloads/drugs/guidancecomplianceregulatoryinformation/guidances/ucm073384.pdf>. Accessed 14.06.11, 2011.
267. Zhang J, and Michniak-Kohn B. Investigation of microemulsion microstructures and their relationship to transdermal permeation of model drugs: Ketoprofen, lidocaine, and caffeine. *International Journal of Pharmaceutics*. 2011;421(1):34-44.
268. . Standard laboratory viscometers for liquids. <http://en.wikipedia.org/wiki/Viscometer>. Updated 20 April 2015, at 00:21.

Appendix

Materials and Methods

This chapter contains general materials and methods used in individual chapters of this thesis. Common laboratory techniques have been used in regards to solutes penetration in skin such as excised human skin preparation and transdermal delivery using Franz diffusion cells. This chapter starts with a list of chemicals that have been used and then experimental methods and procedures follow.

Chemicals

Caffeine, naproxen, minoxidil, lidocaine, ethanol, oleic acid (OA), eucalyptol (EU), polyethylene glycol 400 (PEG400) and polyethylene glycol 6000 (PEG6000), cholesterol, dilauroyl L- α -phosphatidylcholine (DLPC) were purchased from Sigma-Aldrich Pty. Ltd. (Sydney, Australia). Mineral oil (MO) was purchased from Galtex (Australia, Ltd), Glycerol from Ajax (a division of Naplex industries, Australia Pty. Ltd), Polyoxyl -20 Oleyl ether (Volpo-N20) was purchased from CRODA (Croda Europe Ltd, United Kingdom) and Polyoxyl 10 Oleyl ether (Volpo-N10, also known as Brij96v) from UNIQEMA (Wilton, United Kingdom), Decyl polyglucoside (DPGluc, sold as Oramix NS 10) was obtained from SEPPIC SA (France). All chromatography reagents were analytical grade.

Drug models

All drugs have been chosen according to their lipophilicity ($\log P$) and molecular weight (< 500) that are considered to be the most important physical properties determining penetration through human skin. The physicochemical properties of the model compounds are shown in Table 1

Table 1 Physicochemical properties of model compounds [Molecular weight (MW g/mol); Lipophilicity (Log P); Melting point (MP °C); Molar volume (MV), Solubility in aqueous solution (S_{aq} mg/L); Dissociation constant (pKa)]

Compound	MW ^a	Log P ^a	MP ^a	MV ^b	S _{aq}	pKa ^a
Caffeine	194.19	-0.07	238	151.8	21600	10.4
Minoxidil	209.25	1.24	248	214.6	2200	4.61
Lidocaine	234.34	2.44	68.5	89.7	4100	7.9
Naproxen	230.26	3.18	153	142.6	15.9	4.2

^aChemIDplus advanced-chemical information with searchable synonyms, structure, formulas <http://chem.sis.nlm.nih.gov/chemidplus/>

^bHSPiP program (Steven Abbott of Steven Abbott TCNF Ltd, ©2011 Steven Abbott and Johann Wiechers)

Human skin preparation:

Skin preparation methods: full-thickness skin

The skin was provided by female donors undergoing elective surgical procedures. Ethical approval was given by The University of Queensland Human Research Ethics Committee (HREC Approval no. 2008001342) and donors gave informed consent.

The skin was placed stratum corneum down in a shallow tray and the fat was surgically excised with a scalpel and discarded as pathological waste. In this process, the fat was removed as completely as possible, taking care not to cut into the dermis below. The remaining full thickness skin was placed flat on 2 sheets of Whatman filter paper, inside a labelled manilla folder and sealed in an airtight ziplock plastic bag with air expelled. The full thickness skin was frozen and stored flat at -20°C

Heat separated epidermal membrane

(Method of Kligman and Christopher 1963) (149)

The full thickness skin was immersed in hot water (60°C) for up to 60 seconds. After removal of skin from the water and draining of excess water, the skin was placed with stratum corneum side up on a cork board and secured with pins with slight stretching. Using a blunt probe, the epidermis was carefully peeled from the dermis, taking care not to tear it. The dermis was discarded, unless required.

The separated epidermal membrane (EM) was placed in a shallow tray containing about 30mm of water, so that the oily outer water resistant layer of the EM was facing up. The EM was unrolled and carefully removed from the water on a piece of Whatman 541 filter paper. The paper and EM were laid flat to air dry, placed on a cardboard support in a sealed zip-lock bag and frozen at -20°C until required

Preparation of the stratum corneum

The stratum corneum was prepared from epidermal sheets by trypsin digestion (149). The full-thickness skin was immersed in water at 60°C for 1 min that allowed the epidermis to be teased off the dermis. The epidermis was floated overnight on a solution of 0.01% trypsin in phosphate buffer saline (PBS) at 37°C. The viable epidermis was scraped off using cotton buds and the remaining stratum corneum membrane was rinsed several times with distilled water. The isolated stratum corneum sheets were placed flat on aluminium foil and stored at -20°C until use.

Skin integrity:

To assess the resistance of the epidermis, samples of epidermis were mounted in Franz cells: the receptor chamber was filled and 0.5-1 mL of PBS was added to the donor chamber. The cells were equilibrated for 30 mins before transdermal electrical resistance measurement was performed using a standard Multimeter with silver and silver chloride (Ag & AgCl) electrodes one into each chamber.

Any reading above 20 K Ω is satisfactory (45, 265) a resistance less than 20 K Ω indicates that the epidermal integrity may be compromised and the membrane should be replaced. PBS was removed from the donor chamber and the surface of the skin gently blotted dry with tissue paper before application of the solutions. The receptor chamber was also emptied and refilled with new PBS.

The silver and silver chloride (Ag & AgCl) electrodes were prepared, according to the Therapeutics Research Centre SOP (14/07/10), as described below:

Two silver rods (approx. 6 cm X 2-3 mm diam.) were polished with sandpaper before being immersed in 1M KCl solution in a small beaker, not touching each other. The rods were connected to a constant current power supply (500 μ A) for 1h. The AgCl electrode became coated with a black AgCl deposit.

Skin permeation studies

Franz Diffusion Cells

In this thesis, **Chapters 3, 4 and 5** examined penetration from various formulations using excised human epidermal membranes and full-thickness skin. Franz Diffusion Cells are the most commonly used method for transdermal penetration studies. The membranes were cut into discs (2 cm diameter), and mounted stratum corneum side uppermost between the glass surfaces of the donor and receptor compartments. Vacuum grease was used as a sealant on the edges that were not exposed to the penetrant. The exposed skin surface area was 1.33 cm². Clamps were used to hold the cells together. The receptor was filled with an appropriate buffer (usually PBS) and the required dose of the test substance was applied to the membrane surface. The diffusion cells was placed in a perspex holder in a water bath, to maintain the receptor phase temperature at 35°C, over a magnetic 15 point stirring plate. Magnetic stirrers in the bottom of each receptor chamber maintained mixing in the receptor fluid. Samples of receptor phase (200µl) were removed at regular time points and replaced with same amount of fresh PBS buffer (152). Drug concentration in receptor samples was determined by HPLC.

3.5.2 High performance liquid chromatography (HPLC)

3.5.2.1 Standard curve Samples preparation and analysis

Caffeine samples were dissolved in (PBS) pH 7.4. The internal standard was theophylline (5µg/mL) dissolved in the same solvent as the samples. Samples were analysed by HPLC.

Minoxidil samples were dissolved in methanol then diluted using PBS pH 7.4. The internal standard was Propyl paraben (5µg/mL) dissolved in the same solvent. Samples were analysed by HPLC.

Lidocaine samples were dissolved in PBS pH 7.4. The internal standard was Bupivacaine 5µg/ml dissolved in the same solvent as the samples. Samples were analysed by HPLC.

Naproxen samples were dissolved in methanol then diluted using PBS pH 7.4. The internal standard was Indomethacin 10µg/ml dissolved in the same solvent. Samples were analysed by HPLC

All samples were analysed using HPLC system consisting of Shimadzu SIL-6B SCL-10 a VP system controller, a SPD-10AV UV-VS detector, LC-10AD pump and an auto injector. The mobile phase was pumped across the system at 1ml/min flow rate. The column was a Phenomenex Luna 5µ C18 (150x4.6mm).

Chromatographic conditions

Table 2 Schedule of operating conditions for chromatographic analyses

	Drug name			
	Caffeine	Minoxidil	Lidocaine	Naproxen
Wavelength	273 nm	281 nm	210 nm	230 nm
Mobile phase	20mL ACN, 20ml THF, 5ml acetic acid,950ml H ₂ O	0.01M NaH ₂ PO ₃ ,60% H ₂ O,40%ACN,2.5m M SDS	0.05M Na ₂ HPO ₄ buffer 73%, 27%ACN	45% CAN, 20% Methanol, 35% water and 4mL Acetic acid
Internal standard (IS)	Theophylline (5 µg/ml)	Propyl paraben (5 µg/ml)	Bupivacaine (10µg/ml)	Indomethacin (10µg/ml)
Dissolution solvent	PBS	Methanol	PBS	Methanol
HPLC system	#4 Shimadzu class VP software and Excel 2002	#4 Shimadzu class VP software and Excel 2002	#4 Shimadzu class VP software and Excel 2002	#4 Shimadzu class VP software and Excel 2002

Validation method

Validation of assays includes testing for linearity, range, accuracy, precision, detection limit (DL) and quantitation limit (QL) according to FDA guidelines (266). The DL and the QL were based on the standard deviation of response (Q) and the slope of calibration curve (S).

$$DL=3.3Q / S$$

$$QL=10Q / S$$

Stock solutions (1mg/mL) of each compound were prepared by dissolving an accurate amount of each compound in the solvents shown in Table 2. The standard curve was then concentrated by serial dilutions of the stock dilution to the concentration differences shown in Table 3.3. Analysis was based on peak areas. Caffeine, lidocaine and naproxen were validated using 3 sets of standard curves plus 3 extra samples of lower limit of quantification for caffeine and lidocaine in one day. The minoxidil method was validated using a set of standard curves plus 2 extra samples for three days (interday) and one set of calibration curves plus 2 extra samples in the morning and afternoon (intraday) (See Table 3).

Table 3 Validation results

	Drug							
	Caffeine		Minoxidil				Lidocaine	Naproxen
Linearity	0.1-10 (µg/ml)		0.05-6 (µg/mL).				0.3-10 (µg/ml)	0.15-10 (µg/ml)
Accuracy	-2.0%	Theoretical Conc.	Mean of	SD	CV%	Error	-0.5%	-1.6%
		µg/mL	d conc			%		
		0.5	0.47	0.01	1.5	-6.81		
		1	0.95	0.01	0.9	-5.2		
Precision	2.4%	Level	Mean	SD	% cv		3.6%	4%
		0.3µg/mL	0.31	0.01	1.9			
		3µg/mL	2.98	0.06	2.1			
Limit of quantitation	0.1 (µg/ml)		1.48 (µg/ml)				0.3215 (µg/ml)	0.15 (µg/ml)

Determination of Solubility in the vehicles or formulations (S_v)

S_v was determined in saturated solutions of the compounds in each vehicle or formulation. An excess amount of the compound was added to 5 ml of the vehicle or formulation and the samples were incubated in a water bath at 32°C for 24 h, with continuous magnetic stirring. The samples were then centrifuged at 4000 rpm for 15 min and the supernatants were analysed by validated HPLC methods, after appropriate dilution where necessary (106). The S_v was described in **Chapters 3, 4 and 5**.

Determination of solubility in the stratum corneum (S_{sc})

Discs of stratum corneum (4 replicates for each compound) were weighed before using. They were then equilibrated in a saturated solution 1mL of each solute at 32°C for 24 h, according to established methods (150). At the end of the incubation period, the stratum corneum was removed, blotted dry and extracted with 1 mL 70% ethanol/water for another 24 h, at the same temperature used for equilibrium (32°C). The S_{sc} was determined from the amount of recovered model compound in the extraction fluid, measured by HPLC divided by the thickness and the area of the stratum corneum. The S_{sc} was examined in **Chapters 3, 4 and 5**.

Solvent uptake

The total solvent uptake into the stratum corneum was determined from the weight difference of a piece of the dry stratum corneum (about 0.6 mg) soaked in individual solvents

(1 mL) for 24 h at 35°C. The stratum corneum pieces were wiped three times with Kimwipe tissues before being weighed again. Solvent uptake was described in **Chapters 3 and 4**.

Tape stripping

This technique has been used in **Chapters 4, 5 and 6**. It is a technique used to remove the stratum corneum from skin by applying adhesive tape to the exposed skin surface, followed by careful removal. After Franz diffusion studies were completed, skin was washed 3 times with an ethanol moistened cotton bud or tissue. These wash samples were saved separately for HPLC analysis. After 10 min air drying, the skin was subjected to up to 20 tape strips to separate the stratum corneum from the epidermis. D-Squame tape (CuDerm Corp., USA) was applied to the exposed skin surface for about 5 s at a standard pressure and then carefully removed. Individual tapes were placed into separate vials and soaked overnight with 2 mL methanol before being analysed by HPLC. The amount of absorbed material in each tape was then determined. It represented material deposited within the stratum corneum. The result of the first tape was discarded, as this represented surface deposited material only.

Skin extraction.

Subsequent to tape stripping, the remaining skin was sliced into small sections; homogenised and extracted overnight with 2 mL methanol under constant shaking. Caffeine and naproxen concentrations in the extracts were determined by HPLC.

Extraction of skin was described in **Chapters 4, 5 and 6**.

Follicular casting

We used a technique known as the Lademann technique. It allows drugs deposited within appendages to be sampled and quantified. The surface and stratum corneum-deposited drugs were first removed by tape stripping 20 times. Following tape stripping, one drop of superglue was placed on a frosted section of a glass microscope slide, which was then pressed onto the surface of the stripped skin and held in place under light pressure for several minutes. When the glue was hard, the slide was peeled carefully from the skin, taking the contents of the skin appendages with it. The superglue was dissolved by rubbing with acetone-soaked cotton buds (4 times) and the individual cotton buds containing the sampled follicular contents were soaked overnight in 2 mL methanol before vortexing and quantitation by HPLC. This technique was used in **Chapters 5 and 6**.

Open and closed hair follicles techniques

Hair follicle plugging

Our group developed a method to plug the hair follicles on excised skin to evaluate their contribution in permeability across the skin. According to this method we closely identified all the hair follicles in a marked region under the microscope (ZEISS, stemi 2000-C, Schott (Germany) KL (200LED)). The plugging procedure involved applying 0.1 μL acriflavine solution (dissolved in milliQ water) to form a globule around the follicle and subsequently adding 0.1 μL of ethyl cyanoacrylate, (Loctite Super Glue, Henkel, USA) on top of it. The polar monomers of cyanoacrylate polymerised when they came in contact with the water molecules in the presence of acriflavine dye. This dye-sensitised polymerisation forms long and strong chains, thus plugging the skin and hair follicle. This technique was used in **Chapters 5**

Validation for hair follicle plugging method

As this is a new method, we wanted to test its efficacy by conducting *in vitro* skin absorption studies. As many of the follicles that could be identified under the microscope were plugged by the above technique. Then 1 mL of 3% (w/v) solution of caffeine in water was applied as the donor solution, with PBS at pH 7.4 as the receptor solution. The donor chamber was wrapped with parafilm after adding of the solution to prevent evaporation. At different times over 12 hours, 200 μL of the receptor solution was withdrawn and replaced with the same amount of fresh PBS. The sample thus withdrawn was analysed for caffeine levels by sensitive and rapid HPLC. The sequence of events is shown in Figure 1.

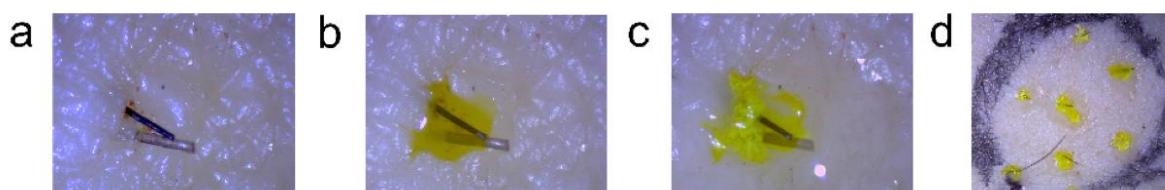


Figure 1 Method of hair follicle plugging (a. hair follicle identification; b. application of 0.1 μL acriflavine solution dissolved in milliQ water; c. application of 0.1 μL of ethyl cyanoacrylate (super glue); d. overview of plugged hair follicles in the exposed area.

Nanoemulsion formulation preparation

The formulations were prepared by dissolving Volpo-N10 (surfactant) in ethanol (co-surfactant). Then, oleic acid or eucalyptol (oil) was dissolved in the surfactant/ co-surfactant mixture, followed by gentle mixing with PBS. The surfactant/co-surfactant (S/Co-S) weight ratio was 1:1 and the weight ratio of oil: S/Co-S was 0.6:1:1. The resulting nanoemulsion was a clear semi-liquid at room temperature. Caffeine, minoxidil and naproxen at 3% w/w, 2%w/w and 2% w/w, respectively were dissolved in the nanoemulsions and control solutions. This preparation method was used **Chapters 4 and 5**.

Pseudo-ternary phase diagram

Oleic acid and eucalyptol were used as oil phase (O), Brij 96v was used as the surfactant, and ethanol was used as the co-surfactant. The mixture of O with S/Co-S was prepared at w/w ratios 0.6:1:1. Then, the O/(S/Co-S) mixture was titrated with water step by step. In each step a mixer agitated the mixture to mix it thoroughly and the sample was checked visually. If the sample was clear, it has become a nanoemulsion but if it was cloudy, it had not become a nanoemulsion. The technique was designed to find the area of nanoemulsion existence to be as correct as possible (267). Once the concentration ratio of the nanoemulsion was selected, the drug was loaded and physicochemical properties were tested at ambient temperature. The preparation was described in **Chapter 4**.

Vesicle preparation

Different vesicles were prepared with excipient mixtures. For all vesicles, the excipients were mixed in a rotary flask in different ratios, followed by glass beads (4 g) and chloroform (3 mL). Once the lipids were dissolved, the solvent was gradually evaporated on a rotary evaporator at 30 °C until a lipid film formed on the wall of the flask. The flask was set aside for 2 hours to eliminate residual chloroform, after which the lipid film was stirred with 2 mL caffeine solution (2% in water) for 2 hours at 30 °C. The liposome suspensions were extruded through a polycarbonate membrane with pore size 100 nm using the Liposofast extruder (AVESTIN, Inc., Ottawa, Canada). Thirty-one cycles of extrusion were performed for each vesicle type. The study was described in **Chapter 6**.

Encapsulation efficiency

To separate the non-encapsulated drug, the vesicle suspensions were centrifuged at 14000 rpm for 30 min at room temperature. The amounts of solute in the supernatant and also in the clear solution were analysed by HPLC. Drug encapsulation efficiency (EE%) was

calculated as: $EE\% = 100 * \text{mass of incorporated drug} / \text{total mass in vesicle preparation}$. The study was described in **Chapter 6**.

Nanoemulsion and vesicle characterisation (These techniques were used in **Chapters 4 and 6**.)

Nanoemulsions were characterised by transmittance, droplet size, reflection index, electrical conductivity and viscosity)

Vesicles were characterised by droplet size, zeta potential and polydispersity index (PDI).

Transmittance (Clarity)

The transmittance (T) of a sample is the ratio between the intensity of light that has passed through a sample to the intensity of light when it entered a sample ($T = I_{\text{incident}} / I_{\text{transmitted}}$). It can also be expressed as a percentage ($T \times 100$). Transmittance measured under standard conditions can be used as a measure of the clarity of a sample. It is generally accepted that nanoemulsions are characterised by transmittance readings >90%. The clarity of nanoemulsions in this work was determined by using a spectrophotometer (Hitachi U-1100; acrylic cuvettes 10X10X45mm) at a wavelength of 650nm.

Dynamic light scattering (DLS)

Size (Z-average size) and polydispersity index (PDI (the width of particle size) of microemulsions were measured using a Zetasizer Nano ZS (Malvern Instruments, Ltd, Malvern, UK). The diameter of a sphere is determined by measuring the speed of the random diffusion of molecules in the liquid due to the bombardment by surrounding solvent molecules using the Dynamic Light Scattering (DLS) method (Malvern). The system contains the optical unit for collection of raw data from samples, cells to hold the samples and controls and software which calculates the results using established theories. The size measurements were conducted using standard operating procedures (SOP) and reflective index values for the water and oil phases. Nanoemulsions were diluted 1:100 in water and measured in polystyrene cuvettes at 25°C.

Refractive index

The refractive indexes of nanoemulsion samples were measured with a refractometer (RFM 34) at room temperature.

Electrical conductivity (EC)

Nanoemulsion phase change analysis can be carried out by observing changes in conductivity with the addition of water to the system. Phase changes are indicated by a “percolation point”, over which a drop in conductivity is observed. Clarification of the concentration ranges within which an O/W or W/O nanoemulsion is formed is confirmed using a Digitor 31/2 Digit multimeter model Q1563. The values of EC measurements were performed in triplicate using an electrical conductivity meter; this was done by using AgCl and Ag conductivity electrodes at room temperature. The O/W nanoemulsion is conductive, however, W/O emulsions show much greater resistance. Therefore, the conductivity switched between two plateaus corresponding to water-continuous and oil-continuous structure (202).

Viscosity measurements

The nanoemulsion viscosity was determined using a glass capillary viscometers or Ostwald viscometers (Figure 2), named after Wilhelm Ostwald, at ambient temperature ($24^{\circ}\text{C} \pm 1$). Another version is the Ubbelohde viscometer, which consists of a U-shaped glass tube held vertically in a room temperature. In one arm of the U is a vertical section of precise narrow bore (the capillary) glass. Above there is a bulb, with another bulb lower down on the other arm. In use, liquid is drawn into the upper bulb by suction, and then allowed to flow down through the capillary into the lower bulb. Two marks (one above and one below the upper bulb) indicate a known volume. The time taken for the level of the liquid to pass between these marks is proportional to the kinematic viscosity. Most commercial units are provided with a conversion factor, or can be calibrated by a fluid of known properties. The time required for the test liquid to flow through a capillary of a known diameter of a certain factor between two marked points is measured. By multiplying the time taken by the factor of the viscometer, the kinematic viscosity is obtained (268).



Figure 2 Ostwald viscometers measure the viscosity of a fluid with a known density (268)

Zeta potential measurements

Zeta potential is the potential at the slipping or shear plane at the boundary between the mobile/diffuse layer and immobile/stern layer. The Zeta potential of liposomes was determined by dynamic light scattering (Zetasizer Nano ZS, Malvern Instruments, Ltd, Malvern UK) at room temperature using polystyrene cuvettes after dilution with water to the ratio 1:50.

Multiphoton microscopy (MPM)

Multiphoton microscopy (MPM) was used to assess the effect of the formulations in the stratum corneum. A DermalInspect system (JenLab GmbH, Jena, Germany), coupled to an ultra-short-pulsed, mode-locked, 80-MHz Titanium Sapphire laser (Mai Tai, Spectra Physics, Mountain View, California, USA) was used to image the skin in **Chapter 4**. For the MPM, skin samples were prepared to match the experimental conditions of *in vitro* Franz cell studies. An infinite dose from F2 EU and OA was applied to full-thickness skin. Samples of untreated skin were used as controls. After 8 h, the donor from the Franz cell was removed and the epidermis swiped gently with water and blotted dry with tissue. Then, these skin pieces were placed onto a microscope slide with a drop of water on the skin surface and protected with a cover slide.(108) Images were captured at 740 nm two-photon excitation. The skin was imaged at four depths, from the superficial surface, corresponding to the *stratum corneum* (~5-10 μm), *stratum granulosum* (~15-20 μm), *stratum spinosum* (25-30

μm) and *stratum basale* (35-40 μm). Keratinocyte morphology was used to confirm each of these layers.

LaVision Multiphoton Microscope

LaVision Multiphoton Microscope (LaVision BioTec GmbH, Germany) was used to assess the effect of these formulations in hair follicles and the area around hair follicles. A multiphoton system, coupled to an ultra-short-pulsed Titanium Sapphire laser (Mai Tai, Spectra Physics, Mountain View, California, USA) was used to image the skin. Full-thickness abdominal skin was mounted in Franz diffusion cells and a finite dose of acriflavine in the nanoemulsion formulations containing EU and OA and control (water) was applied. Samples of untreated skin were used as controls. After 24 h, the cells were dismantled and the skin was rinsed gently with water and blotted dry with a tissue. It was then placed directly on a microscope slide. Images were captured by two photon excitation at 740 nm. The skin was imaged at different depths, from the superficial surface, corresponding to the *stratum corneum* (~5-10 μm), *stratum granulosum* (~15-20 μm), *stratum spinosum* (25-30 μm) and *stratum basale* (35-40 μm). Keratinocyte morphology was used to confirm image depth in each of these layers. Image analysis was done using Image J (Wayne Rasband, National Institutes of Health, USA). These images were used in **Chapter 5**.